Mitigating Negative Transport Externalities in Industrialized and Industrializing Countries

---

vorgelegt von
Amit Agarwal
geboren in Jaipur, Indien

von der Fakultät V – Verkehrs- und Maschinensysteme
der Technischen Universität Berlin
zur Erlangung des akademischen Grades

Doktor der Ingenieurwissenschaften
-Dr.-Ing.-

genehmigte Dissertation

Promotionsausschuss:

Vorsitzender:	Prof. Dr. Oliver Schwedes
Gutachter:	Prof. Dr. Kai Nagel
Gutachter:	Prof. Dr. Kalaga Ramachandra Rao
Gutachterin:	Prof. Dr. Regine Gerike

Tag der wissenschaftlichen Aussprache: 03. März 2017

Berlin 2017

Man needs difficulties in life because they are necessary to enjoy the success.

Dr. A. P. J. Abdul Kalam

Acknowledgments

This dissertation was funded by the German Academic Exchange Service (DAAD) within the research project *Mitigating Negative Transport Externalities in industrialized and newly industrializing countries* (MiNTE).

Important data for the Munich Case Studies was provided by the Municipality of Munich, more precisely by 'Kreisverwaltungsreferat München' and 'Referat für Stadtplanung und Bauordnung München'. Important data for the Patna Case Studies was provided by the Innovative Transport Solutions (iTrans), New Delhi, India.

I take immense pleasure in thanking to my advisor, Kai Nagel at Technical Universität Berlin, whose encouragement, supervision and guidance from the beginning to the concluding level enabled me to finish this work in the first place. Along with my advisor, my thanks also go out to other committee members, Kalaga Ramachandra Rao at Indian Institute of Technology, Delhi and Regine Gerike at Technische Universität Dresden for serving as my committee members even at hardship.

I am greatly indebted to Benjamin Kickhöfer and Gregor Lämmel, German Aerospace Center (DLR) for consistent support, fruitful discussions and useful suggestions to complete this dissertation.

I am very thankful to the following people, who helped me during my work on this thesis in many respects: Andreas Neumann, Daniel Röder, Dominik Ziemke, Ihab Kaddoura, Jakub Wilk, Joschka Bischoff, Kalaga Ramachandra Rao, Michael Zilske, Michal Maciejewski, Simon F. Six, Theresa Thunig. I would like to thank H. Schwandt and N. Paschedag at the Department of Mathematics (Technical Universität Berlin), for maintaining our computing clusters.

Finally, I am deeply grateful to my beloved mother Umrao, father Suresh, for their blessings, my sisters Barkha and Shiva, my wife Vandana and my friends for their support and encouragement during this exciting and challenging period of my life what allowed me to focus on my research.

Table of Contents

Acknowledgments v

Table of Contents vii

List of Figures xiii

List of Tables xvii

List of Algorithms xix

Abstract xxi

Zusammenfassung xxv

1 General Introduction 1
- 1.1 Motivation . . . 1
- 1.2 Background of the research problem . . . 2
  - 1.2.1 Externalities in the transport sector . . . 2
  - 1.2.2 Economic valuation . . . 3
  - 1.2.3 Heterogeneous traffic . . . 5
- 1.3 Problem definition . . . 6
- 1.4 Research objectives . . . 7
- 1.5 Research approach . . . 9
  - 1.5.1 Travel simulator . . . 9
  - 1.5.2 Internalization of external costs . . . 9
  - 1.5.3 Traffic and link dynamics . . . 10
- 1.6 Thesis road-map . . . 10

2 Overview of Simulation Framework 13
- 2.1 Context . . . 13
- 2.2 Travel simulator – MATSim . . . 13
  - 2.2.1 Simulation inputs . . . 13
  - 2.2.2 MATSim cycle . . . 14
  - 2.2.3 Simulation outputs . . . 18
- 2.3 Summary . . . 18

Part I Transport Externalities

3 Literature Review of Transport Externalities **21**
3.1 Context . . . 21
3.2 Policy measures . . . 21
3.2.1 Traffic restrain measures . . . 21
3.2.2 Traffic control measures . . . 23
3.2.3 Vehicle and fuel side measures . . . 24
3.2.4 Road pricing . . . 24
3.3 Rationale . . . 25
3.3.1 Combined pricing . . . 25
3.3.2 Backcasting . . . 27
3.4 Research approach . . . 27
3.4.1 Combined pricing . . . 28
3.4.2 Backcasting . . . 28

4 Policy Measure : Combined Pricing **29**
4.1 Overview . . . 29
4.2 Pricing negative externalities . . . 29
4.2.1 Congestion cost . . . 29
4.2.2 Emission cost . . . 30
4.2.3 Internalization . . . 32
4.3 Test example . . . 32
4.4 Case study : Munich . . . 34
4.4.1 Input . . . 34
4.4.2 Base case . . . 36
4.4.3 Policy cases . . . 37
4.5 Results . . . 38
4.5.1 BAU: amplitude of externalities . . . 38
4.5.2 Pricing: system performance . . . 40
4.5.3 Pricing: driving forces . . . 41
4.5.4 Pricing: spatial distribution . . . 45
4.6 Discussion . . . 47
4.6.1 Commercial traffic . . . 47
4.6.2 Externalities from public transit . . . 48
4.6.3 Choice dimensions . . . 48
4.6.4 Improved scenario setup . . . 48
4.6.5 Pricing local emission exposure . . . 48
4.6.6 Policy implications . . . 49
4.7 Summary . . . 49

5 Policy Measure : Backcasting **51**
5.1 Overview . . . 51
5.2 Background . . . 51
5.2.1 Policy objective . . . 51
5.2.2 Historic trends . . . 51
5.2.3 Policy roadblocks . . . 52
5.3 Methodology . . . 54
5.3.1 Research problem . . . 54
5.3.2 Parametrized backcasting . . . 55

5.4 Scenario set up . . . 55
5.5 Results . . . 55
5.5.1 Extent of emissions costs . . . 56
5.5.2 Changes in emissions costs . . . 57
5.5.3 Changes in pollutant types . . . 59
5.5.4 Economic assessment . . . 61
5.6 Discussion . . . 63
5.6.1 Share of road transport sector . . . 63
5.6.2 Base and projected year demand . . . 63
5.6.3 Evaluated avoidance charge . . . 64
5.7 Summary . . . 64

Part II Mixed Traffic

6 Literature Review of Traffic Flow Model **69**
6.1 Context . . . 69
6.2 Homogeneous traffic modeling . . . 69
6.2.1 Queue models . . . 69
6.2.2 Discretized models . . . 70
6.2.3 Comparison with the queue models . . . 71
6.3 Heterogeneous traffic modeling . . . 72
6.3.1 Traffic dynamics . . . 72
6.3.2 Link dynamics . . . 74
6.4 Rationale . . . 75
6.4.1 Traffic dynamics . . . 75
6.4.2 Link dynamics . . . 76
6.5 Research approach . . . 76

7 Extensions of the Queue Model **79**
7.1 Overview . . . 79
7.2 Methodology . . . 79
7.2.1 Traffic dynamics : without holes . . . 79
7.2.2 Traffic dynamics : with holes . . . 81
7.2.3 Comparison of the traffic dynamics . . . 82
7.2.4 Link dynamics : seepage . . . 82
7.3 Experimental design . . . 84
7.3.1 Set up . . . 84
7.3.2 Steady state . . . 84
7.4 Fundamental Diagrams (FDs) . . . 85
7.4.1 Traffic dynamics : without holes . . . 85
7.4.2 Traffic dynamics : with holes . . . 87
7.5 Sensitivity . . . 91
7.5.1 Storage capacity . . . 92
7.5.2 Bicycle mixing ratio . . . 94
7.6 Spatio-temporal plots . . . 98
7.7 Discussion . . . 99
7.7.1 Validation with real-traffic data . . . 99
7.7.2 Passing link dynamics . . . 99

7.7.3 Seepage link dynamics . . . 100
7.7.4 Speed of backward traveling holes . . . 100
7.8 Summary . . . 101

8 Real-World Simulation Experiments 103
8.1 Overview . . . 103
8.2 Real-world evacuation . . . 103
8.2.1 Simulation inputs . . . 104
8.2.2 Simulation set up . . . 105
8.2.3 Simulation results . . . 105
8.3 Computation performance . . . 107
8.3.1 Simulation time in MATSim . . . 108
8.3.2 Simulation set up . . . 109
8.3.3 Computational hardware . . . 109
8.3.4 Outcome . . . 110
8.3.5 Average simulation time . . . 111
8.4 Discussion . . . 112
8.4.1 Application of seepage . . . 112
8.4.2 Comparison with other models . . . 112
8.5 Summary . . . 112

Part III Integrated Scenario

9 Patna Scenario 115
9.1 Overview . . . 115
9.2 Scenario background . . . 115
9.3 Inputs . . . 116
9.3.1 Network . . . 116
9.3.2 Demand . . . 117
9.3.3 Travel modes . . . 119
9.4 Calibration . . . 120
9.4.1 Calibrator : Cadyts . . . 120
9.4.2 Utility function . . . 121
9.4.3 Simulation set up . . . 123
9.4.4 Calibration results . . . 124
9.5 Policy measures . . . 127
9.5.1 Policy scenarios . . . 129
9.5.2 Policy set up . . . 129
9.5.3 Bicycle superhighway connectors . . . 130
9.6 Results . . . 131
9.6.1 Congestion patterns . . . 131
9.6.2 Modal split . . . 132
9.6.3 Mode switcher analysis . . . 133
9.6.4 Emissions calculation . . . 136
9.7 Discussion . . . 139
9.7.1 Plans from traffic counts . . . 139
9.7.2 Calibration of utility parameters . . . 139
9.7.3 Inclusion of public transit . . . 140

9.7.4 Policy implications . . . 140
9.7.5 Benefit-cost analysis . . . 141
9.8 Summary . . . 141

10 Conclusions and Further Challenges **143**
10.1 Conclusions . . . 143
10.2 Summary and future challenges . . . 147

A Spatial Averaging **151**
A.1 Parametric equation . . . 151
A.2 Spatial smoothing . . . 151

B Queue Model **155**
B.1 Consequences for the link geometry . . . 155
B.2 Average bicycle passing rate . . . 156
B.3 Spatio temporal trajectories . . . 156
B.4 Capacity update in queue model . . . 157
B.4.1 QSim structure . . . 157
B.4.2 Fast capacity update . . . 158
B.4.3 Performance analysis . . . 159
B.5 Scaling of a scenario . . . 159
B.5.1 Sample sizes in MATSim . . . 159
B.5.2 Traffic patterns . . . 161

C Patna Scenario **163**
C.1 Patna external demand . . . 163

List of Symbols and Acronyms **165**

Bibliography **169**

List of Figures

1.1 A schematic representation of nearly homogeneous and heterogeneous traffic. 6

2.1 MATSim cycle. 15
2.2 An illustration of re-planning over iterations. 17

Part I Transport Externalities

4.1 A small test example to compute the external costs. 33
4.2 Road network of Munich Metropolitan Area (MMA). 34
4.3 Re-planning over the iterations for different scenarios. 36
4.4 Share of car trips, emission and congestion costs for different user groups of BAU scenario. 39
4.5 Changes in the average trip travel time for mode switchers and retainers. . 43
4.6 Toll payments (in EUR) over time of day. 44
4.7 Absolute emissions (in g) and delays (in h). 45
4.8 Changes in the NO_2 emissions (in g) and delays (in h). 46

5.1 GHG emissions for EU-28. 52
5.2 Divergence between the emissions from new cars produced under laboratory and real-world conditions. 53
5.3 Contribution of sub-population in the emission costs for different regions. . 56
5.4 Changes in the emission costs (in %) for different sub-population and different region. 58
5.5 Effect of the ECMFs on the CO_2 emissions for respective sub-population and area. 59
5.6 Changes in the $NMHC$ emissions and average trip distance for urban and freight sub-populations with respect to BAU. 61

Part II Mixed Traffic

6.1 Schematic of the seepage link dynamics. 74
6.2 Queue model extensions in MATSim. 77

7.1 Schematic diagram differentiating FIFO and passing link dynamics. 80

7.2 Comparison of the FDs from simulations of the car vehicle class. Traffic dynamics = with and without holes; link dynamics = FIFO. 82
7.3 Network for race track experiment. 84
7.4 Truncated box plots (inset) showing variations in the flow and speed at different densities. 85
7.5 FDs from simulations of car only and bicycle only simulations. Traffic dynamics = without holes; link dynamics = FIFO. 85
7.6 FDs from simulation of car and bicycle vehicle classes. Traffic dynamics = without holes; link dynamics = passing. 86
7.7 FDs from simulation of car and bicycle vehicle classes, and bicycle is considered as seep mode. Traffic dynamics = without holes; link dynamics = seepage. 87
7.8 FDs from simulations of single vehicle classes (car, truck, motorbike and bicycle). Traffic dynamics = with holes; link dynamics = FIFO. 88
7.9 FDs from simulation of equal modal split (in PCU) of car and bicycle. Traffic dynamics = with holes; link dynamics = passing. 89
7.10 FDs from simulation of equal modal split (in PCU) of car, motorbike and bicycle. Traffic dynamics = with holes; link dynamics = passing. 89
7.11 FDs from simulation of equal modal split of car and bicycle, and bicycle is considered as seep mode. Traffic dynamics = with holes; link dynamics = seepage. 90
7.12 FDs from simulation of equal modal split of car, motorbike and bicycle. Bicycle and motorbike are considered as seep modes. Traffic dynamics = with holes; link dynamics = seepage. 91
7.13 FDs with storage capacity equivalent to 2 lanes. Traffic dynamics = with holes. 92
7.14 Flow density contours from the simulations of car and bicycle vehicle classes. Traffic dynamics = with and without holes; link dynamics = passing. 94
7.15 Average bicycle passing rate contours from the simulations of car and bicycle vehicle classes. Traffic dynamics = without holes; link dynamics = passing and seepage. 96
7.16 Average bicycle passing rate contours from the simulations of car and bicycle vehicle classes. Traffic dynamics = with holes; link dynamics = passing and seepage. 96
7.17 Speed density profiles from the simulations of car and bicycle vehicle classes. Traffic dynamics = with holes; link dynamics = passing and seepage. 97
7.18 Space time trajectories at density 13.33 PCU/km. 98

8.1 Evacuation Patna network for the experiment. 104
8.2 Comparison of the evacuation progress. 107
8.3 Average simulation time for 200 runs of Patna scenario 110

Part III Integrated Scenario

9.1 Patna road network, survey and activity location zones. 116
9.2 Comparison of 24 h simulation and real traffic counts. 126
9.3 Income (in USD) distance (in km) distributions for initial plans and calibrated plans. 127
9.4 Patna network with bicycle superhighway. 130

9.5 Modal share of urban travelers during identification of bicycle superhighway connectors. 131
9.6 Comparison of the congestion patterns at 08:00:00 for three scenarios. . . . 132
9.7 Absolute emissions for Patna BAU scenario. 136
9.8 Change in emissions (in %) for the BSH-b and BSH-mb scenarios with respect to BAU scenario. 137
9.9 Absolute NO_2 emissions for BAU scenario and changes in NO_2 emissions for BSH-b and BSH-mb policy measures. 138

B.1 FDs from simulation of equal modal split (in PCU) of car and bicycle using fast capacity update approach. Traffic dynamics = with holes, link dynamics = passing. 158
B.2 An illustration of traffic patterns. Traffic dynamics = with holes; link dynamics = passing. 160

List of Tables

1.1 Organization of the thesis. 10

Part I Transport Externalities

3.1 Different measures to improve the air quality and/or reduce the congestion externality. 22

4.1 Emission cost factors. 31
4.2 Key indicators for user groups of Munich Metropolitan Area (MMA). . . . 35
4.3 Behavioral parameters. 36
4.4 Modal split from reference studies, initial demand and calibrated base cases. 37
4.5 Policy cases. 38
4.6 Key indicators for all pricing schemes (in $M\ EUR$) per typical working day. 40
4.7 Changes in the car share (% points) with respect to BAU for all pricing schemes. 42
4.8 Average toll payments (EUR) per car trip for all pricing schemes. 42
4.9 Average toll levels ($EURct/km$) in the car mode for peak and off-peak hours. 43
4.10 Contributions of the externalities to the ECI toll levels ($EURct/km$) for the car mode in peak and off-peak hours. 43

5.1 Absolute and share of the emission costs ($M\ EUR$) for BAU scenario. . . . 56
5.2 Changes in the car trips (in % points) with respect to BAU for various ECMF. 58
5.3 Toll values (in EUR/km) differentiated for sub-population and area. 62
5.4 Absolute changes in the system welfare with respect to BAU scenario. . . . 62

Part II Mixed Traffic

8.1 Average trip time (in min) for various scenarios. 106
8.2 Average simulation time per iteration (in sec). 111

Part III Integrated Scenario

9.1 Average income (in INR) statistics for Patna city. 116

9.2 Values of time and vehicle operating costs. 117
9.3 Modal attributes for Patna scenario. 120
9.4 Utility parameters converted to MATSim format. 124
9.5 Calibrated utility parameters. 125
9.6 Modal splits for urban demand. 126
9.7 Modal splits for urban travelers (in %) for various policy scenarios. 133
9.8 Analysis for number of trips of mode switcher/retainer. 134
9.9 The changes in average speeds for mode switcher/retainer with respect to first iteration. 135

B.1 Average simulation time per iteration (in *sec*) for fast and slow capacity update approaches. 159

C.1 An example of hourly classified traffic counts data. 163
C.2 Share of through and commuters traffic. 164
C.3 Origin-destination (O-D) matrix for through traffic. 164

List of Algorithms

7.1 Seepage algorithm for the queue model. 83

9.1 Identification of the bicycle superhighway connectors. 130

Abstract

The ongoing urbanization process all around the globe is likely to increase transport-related negative externalities e.g., congestion, air pollution, climate change etc. This situation is severe in rapidly expanding cities where the demand for motorized transport is rising. This has increased the pressure on the policy makers to devise policies to tackle the problem. In this context, this thesis considers following objectives:

1. Investigation of the policy measures in a simulation framework a) to abate the transport negative externalities while considering the inter-relationship between different externalities and b) to achieve the politically goals.

2. Development of a computationally efficient model to simulate heterogeneous traffic conditions.

With the first objectives, the idea is to investigate the policy measures for industrialized nations; this is addressed in the first part of the thesis. In a simulation environment, marginal social cost pricing allows to correct for the inefficiencies due to exclusion of external costs from behavioral decision making process and to derive real-world policy recommendations. The first part of the thesis investigates and compares the effect of congestion pricing on emissions levels and the effect of emission pricing on congestion levels while considering the heterogeneity in the individual attributes and choice behavior. Derived from the inter-relationship between the two externalities, a joint internalization of vehicular congestion and emissions is proposed. It is applied to a real-world scenario of the Munich metropolitan area in Germany. It is found that the joint internalization moves the car transport system towards the optimum, measured by a strong decrease in congestion and emission costs. In this context, it has been shown for analytical models considering more than one externality, that the correlation between the externalities needs to be taken into account. Typically, in order to avoid overpricing, this is performed by introducing correction factors which capture the correlation effect. However, the correlation structure between, say, emission and congestion externalities changes for every congested facility over time of day. Additionally, the possible efficiency gains highly depend on the implicit price elasticity of demand, which again, depends on the availability of substitutes to car travel. For the Munich case study, it is shown that the iterative calculation of prices based on cost estimates from the literature allows to identify the amplitude of the correlation between the two externalities under consideration. Further, at the disaggregated level, the results show that pricing emissions moves individuals to shorter distance routes, whereas pricing congestion pushes towards longer distance routes. That is, despite the correlation

between the two externalities, isolated pricing strategies influence route choice behavior by tendency into opposite directions.

In real-world politics, policy setting often follows so-called *backcasting* approaches where goals are predefined, and policy measures are implemented to reach those goals. The first part also presents an parametric approach to identify the gap between toll levels derived from environmental damage cost internalization and toll levels to achieve the political goal of 20% reduction in GHG emissions of transport sector until 2020 with respect to 1990 levels. For this purpose, damage costs internalization is applied to the scenario of Munich metropolitan area again and it is shown that the desired reduction in CO_2 emissions is not reached. Further application of the parametric internalization approach with damage cost estimates from the literature yields toll levels that are by a factor of 5 too low in order to reach the predefined goal. When aiming at emission costs reductions of 20%, the damage cost estimates are even by a factor of 10 too low. It is shown that the major contribution to the overall emission reduction stems from behavioral changes of (reverse) commuters rather than from urban travelers; under some circumstances, the latter even increase their CO_2 emission levels. An economic assessment indicates that a toll equivalent to 5 times of the toll from the damage cost internalization approach increases the system welfare 6 times.

The second part of the thesis treats the second objective (development of a computationally efficient model to simulate heterogeneous traffic conditions) mainly in the context of industrializing nations where mixed traffic conditions prevail. In such conditions, it becomes necessary to develop a heterogeneous traffic flow model to include all vehicle classes while keeping the model equally computationally efficient. In this direction, the second part proposes a fast Spatial Queue Model (SQM) to produce realistic flow dynamics by introducing *backward traveling holes* for mixed traffic conditions. In the proposed approach, the space freed by a leaving vehicle on the downstream end of the link is not available immediately to the following vehicle, rather depends on the speed of backward traveling holes. This results in triangular Fundamental Diagrams (FDs) for traffic flow where the slope of the left branch is approximately equal to the minimum of the vehicle speed and link speed whereas the slope of the right branch is approximately equal to the speed of the backward traveling holes. With the help of FDs from the simulation of several vehicle classes, it is demonstrated that as the maximum speed of the vehicle class decreases, the density at which the maximum flow is achieved, increases and the maximum flow decreases.

In a similar direction, the second part also introduces *seepage* link dynamics to the SQM. Seepage is predominately common on urban streets of most of the industrializing nations. In this model, due to higher maneuverability and smaller size, smaller vehicles (e.g., bicycle, motorbike) move continuously across the gaps between the stationary or almost stationary vehicles and come in front of the queue to leave prior to other queued vehicles. The FDs from simulation of equal modal split of car and bicycle show that the flow characteristics of bicycle is marginally affected by the presence of cars but on the contrary, the flow characteristics of the car is significantly affected by the presence of bicycles. Further, it has been shown that in a traffic stream, seepage is more effective for faster seep mode (e.g., motorbike) than slower seep mode (e.g., bicycle).

Finally, in the second part, a comparison of the computational performances from the

simulations using various traffic and link dynamics of the queue model is presented. An additional data structure to maintain the backward traveling holes, increases the average simulation time marginally for all three sample sizes (1%, 10%, 100%). However, the search for seep mode on every link of the network is appeared to be resource-intensive with respect to the other link dynamics of the queue model. The rate of increase in the average simulation time using the seepage link dynamics for different sample sizes is significantly higher than the rate of increase in the average simulation time of other link dynamics of the queue model.

The third part integrates the two objectives and presents a real-world scenario of Patna, India with a goal of reduction in emissions externality towards sustainable transport. This part exhibits the steps for demand generation and calibration of the scenario. The urban demand is generated using the trip diaries whereas the external demand is generated using hourly trip counts. For the latter, Calibration of dynamic traffic assignment (Cadyts) is extended to mixed traffic conditions. To include diverse income effects in the behavioral decision making process of the individual, the individual income is included in the scoring function. The scenario is calibrated to evaluate the Alternative (mode) specific constants (ASCs) for different modes. The calibrated scenario is used for policy testing. Based on the traffic characteristics and composition, a *bicycle superhighway* is proposed along the existing railway line. An iterative process is proposed to identify the optimum locations of the connectors between bicycle superhighway and existing network. A what-if policy measure is considered in which motorbike is also allowed on the bicycle superhighway. Both policy measures increase the share of the bicycle significantly. To estimate the emissions for the two policy measures, the Emission Modeling Tool (EMT) is extended to mixed traffic conditions. It is shown that if only bicycle is allowed on the bicycle superhighway, significant reduction in emissions are observed in the inner city. However, as soon as the motorbike is also allowed on it, significant increase in the emissions are observed along the bicycle superhighway in the inner city of Patna which emphasizes the need of enforcements to stop motorbikes on the bicycle superhighway. With this, the third part demonstrates that significant reduction in emissions can be obtained in the situations where a pricing measure is difficult to implement.

To summarize, this thesis focuses on the evaluation of policy measures in a simulation framework to extract the valuable information for the policy makers to tackle the problem of negative transport externality in the industrialized nations as well as industrializing nations. For the latter, this thesis also extends a computationally efficient traffic flow model to simulate the heterogeneous traffic conditions. Finally, with several case studies, the thesis shows the scope of devising policy recommendations based on the scenario specifications.

Zusammenfassung

Es ist anzunehmen, dass die aktuell stattfindende globale Urbanisierung negative externe Effekte des Verkehrssektors wie z.B. Stau, Luftverschmutzung sowie den Klimawandel verstärkt. Die Situation ist besonders schwerwiegend in aktuell stark wachsenden Städten, in denen auch die Verkehrsnachfrage steigt. Somit steigt der Druck auf politische Entscheidungsträger Maßnahmen zu ergreifen, um den genannten Problemen entgegenzuwirken. Ausgehend von diesem Spannungsfeld, verfolgt die vorliegende Dissertation folgende Ziele:

1. Die Untersuchung von Maßnahmen in einem Simulationsmodell a) zur Verringerung der negativen externen Effekte unter Berücksichtigung der gegenseitigen Abhängigkeiten der verschiedenen externen Effekte sowie b) zum Erreichen politisch motivierter Ziele.

2. Entwicklung eines laufzeiteffizienten Modells zur Simulation heterogener Verkehrsbedingungen.

In Bezug auf das erste Ziel, werden zunächst Maßnahmen im Kontext industrialisierter Länder untersucht; dies stellt den ersten Teil der Dissertation dar. Hierfür wird ein Simulationsmodell verwendet, in welchem eine Bepreisung auf Basis marginaler sozialer Kosten eine Korrektur der Ineffizienzen, die aufgrund der Nichtberücksichtigung von externen Kosten in Entscheidungsprozessen entstehen, ermöglicht und somit die Ableitung von Maßnahmenempfehlungen erlaubt. In diesem ersten Teil der Dissertation wird die Auswirkung von Staubepreisung auf Emissionen sowie die Auswirkung von Emissionsbepreisung auf Stau untersucht und verglichen, wobei die Heterogenität in den Attributen der Individuen sowie in deren Entscheidungsverhalten in Betracht gezogen wird. Auf Basis der beiderseitigen Abhängigkeit zwischen den genannten externen Effekten, wird eine gleichzeitige Internalisierung von Stau- und Emissionseffekten vorgeschlagen. Diese Maßnahme wird in einem realistischen Simulationsszenario für die Metropolregion München angewendet. Es kann gezeigt werden, dass die vorgeschlagene gleichzeitige Internalisierung das Verkehrssystem des motorisierten Individualverkehrs in Richtung des Systemoptimums bewegt, was durch einen starken Rückgang in Stau- und Emissionskosten charakterisiert ist. In diesem Zusammenhang wurde für analytische Modelle, die mehr als einen externen Effekt betrachten, gezeigt, dass die Korrelation zwischen den externen Effekten berücksichtigt werden muss. Um eine Überbepreisung zu vermeiden, werden typischerweise Korrekturfaktoren verwendet, die den Korrelationseffekt aufgreifen. Die Korrelationsstruktur zwischen Emissions- und Stauexternalitäten ändert sich jedoch für jede bestaute Infrastruktur im Laufe des Tages. Weiterhin hängen mögliche Effizienzgewinne stark von der

impliziten Preiselastizität der Nachfrage ab, welche wiederum von der Verfügbarkeit von Alternativen zur Fortbewegung mit dem Auto abhängt. Für das München-Szenario wird gezeigt, dass die iterative Berechnung von Preisen auf Basis von Kostenschätzungen aus der Literatur eine Bestimmung des Ausmaßes der Korrelation der beiden berücksichtigten externen Effekte erlaubt. In einer disaggregierten Betrachtung zeigen die Ergebnisse weiterhin, dass eine Emissionsbepreisung die Verkehrsteilnehmer dazu veranlasst kürzere Routen zu wählen, während eine Staubepreisung zur Wahl längerer Routen bewegt. Dies bedeutet, dass trotz der Korrelation beider externer Effekte, isolierte Bepreisungsstrategien das Routenwahlverhalten tendenziell in gegensätzliche Richtungen beeinflussen.

In realer Politik basiert die Festlegung von Maßnahmen häufig auf sogenannten *Backcasting*-Ansätzen, bei denen im Voraus Ziele definiert und Maßnahmen in Kraft gesetzt werden, um diese Ziele zu erreichen. Im ersten Teil der Dissertation wir ferner ein parametrischer Ansatz vorgestellt, mit dem der Unterschied zwischen der nötigen Mauthöhe zur Internalisierung der Umweltschadenskosten und der nötigen Mauthöhe zum Erreichen des politischen Ziels einer 20-prozentigen Reduktion von Treibhausgasemissionen (GHG) des Verkehrssektors bis 2020 gegenüber dem Niveau von 1990 ermittelt werden kann. Zu diesem Zwecke wir die Internalisierung der Schadenskosten abermals auf das Szenario für die Metropolregion München angewendet. Es wird gezeigt, dass die gewünschte Reduktion der CO_2-Emissionen nicht erreicht wird. Eine weitere Anwendung des parametrischen Internalisierungsansatzes mit Schadenskostenschätzungen aus der Literatur führt zu Mauthöhen, die um einen Faktor 5 zu niedrig sind, um das gesetzte Ziel zu erreichen. Um Reduktionen der Emissionskosten von 20% zu erreichen, sind die Schadenskostenschätzungen sogar um einen Faktor 10 zu niedrig. Es wird gezeigt, dass der Hauptbeitrag zur Emissionsreduktion eher auf Verhaltensänderungen der Auspendler als auf jenen der innerstädtischen Verkehrsteilnehmer basiert; unter bestimmten Umständen erhöht sich sogar der CO_2-Ausstoß der Letzteren. Eine ökonomische Untersuchung deutet darauf hin, dass eine Maut, die dem Fünffachen der Maut auf Basis der Schadenskosteninternalisierung entspricht zu einer sechsfachen Steigerung der Wohlfahrt im Gesamtsystem führt.

Im zweiten Teil der Dissertation wird das zweite Ziel (Entwicklung eines laufzeiteffizienten Modells zur Simulation heterogener Verkehrsbedingungen) hauptsächlich im Kontext von Entwicklungsländern behandelt, in denen häufig heterogene Verkehrsverhältnisse vorherrschen. Diese Bedingungen erfordern die Entwicklung eines heterogenen Verkehrsflussmodells, um alle Fahrzeugklassen einschließen zu können, während die rechentechnische Effizienz des Modells erhalten bleibt. Daher wird im zweiten Teil der Dissertation ein schnelles Spatial Queue Model (SQM) vorgestellt, mit dem realistische Verkehrsflussdynamiken durch Berücksichtigung sich rückwärtsbewegender Lücken unter heterogenen Verkehrsbedingungen produziert werden. In diesem Ansatz steht der Raum, der frei wird, wenn sich ein Fahrzeug Richtung Ende der Netzwerkkante bewegt, nicht unmittelbar für nachfolgende Fahrzeuge zur Verfügung, sondern hängt vielmehr von der Geschwindigkeit der sich rückwärts bewegenden Lücken ab. Dies führt zu dreiecksförmigen Fundamentaldiagrammen (FDs) des Verkehrsflusses, sodass die Steigung des linken Asts näherungsweise gleich dem Minimum aus Fahrzeuggeschwindigkeit und Netzwerkkantengeschwindigkeit ist, während die Steigung des rechten Asts näherungsweise gleich der Geschwindigkeit der sich rückwärts bewegenden Lücke ist. Mit Hilfe der FDs der Simulation verschiedener

Fahrzeugklassen wird gezeigt, dass mit abnehmender Höchstgeschwindigkeit der Fahrzeugklasse die Dichte, bei der der höchste Verkehrsfluss erreicht wird, steigt und der maximale Verkehrsfluss sinkt.

Mit einem ähnlichen Ziel werden im zweiten Teil der Disseration ferner sog. *Seepage* Link Dynamics in das SQM integriert. Seepage (Durchschlängeln) ist ein typisches Phänomen auf urbanen Straßen in den meisten Entwicklungsländern. Seepage beschriebt das Phänomen, dass sich kleinere Fahrzeuge wie bspw. Fahrräder oder Motorräder aufgrund ihrer höheren Manövrierbarkeit und ihrer geringeren Größe kontinuierlich durch die Lücken zwischen stehenden oder fast stehenden anderen Fahrzeugen bewegen und somit zum Ende der Warteschlange vorrücken und diese vor den anderen Fahrzeugen verlassen. Die FDs von Simulationen mit gleichem Modal Split von Autos und Fahrrädern zeigen, dass die Flusseigenschaften der Fahrräder nur marginal durch das Vorhandensein von Autos beeinflusst werden, während die Flusseigenschaften von Autos signifikant durch das Vorhandensein von Fahrrädern beeinflusst werden. Weiterhin wurde für einen Verkehrsstrom gezeigt, dass Seepage effizienter für schnellere Verkehrsmittel wie z.B. Motorräder ist als für langsamere.

Schließlich wird im zweiten Teil der Dissertation ein Vergleich der rechentechnischen Performanz aus verschiedenen Simulationen, in denen die unterschiedlichen Verkehrs- und Kantendynamiken des Queue-Modells verwendet werden, gezogen. Die zusätzliche Datenstruktur zur Behandlung der sich rückwärts bewegenden Lücken erhöht die durchschnittliche Simulationszeit nur marginal in allen drei verwendeten Simulationssamples (1%, 10%, 100%). Die nötigen Zwischenspeicherung zur Berücksichtigung von sich durchschlängelnden Fahrzeugen auf den einzelnen Kanten (Seepage) hingegen stellt sich als ressourcenintensiv im Vergleich zu den sonstigen Kantendynamiken des Queue-Modells dar. Die Steigerungsrate der durchschnittlichen Simulationszeit bei Berücksichtigung von Seepage Link Dynamics ist signifikant höher als die Steigerungsraten der durchschnittlichen Simulationszeit der anderen Linkdynamiken des Queue-Modells.

Im dritten Teil der Dissertation werden die beiden Ziele zusammengeführt und anhand eines realistischen Simulationsszenarios für Patna in Indien veranschaulicht mit dem Ziel externe Effekte durch Emissionen zu reduzieren und ein nachhaltiges Verkehrssystem zu erreichen. In diesem Teil der Dissertation werden die Schritte zur Generierung der Verkehrsnachfrage sowie zur Kalibrierung des Szenarios dargelegt. Die städtische Verkehrsnachfrage wird auf Basis von Reisetagebüchern erstellt, während der Pendlerverkehr auf Basis stündlicher Verkehrszählungen generiert wird. Für Zweiteres wird das Kalibrierungstool Calibration of dynamic traffic assignment (Cadyts) zur Berücksichtigung heterogener Verkehrsbedingungen angepasst. Um unterschiedliche Einkommenseffekte in den verhaltensbasierten Entscheidungsprozess der Verkehrsteilnehmer einzubeziehen, wird das individuelle Einkommen in die Bewertungsfunktion integriert. Das Szenario wird kalibriert, um die alternativenspezifische (verkehrsmittelspezifische) Konstante Alternative (mode) specific constants (ASCs) für verschiedenen Verkehrsmittel auszuwerten. Das kalibrierte Szenario wird zur Maßnahmenuntersuchung verwendet. Ausgehend von den Charakteristika des Verkehrsgeschehens und der Zusammensetzung der Verkehrsmittel, wird ein *Fahrradschnellweg* (Bicycle Superhighway) entlang einer existierenden Eisenbahnlinie vorgeschlagen. Ein iterativer Prozess wird verwendet, um die optimalen Orte für Verbindungen zwischen dem Fahrradschnellweg und der existierenden Infrastruktur

zu bestimmen. Dies wird mit einem Alternativszenario, in dem auch Motorräder auf dem Fahrradschnellweg zugelassen sind, verglichen. Beide Maßnahmen tragen zu einer signifikanten Erhöhung des Fahrradanteils bei. Um die Emissionen unter beiden Maßnahmen abzuschätzen wird das Emission Modeling Tool (EMT) für heterogenen Verkehrsbedingungen erweitert. Es wird gezeigt, dass signifikante Reduktionen der Emissionen in der Innenstadt zu verzeichnen sind, falls Fahrräder als einziges Verkehrsmittel auf den Fahrradschnellwegen erlaubt sind. Sobald jedoch auch Motorräder auf dem Fahrradschnellweg zugelassen werden, ist ein signifikanter Anstieg der Emissionen entlang des Fahrradschnellwegen in der Innenstadt von Patna zu beobachten, was die Notwendigkeit solche Verkehrsmittel von Fahrradschnellwegen zu verbannen verdeutlicht. Hierdurch wird im dritten Teil der Dissertation gezeigt, dass signifikante Emissionsreduktionen auch unter Bedingungen, in denen die Umsetzung von Bepreisungsmaßnahmen schwierig ist, erreicht werden können.

Zusammenfassend liegt der Schwerpunkt dieser Dissertation auf der Bewertung von Bepreisungsmaßnahmen mittels eines Simulationsmodells mit dem Ziel nützliche Informationen für Entscheidungsträger abzuleiten, die geeignet sind, um negativen externen Effekten des Verkehrs sowohl in Industrie- als auch Entwicklungsländern entgegenzuwirken. Für letztere wird in dieser Arbeit ein effizientes Verkehrsflussmodell zur Simulation heterogener Verkehrsbedingungen vorgestellt. Schließlich wird in mehreren Fallstudien das Spektrum möglicher Maßnahmen auf Basis verschiedener Szenarien gezeigt.

Chapter 1

General Introduction

1.1 Motivation

The number of urban agglomerations with a population of 10 $Million(M)$ or more will increase from 10 to 41 in the period from 1990 to 2030 (United Nations, 2014). The fast pace of urbanization[1] is accompanied by a faster rate of economic and social transformations in urban areas relative to rural areas. This rapid urbanization is driven by a rapid growth in urban population[2]. The major shift is towards the urban economy and this will amplify the demands for basic services like power, transport, housing and water steeply.

In last few decades, due to unplanned and inadequate infrastructure, the urbanization process has increased the dependency on road transport which results into high vehicle usage. The problem is expected to become more severe because the total number of cars across world is expected to rise between 2.2 to 2.6 times from the 2010 levels until 2050 (WEC, 2011, p. 62). Clearly, this would depend on the government intervention for regulating future policies. The rise is more profound for non-OECD countries.[3] Historically, the focus of the motorization is limited to automobile. However, the role of motorized two-wheelers (motorcycles, motorbikes, scooters) cannot be neglected due to their significant contribution in the motorization of the developing nations. E.g., Asia accounts for more than 75% of global motorized two-wheelers fleet, of which China accounts for roughly 50% and India accounts for about 20% (WBCSD, 2004). In India, the registered number of cars has increased from 0.16 M to 24.8 M in the time frame of 1951-2013; the registered number of motorbikes jumped to 132.5 M in 2013 up from 0.03 M in 1951.[4] After 1980, the rate of increase for the latter is significantly higher With the rapid increase in the number of motorized vehicles, the severity of congestion, emissions and noise will also increase in existing and future mega-cities[5]. Additionally, in absence of planned and

[1] It is defined as the average annual rate of change in urban percentage.

[2] The share of urban population was only 30% in 1950 which is increased to 54% in 2014; it is predicted that by 2050, about 66% of the world's population will reside in urban areas (United Nations, 2014).

[3] This increment is between 430-557% and 36-41% for non-OECD and OECD countries (WEC, 2011, pp. 65–66). Refer to http://www.oecd.org for a complete list of OECD countries.

[4] These numbers are taken from https://data.gov.in/catalog/total-number-registered-motor-vehicles-india.

[5] A mega-city is usually defined as a metropolitan area with more than 10 M inhabitants (United Nations, 2014).

adequately managed infrastructure, and policies to ensure the benefits of city life, the urban areas are unequally expanded. This rapid and unplanned growth in urban sprawl endangers sustainable development (United Nations, 2014). This emphasizes the need for a tool designed to model the travel demand and thereby test the impact of regulating policies on the decision making of individual travelers. Thus, this thesis focuses on two important issues in the context of rapid urbanization processes. These are –

1) Evaluation of policies to abate the external effects in the transport sector.

2) Modeling of the travel demand from a large urban agglomeration under heterogeneous traffic conditions.

This chapter highlights the background of the research problems in the context of rapid urbanization processes in Sec. 1.2, followed by the problem definition in Sec. 1.3. The research objectives for the thesis are listed in Sec. 1.4. The research approach is briefly explained in Sec. 1.5 and the road map of the thesis is placed in Sec. 1.6.

1.2 Background of the research problem

1.2.1 Externalities in the transport sector

As discussed in the previous section, in last few decades, due to unplanned and inadequate infrastructure, the urbanization process has increased the dependency on road transport which results into high vehicle usage. Consequently, the externalities from the transport sector are rising. According to Buchanan and Stubblebine (1962, p. 372), an externality exists –

> "the utility of an individual, A, is dependent upon the "activities", $(X_1, X_2, \cdots, X_m)$, that are exclusively under his own control or authority, but also upon another single activity, Y_1, which is, by definition, under the control of a second individual, B, who is presumed to be a member of the same social group."

Thus, an externality can be associated with positive (benefits) or negative (costs) effects, which an activity imposes on another entity (individual/firm). Due to improvements in the transport sector, positive externalities (desirable side-effects) such as increased accessibilities, increased land values, emergency services, agglomeration benefits, etc., become apparent. In contrast, there exist negative externalities which are imposed on the society or community. Some of the major externalities are:

i) **Accident costs:** With the introduction of additional cars on the streets, the accident externalities could be (Newbery, 1988; Jansson, 1994):

   a) higher accident risks[6] for other vehicles and unprotected road users and

   b) accident effects on the rest of the society in terms of ambulance transport, hospital treatment, etc.

[6] According to (Newbery, 1988, p. 169), the probability of the accidents depends on the vehicular encounters (i.e., passing or other interactions). Then, the accidents are proportional to the square of the traffic flow. In the similar context, this thesis also estimates the average bicycle passing rate in Sec. 7.5.2.2.

ii) **Congestion costs:** Generally, the decision about making a (private vehicle) trip is governed by the private costs of making trip against expected benefits of the trip. Travelers ignore the additional congestion that they cause to others due to the presence of their vehicles. The magnitude of the congestion costs is continuously rising; e.g., average yearly delay per auto commuters has increased from 18 Hour (h) in 1982 to 42 h in 2014 for US urban areas (Schrank et al., 2015).

iii) **Air pollution costs:** Exhaust emissions from the motorized vehicles is a major source of air pollution releasing a variety of emissions. These are categorized as follows:[7]

a) **Green House Gases (GHG)** Combustion of the fossil fuels emits Carbon Dioxide (CO_2) which does not impair human health directly but exacerbate global warming (GHG trap the heat in the atmosphere and consequently elevate global warming).[8]

b) **Local pollutants** Nitrogen Oxides (NO_x), Nitrogen Dioxide (NO_2), Particular Matter (PM), Non-Methane Hydrocarbons ($NMHC$), Sulfur Dioxide (SO_2), etc., are other major pollutants which affect the human health adversely such as, irritation in the respiratory system and in the lungs, coughing, choking, etc., which are proven to yield long-term health damages.

In contrast to other externalities, emission costs are imposed on a larger group of persons and for a longer period of time. Air pollution costs are related to other externalities; for instance, as a consequence of congestion, corresponding to the average yearly delay per car, average additional fuel consumption per person per year has escalated from 4 Gallons in 1982 to 19 Gallons in 2014 (Schrank et al., 2015). The data is averaged from 471 US urban areas.

iv) **Noise pollution costs:** Similar to emissions, noise pollution also affects health adversely (e.g., hearing problems, sleeping disorders, cardio-vascular disease, stress related heart problems, etc.; Stassen et al., 2008; Babisch et al., 2013). This could arise due to continuous honking, acceleration/deceleration of more powerful engines, tire/road contact, etc.

Here onwards, the term externality refers to negative externality or negative external costs unless otherwise stated. This thesis mainly focuses on congestion and emission externalities.

1.2.2 Economic valuation

As discussed before, negative externalities impose significant negative impacts on the health, climate, etc.; however, quantification and monetization of these externalities is very difficult due to the nature of their impacts (indirect, long-term, uncertain, etc.; Litman,

[7] A general categorization is primary and secondary. The primary pollutants are emitted directly into the atmosphere whereas the secondary pollutants results from the chemical reactions between between pollutants in the atmosphere. This thesis considers only primary pollutants for all analyses and estimation approaches.

[8] Apart from the CO_2, there are other GHG e.g., Methane, Nitrous oxide which contribute to the global warming. However, the focus of this thesis is limited to the CO_2 only.

2012). The costing of externalities is composed of two steps (Zhang et al., 2004, pp. 44-46): a) quantifying the externality and b) economic valuation of the physical impacts of the externality. In the literature, several techniques are available for monetizing different externalities (Zhang et al., 2004; Maibach et al., 2008).[9] For congestion and emission externalities, different options are briefly described next.

1.2.2.1 Congestion costs

In order to estimate congestion cost, speed-flow relations, value of time and demand elasticities can be used (refer to Zhang et al., 2004; Maibach et al., 2008, for detailed descriptions). The possible different components of congestion costs are higher travel time, vehicle provision and operating costs, disamenities in the crowded system, additional fuel costs, etc.

The economic valuation of the congestion costs due to increased travel time is estimated mainly using the value that travelers place on travel time savings (Value of Travel Time Savings (VTTS)) or delays. There are several methods to estimate the travelers' valuation of time savings, however, broadly, they are categorized as: revealed preferences (RP) and stated preferences (SP) (Zhang et al., 2004). In the former approach, the VTTS is estimated using the observed behavior of individual travelers, where travelers trade-off time and money to exercise a choice between two or more alternatives. In the latter approach, the VTTS is estimated using the stated or indicated preferences for hypothetical travel cost and time alternatives. The increases in the travel time can account for about 90% of the economic congestion costs (Maibach et al., 2008).

1.2.2.2 Air pollution costs

In general, air pollution costs include the damage cost of pollutants, health costs, human mortality/morbidity, reduced visibility, corrosion of materials, crop losses, impacts on biodiversity and damages to the climate (Zhang et al., 2004, pp. 316-317; Maibach et al., 2008, p. 46). Transport literature suggests to use the *impact pathway approach*[10] to estimate the marginal external costs of air pollution and noise.

Air pollution costs together with climate change costs have a high level of complexities and uncertainties (Tol, 2005) which makes the estimation of the damage costs very difficult.

Damage cost approach The marginal damage cost of carbon emissions is defined as the net present value of the impact of one additional Ton (*ton*) of carbon[11] over the next 100 years which is emitted to the atmosphere today (Watkiss et al., 2005; Downing et al., 2005). It is also known as social cost of Carbon (SCC). Thus, in simpler words, the

[9] The readers are advised to look on Weinreich et al., 1998; Mayeres et al., 1996; Maibach et al., 2008, for different methodologies adopted to estimate the external costs of transport and different levels of the external costs.

[10] The impact pathway approach (IPA) is a detailed way to value the air quality changes and it uses location-specific detailed modeling to evaluate the physical impacts of air pollution (Maibach et al., 2008, pp. 47-49; Bickel et al., 2006).

[11] In literature, the (damage or avoidance) cost estimates are expressed either in money unit per *ton* of carbon (C) (Watkiss et al., 2005; Clarkson and Deyes, 2002; Downing et al., 2005) or per *ton* of CO_2 (Maibach et al., 2008). The conversion between these is possible using the molecular weights i.e., 1 *ton* C = 44/12 = 3.667 *ton* CO_2. In this thesis, the latter is used.

damage costs are the costs imposed on the society due to a unit increase in the emissions of different pollutants.[12] The damage cost approach follows the impact pathway approach. This approach is preferred for internalizing the external costs (Maibach et al., 2008).

Avoidance cost approach Avoidance costs are actual or imputed costs to prevent the environment deterioration until a desired extent is termed as avoidance costs (Maibach et al., 2008). The uncertainty range in the damage costs is very high (Tol, 2005; Downing et al., 2005), therefore use of the avoidance costs approach is more acceptable from a political and practical point of view and preferred for a long-term reduction target (Maibach et al., 2008; Bickel et al., 2006; Weinreich et al., 2000). As an alternative to the damage costs, this approach avoids the uncertainties to assess the damage costs by assessing the costs of avoiding CO_2 emissions. Often, these costs are also called as mitigation costs or abatement costs. The avoidance costs may vary over time and may differ from region to region because it is derived from the desired set of goals for a particular region.

1.2.2.3 Aggregation of external costs

An externality arises if an individual considers only his private costs in his mobility decision making process rather than including the external costs he may impose on others. The Marginal Social Cost (MSC) is the sum of Marginal Private Cost (MPC) and Marginal External Cost (MEC) (Walters, 1961; Turvey, 1963). Thus, the presence of an externality shows a diversion between MSC and MPC. Aggregation of these external costs amounts to a significant share of a country's Gross Domestic Product (GDP): For example[13],

(a) Creutzig and He (2009) estimate the total external costs by motorized traffic in Beijing to range between 7.5% and 15% of the city's GDP,

(b) according to Essen et al. (2011), the total external costs in the European Union (EU)-27 plus Norway and Switzerland is estimated to approximately 5 to 6% of the union's GDP,

(c) total external costs for Auckland, New Zealand amounts up to 2.23% of region's GDP in 2001 (Jakob et al., 2006).

1.2.3 Heterogeneous traffic

Heterogeneous traffic is the traffic stream in which more than one type of vehicles with different static and/or dynamic characteristics are present. Heterogeneous traffic is widespread. However, the degree of heterogeneity is non-uniform; it is significantly higher in the industrializing nations than in the industrialized nations. The pace of urbanization is highest for Asia (United Nations, 2014). Urban roads in most of the Asian cities are full of heterogeneous vehicles which can be differentiated based on their static and dynamic characteristics:

[12] Use of "Dose-response function" to estimate the damage costs is quite common and it is followed by an air dispersion model to estimate the exposure of local pollutants (Zhang et al., 2004, pp. 321-343).

[13] The estimates differ from study to study and region to region due to adopted methodology and factors for estimation and underlying assumptions.

a) **Static characteristics:** Static characteristics include the physical dimension (length, width, height) and weight of the vehicle. The vehicle could be as small as a *bicycle* (or cycle)[14] and as big as a multi-axle truck.

b) **Dynamic characteristics:** The capability to accelerate and decelerate, speed, power are dynamic characteristics.

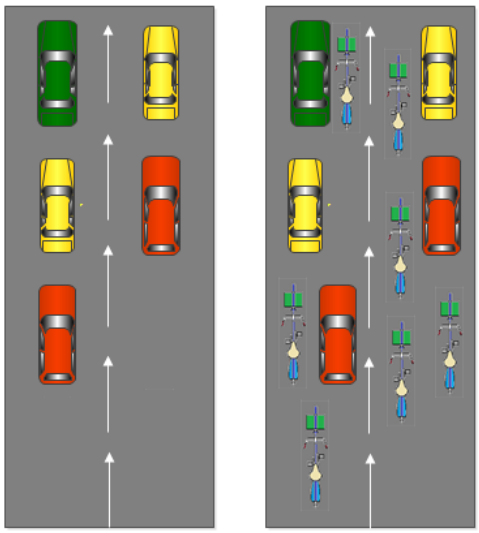

Figure 1.1: A schematic representation of nearly homogeneous (left) and heterogeneous traffic (right) (vehicle types and figures are not to scale; Agarwal, 2012).

Fig. 1.1 shows a schematic representation of homogeneous (left) and heterogeneous traffic (right) conditions. In the former case, vehicles follow each other and stay behind the queued vehicle. On the contrary, on the right, the traffic stream has parallel/staggered vehicles in the same lane which depicts the absence of lane discipline. Motorized (car, motorbike/motorcycle, bus, auto-rickshaw, etc.) and non-motorized (bicycle/bike, cycle-rickshaws, animal carts, etc.) vehicles share the common road space. Consequently, the traffic flow is interrupted. Both, static and dynamic characteristics affect the driving behavior and consequently, the traffic flow; for instance, motorbike and bicycle occupy almost same space on the road but the former has higher acceleration and speed than the latter. Similarly, a heavy vehicle has poorer acceleration and speed capabilities and thus takes more time to maneuver, and occupies more space on the road than a car.

1.3 Problem definition

As illustrated before in Sec. 1.2.1, urbanization and transport externalities are inter-linked. The presence of negative externalities is known to result in inefficiencies unless the underlying external costs are reflected in the market prices for mobility, i.e., considered in

[14] Many studies use the term *bike* to represent the bicycle which is a common practice in the European context. However, the term bike is also used to represent motorized two-wheelers (motorcycles/motorbikes) in most of the industrializing nations, therefore, this thesis uses the term *bicycle* to refer non-motorized two-wheeler.

people's mobility decisions. Eventually, these inefficiencies can lead to market failure and losses in system welfare.

One option in order to correct the market failure and reduce the efficiency loss, is to aim for behavioral changes of people. From the economic literature, it is known that internalizing external effects by a tax can change behavior and, thus, can increase the welfare of the society (Pigou, 1920). Ideally, all external costs need to be included in the tax; however, from a global perspective, the rise in the CO_2 emissions has gained more attention due to its irreversible climate change effects. To abate it, the international communities agree to set an aim to hold the increase in the average global temperature to well below 2° Celsius (European Commission, 2011; FCCC/CP/2015/L.9/Rev.1, 2016). EU transfered this to a sub-aim of cutting global GHG emissions by at least 20% until 2020 with respect to 1990 levels (2008/101/EC, 2008). The pace of urbanization and motorization in the industrializing nations could offset the projected course for holding the increase in the average global temperature (Wright and Fulton, 2005). On top of this, the presence of mixed traffic conditions and underlying driving behavior impose another layer of difficulty to estimate and monetize the external costs.

The presence of heterogeneous traffic conditions adversely affects the performance of traffic streams due to complex maneuvers and intensifies the transport externalities. The driving behavior in heterogeneous traffic conditions is different than it is observed under homogeneous conditions (e.g., see Fig. 1.1). Modeling of such traffic conditions is complex and a challenge for traffic planners because homogeneous traffic flow models or conventional car following models are not applicable.

The use of simulations is becoming quite common to replicate complex transport systems, to model traffic flow, to predict the user behavior, to forecast the future possible trends, to evaluate the various policy measures and to visualize the traffic. However, the rapid – often unplanned – urbanization brings serious concerns in terms of computational efficiency for simulating travel demand of such large systems. A variety of simulators exists, which can be differentiated based on model abstraction, reliability of the results, etc. Many such simulators use iterative algorithms to determine a dynamic user equilibrium. However, the simulation of a whole day of traffic of a large urban network takes a lot of CPU time (Gawron, 1998). In particular, simulators with a high level of detail are resource-intensive and require high performance computing systems. Access to such systems is not very common.

1.4 Research objectives

Derived from the foregoing discussion, for this thesis, two major objectives are contemplated. These are:

1) To investigate policy measures in order to abate the transport negative externalities while considering
   a) the inter-relationship between different externalities and
   b) politically motivated goals.
2) To develop an efficient model to simulate the the mixed traffic conditions which can replicate the traffic patterns realistically.

Clearly, these objectives are not isolated, but rather interrelated by the means of requirement of a simulation framework to simulate the mixed traffic conditions and evaluation of the policy measures for a large-scale urban agglomeration. It is noteworthy that despite of the other available simulators for mixed traffic conditions (e.g.,Vissim, Manjunatha et al., 2013; SiMTraM, Mathew et al., 2013) a multi-agent simulation framework for homogeneous traffic conditions is extended to simulate the heterogeneous traffic conditions such that the extended model is still computationally efficient.

Based on the above, this thesis is split into three parts as showed in Tab. 1.1. The first two parts address and sub-categorize the two objectives. Part I tries to optimize the system using the damage costs estimates from the literature and to identify the gap between toll levels derived from environmental damage cost internalization and toll levels to achieve the political goal of 20% reduction in GHG emissions of transport sector until 2020 with respect to 1990 levels. In the former, emphasis is given on the inter-relationship between the two transport externalities – congestion and emissions – and a combined pricing scheme is proposed to internalize both externalities simultaneously. Further, Part II constitutes the simulation of traffic streams with mixed traffic conditions using an multi-agent based simulation framework. The main network loading algorithm of the simulation framework is a queue model, which is extended to introduce backward traveling holes and seepage link dynamics in order to replicate the real-world conditions mainly in the industrializing nations. In the last part, a real-world scenario of Patna, India is presented to address the both objectives together in the context of the industrializing nations. A few policy measures are proposed and investigated in order to abate the emissions externality.

In the literature, several policy measures are available which can be differentiated based on the scope of the application (short/long term), aim of the measures, etc. Timilsina and Dulal (2011) categorize the policies to abate the transport externalities into following three categories.

1) Fiscal policies – fuel/emission/congestion tax, subsidies for clean fuel and vehicles, Public Transport (PT)

2) Regulatory policies – standards for vehicle and fuel technologies

3) Planning and investment policies – land-use or urban planning, infrastructure investments.

In addition to this classification, Kickhöfer (2014, pp. 3-4) divides the different levels of political efforts in four categories ('Four E'):

1) Engineering – vehicle and fuel technologies

2) Education – change in behavior by spreading awareness

3) Enforcement – regulatory measures (e.g., speed limits)

4) Economy – fuel tax, tolls

The engineering and economy measures are the regulatory and fiscal policies from the former classification. In this thesis, fiscal policies (economy) are tested in Part I and planning policy is tested in Part III whereas rest are beyond the scope of this thesis.

1.5 Research approach

This section briefs about the research approach adopted in this thesis. A detailed description is given in Secs. 3.4 and 6.5.

1.5.1 Travel simulator

In order to simulate the travel demand in mega-cities, a simulator which can handle the large-scale scenarios is required. For this, an activity-based, multi-agent simulation framework, Multi-Agent Transport Simulation (MATSim) is chosen due to several reasons; e.g.,

a) It has a high degree of modularity which is important to integrate/develop the extensions.

b) The network loading algorithm of this framework is a queue model which controls agents at entry/exit of the link and never in between (Gawron, 1998; Cetin et al., 2003). This makes it computationally fast and therefore suitable for the large-scale scenarios.

c) It provides the dynamic locations of all the agents in the simulation which is required to identify the highly differentiated, time-dependent toll values corresponding to the emission and congestion costs.

d) The model is embedded into an iterative co-evolutionary algorithm (see Sec. 2.2.2), in which agents interact, learn and adapt to the system in general and to the price levels in particular.

Further details of the MATSim framework are provided in Ch. 2.

1.5.2 Internalization of external costs

The vehicle-specific, time-dependent external costs of emissions are calculated using the approach by Kickhöfer and Nagel (2016b) and external costs of congestion is estimated using the approach by Kaddoura and Kickhöfer (2014). These approaches are marginal cost pricing approaches which returns the time-dependent agent-specific (individual) tolls. The individual tolls are included in the decision making process of every agent and consequently, agent reacts to this by changing route, mode, time, etc. Thus, these individual toll levels change over the iterations and eventually converging to a stable traffic flow regime.

A joint internalization approach is proposed to internalize the external costs from emissions and congestion in order to capture the correlation between these two externalities. A hypothesis is defined to test that "combining the toll levels obtained from the separate pricing schemes would not yield toll levels above those of the economic optimum". The isolated and combined pricing schemes are economically assessed in order to establish the policy implications for real-world situations. Thereafter, a parametric backcasting approach is proposed to identify the necessary avoidance charge in order to achieve the political goal of 20% reduction in GHG emissions of transport sector until 2020 with respect to 1990 levels.

1.5.3 Traffic and link dynamics

The default variant of the queue model in MATSim follows First-in-first-out (FIFO). The queue model is then extended to allow passing of slower vehicle by faster vehicles (Agarwal, 2012; Agarwal et al., 2015). However, the traffic dynamics of the queue model is impractical due to the absence of the intra-link interaction i.e., space origination from leaving vehicle on the downstream end of the link is available immediately at upstream end of the link. This is overcome by introducing backward traveling holes (Charypar et al., 2007b; Eissfeldt et al., 2006) for mixed traffic conditions into the existing queue model. Further, a link dynamics – named as seepage – is added to the queue model. This is a common behavior in the industrializing nations where the smaller vehicles are in abundance. Due to higher maneuverability, the smaller vehicles do not stop at the end of the queue instead seep through the space available between the vehicles to come in front of the queue (Oketch, 2000; Asaithambi et al., 2013; Nair et al., 2011).

1.6 Thesis road-map

This thesis is organized as follows. Ch. 2 presents the travel simulators for all the experiments in the thesis. It also lists the required inputs and illustrates the mechanism of the underlying co-evolutionary algorithm. In addition to this, the chapter also briefs about different modules for re-planning.

Afterwards, this thesis is divided into three parts as shown in Tab. 1.1.

Table 1.1: Organization of the thesis.

Part I (Chs. 3 to 5) **Transport Externalities**	**Part II (Chs. 6 to 8)** **Mixed Traffic**
• Review of the policy measures to abate the transport externalities. • Policy measure: combined internalization for air pollution and congestion externalities. • Policy measure: parametric backcasting. • Real-world scenario: Munich Metropolitan Area (MMA).	• Review of the existing traffic flow models for mixed traffic conditions. • Queue model extension: with holes traffic dynamics. • Queue model extension: seepage link dynamics. • Application of the queue model extensions to a real-world scenario of Patna, India.
Part III (Ch. 9) **Integrated Scenario**	
• Scenario: Patna, India. • Scenario generation using trip diaries and traffic counts. • Calibration using Cadyts for mixed traffic. • Emission Modeling Tool (EMT) for mixed traffic conditions. • Policy measures.	

Part I contains three chapters. Ch. 3 reviews the transport literature for congestion and emission externalities. It lists several policy measures in order to abate the transport negative externalities. Ch. 4 first internalizes individual external costs (emission and congestion) and then proposes a combined pricing schemes by internalizing both external costs components simultaneously. These pricing schemes are applied to a real-world scenario of Munich metropolitan area. In Ch. 5, another policy measure is tested with aim to cut down the CO_2 emission by 20%. It is determined by what factors the damage costs should be increased in order to achieve this target.

Part II starts with the discussion of various queue models in Ch. 6. Arguments for and against the usage of the queue model are discussed in detail. It also highlights the other traffic flow models from the literature to explain the rationale behind the use of queue model in the thesis. Further, in Ch. 7, the queue model is extended by introducing backward traveling holes for both, homogeneous and heterogeneous traffic conditions. This will provide the ability to simulate and observe the intra-link interaction between the vehicles. In the Ch. 7, the queue model is extended again to allow smaller vehicles pass through the gaps between stationary vehicles (seepage). For various link and traffic dynamics, Fundamental Diagrams (FDs) are plotted to show the relationship between the fundamental variables (flow, density and speed). Several experiments are performed in Ch. 8 to apply the proposed queue model extensions. Various link and traffic dynamics of the queue model are compared in terms of the computational efficiency for different sample sizes.

Part III starts with a real-world scenario of Patna in Ch. 9. It illustrates the scenario set up and synthesis of external demand by extending Calibration of dynamic traffic assignment (Cadyts) to mixed traffic conditions. Thereafter, the calibration and validation of the scenario is presented. Based on the given modal share and traffic characteristics, a bicycle superhighway is proposed for Patna. The impact of the bicycle superhighway on the overall modal share, average speeds is evaluated. For the policy measures, the emissions are estimated by extending the Emission Modeling Tool (EMT) to mixed traffic conditions. Ch. 10 concludes the thesis and lays the way forward for future research.

Chapter 2 Overview of Simulation Framework

2.1 Context

A variety of travel simulators exists, which can be differentiated based on model abstraction, reliability of the results, etc. Many such simulators use iterative algorithms to determine a dynamic user equilibrium. However, the simulation of a whole day of traffic for a large urban network takes a lot of CPU time (Gawron, 1998). In particular, simulators with a high level of detail are resource-intensive and require high performance computing systems. Access to such systems is not very common. In this thesis, an multi-agent based simulator is used which is computationally efficient (see Sec. 8.3). This chapter provides an overview of the simulation framework and emphasizes the features briefly. Detailed information about the technical infrastructure has been published in many previous studies (e.g., Balmer et al., 2009, 2005a; Raney and Nagel, 2004, 2006; Horni et al., 2016b).

2.2 Travel simulator – MATSim

MATSim is an open-source, activity-based transport simulation framework designed to simulate large-scale scenarios (Balmer et al., 2009). It is, therefore, chosen for all simulation runs. The simulator is implemented in Java programming language (Java). It is based on the co-evolutionary principle. The MATSim cycle is explained in Sec. 2.2.2.

2.2.1 Simulation inputs

This section highlights various inputs for the simulator. In general, the input files are in the Extensible Markup Language (XML) data format. The information is entered in most cases into the International System of Units (French: Système international d'unités, SI unit).

2.2.1.1 Essential inputs

Physical boundary condition (network data), initial demand (daily plans of all individual travelers) and various configuration parameters are minimal essential inputs.

Network The road network for any scenario is essential for the simulation. It contains the physical properties of network geometry; e.g., coordinates[1] of nodes, unique node and link identifiers, link (edge, arc) length, link capacity (see Sec. 7.2), maximum speed on the link, allowed modes on the link, number of lanes, type of the link, etc.

Plans The second essential input is the travel demand in terms of daily plans of the individual travelers.[2] The daily plan of an agent is an approximate travel diary of the agent, which he/she plans to do over the day. It encodes the information about the various activities, leg (with travel mode) between two activities, departure time, etc. In general, a trip is made from one "behavioral" activity to next (e.g., home to work, work to shopping etc.). The trip typically consists of multiple legs with intervening "stage" activities (e.g, PT interaction) (see Nagel, 2016a, for an example). A MATSim plan has information about legs and trips are reconstructed by identifying the stage activities.

The whole collection of plans of all agents is also called as population. At least one plan must be assigned for each person. The maximum number of the plans in the choice set an agent is a configurable parameter, however, only one plan is marked as the *selected plan* which is executed in the mobility simulation.

Configuration A few scenario specific configuration parameters are essential for the simulation e.g., parameters related to the mobility simulation (see Sec. 2.2.2.1), scoring (see Sec. 2.2.2.2), re-planning (see Sec. 2.2.2.3), etc., (see Horni and Nagel, 2016, for more details about inputs and configuration).

2.2.1.2 Optional inputs

Apart from the essential inputs, there are several other inputs which are used depending on the requirements of the scenario; e.g., counts, public transit schedule, facilities, vehicle type data, emission data, etc. For instance, vehicle type data is only required to simulate heterogeneous traffic, emission data is essential while estimating and/or internalizing the external costs for emissions. These additional inputs are also passed to the configuration of the simulation.

2.2.2 MATSim cycle

The network loading algorithm of the simulation framework is embedded into an iterative co-evolutionary algorithm (Balmer et al., 2009) in which every agent learns and adapts to the system. This process is composed of the following three steps:

2.2.2.1 Mobility simulation – Mobsim

In the first step, daily plans of all individuals are loaded on the network simultaneously, therefore this step is also called as plans execution. There exists two main mobility simulations (mobsims), namely QSim and JDEQSim (Waraich et al., 2009), however, a configurable external mobsim can also be used. The default network loading algorithm

[1] All coordinates must be converted to a common system e.g., "European Petroleum Survey Group (EPSG)" code. This helps in visualization using external applications.

[2] In the simulation, individual traveler is referred to as an 'agent'.

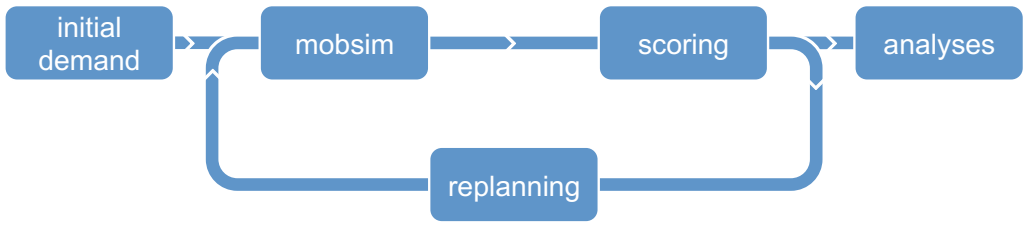

Figure 2.1: MATSim cycle (Horni et al., 2016a).

in MATSim is so called queue model (QSim; Gawron, 1998; Cetin et al., 2003), which can simulate the large-scale scenarios in reasonable computation time. By default, the queue model in the simulation framework respects the FIFO order in which the traffic dynamics are modeled with the waiting queues. The JDEQSim is a Java reimplementation of an event-based parallel queue simulation called DEQSim (Charypar et al., 2007a,b). The basic implementation methodology of the queue model (QSim) and other proposed extensions are elaborated in detail in Ch. 7.

2.2.2.2 Plans evaluation – Scoring

A econometric utility is assigned to each plan in order to model the choice of different routes and modes. This utility (or score) is evaluated using a utility (or scoring) function which indicates the performance of the plan. A plan's utility (S_{plan}) is represented by:

$$S_{plan} = \sum_{q=0}^{N-1} S_{act,q} + \sum_{q=0}^{N-1} S_{trav,mode(q)} \tag{2.1}$$

where N is the number of activities, $S_{act,q}$ is the utility for performing an activity q and $S_{trav,mode(q)}$ is the (typically negative) utility for traveling to the activity q. In short, the utility earned from performing an activity is given by[3]

$$S_{act,q} = \beta_{dur} \cdot \ t_{typ,q} \cdot \ln(t_{dur,q}/t_{0,q}) \tag{2.2}$$

$$t_{0,q} = t_{typ,q} \cdot \exp(\frac{-10}{\frac{t_{typ,q}}{1h} \cdot p}) \tag{2.3}$$

where $t_{dur,q}$ and $t_{typ,q}$ are actual and typical durations of the activity q, respectively. β_{dur} is the marginal utility of activity duration (also called as marginal utility of activity performing). $t_{0,q}$ is the minimal duration, which essentially has no effect as long as dropping activities are not allowed. The p is designed such that all activities with the same value

[3]See Charypar and Nagel (2005) and Nagel et al. (2016a), Section 3.2, for a more detailed description.

of p result in the same utility value ($= 10 \cdot \beta_{dur}$) at their typical durations.[4]

The mode-specific direct utility from traveling by any mode is described by (Nagel et al., 2016a, pp. 27–29):

$$\begin{aligned} S_{trav(q)} = C_{mode(q)} + \beta_{trav,mode(q)} \cdot t_{trav,q} \\ + (\beta_m \cdot \gamma_{d,mode(q)} + \beta_{d,mode(q)}) \cdot d_{trav,q} \end{aligned} \tag{2.4}$$

where $t_{trav,q}$ and $d_{trav,q}$ are the travel time and distance between activity q and $q+1$. $C_{mode(q)}$ is the Alternative (mode) specific constant (ASC), $\beta_{trav,mode(q)}$ is the marginal utility of traveling by mode $mode(q)$, β_m is the marginal utility of money, $\gamma_{d,mode(q)}$ is the mode-specific monetary distance rate and $\beta_{d,mode(q)}$ is the marginal utility of distance.

2.2.2.3 Plans re-planning

After executing and scoring the plans, re-planning is performed in which a new plan is created (plan innovation) or a plan is selected from the choice set (plan selection). In the former, a new plan is generated for a configurable predefined share of agents. The new plan is generated by modifying an existing plan with respect to the predefined choice modules. Several innovative choice dimensions are available e.g., Mode Choice Module (MCM), Route Choice Module (RCM), Time allocation mutator Module (TAMM), etc. The new plan is then executed in the next iteration.

Route choice module This is the most common re-planning strategy in which a time-dependent implementation of Dijkstra algorithm (Dijkstra, 1959) is used. The shortest path is calculated based on the link travel time and other generalized costs (if any). The travel time is computed from the last iteration of the simulation, aggregated into configurable time bins (typically 15 Minutes ($mins$)) and then used as the generalized cost of the link in network graph (see Balmer, 2007; Jacob et al., 1999, for more details). The new route is assigned to the leg of the agent's plan, and then this plan is executed in the mobility simulation.

Mode choice module This module is categorized in three parts.

[4]Simplifying Eqs. 2.2 and 2.3 and using $p = 1$, the $S_{act,q}$ can be written as:

$$S_{act,q} = \beta_{dur} \cdot 10 \cdot 1h + \beta_{dur} \cdot t_{typ,q} \cdot \ln(t_{dur,q}/t_{typ,q}) \Rightarrow S_{act,q}\Big|_{t_{dur,q}=t_{typ,q}} = \beta_{dur} \cdot 10h$$

i.e., all activities at their typical durations ($t_{typ,q}$) will have same utility of performing. Therefore, it is named as *uniform* computation. This setting is used throughout this thesis for consistency. Recently, as an alternative a *relative* approach was introduced, in which $t_{0,q}$ is defined as follows (Nagel et al., 2016b, pp. 538-539):

$$t_{0,q} = t_{typ,q} \cdot \exp(\frac{-1}{p})$$

such that the utility of performing for activity q at their typical duration depends on the typical duration of the activity q. The relative approach would be the preferred approach in future.

$$S_{act,q} = \beta_{dur} \cdot t_{typ,q} + \beta_{dur} \cdot t_{typ,q} \cdot \ln(t_{dur,q}/t_{typ,q}) \Rightarrow S_{act,q}\Big|_{t_{dur,q}=t_{typ,q}} = \beta_{dur} \cdot t_{typ,q}$$

a) `ChangeSingleTripMode` The travel mode of one leg in an agent's plan is randomly chosen from a given list of modes while making sure that new mode is different than existing mode.

b) `SubtourModeChoice` In this module, the travel mode of a sub-tour is changed randomly. In addition to that, this module ensures that the chosen mode is available at the activity location.

c) `ChangeTripMode` This module is same as `ChangeSingleTripMode` with the sole difference that in this module, the travel modes of all trips in an agent's plan are randomly chosen from a given list of modes (see Rieser et al., 2009; Grether et al., 2009, for more details).

Afterwards, for the new mode, a new route is assigned to the corresponding leg of the agent's plan, and then this plan is executed in the mobility simulation.

Time allocation mutator module This module is responsible for modifying the departure time and/or activity duration of an activity for the selected agent (see Balmer et al., 2005a, for more details). The new time is randomly chosen between a so-called *time mutation range* according to the uniform distribution. The default value for the configurable time mutation range is set to $[-2h, +2h]$.

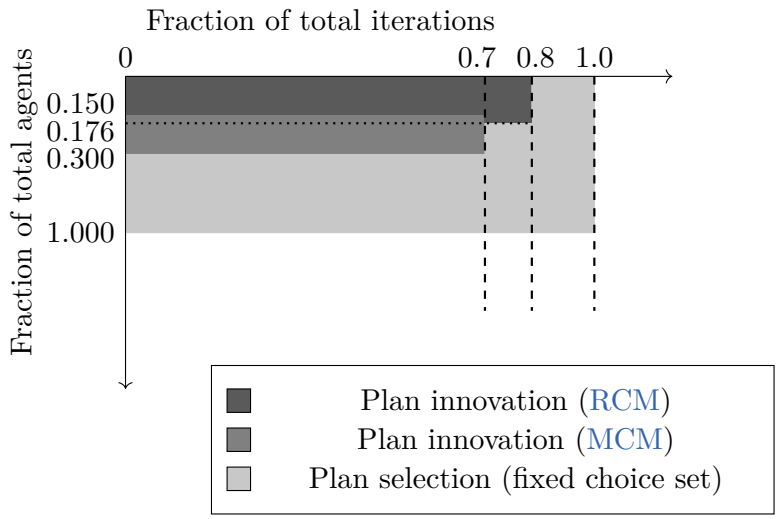

Figure 2.2: An illustration of re-planning over iterations.

Innovation switch-off The plans innovation process continues until a fixed number of iterations which is a configurable parameter. A brief illustration of re-planning is given in Fig. 2.2. In this, 15% of the agents are allowed to change the mode until 70% of the iterations, another 15% of the agents are allowed to change the route until 80% of the iterations. For each innovative module, a weight is assigned and the weights of all innovative modules are converted to probabilities. In this example, after 70% of the iterations, the weights are 0.15 and 0.7 which are re-scaled to probabilities as 0.176 ($= 0.15/(0.15 + 0.70)$) and 0.824 ($= 0.7/(0.15 + 0.70)$) respectively. The rest of the agents, and after 80% of the iterations all agents, select a plan from their generated choice sets.

Plan selection The choice set of a person can have n number of plans which is a configurable parameter. However, exactly one plan is marked as selected which will eventually be executed in the next iteration. During plans innovation, one of the plans from the choice set is modified as explained above, added to the choice set and marked as selected.[5] For the agents which do not undergo the innovation, one of the plans from the choice set is selected to execute in the next iteration. A plan could be selected using several strategies (e.g., `KeepLastSelected`, `BestScore`, `SelectExpBeta`, `ChangeExpBeta`, `SelectRandom`, etc.). In all experiments of this thesis, the plan selection is performed according to a probability distribution which converges to Multinomial Logit (MNL) model (i.e., `ChangeExpBeta`; Nagel and Flötteröd, 2012).

By repeatedly performing the steps above, an iterative process is initiated which results in the stabilized simulation outputs.

2.2.3 Simulation outputs

By default, MATSim generates some output to monitor current progress e.g., log files, score statistics, leg histograms, etc. Every action in MATSim is recorded as an event (e.g., `ActivityEndEvent`, `PersonDepartureEvent`, `PersonEntersVehicleEvent`, `VehicleEntersTrafficEvent`, `LinkLeaveEvent` ... `ActivityStartEvent`; see Figure 2.2 in Rieser et al., 2016) and then optionally written at the end of iteration. The event file is then used for post-processing and advanced analyses.

2.3 Summary

An activity-based transport simulation framework is used for all the simulation experiments. The main network loading algorithm of the simulator is a computationally efficient queue model which makes it possible to simulate large-scale scenarios with different sample sizes. It provides the dynamic locations of all agents in the simulation. This depicts the microscopic nature of the simulator and is useful to test the decision making process of individual travelers using co-evolutionary algorithm.

[5] If maximum number of plans in the choice set of a person is reached, the worst plan is removed from the choice set.

Part I

Transport Externalities

Chapter 3

Literature Review of Transport Externalities

3.1 Context

In last few decades, due to unplanned and inadequate infrastructure, the urbanization process has increased the dependency on road transport which results into high vehicle usage (see Sec. 1.2). It results into higher network densities, longer travel time, higher fuel consumption, etc. Eventually, the pollution levels are rising which affect the health conditions adversely. Congestion, air pollution, noise pollution, accidents, etc., are some examples of the undesirable by-products of urbanization. These are grouped as transport externalities and can account to significant share of GDP (see Sec. 1.2.1).

In transport economics, about a century ago, Pigou (1920) and Knight (1924) propose a pricing mechanism to correct the market failures. These market failures emerge due to the exclusion of the transport externalities in the behavioral decision making process of individual travelers.

In the more general transport literature, several policy measures are available, which can be differentiated based on their motives, scope of the applications, etc. A few important policy measures are discussed in this chapter. Subsequently, two pricing schemes are proposed and applied to a real-world large-scale scenarios of Munich metropolitan area in the Chs. 4 and 5. The content of this part is loosely integrated from Agarwal and Kickhöfer (2015, 2016).

3.2 Policy measures

With the recent advances in the technology, there are several policy measures that are helpful in abating the transport externalities – in particular emission and congestion external costs – at various scales in long and short term. This chapter compiles most of the policy measures in different categories (see Tab. 3.1) and are discussed next.

3.2.1 Traffic restrain measures

There are many examples available in the transport literature, where different kind of traffic-restrain measures were successfully applied. E.g., in 1970, the private car users

Table 3.1: Different measures to improve the air quality and/or reduce the congestion externality.

Measures	Examples	Studies
Traffic restrain measures	restrict private vehicles inside city, speed restriction, odd-even car restriction scheme, bus only lane, dropping a lane, etc., parking policies	Elmberg (1972), Buehler and Pucher (2011), Zhou et al. (2010), Cai and Xie (2011), Fernandes et al. (2014), Madireddy et al. (2011), Qu et al. (2003), Ghafghazi and Hatzopoulou (2014), Basso et al. (2011), Calthrop et al. (2000), and Wall (2011)
Traffic control measures	traffic signal optimization, integration with emission or fuel consumption models	Li et al. (2004), Osorio and Nanduri (2015a,b), and Madireddy et al. (2011)
Vehicle and/or fuel technology measures	use of hybrid, hydrogen, electric vehicle, fuel cell vehicles, bio fuels, etc., use of ethanol	Romm (2006), Leong et al. (2002), and Gajjar and Mondol (2015)
Isolated road pricing measures	cordon toll, carbon/fuel tax, marginal emission pricing, exposure toll	Daniel and Bekka (2000), Beevers and Carslaw (2005), Kickhöfer and Nagel (2016b), Kickhöfer and Kern (2015), Rotaris et al. (2010), and Parry et al. (2007)
Integrated road pricing measures	combined pricing for multiple externalities e.g., emission, congestion, noise, etc.	Calthrop and Proost (1998), Proost and van Dender (2001), Li et al. (2012), Wang et al. (2014), Sharma and Mathew (2011), Ferguson et al. (2011), and Aziz and Ukkusuri (2012)
Backcasting	Goal driven policies and pricing	Geurs and van Wee (2000, 2004) and Hickman et al. (2009)

were restricted in central area of Gothenburg city and satisfactory results were achieved (Elmberg, 1972). Similarly, the share of bicycle (bike) and PT trips is increasing significantly in the last three decades in Freiburg by restricting car usages, improving PT and promoting bicycle and walk modes (Buehler and Pucher, 2011). Clearly, on demand side, traffic restrain schemes help to reduce the emission levels for short term. For instance, implementation of odd and even car numbers on alternative days during Beijing Olympic games in 2008 was effective in terms of reducing short term traffic related air pollution (Zhou et al., 2010; Cai and Xie, 2011). Similarly, dropping a lane in the evening peak hours produces least average emissions among other traffic restriction measures (bus only lane, closure of the road), evaluated for an central arterial in Lisbon (Fernandes et al., 2014). However, these improvements cause rise in emissions on alternative roads.

In the transport literature, there is sufficient evidence of using and modeling parking policies with the different objectives. Calthrop et al. (2000) show that the pricing of parking and road use needs to be simultaneously determined and this eventually generates highest welfare gains. Further, the authors also show that the second-best resource cost pricing of all parking spaces produces higher welfare gains than the use of a single-ring cordon scheme. Similarly, an environmentally-linked pricing charging policy is designed for the parking fleet in Winchester (Wall, 2011) i.e., higher discounts for the vehicles with

the lower CO_2 bands and free annual permits for electric or hybrid car owners. On the application of this scheme, some positive influence on the fleet size are observed.

In some studies, it has been showed that speed limit reduction measures also help to bring down emissions on freeway (Qu et al., 2003) and on urban arterial (Madireddy et al., 2011). Basso et al. (2011) compare several different congestion management policies i.e., congestion pricing, transit subsidies, dedicated bus lanes, using numerical analysis of a simple model. The authors find that the dedicated bus lanes are better stand-alone policy than transit subsidization and congestion pricing, and the congestion pricing is marginally better than transit subsidization.

On the contrary, some measures result in higher emissions. For instance, Ghafghazi and Hatzopoulou (2014) quantify the effect of different traffic calming measures (speed humps, speed bumps, speed limit) on vehicle emission. The authors test the isolated traffic-calming measures at a corridor level and area-wide calming measures using a scenario of Montreal, Canada. Despite of a decrease in the vehicle kilometer traveled, both measures lead to a modest increase in the emissions. Similarly, in an another study by Panis et al. (2006), the authors find that the active speed management has no significant positive impacts on the emissions. The authors also suggest that in order to determine the environmental impacts of any traffic management and control policy, it requires a detailed analysis of not only the average speeds but also other aspects of vehicle operation such as acceleration, breaking, etc.

3.2.2 Traffic control measures

Many studies try to optimize the signal cycle length at an intersection in order to reduce the fuel consumption and emissions. A performance index function for optimization of the signal cycle length is defined by integrating traffic quality, fuel consumption and emissions at intersections (Li et al., 2004). The model is then applied to an intersection of Nanjing city. On application of the traffic light coordination scheme on an urban arterial, the emission reduction in the order of 10% is expected (Madireddy et al., 2011). However, this does not include the possible rebound effects in the medium to long term due to reduction in the travel times.

A stochastic microscopic traffic simulation model and an instantaneous vehicular fuel consumption model is integrated within a simulation based optimization algorithm and applied to signal control problem (Osorio and Nanduri, 2015a). The methodology is applied to Swiss city of Lausanne and reductions in the travel time and the fuel consumption is obtained. In another similar study, a meta-model is presented by combining a macroscopic analytical emission model with a microscopic simulation model. It is also applied to Swiss city of Lausanne (Osorio and Nanduri, 2015b). The signal plans derived using the proposed approach, outperform the signal plans derived by either of the microscopic or macroscopic models. The empirical analysis shows that a signal plan derived using the proposed approach provides significant monetary savings at network level and reduces the emissions at link level.

3.2.3 Vehicle and fuel side measures

In 1970, in order to control the air pollution on a national level, United States federal law had designed a Clean Air Act. Under the CAA § 201-219; USC § 7521-7554, standards for the motor vehicle emissions (in $Gram(g)/Kilometer(km)$) and fuel standards are set and tightened over time. Similarly, the main focus of EU's regulation scheme for the transport sector is on improvement of the fuel and vehicle technology, which is expected to reduce emissions significantly (see more details in Sec. 5.2). Leong et al. (2002) compare the average emission rates while using alternative fuels (gasoline blended with different % of ethanol) and vehicle technologies (different catalytic converters). The authors find that alternative fuels and technologies are able to reduce the volatile organic compounds significantly from the automobile emissions.

Romm (2006) reviews the technical literature on alternative fuel vehicles and emphasizes the need of the alternative fuel vehicles to reduce the global GHG. In this direction, initiatives across the world are taken and also some positive effects are achieved. For instance, in EU, the average emission from new cars registered in 2014 is 123.4 $g\ CO_2/km$, significantly below the 2015 target of 130 $g\ CO_2/km$ (EEA, 2015). It means that new cars will generate less emissions, however, the market penetration of these technologies will decide the overall improvements in the CO_2 levels. The possible extent of improvements from vehicle and fuel technologies are shown in a study by Gajjar and Mondol (2015). The authors consider the potential impacts of the introduction of the vehicle technology into South Africa. It has been showed that an aggressive uptake (about 56% of the total fleet) of battery/plug-in hybrid/hybrid electric vehicles will lead to about 8% drop in GHG emissions when compared to the conventional vehicles by 2030.

3.2.4 Road pricing

May (2013) reports that road pricing can contribute in reducing GHG, congestion and improving the air quality, noise levels, etc. The focus of this thesis is mainly limited to the pricing for the congestion and emission external costs.

Congestion externalities occur, since every vehicle on the network imposes costs on the other vehicles in terms of increased travel time. These costs are not compensated by any market mechanism, and are therefore not considered in the people's decisions. The theory on time allocation suggests that an affected person explicitly loses *utility from travel time* which e.g., depends on the comfort and pleasantness of the transport mode. Additionally, that person implicitly loses *time as a resource*, which could be used to perform a beneficial activity (Jara-Díaz, 2007; Börjesson and Eliasson, 2014). Exhaust emission externalities occur, since vehicular traffic emits NO_2, PM, SO_2, etc., which are the main components of the air pollution and these in turn are responsible for adverse effects on the health and living conditions.

Exclusion of these adverse effects from the people's mobility decision results in market failure. In order to correct for these market failures, planners and policy makers may look for measures which reduce the efficiency losses caused by the negative externalities. One option in this context is to aim for the behavioral changes of people which increase the efficiency of the system. For almost a century, it is known that internalizing external effects by a tax can change users' behavior and increase overall benefits (Pigou, 1920). Therefore,

many past contributions have investigated on the impact of internalizing external costs. Some studies focus on finding theoretically optimal congestion tolls (see, e.g., Vickrey, 1969; Henderson, 1974; Arnott et al., 1993a), and other studies examine the effect of the congestion pricing strategies on the emission levels (see, e.g., Daniel and Bekka, 2000; Beevers and Carslaw, 2005).

Towards practical implementation side, congestion pricing schemes have been introduced in Singapore, London, Stockholm (Eliasson et al., 2009), and Gothenburg (Börjesson and Kristoffersson, 2015). An air pollution toll has been implemented in Milan in 2008 (Rotaris et al., 2010). Even though focus and naming are rather driven by the political discussions, all pricing schemes have effects on both, the congestion and the environment. For the air pollution toll in Milan, it is found that the positive effects were decreasing over the time and in four years, exempted newer car entering the cordon area increased by 478% and commercial vehicles increased by 1400% (Beria, 2015). Percoco (2014) argues that road pricing in Milan has only limited effects on the environmental quality and congestion because of an increase in polluting vehicles (motorbikes) and non-polluting vehicles (LPG, bi-fuel and hybrid cars) which are exempted from the toll. Additionally, no significant changes in the flows of prohibited vehicles entering into the city center are observed (Percoco, 2015). Similarly, Whitehead et al. (2014) investigate the impact of congestion pricing on the demand of the new exempted energy efficient vehicles in Stockholm. They show that the demand for the exempted energy efficient vehicles increases with a stronger effect on the commuters.

Substantially less effort has been undertaken to develop exhaust emission internalization strategies. A marginal-cost based pricing scheme for exhaust emission is presented and then applied to Munich Metropolitan Area (MMA) (Kickhöfer and Nagel, 2016b). Another marginal-cost based pricing scheme for the emission exposure is presented and applied to the same scenario (Kickhöfer and Kern, 2015). The latter reports higher reductions in the emissions.

3.3 Rationale

3.3.1 Combined pricing

Very little research has focused on combined pricing schemes, even though it is well known that these different external effects of the transportation are positively correlated (see, e.g., Barth and Boriboonsomsin, 2009; Beamon and Griffin, 1999). On the contrary, with a simple example, Nagurney (2000) shows that the improvements in travel times may lead to an increase in the emissions. Thus, abating congestion and emission can, under certain conditions, turn out to be conflicting goals.

Despite the limited real-world implementations, pricing strategies offer – especially in a simulation context – a great opportunity to estimate the magnitude of potential efficiency gains and to identify and avoid possible flaws before the implementation. Especially, a thorough investigation about the interrelationship of congestion and air pollution externalities seems promising. In the literature, this potential is, however, only reflected by a relatively small number of contributions. This lack of research might be explained by the fact that the time losses (and in consequence congestion levels) can be obtained relatively

easily from the standard transport simulation tool-kits, but environmental impacts other than CO_2 require rather sophisticated (post-processing) models and the *true* marginal costs (and in consequence damage levels) are hard to obtain.

Proost and van Dender (2001) and Chen and Yang (2012) use analytical approaches with static traffic flow models; the former considers external effects of congestion, emission, accident and noise for a large-scale scenario of Brussels in Belgium, and the latter obtains Pareto system optimum link flow patterns by simultaneous minimization of travel times and emissions. Li et al. (2012) propose a stochastic, sustainable toll-design model for congestion and environment externalities with uncertainty in the demand. Wang et al. (2014) use a small test network while considering the carbon emission costs with the generalized cost of travel. In the similar direction, Ferguson et al. (2011) characterize the system performance by considering total travel time, VOC emissions, NO_x emissions and Carbon Monoxide (CO) emissions. One of them is minimized and trade-off with other is studied. Sharma and Mathew (2011) formulate a multiobjective optimization approach which minimizes emissions and travel time. The authors use a speed-dependent emission functions for various transport modes. Aziz and Ukkusuri (2012) integrates the speed-dependent CO emissions and travel time in the system optimum objective function. However, none of the study considered the detailed emission modeling in which cold and warm emissions are estimated dynamically based on the vehicular characteristics, parking duration, traveled distance, speed of the vehicle etc.

Shepherd (2008) demonstrates a method to optimize the average toll of car use for congestion, CO_2 and accident externalities. The author compared the simple constant cost models to a more complex models for CO_2 and accident costs. It has been shown that the more complex and accurate emission model gives a better and lower estimates of CO_2 than the fixed cost model. The CO_2 costs decreases by 1.8% and 3.8% for the fixed cost model and the more accurate model, respectively. This highlights the need of a more accurate emission model.

To the knowledge of the author, there exists no contribution, attempting a joint internalization of congestion and air pollution externalities in an agent-based framework with dynamic traffic flows and activity-based demand for a whole metropolitan area. This thesis attempts to close this gap by proposing a combined pricing scheme for congestion and air pollution externalities (see Ch. 4). Hence the major objectives are

a) to investigate the aggregated and disaggregated effects of the correlation between congestion and air pollution externalities on the toll levels and the agent behavior,

b) to determine the individual vehicle-specific, time-dependent toll levels that include both externalities under consideration,

c) to test a hypothesis that

> "combining the toll levels obtained from the separate pricing schemes would not yield toll levels above those of the economic optimum" ,

d) to analyze the driving forces behind the increase in the system performance of different user groups,

e) to identify the amplitude of the correlation between congestion and air pollution externalities, which allows the investigation of their isolated impact on the overall toll level, e.g., in peak and off-peak hours, and

f) to emphasize on relevant policy recommendations by deriving the corrected average cost factors per vehicle kilometer for the different user groups of the population.

3.3.2 Backcasting

In real-world politics, the focus is typically on so-called 'backcasting' approaches (Geurs and van Wee, 2000, 2004; IWW et al., 1998) rather than on marginal cost pricing strategies. The idea behind backcasting is to set the political goals, and implement a number of policy measures in order to achieve these goals towards a sustainable future transport. For example, in a study, the backcasting approach is used to achieve the 2025 CO_2 reduction targets for United Kingdom (Hickman et al., 2009) and it is shown that with the current trends, chances to achieve these targets are slim and therefore, several policy pathways are identified to help to achieve the transport CO_2 reduction targets. In another study by Banister and Hickman (2009), the authors highlight that assumed progress in the technological penetration is over-optimistic, and integration of the technological and behavioral policy interventions are required. Towards the vehicle/fuel technology, another study finds that even the highest estimates of the social cost of carbon from the literature is not able to justify the mass introduction of the low/zero emission vehicles/fuel technologies (Liu and Santos, 2015). Further, the authors accept that, possibly, these could be justified if the social cost of carbon is revised upwards. Therefore, in order to achieve the CO_2 reduction targets, the behavioral changes forced by the pricing measures are necessary. The backcasting procedure implicitly defines implementation (= avoidance/abatement/mitigation) costs and ignores the damage costs (= social costs of carbon; see Sec. 1.2.2.2) approach (see, Watkiss et al., 2005; Link et al., 2014; Maibach et al., 2008, for detailed discussion about the damage and avoidance costs).

In the light of the above, the following research questions arise which are responded to in Ch. 5.

a) To what extent pricing schemes, in particular the internalization of air pollution externalities, would contribute to the political goal, and

b) how (additional) prices would need to be set in order to reach this target or, in other words, how different the price levels of a (best-practice) damage cost approach are compared to the backcasting approach.

3.4 Research approach

As depicted in Sec. 3.3.1, this thesis proposes a combined pricing scheme to internalize the congestion and emission externalities simultaneously (see Ch. 4). Thereby, the concept of marginal social cost pricing (Turvey, 1963), is used in many previous studies to identify an optimal toll analytically (Vickrey, 1969; Arnott et al., 1993b; Lindsey and Verhoef, 2001). However, these simplified approaches are less appropriate for the large-scale scenarios with

dynamic demand which evolves differently over the space and time. The complexity increases in such scenarios and the analytical calculation of such highly differentiated tolls by the user behavior in space and time is not feasible. An agent-based simulation framework can bridge this gap: it facilitates to identify the agents who are causing externalities and to charge them with the corresponding price. For this, the activity-based, multi-agent simulation framework, MATSim, is chosen (see Sec. 2.2). The network loading algorithm of this framework is a queue model which is computationally very fast and therefore suitable for the large-scale scenarios (see Ch. 7).

3.4.1 Combined pricing

In the first step, Ch. 4 investigates the effect of congestion pricing on the emission levels, and the effect of emission pricing on the congestion levels. For this purpose, the marginal congestion pricing approach by Kaddoura and Kickhöfer (2014) and the marginal emission pricing approach by Kickhöfer and Nagel (2016b) are applied to a real-world scenario of the Munich Metropolitan Area (MMA) in Germany (see Sec. 4.4). In the second step, the two pricing approaches from above are combined in a joint pricing scheme (see Sec. 4.2.3). The outcomes are optimal emission-congestion levels for a particular case study. The methodology that is developed can, however, be applied to any number of externalities and any scenario worldwide.

3.4.2 Backcasting

The need of backcasting approach in the context of CO_2 emissions is argued in great detail in Sec. 5.2. In order to answer the research questions from Sec. 3.3.2, in the first step, the marginal cost-based pricing scheme for exhaust emissions is applied to the real-world scenario of MMA similar to the isolated pricing for exhaust emissions in Ch. 4. Further, for backcasting approach, the objective is to identify the necessary additional prices, as multiples of the original damage cost estimates, in oder to achieve the 2020 CO_2 reduction targets for MMA. Thus, the emission cost factors from the literature (Maibach et al., 2008) are increased by a multiplication factor following a parametric approach (see Sec. 5.3.2) and then these factors are applied to the MMA scenario. Further analysis is provided in Sec. 5.5.

Chapter 4

Policy Measure : Combined Pricing

4.1 Overview

As discussed previously in Ch. 3, there are several measures to abate the increasing transport negative externalities. The choice of a measure is driven by different objectives (e.g., reduce congestion, improve traffic conditions, reduce emissions, etc.) depending on the scenarios, however, it has been showed that the transport externalities are correlated. In this research direction, this chapter proposes a joint internalization approach to include the cost of multiple transport negative externalities. In this thesis, only emissions and congestion externalities are considered. The joint internalization is applied in an agent-based framework with dynamic traffic flows and activity-based demand for a real-world MMA. This chapter is an edited version of Agarwal and Kickhöfer (2015, 2016).

4.2 Pricing negative externalities

This section first demonstrates the methodology used to calculate the congestion and emission costs. Furthermore, the process of internalization of these external costs into the user's decision making process is presented. For illustration purpose, a small example is displayed.

4.2.1 Congestion cost

Traffic congestion is a common problem on major urban arterials. Individual travelers impose delay on others; these delays create negative externalities if unpaid or unaccounted into the behavioral decision making process of the individual traveler. To identify the delays for each agent, the queue model in MATSim facilitates the flexibility to identify the link enter, link leave times of agents (see Sec. 7.2). Hence, it keeps the track of agents which is essentially required to find the delay causing agents and affected agents.

Delay Delay is in this thesis defined by the difference between the actual travel time on a link and the link's free speed travel time ($t_{l,free}$; see Eq. 7.1). That is, delays are calculated on a per-link basis and not for the entire routes. Further, in this thesis, only

recurrent delays (a normal weekday traffic congestion) are considered, i.e., delays due to accidents, bad weather, special events, etc., are not considered.[1] The tool to compute individual delays and then to internalize those by a marginal social cost pricing scheme in the MATSim framework is taken from Kaddoura and Kickhöfer (2014) and briefly described below.

Delay computation This approach tracks routes and travel times of all agents to calculate the time-dependent, agent-specific delay on each link. The delay is computed whenever an agent is leaving a link. The flow capacity ($c_{l,flow}$) restricts the outflow i.e., number of vehicles that can leave a link and thus, a demand higher than flow capacity leads to bottleneck congestion. In order to move an agent across a node, the minimum time gap between two consecutive agents cannot be less than the minimum allowed time headway i.e., $\tau_{l,min} = \frac{1}{c_{l,flow}}$. Thus, if two agents arrive on the downstream end of the link at a time gap less than $\tau_{l,min}$, delay occurs. The delay results from agents who have left that link before the delayed (or affected) agent and who are using capacity and blocking the link. Thus, these downstream agents (agents which left first and consumed the flow capacity) are named as 'causing agents'.

In the agent-based framework, causing and affected agents can then be identified. The former can therefore be charged with a monetary equivalent of the sum of marginal delays they have caused to others. The marginal delay is hereby defined as the maximum time for which an agent can block a link i.e., inverse of the flow capacity of a link. Since congestion is – in contrast to emissions – inherent to road traffic, the behavioral parameters can be used to convert delays into monetary units. This is done using the approximate average VTTS of the car mode.[2] An example, to demonstrate the procedure numerically, is provided in Sec. 4.3.

4.2.2 Emission cost

The Emission Modeling Tool (EMT) was initially developed by Hülsmann et al. (2011) and further improved and extended by Kickhöfer et al. (2013). The tool is coupled with the MATSim framework. Currently, emissions are calculated for free flow and stop&go traffic state.[3] The total emissions consist of cold and warm emissions.

[1] The non-recurrent delay can be as high as 60% of the total delay (Lindley, 1987); however, according to Hall (1994), the share of the non-recurrent delay would not be so high if highways are not congested on the first place.

[2] The VTTS is defined as the individual willingness-to-pay for reducing the travel time by one h. For linear utility functions, it is the ratio of the marginal utility of travel time and the marginal utility of money. The former is the sum of the disutility for traveling ($\beta_{trav,mode(q)}$) and the negative utility of time as a resource ($-\beta_{dur}$). Please note that the person-specific VTTS in MATSim can vary significantly with the time pressure which an individual experiences. This is because of the non-linear utility function for performing activities, influencing the actual value of β_{dur}.

[3] Though Handbook on Emission Factors for Road Transport (HBEFA) provides emission levels for four traffic states, namely, free flow, heavy, saturated and stop&go, the emissions are estimated for free flow and stop&go traffic states only because: a) The network loading algorithm of MATSim is a simple queue model (see Sec. 7.2) which provides the locations of the vehicles during entry/exit of the link and nowhere else on the link. The approximate location of start of the stop&go traffic state is estimated using free flow speed, actual speed, stop&go speed and link length (Kickhöfer, 2014, p. 41). b) The differences between the emissions during first three traffic states are marginal whereas the difference between the emissions during free flow and stop&go traffic states is significant.

1) Cold emissions or cold-start emissions are emitted during warm-up phase of the vehicle and essentially depend on parking duration, distance traveled, and vehicle characteristics.

2) Warm emissions or hot-start emissions are emitted during driving and essentially depends on the engine type, road category and speed of the vehicle.

The vehicle characteristics (vehicle type, age, cubic capacity, fuel type), engine type, road category are taken from the initial inputs whereas the dynamic attributes (parking duration, distance traveled and speed of the vehicle) are determined from the simulation at the end of each iteration. Thereupon, the cold and warm emissions (in g) for each agent on each link are calculated using the HBEFA database[4] as follows:

1) **Cold emissions:** The cooling of the vehicles is determined by the parking duration (in 1 h time bins up to 12 h and assumed as fully cooled down for the parking durations longer than 12 h). The cold emissions are generated up to a distance of 2 km, depending on the cool-down time. This information together with the vehicle characteristics is used to look up the HBEFA emission factors[5] (in g). Categories of 0-1 and 1-2 km are used to distribute the cold emissions on the links after the vehicle has been started.

2) **Warm emissions:** The vehicle-specific travel time on a link derived from the simulation is used to identify the different traffic states (free flow, stop and go, or both). Similar to the cold emissions look up, the information about traffic states, road type and vehicle characteristics are used to look up the HBEFA emission factors (in g).

Furthermore, Kickhöfer and Nagel (2016b) develop a method to calculate the time-dependent, vehicle-specific emission tolls. In that method, the vehicle- and link-specific time-dependent emissions obtained from the EMT, are converted into monetary units (emission costs) using unit damage costs (see Sec. 1.2.2.2). The uncertainty range in the estimation of the unit damage costs is very high (Tol, 2005; Downing et al., 2005) and these costs rise over time (Watkiss et al., 2005; Clarkson and Deyes, 2002). However, for this thesis, the unit costs are taken from Maibach et al. (2008) and from here onwards called emission cost factors (see Tab. 4.1).

Table 4.1: Emission cost factors. Source: Maibach et al. (2008).

Emission type	Cost factor (EUR/ton)
Carbon Dioxide (CO_2)	70
Non-Methane Hydrocarbons ($NMHC$)	1,700
Nitrogen Oxides (NO_x)	9,600
Particular Matter (PM)	384,500
Sulfur Dioxide (SO_2)	11,000

[4]For the test example and for the MMA scenario, HBEFA version 3.1 is used.
[5]The HBEFA does not provide cold start emissions for heavy goods vehicles, therefore, using values corresponding to an average passenger car.

4.2.3 Internalization

Internalization is the process by which the external effects are included into the behavioral decision making of the individuals by setting prices according to their MECs. By default, the MATSim utility function only incorporates the MPC which correspond to spending time and money for traveling to the planned activities (see Eqs. 2.1 and 2.4). The MSC are the sum of MPC and MEC (see, e.g., Walters, 1961; Turvey, 1963).

Following Eq. 2.4, the simplified mode-specific direct utility from traveling by car or PT for the case study of Munich is written as:

$$\begin{aligned} S_{car(q)} &= \beta_{trav,car(q)} \cdot t_{trav,q} + \beta_m \cdot \gamma_{d,car(q)} \cdot d_{trav,q} \\ S_{PT(q)} &= C_{PT(q)} + \beta_{trav,PT(q)} \cdot t_{trav,q} + \beta_m \cdot \gamma_{d,PT(q)} \cdot d_{trav,q} \end{aligned} \tag{4.1}$$

The MEC for congestion and emissions are computed according to Secs. 4.2.1 and 4.2.2 respectively, and subsequently, considered in the utility-based learning cycle of MATSim as follows:

$$S_{car(q)} = \beta_{trav,car(q)} \cdot t_{trav,q} + \beta_m \cdot (\gamma_{d,car(q)} \cdot d_{trav,q} + \Delta m_q) \ . \tag{4.2}$$

where, Δm_q is the vehicle-specific, time-dependent tolls corresponding to the external costs.

At this point, it is important to note that the individual toll levels change over the iterations, converging to a stable point once the traffic flows stabilize. This is due to the fact that the presented approach is embedded into the iterative co-evolutionary algorithm (see Sec. 2.2.2): In the first iteration, the process starts with charging agents for the delay and the emissions they caused. This is simply the sum of both effects, and on a crowded street segment the toll levels are high. As a reaction, some agents opt for other alternatives (mode/route) in the next iteration to improve their overall utilities. This selection between alternatives follows a probability distribution which converges to a multinomial logit model (Nagel and Flötteröd, 2012). In consequence, the toll levels will drop and attract more agents in the subsequent iteration, yielding again higher tolls. That is, over the iterations, the simulation finds a toll level which considers the correlation between the two externalities under consideration without explicitly calculating the correction factors.

4.3 Test example

This section provides a small example in order to illustrate the computation of the time-dependent vehicle-specific congestion and emission tolls.

Set up Each link in Fig. 4.1 is 100 $Meter(m)$ long and only one agent every 4 $Second(sec)$ is allowed to move to the next link i.e., marginal delay (τ_{min}; see Sec. 4.2.1) will be 4 sec. Two agents depart at $t = 0$ by car and reach the end of the link simultaneously at $t = 4$.[6]

[6] Please note that, in order to improve the computational efficiency, the queue model controls agents only at link entry/exit and never in between (see Sec. 7.2 for further details about the queue model). Therefore, both agents can reach at the end of the link simultaneously, however, agents will leave the link while respecting the flow capacity (outflow) of the link and storage capacity of the downstream link.

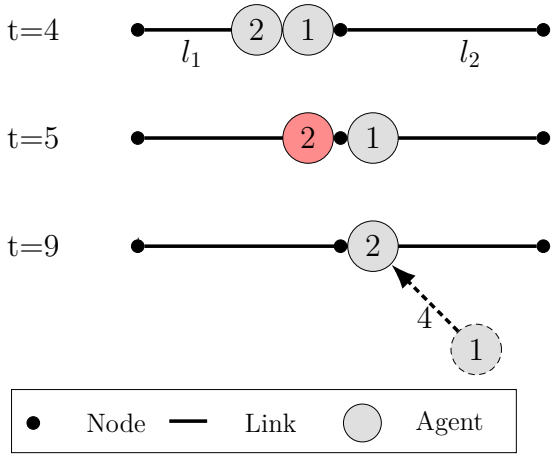

Figure 4.1: A small test example to compute the external costs. The delayed agent is shown in red.

Congestion costs Since the free speed travel time on the link (l_1) is 5 *sec*, both agents would like to leave the link (l_1) at $t = 5$. However, the flow capacity only allows agent 1 to leave at $t = 5$ and then agent 2 to leave at $t = 9$. That is, agent 2 has to wait for 4 *sec* on the first link with agent 1 being responsible for that delay. Hence, agent 1 will be charged with the monetary equivalent of 4 *sec*, yielding to an individual toll of 4 $sec \cdot VTTS_{car} = 1.4$ $Eurocent(EURct)$. Though, there are only two agents in the example, the procedure is same if there are more agents on the link l_1. For instance, if there are N agents in the queue on the link l_1, the delay of the Nth agent is charged to all causing agents until all causing agents are identified or all delay has been charged, i.e., charging in the order $N - 1^{th}$, $N - 2^{th}$, ... 2nd, 1st with a maximum delay of 4 *sec* (= inverse of flow capacity) per agent.

Emission costs Emissions are calculated for both agents on both links as described in the Sec. 4.2.2. It is assumed in this case that both vehicles have fully cooled down, i.e., experienced a parking duration of minimum 12 h. Thus on the first link for the first vehicle, parking duration, distance traveled and average speed are 12 h, 100 m and 20 m/sec (= 100 m/5 *sec*), respectively. The same calculation for the second vehicle yields 12 h, 100 m and 11.11 m/sec (= 100 m/9 *sec*). For illustration purpose, the two vehicles are assumed as identical passenger petrol cars with 4-stroke engines. The links are assumed as urban city roads with speed limit of 60 km/h. Using vehicle characteristics together with this data returns the cold and warm emissions from the HBEFA database. These emissions are then converted into monetary units using the emission cost factors in Tab. 4.1. This yields an individual toll of 0.9 *EURct* for the cold emissions and 0.12 *EURct* for the warm emissions for the first vehicle on the start link. The same numbers for the second vehicle are 0.9 *EURct* and 0.14 *EURct*, respectively. Clearly, as expected, due to delay, the warm emissions for the second vehicle is higher than for the first vehicle.

4.4 Case study : Munich

This section illustrates the set up and the pricing schemes for the real-world case study of the MMA in Germany. Fig. 4.2 shows the territorial boundary and road network of Munich and MMA.

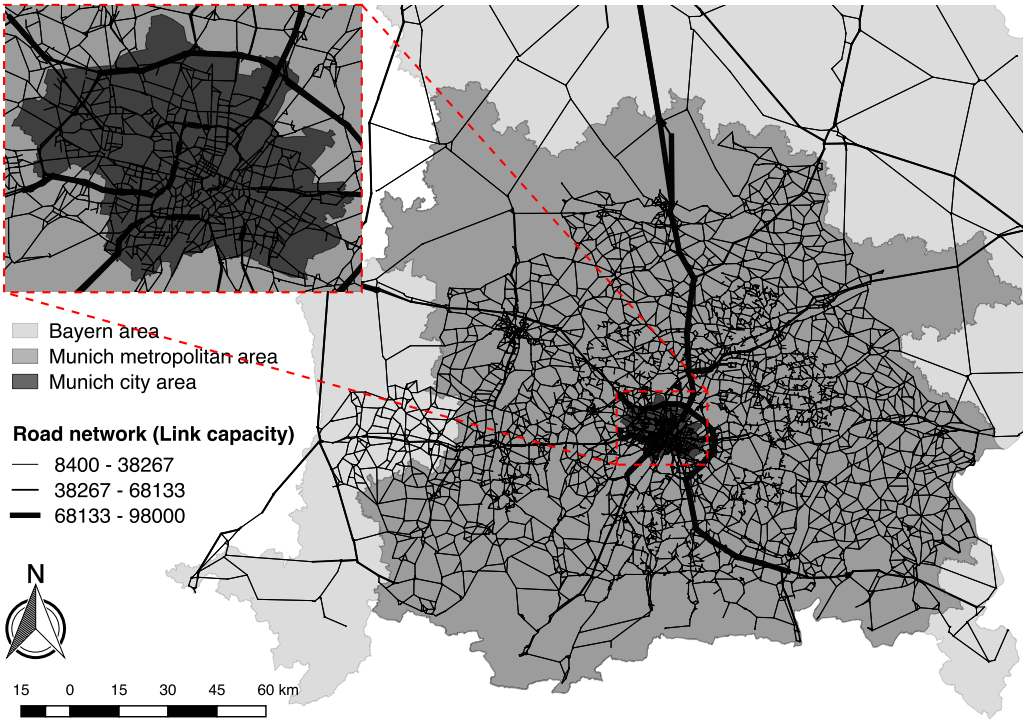

Figure 4.2: Road network of Munich and MMA. Inset shows the Munich map at a higher resolution. The link capacities are for 24 h period.

4.4.1 Input

The initial scenario is taken from Kickhöfer and Nagel (2016b) and modified afterwards, as will be described later in this section.

Network Network data was provided by municipality of Munich (RSB, 2005) in the form of Verkehr In Städten – UMlegung (VISUM) data. This is converted into a MATSim network, which contains 17,888 nodes and 41,942 links. The road network is shown in Fig. 4.2.

Plans The travel demand for the MMA is based on three different data sources (see Tab. 4.2), resulting in four sub-population (or user) groups: urban, commuters, reverse commuters and freight. The number of individuals and travel mode for each user group is shown in Tab. 4.2. A realistic activity-based demand for each of the sub-population is created as follows.

1. Inner urban travel demand is synthesized using detailed survey data based on *Mobility in Germany* (MiD 2002, Follmer et al., 2004). The synthetic demand contains 1,424,520 individuals with detailed vehicle information.

2. Commuters and reverse commuter trips are modeled using data provided by Böhme and Eigenmüller (2006), which contains about 0.5 M individuals, out of these about 0.3 M are commuters and the remaining are reverse commuters.

3. About 0.15 M freight trips are created (0.15 M agents with one commercial trip) from data provided by the German Ministry of Transport (ITP and BVU, 2007).

Table 4.2: Key indicators for user groups of Munich Metropolitan Area (MMA).

User group	Data source	No of individuals [M]	Travel modes
urban	MiD 2002, Follmer et al. (2004)	1.4	car, PT, bicycle, walk,ride
commuter	Böhme and Eigenmüller (2006)	0.3	car, PT
rev. commuter		0.2	
freight	(ITP and BVU, 2007)	0.15	truck

The commuters and reverse commuters are coupled together and named as (rev.) commuters here onwards unless otherwise stated. The urban travelers are confined to Munich city area only, whereas, MMA is also populated by (rev.) commuters and freight trips. In the simulation, the urban travelers use car, PT, bicycle, walk, and ride as transport modes, whereas (rev.) commuters use only car or PT. The freight trips are assumed to use only trucks. PT, bicycle, walk, and ride trips are in the case study assumed to run emission free and without capacity constraints. Therefore, there is no emission and congestion externality for such trips, and thus, such travel modes are grouped together as *non-car* travel modes.

Overall, for computational performance reasons, 1% of total population is used for the present case study. Agents are categorized among three subpopulations (user groups) namely urban, (rev.) commuter, and freight and therefore, results are discussed based on this classification. Tab. 4.3 lists the behavioral parameters used for the case study. In contrast to scenario in Kickhöfer and Nagel (2016b), this chapter, considers two ASCs for the urban and (rev.) commuters user groups (see Sec. 4.4.2).

Choice dimensions As a reaction to the policy cases (see Sec. 4.4.3), new choice sets are generated in the iterative loop of MATSim according to the following rule (see Fig. 4.3): In each iteration,

a) 15% of the total agents are allowed to change their route and

b) 15% of the total agents are allowed to change their travel mode from car to PT or from PT to car.[7]

[7] An urban traveler can switch mode between car and slower PT (speed 25 km/h) and similarly, (rev.) commuters can switch mode between car and faster PT (speed 50 km/h). See Sec. 4.4.2 for details on the slower and faster PT.

Table 4.3: Behavioral parameters.

Parameter	Value	Unit
Source: Kickhöfer (2014)		
Marginal utility of activity duration (β_{dur})	+ 0.96	$util/h$
Marginal utility of traveling by car ($\beta_{trav,car}$)	– 0.00	$util/h$
Marginal utility of traveling by PT ($\beta_{trav,PT}$)	– 0.18	$util/h$
Monetary distance rate by car ($\gamma_{d,car(q)}$)	– 0.30	EUR/km
Monetary distance rate by PT ($\gamma_{d,PT(q)}$)	– 0.18	EUR/km
Marginal utility of money (β_m)	– 0.079	$util/EUR$
Approximate average $VTTS_{car}$	+ 12.15	EUR/h
Approximate average $VTTS_{PT}$	+ 14.43	EUR/h
Calibrated for this case study		
ASC for urban PT	– 0.75	$util$
ASC for (rev.) commuters PT	– 0.3	$util$

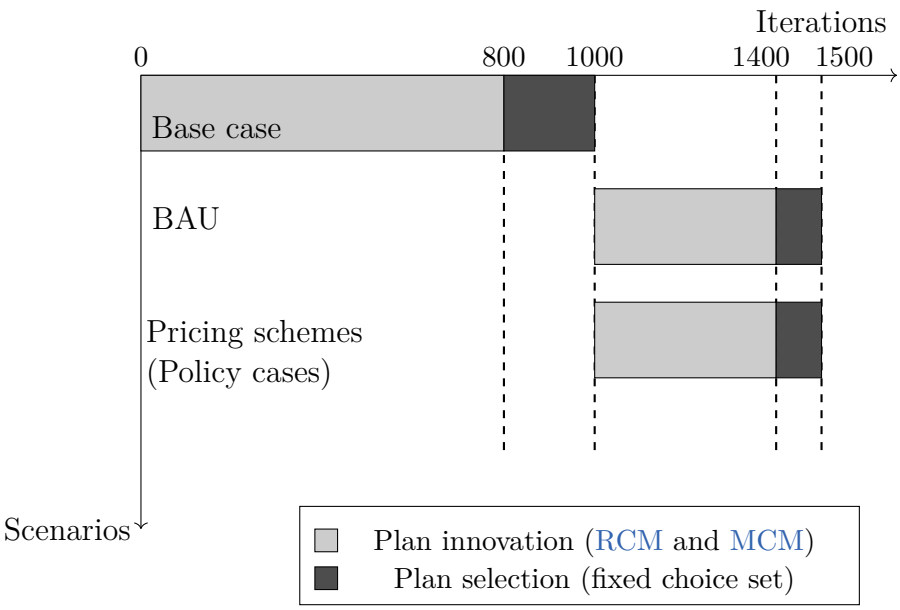

Figure 4.3: Re-planning over the iterations for different scenarios.

The rest of the agents chose a plan from their existing choice set according to a MNL model. After 80% of the iterations, the choice set is fixed and agents can only chose from the existing alternatives. In case of freight, mode choice is not available, i.e., all freight trips use truck mode only.

4.4.2 Base case

Similar to Fig. 2.2, Fig. 4.3 briefs the different scenarios under consideration and their re-planning modules for the case study. A base case is set up by running simulation for 1000 iterations. The ASC for PT in base case of Kickhöfer and Nagel (2016b) was calibrated

assuming a uniform PT speed of 25 km/h for all user groups while matching the modal split for the urban travelers. As a consequence, the modal split for the (rev.) commuters did not match the reference study (see Tab. 4.4, "*Common* PT speed (it.1000)").

Therefore, in this case, the PT speed (25 km/h) for urban travelers is kept, and for (rev.) commuters, it is assumed to be 50 km/h, emulating faster trains between the city center and suburbs. Then, the base case is re-calibrated, eventually resulting in an ASC of -0.3 for (rev.) commuters. Tab. 4.4, "*Different* PT speed (it.1000)", shows the results of this calibration effort. The combined modal split of (rev.) commuters is now very close to the initial plans and the reference study. Because of the decrease in the car share for (rev.) commuters (from 96% to 66%; see Tab. 4.4), there is some relief of capacities on the network. In consequence, the share of the car trips for urban travelers increases from 20.11% to 21.20% which is also closer to the reference study.

Table 4.4: Modal split from reference studies, initial demand and calibrated base cases.

	Urban		(Rev.) commuter	
	car	non-car	car	non-car
Reference study[8]	26.00	74.00	67.00	33.00
Initial demand (it.0)	22.48	77.52	67.97	32.03
Common PT speed (it.1000)	20.11	79.89	96.59	3.41
Different PT speed (it.1000)	21.20	78.80	66.62	33.38

4.4.3 Policy cases

After the calibration of the base case, the simulation is further continued for 500 iterations along with the 'Business As Usual' (BAU) case and three pricing schemes (see Tab. 4.5). The output of the base case after iteration 1000 is used as inputs for all four policy cases. As described in Sec. 4.2.3, different user-specific external costs are internalized for the scenarios listed in Tab. 4.5. The final iterations (1500) of the pricing schemes are compared with the final iteration of BAU. The emission costs, congestion costs and toll payments for all four scenarios are computed as follows:

1. **Emission costs**: The time-dependent and person-specific cold and warm emissions are calculated as described in Sec. 4.2.2. These emissions are then transformed into monetary units using the emission costs factors (see Tab. 4.1). These monetary emission costs are summed up to get the total emission costs in each scenario.

2. **Congestion costs**: As illustrated in Sec. 4.2.1, disaggregated delays are calculated on a per-link basis for each affected or causing agent and then converted into monetary units using the approximate average VTTS. The congestion costs are classified into two categories, namely 'experienced congestion costs' and 'caused congestion costs'. The former are the costs experienced and the latter are costs caused by the agents. Afterwards, these values are summed up to get the total congestion costs for each scenario.

[8] Follmer et al. (2004) for urban travelers and MVV (2007) for commuters and reverse commuters.

3. **System welfare**: In order to perform economic evaluation for all three pricing scenarios, the travel related user benefits are calculated by converting the utility of each agent into monetary terms.[9] The congestion costs and the negative perception of toll payments are both implicitly part of the user benefits. The toll payments are, however, simply transfer payments from users to public authorities. Consequently, the change in the system welfare is defined as the algebraic sum of changes in the emission costs, toll payments, and user benefits.

Table 4.5: Policy cases.

Policy case	Externality	Internalization
Business As Usual (BAU)	none	none
Congestion Internalization (CI)	congestion	see Sec. 4.2.1
Emission Internalization (EI)	emission	see Sec. 4.2.2
Emission and Congestion Internalization (ECI)	both	both

4.5 Results

In this section, the levels of the external costs are illustrated (Sec. 4.5.1) and subsequently, the effects of the pricing schemes on the system performance is presented (Sec. 4.5.2). Furthermore, Sec. 4.5.3 and Sec. 4.5.4 provide more detailed and disaggregated analyses for different agent groups. The emphasis will thereby be put on the driving forces behind the increase in the system performance, and on the isolated impacts of each externality on the overall toll level. All figures in the presentation of the results are for a typical working day and scaled to the full population. The idea behind the comparison of the pricing schemes is

i) to investigate the influence of internalizing one externality on the other externality,

ii) to test whether the correlation between the two externalities in the combined internalization (ECI) yields toll levels that are lower than the algebraic sum of the toll levels from the individual internalization models, and

iii) to test whether the correlation between the two externalities in the combined internalization (ECI) has policy implications.

4.5.1 BAU: amplitude of externalities

For the MMA, the congestion costs amount to approximately 7.3 *M* Euro (*EUR*) which is about twice as much as the emission costs (3.7 *M EUR*). In the transport literature,

[9] The user benefits calculated from the utility of the last executed plan are not same as the user benefits calculated from the logsum over all plans of an agent. The latter (also sometimes called expected maximum utility) considers utility from heterogeneity in the choice set and is in theory the preferable figure for calculating user benefits in MATSim (see Kickhöfer and Nagel, 2016a). However, as the authors point out, the current MATSim implementation might, under certain conditions, yield biased choice sets. In consequence, the last executed plan is used in the present paper.

the congestion cost estimates is found to be higher than the emission cost estimates (see, e.g., Maibach et al., 2008; Parry and Small, 2005) and therefore, the results of this case study are in line with the estimates from the literature.

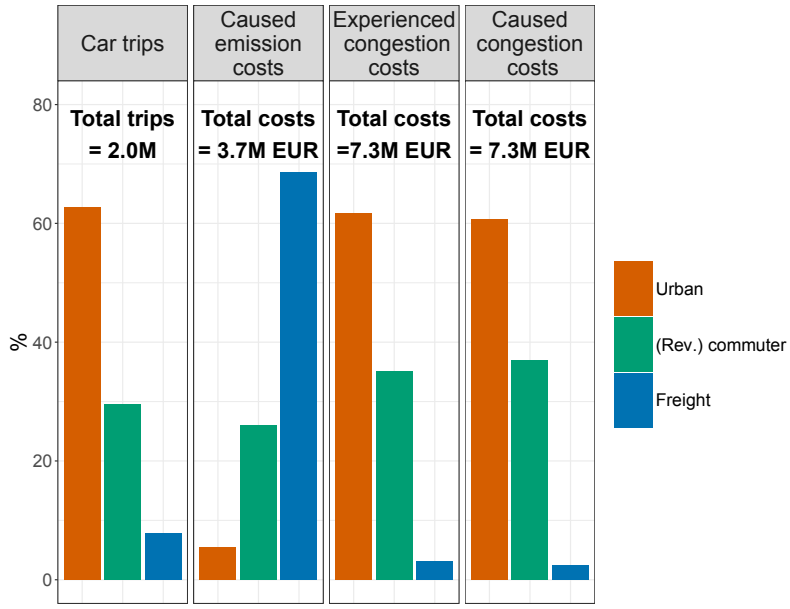

Figure 4.4: Share of car trips, emission and congestion costs for different user groups of BAU scenario.

Fig. 4.4 shows the share of persons and external costs for each user group of the BAU scenario. The caused emission costs of a user group are total costs of emissions produced by all vehicles of that group. Freight trips consists of only about 8% (0.15 M) of all car trips, but is responsible for more than 65% (2.5 M EUR) of the total emission costs. This is due to the fact that the freight vehicles (i) emit more emissions than other vehicles and, (ii) have longer travel distances (mean and median trip distances are 111 km and 69 km, respectively). As explained before in Sec. 4.4.3, congestion costs are classified into two categories, namely 'experienced congestion costs' and 'caused congestion costs' depending on the experience or caused congestion costs by respective user groups.[10] Thus, the experienced congestion costs are also influenced by the agents from other user groups. The share of car trips for urban travelers is more than 60% (1.3 M car trips) of the total car trips. They experience and cause about 4.5 and 4.4 M EUR of the total congestion costs respectively. This is expected since they perform most of the trips and congestion is predominant in urban areas. Together with the freight, they are causing less congestion (i.e., delays) than they experience. On the contrary, (rev.) commuters cause (2.7 M EUR) more than what they experience (2.6 M EUR). In marginal congestion pricing, the agents are charged for the delays they cause to others and therefore *caused congestion costs* will be referred as congestion costs in rest of the thesis.

[10] A recent study by Kickhöfer and Kern (2015) shows that the framework in principle allows for a similar classification in the case of emission costs. However, in this thesis, only *caused emission costs* are considered and referred to as 'emission costs' from here on.

4.5.2 Pricing: system performance

Absolute changes in the external costs, toll payments, user benefits and system welfare as a result of the three different pricing schemes are shown in Tab. 4.6.

Table 4.6: Key indicators for all pricing schemes (in *M EUR*) per typical working day.

	Pricing schemes		
Benefits from ...	**EI**	**CI**	**ECI**
... changes in emission costs (1)	0.10	0.17	0.27
... changes in congestion costs (2)	0.91	3.61	3.96
Changes in travel related user benefits (3)	−2.75	0.44	−2.34
Toll revenues (4)	3.61	3.68	6.78
Changes in system welfare (=1+3+4)	0.96	4.27	4.71

The reduction in the emission costs for EI, CI and ECI pricing schemes are 2.72%, 4.49%, and 7.22% (0.10 *M*, 0.17 *M*, and 0.27 *M EUR*), respectively. These values follow the same trend as in the previous work by Agarwal and Kickhöfer (2015), in which the authors reported the reductions in emission costs of 0.57%, 1.94% and 2.48% for the same pricing schemes. However, that study did not account for different PT speeds (see Sec. 4.4.2), which seems to have an important effect on the price elasticity of car travel demand. The decrease in the emission costs for all pricing schemes is more significant in this chapter which indicates that capturing the elasticities accurately has a major impact on the results. The reduction in the congestion costs for EI, CI and ECI pricing schemes are 12.70%, 49.66%, and 54.44% (0.91 *M*, 3.61 *M*, and 3.96 *M EUR*), respectively.

Internalizing emissions (EI) results in approximately 0.91 *M EUR* less congestion costs. Internalizing congestion (CI) results in approx. 0.17 *M EUR* less emission costs. Thus, pricing one externality has a positive impact on the other externality. That is, the externalities prove to be positively correlated. The positive correlation is also found in the study by Beevers and Carslaw (2005), who show that the London congestion charging scheme reduced NO_x and PM_{10} by 12% and 11.9% respectively between 2002 and 2003. The combined pricing scheme (ECI) exhibits the highest reductions in emission costs (0.27 *M EUR*) and congestion costs (3.96 *M EUR*), and the highest gain in system welfare (4.71 *M EUR*). That is, the combined pricing scheme improves system performance the most.

An interesting observation can be made for the changes in the 'travel related user benefits': they are negative for EI and ECI and positive for CI. This stems from the fact that, for CI, the reduction in the travel times overcompensates the losses from the toll payments yielding a positive change in the user benefits. For EI and ECI, the reduction in the travel times is smaller than the loss from the toll payments yielding a negative change in the user benefits.

To summarize, the following observations are obtained:

a) pricing congestion (CI) results in a decrease of the emissions,

b) pricing emissions (EI) yields a reduction in the congestion,

c) the lowest levels of the external costs are observed in the combined pricing scheme (ECI), and

d) system welfare is highest for ECI.

These findings are confirmed for all user groups under investigation. However, when looking at the effects on the individual user group, some interesting additional observations can be made. In particular:

1. Pricing emissions (EI) diverts freight trips on shorter (Δ average distance $= -0.2\ km$) but more congested links and consequently a slight increase in congestion costs is observed. That is, pricing emissions might yield higher congestion levels (see also later in Sec. 4.5.4). This effect is also observed in a study by Yin and Lawphongpanich (2006), where authors experimented on a 6 node test network and found that the emission internalization may sometimes produce less emissions but higher delays.

2. All three pricing schemes yield a decrease in the user benefits for all user groups except for urban travelers. For them, the gain in the utility from the reduction in the travel times is higher than the loss because of the toll payments which eventually produces higher user welfare. When pricing congestion (CI), this gain overcompensates the losses of the other user groups and finally results in higher user benefits for the whole population (see Tab. 4.6).

For now, the point with the most important policy implication, however, is the following: the sum of the toll revenues from the isolated pricing schemes is roughly 7.29 *M EUR* whereas the total toll revenues for the combined pricing is roughly 6.78 *M EUR*.[11] The lessons learned here are that simply combining the average toll levels from the isolated pricing schemes (EI and CI) for policy making will result in over-pricing. This is due to the correlation between the congestion and air pollution externalities. Thus, the hypothesis that "combining the toll levels obtained from the separate pricing schemes would not yield toll levels above those of the economic optimum", is rejected. The same is likely to be true for a policy which combines the marginal cost factors from the literature, since there are typically no cost estimates for the emissions *given* an existing congestion pricing scheme or cost estimates for the congestion *given* an existing emission pricing scheme.

4.5.3 Pricing: driving forces

The increase in the system performance indicators is a combined effect of users' reactions with respect to two choice dimensions, mode choice and route choice (see Sec. 4.4.1). This section aims at presenting the driving forces behind the increases in the system performance by performing a more in-depth analysis.

Modal split Tab. 4.7 shows the impact of the pricing schemes on the modal split. For the EI case, the share of car trips decreases for (rev.) commuters whereas it increases slightly

[11] This result has been confirmed by two simulations with different random seeds, which are used to initialize the pseudo random number generator in MATSim. A different random seed will eventually result in different simulation outcomes. For an example of the effect of randomness on optimal supply in MATSim, see, e.g., Kaddoura et al. (2015a).

for urban travelers. Because of the higher average toll per trip for (rev.) commuters (see Tab. 4.8), a significant number of car users in this user group switch to PT. This relieves some capacity and leads to an increase in the car share of urban travelers. In contrast, for the CI and ECI case, the car share decreases for both user groups. This is because the average toll per trip for urban travelers is by a factor of 12 higher than in EI. This effect is less pronounced for (rev.) commuters, however, also their toll increases by a factor of 1.5 and 2.5 from the EI to the CI and ECI case, respectively. On the aggregated level, one observes – as expected – that higher the toll, more agents switch from car to PT, depending on the implicit price elasticity of demand. The elasticity is dependent on the availability of substitutes, i.e., if agents are not able to switch mode because of insufficient alternatives, pricing cannot be used to increase the system efficiency. Daniel and Bekka (2000) have found in their models that potential welfare gains decrease with a decrease in the elasticity of demand. The results in this chapter support this finding. On the disaggregated level, however, the agent-based simulation framework exhibits the complex structure of human interactions in transport decisions. Because of capacity relief, pricing car emissions might *in*crease the car share for certain subgroups. Similarly, increasing the toll level (i.e., going from CI to ECI) might *de*crease the reduction in the car share for certain subgroups.

Table 4.7: Changes in the car share (% points) with respect to BAU for all pricing schemes.

	urban	(rev.) commuters	freight
EI	+0.22	−7.04	0.00
CI	−0.66	−16.25	0.00
ECI	−0.48	−23.46	0.00

Table 4.8: Average toll payments (*EUR*) per car trip for all pricing schemes.

	urban	(rev.) commuters	freight
EI	0.16	1.62	16.04
CI	1.96	2.46	0.92
ECI	2.00	4.12	16.96

Travel time Fig. 4.5 shows the change in the average trip travel time for mode switchers and retainers. One observes that the average trip travel time decreases significantly for the agents who retain car as transport mode, as well as for the agents who change from PT to car: the toll in the car mode improves car travel times, so car gets attractive in particular for short trips. In contrast, the travel time is increased for the agents who switch from car to PT. These agents are better off by shifting to the time-consuming PT travel mode than paying toll. Interestingly, with the congestion pricing scheme, the agents who stay in the car mode are shifting to less congested but longer routes (see Fig. 4.8b) in order to dampen their toll. In contrast, the agents who switch from PT to car prefer to pay toll which is compensated by significant reductions in the travel time.

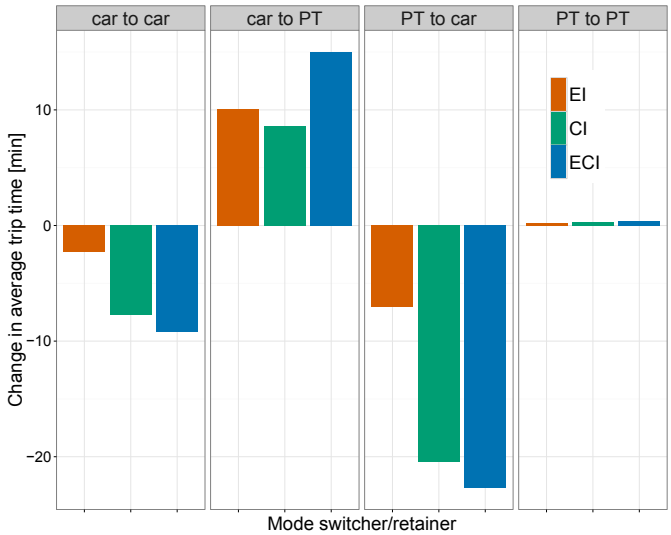

Figure 4.5: Changes in the average trip travel time for mode switchers and retainers.

Peak/off-peak tolls Tab. 4.9 shows the average toll levels in the car mode for peak[12] and off-peak hours, now in *EURct*/*km*. The resulting average toll levels are plausible values:

Table 4.9: Average toll levels (*EURct*/*km*) in the car mode for peak and off-peak hours.

Time	Pricing scheme	urban	(rev.) commuters	freight
Peak	EI	2.61	2.24	14.45
	CI	36.38	3.62	1.28
	ECI	37.83	5.40	15.70
Off-peak	EI	2.56	2.19	14.45
	CI	29.99	2.70	0.63
	ECI	30.46	4.59	15.08

Table 4.10: Contributions of the externalities to the ECI toll levels (*EURct*/*km*) for the car mode in peak and off-peak hours.

Time	externality	urban	(rev.) commuters	freight
Peak	Emissions	2.51 (6.6%)	2.22 (41.1%)	14.44 (92.0%)
	Congestion	35.32 (93.4%)	3.18 (58.9%)	1.26 (8.0%)
Off-peak	Emissions	2.49 (8.2%)	2.18 (47.5%)	14.43 (95.7%)
	Congestion	27.97 (91.8%)	2.41 (52.5%)	0.65 (4.3%)

e.g., Parry and Small (2005) use local pollution costs for automobile as 1.18 *EURct*/*km* for US and UK, and external congestion costs as 2.06 and 4.11 *EURct*/*km* for US and UK

[12]The peak hours are identified as 07:00–10:00 and 15:00–18:00 considering the total travel demand of all user groups in the BAU scenario.

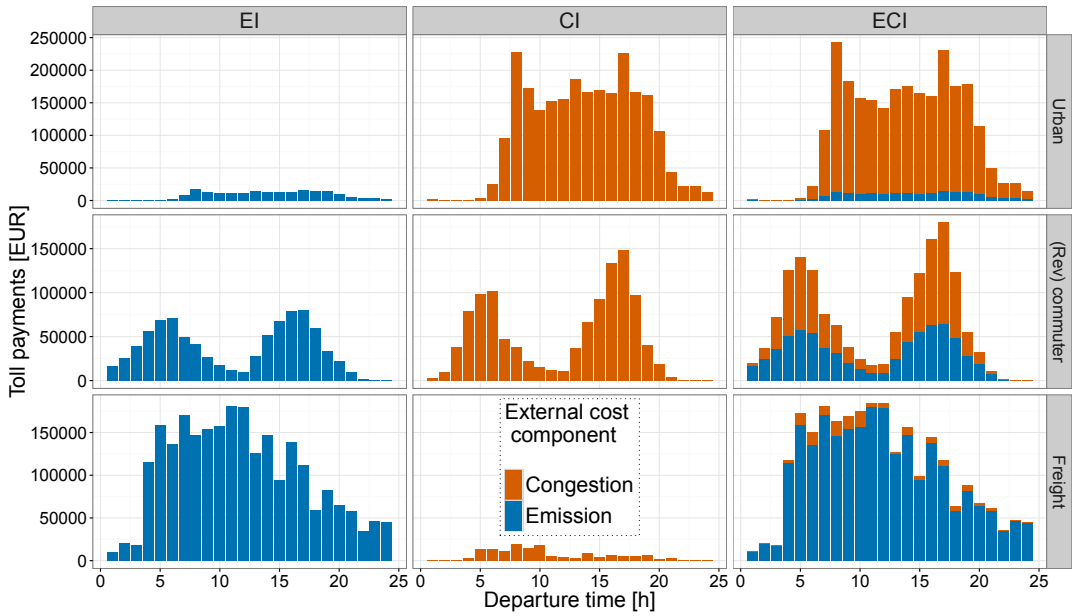

Figure 4.6: Toll payments (in *EUR*) over time of day for all pricing schemes and subpopulations. Values are scaled to full population.

respectively. Clearly, due to higher generated emissions, the toll values for freight trips are very high. Similarly, higher congestion from urban travelers yields higher toll values.

Peak-hour toll levels are – as expected – higher than off-peak tolls. For CI and ECI, urban travelers exhibit a six to ten times higher toll level per vehicle kilometer than (rev.) commuters whereas for EI, this factor is about 1.2 only. On a per-km basis, the influence of the (rev.) commuters is much smaller than that of the urban travelers,[13] however, they travel significantly longer than the urban travelers.[14] This was not yet visible from the tolls per trip in Tab. 4.8. Freight tolls are almost not influenced by congestion pricing since the emission toll dominates the overall price level.

Tab. 4.10 shows the contributions of the two externalities to the overall ECI toll level for peak and off-peak hours. The first important finding is that the contribution of emissions to the overall toll level is higher in off-peak than in peak hours. This is valid for all user groups. In comparison with Tab. 4.9, the figures in Tab. 4.10 additionally exhibit that, in the EI case, the emissions are more strongly overpriced in peak hours than in off-peak hours. To give an example: in EI, peak hour emission prices for urban travelers are 4.0% ((2.61 – 2.51)/2.51) higher than in the ECI case. In off-peak hours, this price difference only amounts to 2.8%. In contrast, in the CI case, the peak hour congestion prices for urban travelers are only 3.0% ((36.38 – 35.32)/35.32) higher than in the ECI case. In off-peak hours, this price difference increases to 7.2%. That is, for a combined pricing scheme, cost estimates from the literature need to be reduced because of the correlation between the air pollution and congestion externalities. For the emission estimates, these reductions should be stronger in peak hours. For the congestion estimates, these reductions should

[13] It is likely that the influence of the (rev.) commuters would reduce and influence of the urban travelers would increase significantly if the exposure of local emissions is priced (i.e., pricing experienced emissions) (Kickhöfer and Kern, 2015).

[14] In BAU scenario, the average trip distances for urban travelers and (rev.) commuters are 6.1 *km* and 72.2 *km* respectively.

be stronger in off-peak hours. Alternatively, the joint internalization model as is proposed in this thesis can help to determine the joint amplitude of the externalities and help to design pricing schemes of any desired complexity, ranging from little price differentiations to highly personalized tolls. For illustration purposes, Fig. 4.6 shows the toll payments for all three pricing schemes and all subpopulations in one hour time bins. It emphasizes the importance of the interrelation of emission and congestion externalities and their variation over time of day and user groups.

4.5.4 Pricing: spatial distribution

The impact of the three pricing schemes on a spatially disaggregated level is presented in this section. The spatial dimension of the external costs in the BAU scenario is shown

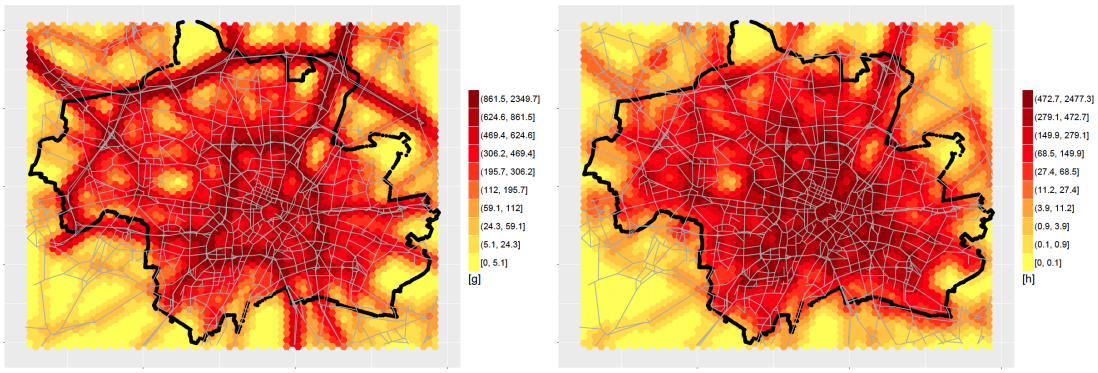

(a) Absolute NO_2 emission (b) Absolute delay

Figure 4.7: Absolute emissions (in g) and delays (in h). Values are scaled to full population.

in Fig. 4.7.[15] The time-dependent and person-specific link-based emissions and delays are presented. Fig. 4.7a shows absolute NO_2 emissions[16] and Fig. 4.7b shows absolute delays. It can be observed that emissions are most important on primary roads (inner and middle ring road, main arterials, and the tangential motorway in the north-west of Munich). In contrast, congestion is evident on almost all roads inside the city area, but not as important on the tangential motorway.

Fig. 4.8 shows the changes in the NO_2 emissions and in delay for the off-peak hours (i.e., 00:00-07:00, 10:00-15:00 and 18:00-24:00).[17] An increase in the emissions or delays is represented by red color, a decrease by green color. The spatial plots in top row (Figs. 4.8a to 4.8c) show the changes in the NO_2 whereas the plots in the bottom row (Figs. 4.8d to 4.8f) show the changes in the delays with respect to the BAU scenario. For the EI case, Figs. 4.8a and 4.8d show that agents are re-routing towards shorter distance routes. This is

[15] For the visual presentation, a Gaussian distance weighting function is used to smooth emissions and delays throughout the area of Munich and surroundings. Uniform hexagonal cells of size 500 m are used for this purpose. The smoothing radius is assumed to be 500 m. In contrast to Kickhöfer (2014) which assumes the emissions at the center of the link, the emissions are linearly distributed on the link. For more information on the exact visualization procedure, please refer to Appen. A.

[16] All important pollutants are considered for pricing. For illustration purposes, the emission plot only shows NO_2.

[17] In the peak hours, the congestion pricing scheme and the combined pricing scheme exhibit similar patterns.

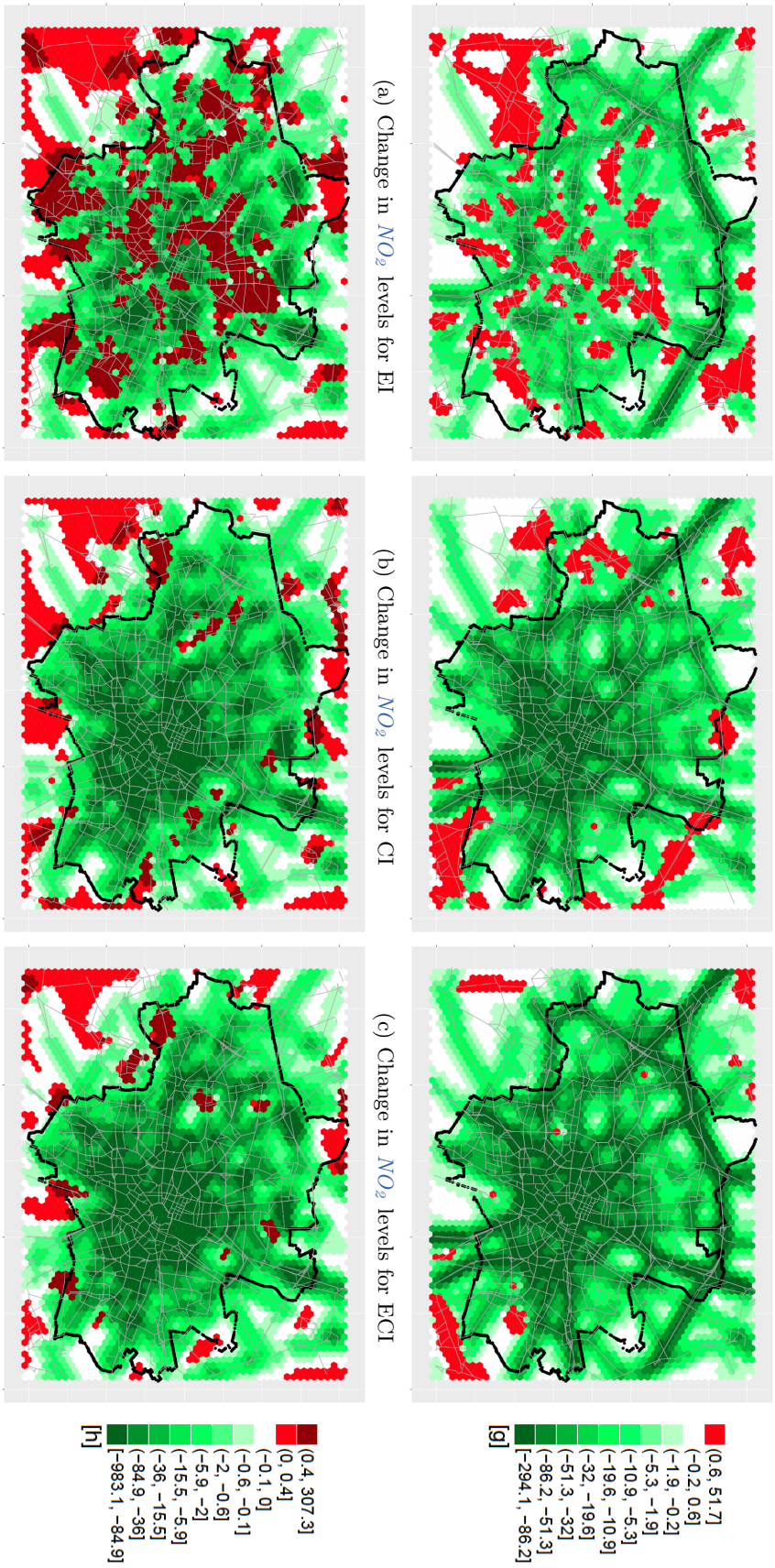

(a) Change in NO_2 levels for EI

(b) Change in NO_2 levels for CI

(c) Change in NO_2 levels for ECI

(d) Change in delays for EI

(e) Change in delays for CI

(f) Change in delays for ECI

Figure 4.8: Changes in NO_2 emissions (in [g]) and delays (in [h]) for all pricing schemes in the off-peak hours. Values are scaled to full population.

indicated by an increase of emissions *and* delays in the inner city. As a consequence, NO_2 emissions are decreased in particular on the north-west tangential motorway and other long-distance routes, basically wherever NO_2 emission was high in the BAU scenario. For the CI case, Figs. 4.8b and 4.8e show that the agents re-route from congested links to non-congested and longer distance routes. Thus, the NO_2 emissions and delays are decreased significantly inside the central areas of Munich. On the contrary, the NO_2 emissions are increased on parts of the tangential motorway where NO_2 emissions were already high in the BAU scenario. The effect of the combined pricing on a spatial level is shown in Figs. 4.8c and 4.8f. Since congestion costs dominate the emission costs, the patterns in the ECI are similar to those from CI. Overall, the combined pricing yields a decrease in the NO_2 emissions *and* delays in most areas of the city.

The lessons learned here are that – for congested regimes – the two pricing schemes (EI and CI) affect the route choice behavior of the agents by tendency into opposite directions: EI towards the shorter distance routes, increasing congestion; CI towards the longer distance routes, increasing emissions. In the combined pricing scheme, the higher toll component (i.e., emission toll on major arterials and tangential motorways, and congestion toll on major arterial inside the city area) wins and eventually, reduces emissions and congestion externalities.

4.6 Discussion

The goal of this chapter is to present a simulation-based approach to calculate and internalize the correct dynamic price levels for the congestion and emission externalities simultaneously. The approach combines activity-based demand with dynamic traffic flow simulations. The behavioral reactions to the time-dependent vehicle-specific congestion and/or emission tolls are modeled for every agent of the system. Clearly, given this complexity of the approach, several assumptions and simplifications are made. In the following, it is discussed to what extent these assumptions and simplifications might influence the results structurally and how they can be used for deriving or evaluating policy interventions.

4.6.1 Commercial traffic

The full behavioral modeling of commercial vehicles is beyond the scope of this thesis (see Schröder et al., 2012; Zilske et al., 2012, for some ongoing work to integrate this in the model). However, to not simply ignore congestion and environmental effects of the commercial vehicles, they are simulated as freight user group in the scenario along with the other user groups. With respect to congestion, other vehicles can delay a truck and a truck can delay other vehicles. In that sense, congestion effects are accounted for. The only assumption here is that one truck uses as much road capacity as one car. That is, the congestion toll for trucks is underestimated. Clearly, the simulation of different vehicle types is possible by accounting for Passenger car unit (PCU) (see Ch. 7), however, the marginal congestion pricing approach is not adapted for the mixed traffic yet. However, this should be tackled in the near future.

With respect to emissions, the vehicle and engine type are assumed to be identical for

all trucks. There is no differentiation by type of commercial vehicle. However, if data is available, the approach in principle allows for this differentiation according to the HBEFA database. That is, the emission toll is as accurate as the underlying demand data allows. In absence of a separate behavioral model for the commercial vehicles, the VTTS for trucks is assumed to be identical to the VTTS of car users, which is certainly lower than the typical values from the literature. Hence, the vehicles will by tendency choose routes with too short distances and too long travel times in comparison to the reality. However, as they are only allowed to change their route (other user groups can additionally switch mode), the effect of this simplification on the overall results is expected to be small.

4.6.2 Externalities from public transit

As a reaction of pricing emissions and/or congestion, an individual car user may switch to more environmentally friendly or less congested transport modes. In this paper, PT is meant to represent all other transport modes and is assumed to run emission and congestion free. This is a valid assumption as long as PT operates as a completely separate system and runs on carbon-free electric power only. In real-world scenarios, however, there exist interactions between individual transport modes and PT. Hence, absolute congestion and emission externalities will be higher than in the case study presented here. It is therefore planned to include the external costs of public transport in the simulations (see, Kaddoura et al., 2015b, for a related study).

4.6.3 Choice dimensions

In this case study, the agents are only allowed to change their route and/or their mode of transport. Incorporating other choice dimensions such as departure time or location choice will certainly have an impact on the results. For instance, the potential efficiency gains depend on the implicit price elasticities of the car travel demand. More options by tendency increase the demand elasticities and with it the potential efficiency gains. That is, the figures presented in this papers are rather at the lower bound of the potential impacts induced by pricing congestion and/or emission externalities.

4.6.4 Improved scenario setup

In this chapter, the scenario setup is improved by introducing a faster PT for (reverse) commuters which is a more viable option to commute between the city center and suburbs (see Sec. 4.4.2). Consequently, the decrease in the emission costs under different pricing schemes is more significant than in the previous study by Agarwal and Kickhöfer (2015). Hence, an improved scenario setup yields more realistic elasticities and is important for estimating the potential welfare gains from pricing schemes.

4.6.5 Pricing local emission exposure

In this chapter, the flat emissions costs are internalized, however, in future, it would be interesting to price the exposure of local emissions (Kickhöfer and Kern, 2015). This will change the results presented in this chapter. E.g., the contribution of the urban travelers in total emissions costs will increase significantly, the agents would prefer to steer on

the longer routes than on the shorter routes in populated areas with many activities (residential, work, shopping, etc.) etc.

4.6.6 Policy implications

The individual tolls in this chapter are obtained by using the idea of the marginal social cost pricing in an agent-based context. Even though the resulting highly differentiated tolls are difficult to implement and it additionally is unclear if users would actually understand the ever-changing price signals correctly, marginal social cost pricing still lays the foundation to derive toll values for reality. The time-dependent vehicle-specific tolls obtained by the presented approach can be aggregated or averaged in many ways, and it is part of the future research to find good pricing schemes which obtain most of the benefits but still remain feasible to implement, always depending on the scenario and the requirements of the case. One option for transferring the insights from the marginal cost pricing into recommendations for the policy makers are the back-calculated tolls presented in the paper (corrected average toll levels per kilometer). They exhibit, for the case study under consideration, the interrelationship between the external cost components and how their respective contribution to the overall effect changes over time of day. Apart from deriving the correct price levels for the policy making, the welfare maximizing system state can be used as a benchmark to evaluate other policies such as traffic calming measures (speed humps/bumps, speed limit restrictions; Buehler and Pucher, 2011; Ghafghazi and Hatzopoulou, 2014), parking policies (Wall, 2011; Attard and Ison, 2015) and traffic control measures (Li et al., 2004; Osorio and Nanduri, 2015b) with respect to the various indicators. This seems a promising road for future applications of the proposed approach.

4.7 Summary

This chapter proposes a joint internalization approach for more than one transport externalities. A real-world example of Munich Metropolitan Area (MMA) is presented. It has been showed that on aggregation, emission and congestion externalities are found to be positively correlated. The combined pricing schemes reduces both externalities to a lowest levels. Furthermore, it is demonstrated that due to correlation between the congestion and air pollution externalities, simply combining the average toll levels from the isolated pricing schemes of policy making will result in over pricing.

For policy implications, it is shown that for a combined pricing scheme, the cost estimates for the literature needs to be reduced. This reduction is stronger in the peak hours for the emission estimates and in the off-peak hours for the congestion estimates. For a large-scale real-world case study, it is shown that this iterative calculation of prices allows to identify the amplitude of the correlation between these two externalities without explicitly calculating correction factors. On a disaggregated level, the congestion and emission pricing schemes affect the route choice behavior of agents by tendency into the opposite directions.

Chapter 5

Policy Measure : Backcasting

5.1 Overview

The use of policy measures for different motivations is quite common, e.g., a traffic restrain scheme was applied to the city of Gothenburg aiming for a better environment in the central business district (Elmberg, 1972).[1] The idea behind backcasting is to set the political goals, and implement a number of policy measures in order to achieve these goals towards sustainable future transport. This chapter first elaborates the need of backcasting approach in the current CO_2 reduction targets. Further, the parametrized backcasting approach in a multi-agent simulation framework is presented. The approach is applied to the MMA; however the approach can be transfered to any scenario worldwide. This chapter is an edited version of Kickhöfer and Agarwal (2015).

5.2 Background

5.2.1 Policy objective

With the knowledge of the negative impacts of the climate change and rising global temperature, EU and international community have agreed on the need to reduce the GHG emissions by limiting the global warming below 2° Celsius (European Commission, 2011; FCCC/CP/2015/L.9/Rev.1, 2016). In order to achieve this goal, the directive 2008/101/EC (2008) sets the goal to reduce the global GHG emissions in the transport sector by at least 20% until 2020 with respect to 1990 levels. In the light of the above, for transport sector, improvement in the fuel and vehicle technology, alternative fuels and propulsion, etc., are the major visions set by EU (European Commission, 2009, 2011).

5.2.2 Historic trends

The passenger and freight transport in Europe has grown more than 40% between 1990 and 2010, and the CO_2 emissions from transport sector has increased by about 300 $Mton$ between 1990 and 2010 (Schoemaker et al., 2012). Fig. 5.1 shows the change in GHG

[1] Please refer to Sec. 3.2, for detailed discussion about the different tolled and non-tolled policy measures.

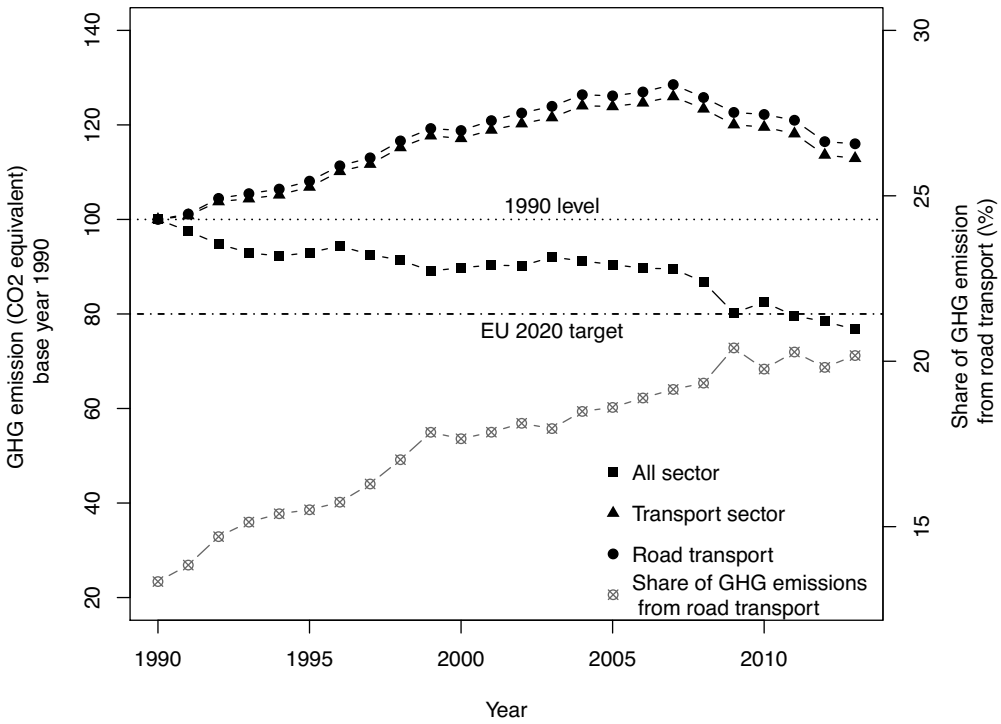

Figure 5.1: Total GHG emissions for EU-28 with respect to 1990 levels. In 1990, total GHG emissions for all sectors, transport sector (excluding international aviation) and road transport was 5420.57, 785.89, 723.15 $Mton$ respectively (Data is taken from European Environment Agency, 2016, online data code: *env_air_gge*).

emissions for EU-28[2] with respect to 1990 levels. The total GHG emissions from all the sectors has already reached to its goal of 20% reduction but on the contrary, an increase of about 10-15% GHG emissions is observed for the road transport sector. In addition to that, the share of road transport GHG emissions is continuously increasing.

5.2.3 Policy roadblocks

Future growth and rebound effect Schoemaker et al. (2012) indicate that from 1990 levels, the passenger and freight transport can grow more than 80% by 2030. Similarly, if the trend continues, with respect to 1990 levels, an increase of about 450 $Mton\ CO_2$ emission from the transport sector can be expected by 2030.

The main focus of EU's regulation scheme for the transport sector is on improvement of the fuel and vehicle technology (Romm, 2006), which is expected to reduce the emissions significantly. In EU, the average emissions from every new car registered in 2014 is 123.4 $g\ CO_2/km$, significantly below the 2015 target of 130 $g\ CO_2/km$ (EEA, 2015). It means that every new car will generate lesser emissions however, importantly, the market penetration of these technologies will decide the overall improvements in the CO_2 emissions.

The improvements in the fuel and vehicle efficiency can lead to reduction of the generalized costs. This in turn can partly neutralize the positive impacts of the technology

[2]See http://europa.eu/about-eu/countries/member-countries/ for a complete list of all EU member countries.

improvements due to the potential *rebound* (or 'takeback') effects resulting from the reduction in the generalized costs (Divjak, 2009; Parry and Small, 2005; Barla et al., 2009).[3] In the transport literature, the magnitude of the rebound effects has low acceptance. Frondel et al. (2012) estimate the rebound effects for Germany in the range of $57 - 62\%$ whereas Wang et al. (2012) find that the average direct rebound effects for passenger transport by urban households is around 96%. A high value of the rebound effects will reduce the CO_2 benefits from the advances in the vehicle and fuel technologies and undermine a particular policy.

Divergence Another point of a great concern from these innovations is the growing divergence between the "type-approved" (emission tests under laboratory conditions) and the on-road CO_2 emission from the vehicles (Mock et al., 2014; EEA, 2014). As shown in Fig. 5.2, the 2015 target of 135 $g\ CO_2/km$ from passenger cars is already achieved. However, the gap between the emissions under laboratory conditions and real-world conditions is increasing steeply in the recent years. That is, the improvements in the vehicle and fuel technology might not be effective under on-road conditions, it might further pull back the reductions in GHG emission.

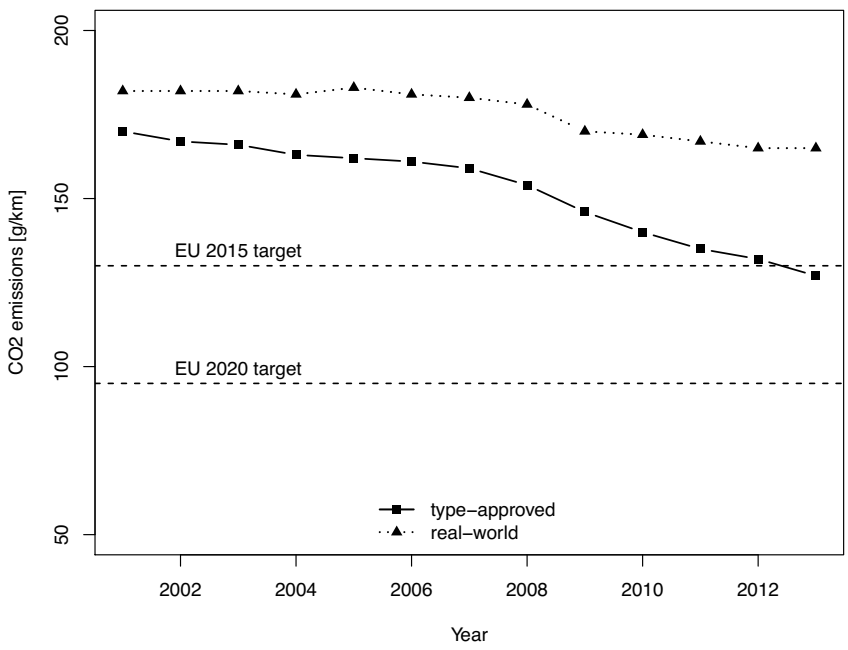

Figure 5.2: Divergence between the emissions from new cars produced under laboratory and real-world conditions (Mock et al., 2014).

[3]The rebound effects are mainly categorized in 'direct' and 'indirect' rebound effects (IPCC, 2014; Thomas and Azevedo, 2013). The former is the increase in the demand due to decrease in the generalized cost with an efficient vehicle/fuel technology; e.g., an fuel-efficient car will have lower operating costs which may increase the vehicle kilometer traveled. The latter is the effects from re-spending of the savings due to the vehicle/fuel technology on other goods or services; e.g., spending fuel savings on a vacation. The combined effect is called as 'economy-wide' rebound effects.

Behavioral changes Emberger (2015) raises some doubts on the EU's transport visions e.g.,

a) there is no policy measures to reduce the car ownership and to obtain higher modal share of more environmental friendly transport,

b) it is not clear, whether the alternative fuel efficiency can compensate the growth of the car usage and rebound effects, etc.

According to Parry et al. (2014), omitting the pricing strategies and focusing only on the technological changes will forgo a major part of the potential welfare improvements. The main focus of the EU transport policy is on the supply side and very little attention is given on the demand side to control the growing demand for transport (EEA, 2008). In order to, implement the alternative vehicle and fuel technology successfully, the behavioral changes are necessary (May, 2013). Clearly, these roadblocks will forfeit a part of the positive effects from the EU's transport policy. Thereby, it will be challenging to achieve the emission reduction targets by 2020. From this, the present chapter presents the backcasting approach to identify the necessary additional price, as multiples of the original damage cost estimates, by including these prices into the behavioral decision making process of the individuals.

5.3 Methodology

5.3.1 Research problem

From Sec. 5.2.1, the objective is to identify the gap between toll levels derived from environmental damage cost internalization and toll levels to achieve the political goal of 20% reduction in GHG emissions of transport sector until 2020 with respect to 1990 levels. The latter, in this thesis, is termed as the avoidance charge. However, a few simplifications are made to reduce the complexity of the research problem and due to unavailability of the disaggregated data. These are as follows.

a) The GHG emissions from the road transport sector and from all transport sectors together (excluding international aviation) follow similar trends over the previous decades (see Fig. 5.1). Therefore, it is assumed that a 20% reduction in GHG emissions is required from the road transport sector also.

b) In the context of the global warming and road transport, the objective of reduction in the GHG emissions is translated to the reduction of CO_2 emissions since CO_2 is a major component among the gases released during the combustion of fossil fuels.

c) The objective is to reduce the EU's GHG emissions, however, the same objective is taken at a smaller scale i.e., for MMA.

d) The travel demand data is available for the survey year (12/2001-12/2002) and therefore, the proposed approach is applied to this demand (MiD 2002, Follmer et al., 2004) rather than forecasting the demand to year 2020.

With the above simplifications, the research problem is reduced to "estimation of the avoidance price to reduce the CO_2 emissions by 20% for MMA with respect to the survey year".

5.3.2 Parametrized backcasting

To summarize, the damage cost approach values the effects of change in the air quality at local and global levels whereas the avoidance cost approach estimates the costs to avoid these effects (see Sec. 1.2.2.2 for detailed description). As mentioned before in Sec. 5.2.1, the EU sets the goal to reduce the global GHG emissions in the transport sector by at least 20% until 2020 with respect to 1990 levels. In absence of any other regional targets for MMA, this chapter adapts a target of 20% reduction in the CO_2 emissions. The marginal social cost pricing schemes can provide the upper bound of the possible efficiency gains in a transport system using the damage cost factors (see Tab. 4.1) from the literature (see also Chs. 3 and 4). Therefore, the aim is to identify the necessary avoidance charge for MMA to achieve the 20% reduction in CO_2 emissions target from road transport sector.

The process of internalizing environmental externalities is based on the MSC as described in Secs. 4.2.2 and 4.2.3. The idea is to identify the order of magnitude of price level differences between the marginal social cost pricing and the backcasting approach. For that purpose, emission cost factors from Tab. 4.1 are increased by a multiplication factor following a parametric approach. Hereon, this factor is referred as Emission Cost Multiplication Factor (ECMF). The increased emission costs are then charged to the agents who eventually consider them in their decision making and react accordingly. The changes in agents' behavior under different levels of ECMFs (see Sec. 5.4) are reported later in the Sec. 5.5.

5.4 Scenario set up

The MMA is again chosen for this approach. The urban travel demand is synthesized using detailed survey data based on *Mobility in Germany* (MiD 2002, Follmer et al., 2004). The inputs and scenario set up for demand generation are explained in Sec. 4.4.1. The base case is also the same as described in Sec. 4.4.2. The base case simulation is run for 1000 iterations and its output is then used as input for the different policy cases:

- The base case is continued for 500 more iterations and is referred to as "Business As Usual"(BAU) case. This is the reference case for comparison with other policy cases.
- Six different ECMFs, namely 1.0, 5.0, 10,0, 15.0, 20.0 and 25.0, are considered and for each ECMF, one simulation is set up by running for 500 iterations.

In each of the pricing schemes, the emission cost factors (see Tab. 4.1) are increased by the above mentioned ECMFs to increase the toll for the agents. The reaction of the agents under various ECMFs is analyzed in the following section.

5.5 Results

The results are classified under two categories

a) based on the geographical area i.e., Munich city area, Munich Metropolitan Area (MMA) and area outside MMA (see Fig. 4.2) and

b) based on the sub-population (also called as user group), namely urban, (rev.) commuters, and freight (see Sec. 4.4.1).

5.5.1 Extent of emissions costs

Table 5.1: Absolute and share of the emission costs ($M\ EUR$) for BAU scenario. All values are scaled to 100% population. The numbers in the brackets show the % share of each sub-population.

Classified based on sub-population for whole area				
	urban	**(rev.) commuter**	**freight**	**total**
	(a)	(b)	(c)	(d=a+b+c)
Total emission costs	0.20 (5.47)	0.96 (25.95)	2.55 (68.58)	3.71 (100.00)
Number of trips [M]	1.27 (62.66)	0.60 (29.52)	0.16 (7.82)	2.04 (100.00)
Total car distance [$M\ km$]	7.81 (11.35)	43.31 (62.95)	17.68 (25.7)	68.8 (100.00)
Classified based on area[4]				
	Munich city	**MMA**	**rest of the area**	**total**
	(a)	(b)	(c)	(d=b+c)
Total emission costs	0.38 (10.24)	1.73 (46.63)	1.98 (53.37)	3.71 (100.00)
Number of links	4804 (11.45)	35317 (84.21)	6624 (15.79)	41941 (100.00)
Total car distance [$M\ km$]	14.04 (20.35)	45.86 (66.66)	22.94 (33.34)	68.8 (100.00)

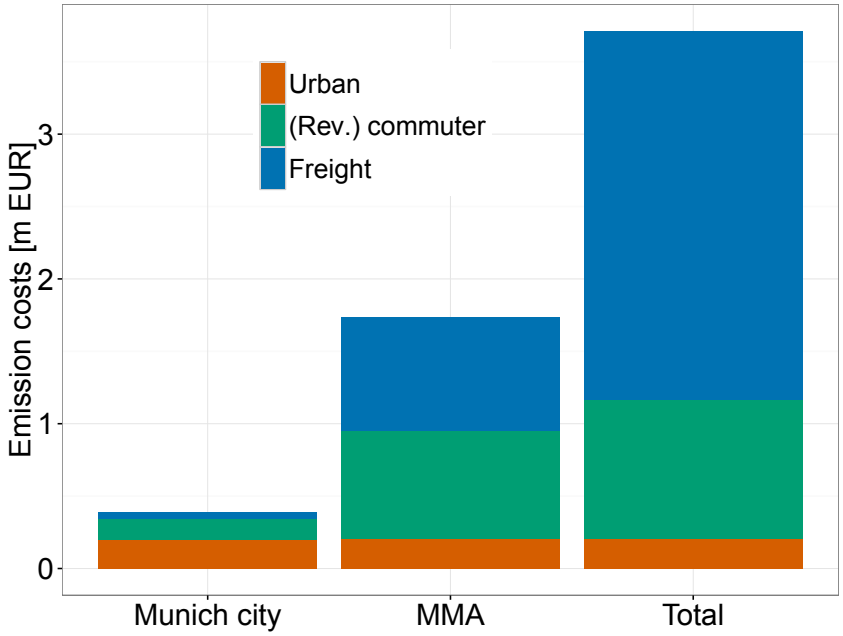

Figure 5.3: Contribution of sub-population in the emission costs for different regions.

[4]The readers should not that since the MMA already includes values inside the Munich city, therefore, only the values for MMA and "rest of the area" sum up to total value.

Tab. 5.1 and Fig. 5.3 show the share of emission costs for BAU scenario categorized based on the geographical area and the sub-population. The absolute daily emission costs caused by all sub-populations for the whole area amount to 3.7 $M\ EUR$. Though, for the whole area, freight car trips represent roughly 7.82% of all car trips, they contribute to approximately 68.58% of the emission costs because freight vehicles emit more emissions than other vehicles and have longer travel distances (mean and median trip distances are 111 and 69 km, respectively). On the other hand, the share of urban car trips is 62.66%, however, it contributes to only 5.47% of total emission costs. Almost all of the emission costs caused by urban sub-population is emitted inside the Munich city whereas the share of emission costs from freight inside the Munich city is very little. Further, most of the emission costs caused by (rev.) commuters are emitted inside the metropolitan area and freight is responsible for most of the emission costs outside metropolitan area.

A comparison of the emission costs from each sub-population can be observed from Fig. 5.3. The Munich city area contributes to only 10% of the total emission costs out of which urban travelers are responsible for more than half of the emission costs (i.e., 0.20 $M\ EUR$ out of 0.38 $M\ EUR$). The emission costs inside MMA (including the emission costs inside Munich city area) is 4 times more than that of the Munich city area and the total distance traveled by car/truck inside MMA is 3 times more than that of the total distance traveled inside the Munich city. Clearly, for the conventional petrol/diesel vehicles, the traveled distance plays an important role to determine the total emission costs.[5]

5.5.2 Changes in emissions costs

Before analyzing the changes in the CO_2 emissions, the impact of the ECMFs on the total emission costs is analyzed. Fig. 5.4 shows the effect of different ECMFs on the emission costs caused by the respective sub-population in different areas. As expected, overall emission costs by tendency decrease with increasing ECMF. This reduction in the emission costs is a combined effect of re-routing and modal shift towards the environmentally friendly modes. As Tab. 5.2 shows, the modal shift is the driving force behind these savings. (Rev.) commuter are better off by already shifting to PT at low values of the ECMFs in all areas. In contrast, in all areas, the emission costs caused by the urban travelers' first decrease marginally (about 0.08%), then increase (about 2%) for $ECMF = 5$ and then decrease again. The significant decrease in the car share of the (rev.) commuters has led to a capacity relief (see Tab. 5.2). As a consequence, the car share for the urban travelers increases and ultimately results in the higher emission costs at $ECMF = 5$. Afterwards, the tolls for the urban travelers become so high that even after further relief in the capacities, the urban travelers are better off by changing to PT transport modes. This, in consequence, eventually diminishes the emission costs of urban travelers. For freight transport where only route choice is allowed, the decrease in the emission costs is – as expected – by far smaller than for the other sub-populations in Metropolitan area and in whole area. On the contrary, in Munich city area, at higher values of ECMFs, a decrease in the emission costs caused by the freight trips is significantly higher than in

[5] Please note that the traffic related to Munich city is included in this case study i.e., the private and commercial traffic of surrounding urban areas are not included in it.

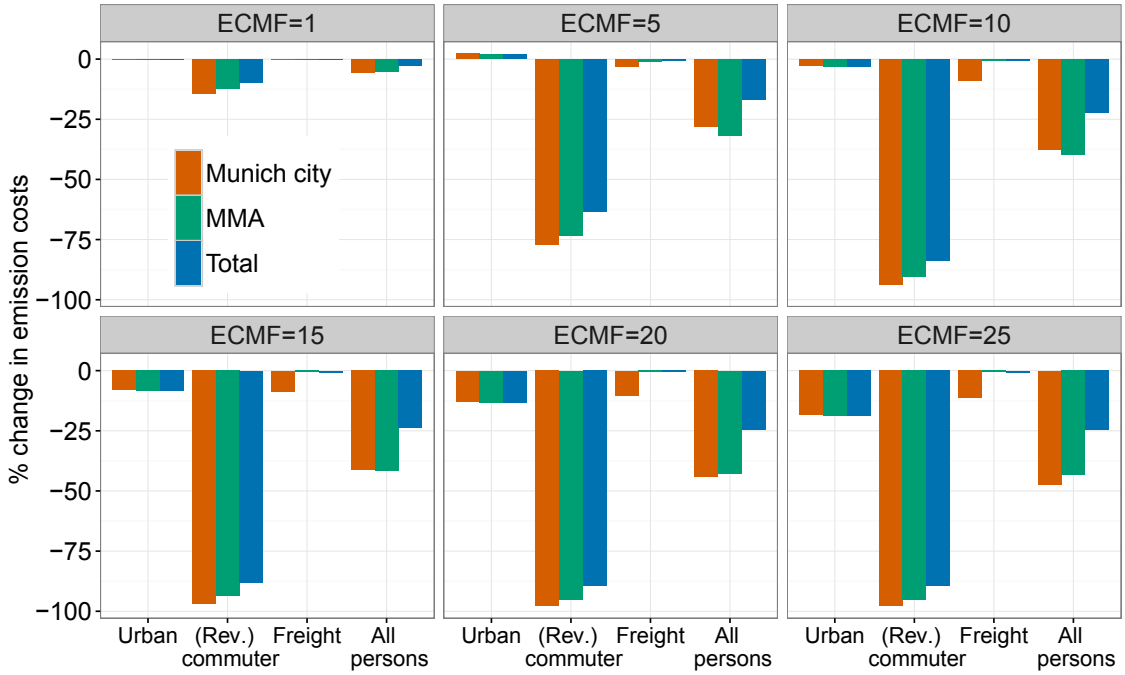

Figure 5.4: Changes in the emission costs (in %) for different sub-population and different region.

other areas because, freight trips are rerouted to outside of the city area.[6]

Table 5.2: Changes in the car trips (in % points) with respect to BAU for various ECMF.

		ECMF					
User group	**BAU**	**1**	**5**	**10**	**15**	**20**	**25**
urban	22.98	0.22	1.39	1.14	0.66	0.20	−0.41
(rev.) commuter	65.57	−7.04	−44.96	−59.57	−62.71	−63.61	−63.67
freight	100.00	No change					
Total	30.72	−0.79	−5.06	−7.29	−8.12	−8.63	−9.15

Overall, for the whole area and all sub-populations, ECMFs and caused emission costs are inversely proportional to each other, i.e., an increase in the ECMF yields a decrease in the emission costs. However, this effect stagnates at higher values of the ECMFs (> 10). Thus, if the objective is to reduce the emission costs of whole area by 20% given the damage cost estimates in Tab. 4.1, a toll level equivalent to 10 times of the damage costs is required, whereas, a factor of 5 is enough to achieve this target inside Munich city and metropolitan areas. However, the objective is to reduce the CO_2 emissions by 20% which is discussed in next section along with the changes in the other pollutants.

[6] From Tab. 5.1, it can be observed that more than half of the emission costs inside Munich city is emitted by urban travelers. Freight trips are responsible only for about 10% (0.04 $M\ EUR$) of the total emission costs inside Munich city. Therefore, the readers should not confuse the big changes in the emission costs for freight inside the Munich city with small changes in the emission costs for freight trips for the whole area.

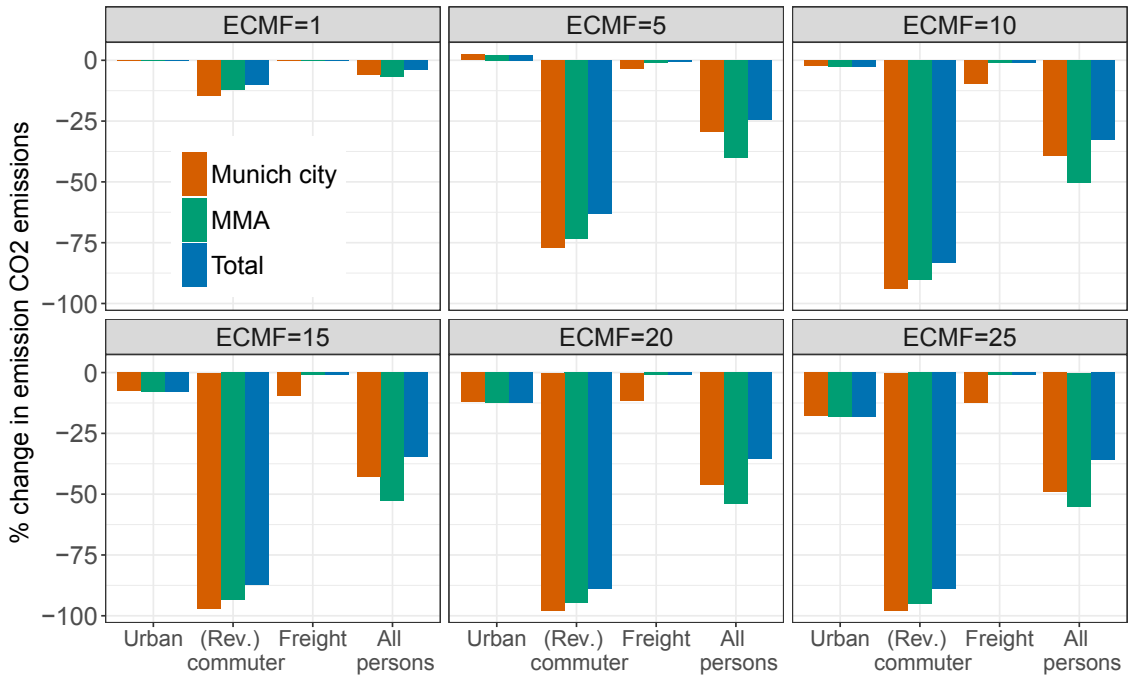

Figure 5.5: Effect of the ECMFs on the CO_2 emissions for respective sub-population and area.

5.5.3 Changes in pollutant types

Following the overall interpretation in the previous section, the impact of different ECMFs on different types of pollutants is presented next. Sec. 5.5.3.1 exhibits the changes in the CO_2 emissions for various sub-population in different areas, whereas, Sec. 5.5.3.2 summarizes the effect of ECMFs on the $NMHC$ emissions for the urban and freight sub-populations which show an exceptional trend.

5.5.3.1 Changes in the CO_2

Fig. 5.5 shows the relative change in CO_2 emissions for various ECMFs on the application of increased damage cost factors. The overall trend for changes in the CO_2 emissions is similar to the changes in emission costs (Fig. 5.4), i.e., for (rev.) commuter, the CO_2 emission decreases significantly with an increase in the ECMF and then become stationary after $ECMF = 15$. For freight, a decrease in the CO_2 emissions is very small except in the city area because, freight reroutes and avoid links inside the city area or shift to shorter distance routes. In contrast, for urban travelers, the CO_2 emission remains almost same at $ECMF = 1$, increases at $ECMF = 5$ and afterwards decreases with an increase in the ECMF. The increase in the CO_2 emissions at $ECMF = 5$ is due to the capacity relief effect (see Sec. 5.5.2).

Interestingly, the emissions reduction target (i.e., 20% reduction in the CO_2 emissions) can be achieved at $ECMF = 5$ (or slightly less) while aggregating all the sub-populations in any area. Recall that for a 20% reduction in the total emission costs, an $ECMF = 10$ or higher for the whole area and an $ECMF = 5$ or higher for Munich city and metropolitan area was necessary. Thus, a common toll (5 times higher than that of from marginal

emission pricing) in all areas can result in 20% lesser CO_2 emissions. Consequently, the avoidance charge of CO_2 will become 350 EUR/ton (see Tab. 4.1 for damage costs of CO_2).

5.5.3.2 Changes in $NMHC$

The emission level of the $NMHC$ emissions, mainly depends on the fuel type, engine type, age of the vehicle and vehicle speed (Haszpra and Szilágyi, 1994). Also, the $NMHC$ emissions are higher for the cold-starts than for a warmed up vehicle (Schmitz et al., 2000; Hoekman, 1992).

For the BAU scenario, the urban travelers contribute to about 39% of total $NMHC$ emissions because:

a) they travel relatively shorter distance (average distance = 6.11 km) and,

b) they perform multiple trips in a day, whereas (rev.) commuters and freight only perform 2 and 1 trip(s) per day, respectively.

All emission pollutants except $NMHC$ emissions show the trend similar to the changes in CO_2 emissions, however, the changes in the $NMHC$ emissions for the urban and freight user groups show an exceptional trend and thus, is presented next. Fig. 5.6a shows the effect of the ECMFs on the exhaust of the $NMHC$ emissions for the urban travelers and freight trips, aggregating for the whole area. With this, the following can be observed:

1. **Urban:** Pricing emission increases the number of urban car trips (see Tab. 5.2) and decreases their average car distance (see Fig. 5.6b). It means, some of the PT users with short trip distance are better off by shifting to the car mode. This eventually results in higher $NMHC$ emissions for the urban travelers. On the contrary, at $ECMF = 25$, even after the decrease in the average trip distance, the $NMHC$ emissions is reduced by more than 2% due to a significant drop in the car share.

2. **Freight:** The freight sub-population is somewhat different than all the other sub-populations. The average trip distance decreases with an increase in the ECMF, but $NMHC$ emission increases. The average trip distance of the freight trips is very high (average distance = 111 km), therefore, it is less likely that the small change in the average trip distance will impact the $NMHC$ emissions significantly. Further, the freight vehicle fleet, fuel type, age of the vehicle do not vary, thus, presumably, the freight trips shift from motorways to local roads increases the $NMHC$ costs.

   It has been observed that total link counts increase with an increase in the ECMF and average trip distance decreases (see Fig. 5.6b) with an increase in the ECMF. That is, the freight trips are shifted from longer links to multiple shorter links. A detailed closer analysis of these numbers show that the major shift occurs from the motorway (faster speed links) to the local and distributor roads (slower speed links). Consequently, the $NMHC$ emission rise with an increase in the ECMF.

This analyses show that the CO_2 reduction target may be achieved at $ECMF = 5$, however, this may also lead to some adverse effects due to the changes in the local pollutants.

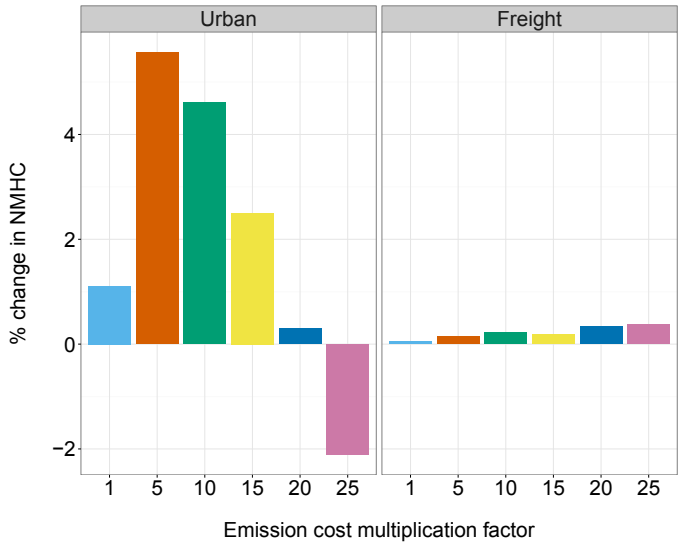

(a) % Change in the *NMHC* emissions

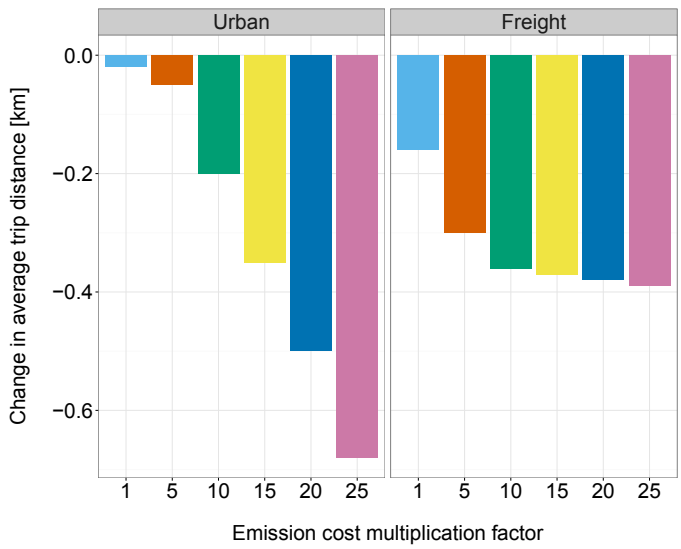

(b) Change in the average trip distance

Figure 5.6: Change in the *NMHC* emissions and average trip distances for urban and freight sub-populations with respect to BAU. The values are aggregated for 100% population.

5.5.4 Economic assessment

This section exhibits an economic analysis to point out the impact of ECMFs on the toll values and system welfare, and to support the findings above. Therefore, only results for ECMF = 1 and 5 are discussed below.

Average toll values The time-dependent, person-specific, link tolls are collected to get the aggregated values under different categories as shown in Tab. 5.3. As expected, the toll values increases with an increase in the ECMF for all sub-populations in all areas (see Tab. 5.3). The freight toll value is significantly higher than the urban and (rev.) commuter because freight vehicle emits higher emissions. In the city area, due to congestion, more

stop&go traffic situations occur which result in higher emissions and higher toll values for freight trips. This happens because freight user group has lesser re-planning choices (freight can select a different route only) and therefore cannot switch to a different travel (emission and congestion free) mode to avoid the congestion. The toll values for $ECMF = 1$ (i.e., toll values for marginal cost pricing) are comparable to the values in the transport literature (also see Sec. 4.5.3). For instance, a central value of 2 $EURct/mile$ is used in the study by Parry and Small (2005).[7]

Table 5.3: Toll values (in EUR/km) differentiated for sub-population and area.

Area	Sub-population	ECMF	
		1	5
	urban	0.03	0.13
Munich	(rev.) commuter	0.02	0.11
city	freight	0.17	0.85
	All persons	0.03	0.14
Munich	urban	0.03	0.13
metropolitan	(rev.) commuter	0.02	0.11
area	freight	0.15	0.75
	All persons	0.04	0.27
	urban	0.03	0.13
Whole	(rev.) commuter	0.02	0.11
area	freight	0.14	0.72
	All persons	0.06	0.37

Table 5.4: Absolute change in the system welfare with respect to BAU scenario. All values are in $M\ EUR$, aggregated for all person in whole area and scaled to 100% population.

	ECMF	
Benefits from ...	**1**	**5**
... changes in emission costs (1)	0.101	0.619
... changes in travel related user benefits (2)	−2.750	−9.626
Toll payments (3)	3.611	15.467
Changes in system welfare = (1) + (2) + (3)	0.962	6.460

System welfare The change in the system welfare is defined as the algebraic sum of changes in the travel related user benefits, toll payments and changes in the emission

[7] The readers are advised to refer to Link et al., 2014; Ricci et al., 2008, for comparison of toll values between various studies and comparison of toll values from different engine types.

costs. Whereas,the travel related user benefits are calculated by converting utility of each agent into monetary terms (see Sec. 4.4.3 for further details on aggregation).

From Tab. 5.4, it can be observed that the overall system gains for $ECMF = 1$ and 5, assuming toll payment as the revenue for the public authorities. Similar patterns are observed for different sub-populations also. Interestingly, the gain in the system welfare at $ECMF = 5$, is 6 times more than that of gain in the system welfare for the damage cost estimates (i.e., marginal emission cost pricing). These additional gains stem from the reduction in congestion externality (see Sec. 4.5.2). Hence, a common toll equivalent to 5 times of the damage costs will not only help in achieving the CO_2 reduction targets but also will generate revenues which could be further re-used in improving the infrastructure.

5.6 Discussion

With the ongoing efforts to bring down the global GHG emissions, there are certain road blocks e.g., growing divergence between CO_2 emissions from the vehicles under the laboratory and under the real-world conditions, continuous growth and rebound effects, etc. In the transport literature, it has been showed that marginal social cost pricing approaches are helpful to reduce the emissions up to a certain level. For pricing air pollution, the damage cost estimates are required. The determination of exact external environmental and health costs is close to impossible since the uncertainty range for these costs is very high. Additionally, the cost factors vary highly depending on the number of affected individuals, buildings, etc. Clearly, with such complexities and political goals, literature suggests the usage of the avoidance cost approach. In this chapter, a parametric backcasting approach is applied to the real-world case study of MMA to determine the avoidance charge to achieve the 20% reductions in CO_2 emissions from transport sector. In this section, the assumptions and simplifications for this case study (see Sec. 5.3.1) are discussed in terms of the influence on the overall results.

The influence of the scenario related assumptions e.g., modeling of commercial traffic, emission and congestion free Public Transport (PT), choice dimensions are already discussed in Sec. 4.6.

5.6.1 Share of road transport sector

The GHG emissions from the road transport sector and all transport sectors together follow similar trends over previous decades, however, from Fig. 5.1, it can be observed that share of GHG emissions from the road transport sector is continuously growing. If the similar trend continues, the required avoidance charge would be higher than the values estimated in this chapter.

5.6.2 Base and projected year demand

The urban travel demand is synthesized using detailed survey data (12/2001 - 12/2002) based on *Mobility in Germany* (MiD 2002, Follmer et al., 2004). Though, the goal is to reduce the GHG emissions by 20% from 1990 levels, however, in absence of any detailed disaggregated data for Munich, the emission reduction target is taken as 20% reduction in

the CO_2 emissions from the survey year. This, is insufficient to determine the true avoidance cost estimates, however, enough to demonstrate the need of the avoidance charge rather than the toll values based on marginal social cost pricing to achieve the 20% reduction in CO_2 emissions. The influence of these simplified assumptions are discussed in the following statements.

a) From Fig. 5.1, it can be observed that the CO_2 emissions from the road transport in years 2001-2002 (survey year) is approximately 20% higher than 1990 levels, it means to reduce the CO_2 emissions by 20% from 1990 levels, the real objective would be to cut the CO_2 emissions approximately by 33.33% from the survey year. Consequently, the avoidance charge would be higher than the estimated values in this chapter.

b) The share of the GHG emissions from the road transport sector is continuously rising (see Fig. 5.1). On the other hand, until 2020, the measures like advances in the vehicle and fuel technology may restrict the further increment in the GHG emissions, however, this would depend on the market penetration of these technologies. Assuming that an aggressive intake of the vehicle and fuel technologies would compensate the CO_2 emissions from future growth and rebound effects, the avoidance cost estimates equivalent to estimates from this chapter are required to achieve the EU emission reduction target.

5.6.3 Evaluated avoidance charge

The damage cost estimates for the CO_2 emissions is 70 EUR/ton (see Tab. 4.1) with lower and upper bounds as 15 EUR/ton and 280 EUR/ton respectively (Krewitt and Schlomann, 2006; Maibach et al., 2008). This value is on higher side while comparing the central estimates from other studies (Maibach et al., 2008, pp. 262-263; Tol, 2005).

The proposed approach finds that to achieve the 20% reduction in the CO_2 emissions, the emissions toll should increase 5 times (i.e., 350 EUR/ton) that of the emissions toll from the damage cost estimates. This implies that a very high toll is required to reduce the CO_2 emissions of transport sector by 20% or this needs to be compensated by some other sector in which the reductions in CO_2 emissions are already ahead of the target.

These simplifications provides several opportunities for future research e.g., i) to forecast the future demand for the projected year and then apply the marginal social cost pricing, and backcasting approach to determine the avoidance charge, ii) to estimate the avoidance charge for the lower and upper bounds of the damage costs, iii) to apply this approach for a greater region (Germany, EU), etc.

5.7 Summary

This chapter points out the probable loopholes in the EU emission reduction targets which can push the emissions far from the target. Further, in this regard, this chapter proposes a parametric backcasting approach and applies it to the real-world scenario of MMA. It has been showed that the damage costs estimates from the literature are not enough to achieve the 20% reduction in the CO_2 emissions. To achieve this goal, the damage cost

estimates should increase approximately 5 times. This may also result in the localized adverse effects. Clearly, the findings are derived under certain assumptions and are very scenario specific, however, a detailed study is required to identify the actual avoidance cost for the whole region.

Part II

Mixed Traffic

Chapter 6

Literature Review of Traffic Flow Model

6.1 Context

In order to model the behavior of the individual traveler in a large urban agglomeration, an efficient traffic flow model is essential. This part briefs about the various traffic flow models from the literature and thereby discusses their limitations in terms of using for the large-scale scenarios.

The main network loading algorithm of MATSim is a so-called queue model. Though the queue model is used in many disciplines, this thesis focuses on the queue models for vehicular traffic. The models and findings from the past studies, relevant to the queue models for vehicular traffic, are explored in this chapter. Moreover, the queue model is extended to simulate the behavior similar to the reality in homogeneous and heterogeneous traffic conditions in Ch. 7. Ch. 8 demonstrates the real-world experiments and compares the computational performances of different traffic and link dynamics of the queue model. The content of this part loosely integrates content from Agarwal and Lämmel (2015, 2016) and Agarwal et al. (2016).

6.2 Homogeneous traffic modeling

6.2.1 Queue models

The credit for origination of queuing theory goes to Erlang (1909). A simple queue model is minimally composed of a) service rate and b) request rate; a queue appears if the request rate is higher than the service rate. In transportation system, the service rate and the request rate are interpreted as supply and demand respectively. In traffic simulators with the queue models, a vehicle travels on a link (road, edge) with an allowed speed until it reaches the downstream end of the link. If inflow to the link is higher than maximum outflow (link capacity), a queue appears. It is simple yet very helpful in traffic flow models due to its computational performance (Gawron, 1998; Simon et al., 1999; Cetin et al., 2003). Besides the already fast base performance of the queue models, additional computing time savings can be obtained from the queue models by scaling down the number of vehicles while at the same time scaling down each link's storage and flow

capacities according to a scaling factor (see Appen. B.5).

There exist various queue models (Point Queue Model (PQM), Spatial Queue Model (SQM), etc.), which can be characterized based on several assumptions. Two important aspects of the queue model are the intra-link and inter-link interactions of the vehicles. The former points to the interaction of the vehicles within the link whereas the latter denotes the interaction of the vehicles on nearby links (e.g., spillback). In this thesis, these are named as link dynamics and traffic dynamics respectively.

6.2.1.1 Point Queue Model (PQM)

A simple queue model is the PQM, in which vehicles are assumed to be stacked on top of each other. Thus, PQM is also known as vertical queue or vertical stack model (Hurdle and Son, 2001; Zhang and Nie, 2005; Zhou and Taylor, 2014). In the PQM, it is assumed that an infinite number of vehicles can be stored on a link, consequently, the length of the queue is zero, and spillback on the upstream link(s) does not occur. In consequence, the inter-link and intra-link interactions are absent (Zhang and Nie, 2005).

6.2.1.2 Spatial Queue Model (SQM)

In the transportation systems, the use of PQM is limited as spillover is common in urban networks. This shortcoming is overcome in SQM (see, e.g., Simon et al., 1999) by having a non-zero length of the queue. Since the physical length of the queue is now non-zero, this is also known as horizontal queue (Kim et al., 2003; Maerivoet and Moor, 2005). In these models, every link has a finite storage capacity which depends on the length of the link, number of lanes, etc. In the SQM, apart from the outflow capacity of the link, a vehicle is allowed to enter the downstream link only if the storage capacity of the downstream link is available. Consequently, in the absence of space on the downstream link, queue reaches onto the upstream link i.e., spill over occurs and therefore, the inter-link interaction of vehicles is present in the SQM.

A few SQMs do not depict intra-link interaction. In such models, – in contrast to the reality – it is assumed that the space originating from the leaving vehicle is available immediately to the following vehicle and subsequently at the upstream end of the link. In other words, on a fully congested link, as soon as a vehicle leaves downstream end of the link, another vehicle enters the upstream end of the link, which is unrealistic.

6.2.2 Discretized models

In the transport literature, many studies try to model the traffic microscopically. This section presents an overview of some of the relevant studies.

Flow dynamics with an intra-link interaction is described by the Kinematic Wave Model (KWM) (also called as Lighthill–Whitham–Richards (LWR) model; Lighthill and Whitham, 1955; Richards, 1956) using the homogeneous traffic conditions on a long crowded road. A stochastic discrete Cellular Automata (CA) model is introduced by Nagel and Schreckenberg (1992) to simulate the homogeneous traffic on a single-lane freeway. In this model, space is divided into cells, time is divided into steps and the state (of the vehicle) is either free (next cell is empty) or jammed i.e., the model is discrete in

nature (Ch. 13; Treiber and Kesting, 2013). The authors find that the model is able to show a start-stop wave, similar to the real freeway conditions.

The KWM realistically describes the queue propagation. Newell (1993) describes a simplified KWM. To numerically solve the full kinematic wave equations, a Cell Transmission Model (CTM) is proposed by Daganzo (1994, 1995) with a computational complexity proportional to the spatial discretization of the links. A stochastic CTM is proposed by Sumalee et al. (2011) to model the stochastic demand and supply. The model is then tested on a hypothetical freeway corridor and an empirical study scenario. However, the model does not incorporate the route choice and FIFO rule at diverges.

In order to reduce the computational burden, a Link Transmission Model (LTM) (Yperman, 2007) is proposed by combining CTM to the cumulative curves of Newell (1993). This model does not have a spatial discretization of the link rather, a complete link is treated as a cell which enhances the computational performances. The traffic propagation under this model is consistent with the KWM. A similar mesoscopic model is proposed by Tordeux (2010) and Tordeux et al. (2014) in which, a particle (vehicle) jumps on a set of sites (road sections) and the jump rate depends on the number of vehicles on the departure and arrival sections. It is shown that the model can reproduce several observed properties of the traffic flow. Clearly, such models obtain more realistic traffic patterns and are more complex. Therefore, higher discretization of the time and space leads to a higher computational time and a higher memory consumption (Nie and Zhang, 2005).

Such detailed model are useful to understand the complex traffic phenomena for small network. However, the usefulness of such models in planning and forecasting context decreases due to the uncertainty for the future demand and the reactions of the travelers. In this direction, Balijepalli et al. (2014) propose a two-regime transmission model (TTM) aiming for a quick model for planning purposes. It is based on the first order traffic flow theory. In contrast to the LTM, this model considers a link in two parts corresponding to the two regimes of the traffic flow (free flow and congested) and models the queue length dynamically based on the shockwave theory. However, the TTM is limited to model the fixed bottlenecks assuming that the bottleneck occurs at the downstream end of a link. As a consequence of the broader discretization, the TTM model may offer the computational advantages over CTM for the same level of time discretization.

In the next section, the LTM and CTM models are compared with the queue models (PQM, SQM) in terms of the traffic flow patterns and required computational efforts for the modeling.

6.2.3 Comparison with the queue models

The differences between PQM, SQM and other models are summarized in many studies (e.g., Zhang and Nie, 2005; Zhang et al., 2013; Frederix et al., 2010). The former two compare PQM, SQM and CTM under dynamic network loading conditions. It is shown that the PQM considerably underestimates the dynamic network travel time. In heavily congested network with spillover, the SQM without kinematic waves also can underestimate the impact of congestion. The latter study compares PQM, SQM and LTM and shows that both PQM and SQM tend to misidentify the flow i.e., lower if the congestion is emerging and higher if the congestion is dissolving. Hurdle and Son (2001) compare the shock wave model with cumulative arrival and departure model in which the latter is

interpreted as PQM and the special case of SQM. It has been shown that both models (shock wave and, cumulative arrival and departure) may yield identical delay estimates. Altogether, there exist many models with varying degree of discretization and abstraction. However, the detailed modeling is resource-intensive and requires high computing systems. E.g., comparing PQM and CTM, the PQM takes the least amount of CPU time and memory whereas CTM takes the most amount of CPU time and memory (Nie and Zhang, 2005).

6.3 Heterogeneous traffic modeling

In absence of the physical segregation, motorized and non-motorized vehicles use the same right of way and thus, increase the vehicular interactions and chances of conflicts. Additionally, the lane discipline and car following methods are scarce and thus modeling such traffic is difficult when applying regular homogeneous traffic flow models. There exists plenty of models to simulate and analyze homogeneous traffic conditions with a varying degree of abstraction and discretization.

6.3.1 Traffic dynamics

There has been a continuous evolution of the CA model after the early CA model by Nagel and Schreckenberg (1992). An attempt is made to study the suitability of the different CA models under mixed traffic condition (Mallikarjuna and Rao, 2007). With the detailed study of several parameters like cell structure, interaction time headways, etc., it is found that the flow declines as the interaction between the vehicles increases.

Similar to the CA model, Gundaliya et al. (2008) develop a grid based approach to include vehicles with different static and dynamics characteristics. In contrast to the earlier CA model (Nagel and Schreckenberg, 1992), the cell size is made smaller such that a vehicle is approximately equivalent to multiple of the cells. The author also compares the simulation time for the CA and grid based models. The former is about about 23 times faster than the latter. The higher degree of discretization explains the higher simulation time. Similarly, the CA model is modified by Mallikarjuna and Rao (2011) to model the heterogeneous traffic conditions without lane-discipline. The authors find that the area occupancy is suitable to describe the heterogeneous traffic. The cell structure and the updating criteria of the cells are modified based on the microscopic traffic variables (e.g., vehicle size, mechanical characteristics, lateral distribution, lateral gaps, etc.). The model results are validated using field data.

Only a limited number of contributions develop models analytically or otherwise to deal with such heterogeneous conditions. The LWR model is extended by Wong and Wong (2002) to include the effect of heterogeneous road users. The model allows overtaking in uncongested as well as congested regimes. In the similar direction, the LWR model is extended analytically for mixed traffic conditions by Zhang and Jin (2002). With an example of the passenger car and truck, the authors show that the model satisfies FIFO if the free flow speeds of both vehicle classes are the same. The authors state that the model can be used to study the traffic evolution at long crowded highways where the low performance vehicles entrap high performance vehicles. Similarly, another analytic multi-

class dynamic network loading model is proposed by Bliemer (2007) which consists of a link and a node model. The former computes the queue inflows and potential outflows and the latter determines the actual outflow depending on the node structure. However, in contrast to the model by Zhang and Jin (2002), it lacks in showing the kinematic waves.

There exist some microscopic models to model the multiple vehicle types simultaneously, which discretize the link for detailed modeling. A multi-class CTM is proposed by Tuerprasert and Aswakul (2010) in which vehicles with different free-flow speed and vehicle length can be included. With the help of 6 network test cases, the authors show that the multi-class CTM is significantly more accurate than single-class CTM without compromising the computational complexities. Similar to the stochastic CTM proposed by Sumalee et al. (2011), Szeto et al. (2011) propose a Monte-Carlo based stochastic CTM. The latter overcome the limitations of the former by considering route choice and FIFO rule at diverges. It also correlates between the model parameters of the flow-density relationship of the various cells. In addition to the former, the latter model is suitable for multi class vehicle types under certain implementation issues. However, both models have higher computational burden due to discretization.

From the above discussion, it is clear that the discretization of links increases the complexity and the computational efforts. Therefore, certain studies focus on somewhat lesser discretization. E.g., Mathew et al. (2013) develop a strip based approach to model mixed traffic conditions while considering lateral movements of the vehicles. The approach is implemented using a simulator Simulation of Urban Mobility (SUMO) (Behrisch et al., 2011). In this model, a lane of the link is divided into several strips and the vehicles are assumed to move laterally along the strips. The number of strips a vehicle can occupy is decided by the vehicle width. Similarly, a LTM for multiple user classes is proposed by Smits et al. (2011) by considering a link and node model. In this model, in free flow regime, a faster vehicle can overtake the slower vehicles and all vehicles follow FIFO in the congested regime.

Arsan and Koshy (2005) present a somewhat different approach than the above. The authors develop an analytical model based on a coordinate referencing technique to include the mixed traffic conditions without lane discipline. In this approach, the entire road is assumed as a single unit and vehicle occupies a specific area on the road which is represented using the coordinates with reference to an origin. The model is then validated by collecting the field data on a 1000 m road stretch.

To summarize the above, there are plenty of models to simulate heterogeneous traffic conditions for mid block sections. However, some lack in the the realistic representation of the traffic conditions, some lack in the applicability for the large-scale urban agglomeration with dynamic demand due to higher degree of complexities. In this direction, a queue model is extended for the mixed traffic conditions in an agent-based simulation framework (Agarwal et al., 2013, 2015). In this, the original FIFO queue model is replaced by an *earliest-link-exit-time* approach such that faster vehicles can overtake slower vehicles in the uncongested regime (see Sec. 7.2 for details). The modification of the queue model increases the simulation time marginally (see Sec. 8.3.1).

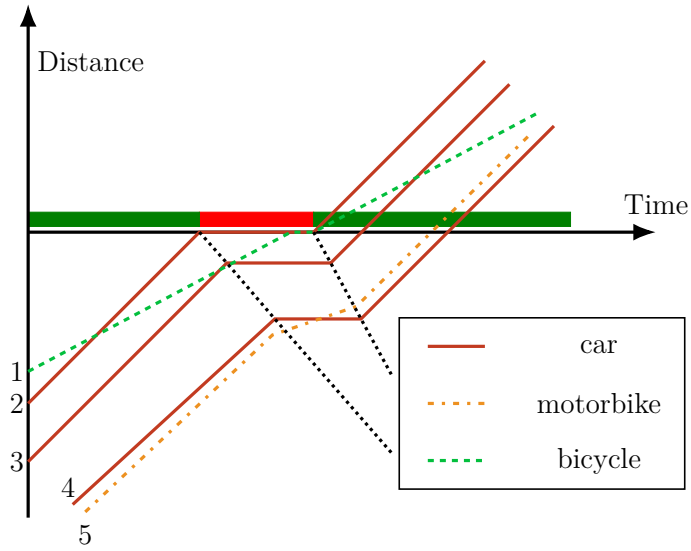

Figure 6.1: Schematic of the seepage link dynamics. Adapted after Oketch (2000).

6.3.2 Link dynamics

The models discussed above do not consider the overtaking of the larger vehicles by smaller vehicles in congested or almost congested conditions. Due to the acute size of smaller vehicles (motorbike, bicycle, etc.), they are non-sensitive to the width of the road but they affect flow of other vehicles remarkably. Moving forward in the similar direction, the present paper investigates the behavior of smaller vehicles in capacity and congested regimes, sometimes called *seepage action* (Oketch, 2000, 2003). In congested regime (where queues build up) and/or at traffic signals, smaller vehicles can pass the faster vehicles by moving continuously across the gaps between stationary congested vehicles, and come in front of the queues (Wang et al., 2004). Fig. 6.1 illustrates the seepage behavior at a traffic signal in which at red signal, motorbike (trajectory 5) and bicycle (trajectory 1) do not stop at the end of the queue (after cars) rather continue traveling towards the front of the queue. Eventually, bicycle and motorbike leave before already queued cars. This behavior is a common practice in the industrializing countries.

Seepage behavior is also known as *lane filtering* (passing between stationary vehicles) (FEMA, 2009), *lane sharing* or *lane splitting* (passing between moving traffic) (FEMA, 2009). In a study in the Paris region, lane splitting is found to be a systematic practice (Aupetit et al., 2014). The findings are derived by monitoring the trips made by 11 motorbike riders for about a month on entire Paris network accounting for 9662 km cumulative distance. In New South Wales, *under the Road Transport Legislation Amendment (Lane Use by Motor Bikes) Regulation 2014*, lane filtering is allowed legally (Centre for Road Safety, accessed 2014) starting from July 1, 2014. This was done in order to reduce congestion and to avoid rear end collisions between motorbikes and cars. Some reports (FEMA, 2009; Hurt et al., 1981) state that the lane splitting is safer due to the increased visibility of motorbikes, on the contrary, some other studies (Clarke et al., 2004; Sperley and Pietz, 2010; MAIDS, 2003) find that this behavior makes motorcyclists more vulnerable and one of the other causes of motorbike accidents. Although, it is a matter of debate to chose between safety and other benefits (congestion and emission reduction, increased

capacity, increased travel time reliability, etc.; Oketch, 2003; FEMA, 2009; Hurt et al., 1981; Sperley and Pietz, 2010; Ellis, 2006), the objective of the thesis is limited to develop a heterogeneous traffic model which is able to handle the existing seepage behavior and to quantify some of the benefits.

In the literature, a few contributions try to study and model this behavior. Oketch (2000) makes an attempt to implement this behavior using the lateral movement model. Nair et al. (2011) present a macroscopic multi-class 'porous model' for seepage, in which the traffic stream is considered as a porous medium, and each vehicle type represents a class. The vehicle class is considered to move through a series of pores and speed is determined by the availability of pores. Asaithambi et al. (2013) address the issue of seepage of motorbikes at traffic signals. The authors use exclusive stopping space for motorcycles (ESSM) in front of the queue at intersections and find it beneficial for all modal splits except when the share of cars is dominant in the traffic composition.[1] Similarly, Fan and Work (2015a,b) develop an analytical *creeping* model as a multi-class generalization of the CTM. Comparing the test results of the creeping model to the porous model, the authors find that the proposed model describes the overtaking and the dynamics of the creeping in the heterogeneous traffic flow.

A related situation is the evacuation of large urban areas, e.g., in the case of tsunamis.[2] As the evacuees usually want to exit the affected area as fast as possible, it is expected that seepage occurs. This situation is addressed in a small evacuation experiment, where pedestrians are evacuated from an open ground to an exit zone (safe place) connected by a narrow street. The seepage behavior of pedestrians is studied under different mixing ratio of the *stationary* cars (Klüpfel and Hebben, 2010).

6.4 Rationale

6.4.1 Traffic dynamics

With the background described above for homogeneous and heterogeneous traffic conditions, it can be noted that the detailed and discretized models are accurate to replicate the realistic traffic flow patters but are resource-intensive. However, minimally,

i) to simulate the demand from an urban agglomeration on a high resolution network,

ii) to predict the behavior of individual travelers under dynamic network loading conditions and

iii) to test the various policies in a planning context,

a computationally efficient model is required which can replicate the realistic traffic flow patters at a link level aggregation. At least for these reasons, this thesis focuses on extending the queue model for the mixed traffic situations rather than addressing the

[1] This behavior of motorbikes and other smaller vehicles (e.g., bicycle or bike) is common in most of the developing nations. Lee and Wong (2016) develop a position choice model for motorbikes. The model is able to replicate the queue formation of the motorbikes in heterogeneous traffic conditions at signalized intersections.

[2] see, e.g., Taubenböck et al., 2013, for a detailed overview of problems that arise when planing the evacuation of whole cities.

more general LWR models or other detailed models. The queue model mainly looks up and stores agents' entry/exit information; however, the link travel time of the agent is not fixed rather dynamically updated based on the state of the link. Thus, the queue model can replicate the realistic queuing and spill-back patterns. However, as discussed in Sec. 6.2.1, *within link dynamics* (intra-link interaction) of the vehicles on the link is missing in the SQMs for the mixed traffic conditions.

The limitation of the missing intra-link interaction in the SQM can be surmounted by integrating backward traveling holes (Charypar et al., 2007b; Eissfeldt et al., 2006) in the SQM. Hence, such SQMs are more realistic and show characteristics similar to the simplified KWM. In fact, Flötteröd (2016b) shows equivalence of such SQM with the double ended queue model. This thesis integrates this concept into an existing SQM to replicate the realistic traffic patters at the cost of a very little additional computational effort. For this, an activity-based travel demand simulator, MATSim (see Ch. 2) is used, which uses a SQM (Gawron, 1998; Simon et al., 1999; Cetin et al., 2003). In this thesis, the proposed approach is called as *with holes* traffic dynamics.

6.4.2 Link dynamics

The seepage models discussed in Sec. 6.3.2 are highly detailed models. Consequently, they are CPU-intensive and unsuitable for simulating large-scale scenarios. The literature lacks for the studies focusing on the modeling of traffic demand under mixed traffic conditions and allowing the seepage action. To the best knowledge of the author, there exist no other simulation framework to model the *seepage* behavior under the highly dynamic conditions observed in the real-world traffic in general and in particular in the case of evacuations. With the help of the proposed approach, it will be possible to simulate the large-scale evacuation scenarios under mixed traffic conditions and allowing seepage behavior. It is assumed that evacuation model also would be more realistic after application of the seepage action.

6.5 Research approach

The default mobility simulation in MATSim is a queue model in which the traffic dynamics is modeled with waiting queues (Gawron, 1998; Simon et al., 1999). The queue model in MATSim is a SQM therefore, from here onwards, queue model refers to the SQM.[3] Fig. 6.2 shows an overview of the various traffic and link dynamics in the queue model. Historically, MATSim simulates the traffic flow of the vehicles by a First-in-first-out (FIFO) queue model without intra-link interaction. For heterogeneous traffic conditions, inclusion of different vehicle classes is necessary which is introduced by Agarwal et al. (2013, 2015). This thesis introduces the intra-link interaction of vehicles (with holes traffic dynamics) in Sec. 7.2.2 and seepage link dynamics in Sec. 7.2.4. For reference purpose, the two pre-existing link dynamics – namely, FIFO and passing of the queue model without holes – are summarized in Sec. 7.2.1.

Further, the relationship between the fundamental variables of the traffic flow (flow,

[3]The queue model in MATSim can behave as PQM by setting sufficiently high value of the link storage capacity (see Sec. 7.2). However, this is omitted in this thesis due to its unrealistic nature.

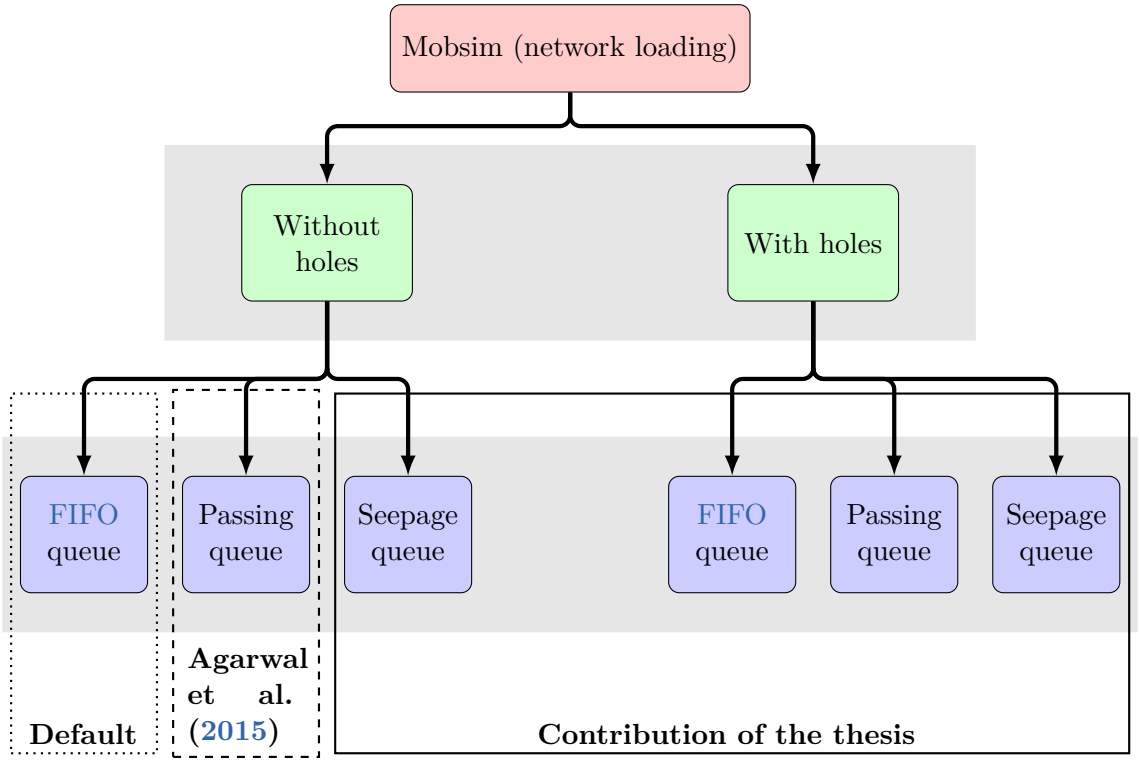

Figure 6.2: Queue model extensions in MATSim.

density and speed) is established using FDs in Sec. 7.4, and the robustness of the models is tested in Sec. 7.5 by showing the flow-density contours, average bicycle passing rate contours, speed-density profiles and spatio-temporal plots. A real-world simulation experiment and a comparison of the computational performances are presented in Ch. 8.

Chapter 7

Extensions of the Queue Model

7.1 Overview

This chapter first exhibit the salient characteristics and implementation of the queue model. The existing link dynamics (FIFO and passing) are explained briefly for the comparison purpose. This is followed by the methodology for the main contributions of the thesis to the queue model model i.e., the *with holes* traffic dynamics and the *seepage* link dynamics are presented. Further, the experimental set up to generate various FDs is demonstrated. The set up is followed by the FDs and robustness tests for different traffic and link dynamics of the queue model. This chapter is an edited version of Agarwal and Lämmel (2015, 2016) and Agarwal et al. (2016).

7.2 Methodology

The network loading algorithm of MATSim is a queue model which tracks agents only at the link entry, exit and never in between. This makes the queue model computationally efficient. The basic functionality of the queue model is presented next.

7.2.1 Traffic dynamics : without holes

In this simulation framework, the physics of a link (l) is determined by the free speed link travel time ($t_{l,free}$), flow capacity ($c_{l,flow}$) and storage capacity ($c_{l,storage}$). These, in turn, are computed from the link length (ℓ_l), number of lanes, and the maximum speed on the link ($v_{l,max}$). The flow capacity or link outflow is the maximum number of vehicles that are allowed to leave the link in one time step (typically 1 sec), whereas the storage capacity of a link is the maximum number of vehicles that can be placed on the link. Different vehicle classes (types) are introduced by Agarwal et al. (2015). A vehicle class[1] minimally needs maximum speed $v_{v,max}$ and PCU of the vehicle class. Thus, different vehicle sizes are taken into account using the vehicle-specific PCU, which is applied both

[1] In the simulation, a vehicle type exhibit the static and dynamic characteristics, e.g., speeds and sizes of car, bicycle (bike), etc. A vehicle is assigned to each agent and this vehicle belongs to one of the predefined vehicle types.

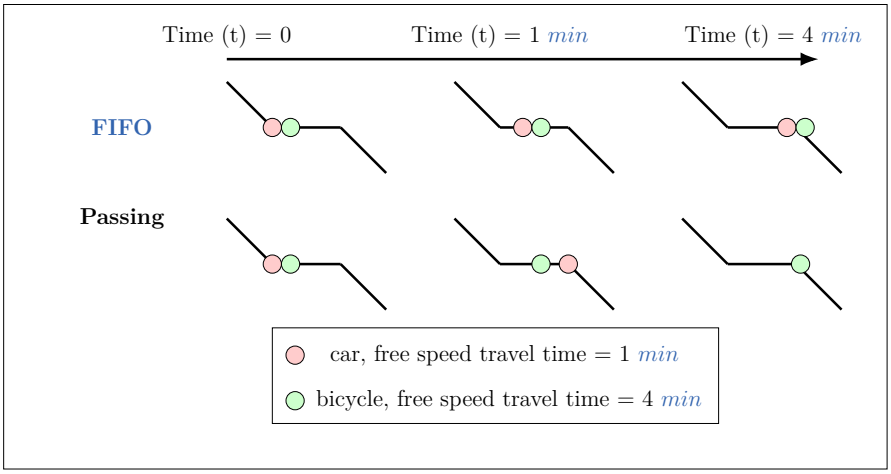

Figure 7.1: Schematic diagram differentiating FIFO and passing link dynamics (adapted after Agarwal, 2016).

to the flow and to the storage capacities. Similarly, the vehicle-specific maximum speeds ($v_{v,max}$) may be lower than the link speed; always, the smaller of the two is used as shown in Eq. 7.1.

The default variant of the queue model in MATSim processes the vehicle queue on each road segment (link) according to the FIFO order. However, the overtaking of the slower vehicle by faster vehicle in free flow regime is also possible by optionally using a passing link dynamics. The free speed travel time on the link ($t^v_{l,free}$) for each entering vehicle is computed as

$$t^v_{l,free} = \frac{\ell_l}{min(v_{l,max}, v_{v,max})} \,. \tag{7.1}$$

Furthermore, the earliest link exit time ($t_{l,earliest}$) is computed as $t_{l,entry} + t^v_{l,free}$, where $t_{l,entry}$ is the time when a vehicle enters the link. Subsequently, the vehicle is added to the queue data structure, and its storage consumption is noted. Afterwards, this queue data structure is sorted based on the earliest link exit time. Consequently, faster vehicles can overtake slower vehicles.[2] A vehicle can leave the link and enter the downstream link provided –

1. the vehicle has spent at least $t^v_{l,free}$ on the link,
2. flow capacity of the link is observed and
3. the downstream link has enough space for the vehicle.

If an agent arrives at the downstream end of the link and flow capacity of the link is available, however, the downstream link does not have enough space, spillback (spillover) occurs.

Further, the introduction of backward traveling holes and seepage behavior to the queue model is presented next.

[2] see Agarwal et al., 2015, for detailed description and comparison of FIFO and passing link dynamics.

7.2.2 Traffic dynamics : with holes

As stated earlier in Sec. 6.2.1, absence of the intra-link interactions make queue propagation unrealistic. It means, freed space from a leaving vehicle at downstream end of the link is available immediately to the following vehicle and eventually at the upstream end of the link. In real-life it takes some time for the free space to arrive on the upstream end of the link (Charypar et al., 2007b; Eissfeldt et al., 2006). Therefore, a so-called *backward traveling holes* are introduced into the existing queue simulation as explained further in the following sections.

7.2.2.1 Hole

The space freed by a leaving vehicle is called as 'hole' or 'gap'. As the name depicts, the holes travel backward i.e., opposite to the direction of the traffic flow. Similar to the vehicle class, a PCU and free speed travel time of the hole ($t^h_{l,free}$) on the link are assigned to the hole. In contrast to $t^v_{l,free}$, $t^h_{l,free}$ is the time required by the hole to reach the upstream end of the link. The PCU of the holes is same as the leaving vehicle and $t^h_{l,free}$ is given by

$$t^h_{l,free} = \frac{\ell_l}{v_h} \tag{7.2}$$

where v_h is the speed of the hole. In this thesis, a constant hole speed of 15 km/h is assumed. This corresponds to the speed of the backward traveling kinematic wave in the KWM. It depends mainly on the *reaction time* of the driver and *length* of the vehicle. The hole speed 15 km/h is equivalent to a reaction time of 1.8 sec (=7.5 $m/(15\ km/h/3.6)$)

7.2.2.2 Backward traveling holes

Corresponding to every leaving vehicle, a hole is generated at the downstream end of the link. This hole is then occupied by the following vehicle; thus the hole propagates one step backward. Similarly, the hole continues until it reaches the upstream end of the link. Consequently, after a critical density, the agents cannot enter the link as long as at least one hole is available at the upstream end of the link. Hence, in this approach, space freed on downstream end of the link is available on upstream end of the link after $t^h_{l,free}$. Thus, this approach implicitly introduces an inflow link capacity restriction (also see Appen. B.1), in addition to the existing outflow link capacity. On the contrary, in the queue model without holes, the freed space is available immediately on upstream end of the link which lets the agents enter from upstream link(s) immediately.

7.2.2.3 Consequences for the link geometry

In order to function properly, a link modeled with holes needs to have certain geometrical properties. The problem is that large-scale assignment networks typically give the maximum (out)flow as each link's most important attribute. However, clearly, the maximum flow on a link cannot be larger than the tip of the FD triangle (see FD for the queue model with holes in Fig. 7.2). So the maximum density on the link has to be large enough to move the tip far enough up to fulfill this condition; somewhat intuitively, the number of

lanes needs to be large enough so that a given flow is physically possible. This is discussed further in Appen. B.1.

7.2.3 Comparison of the traffic dynamics

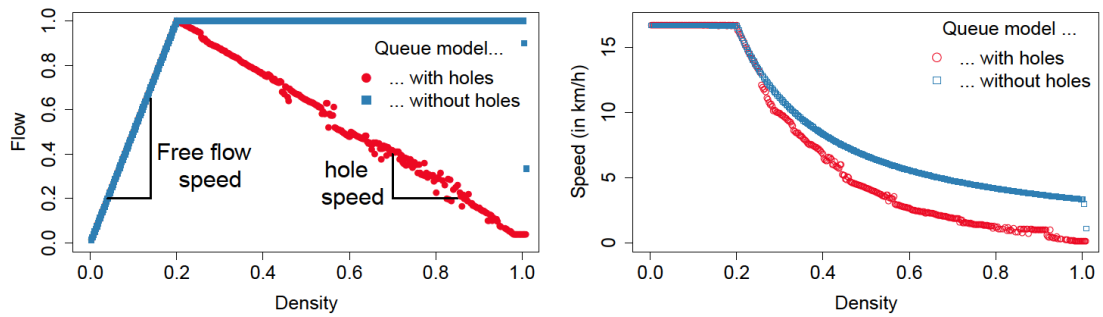

Figure 7.2: Comparison of the FDs from simulations of the car vehicle class. Traffic dynamics = with and without holes; link dynamics = FIFO.

Fig. 7.2 shows a comparison of FDs generated from both traffic dynamics approaches – with and without holes – for a car only simulation.[3] Axes for flow and density are normalized. The FD for the queue model without hole is same as the FD for car with maximum speed 60 km/h in Fig. 7.5. In the free flow regime, both traffic dynamics (with and without holes) show similar behavior i.e., the slopes of the left branches of the FDs are equal to the minimum of the two speeds ($v_{v,max}$ and $v_{l,max}$). Now, since, the intra-link congestion is introduced by inserting holes into the queue model, the free space on the upstream end of the link is not available immediately. Therefore, the slope of the congested branch is reduced to the speed of the backward traveling holes. On the contrary in the queue model without holes, the flow remains constant until density is close to the jammed density and eventually, in the jammed regime, flow decreases to zero with almost vertical slope. It can also be observed that the critical density at which speed starts decreasing is same for both traffic dynamics.[4] However, the rate of decrease in the speed for the queue model with holes is higher than in the queue model without holes. Clearly, the proposed model has produced triangular FD and has a realistic jammed regime.

7.2.4 Link dynamics : seepage

In the direction, similar to the passing queue model, the queue model is further extended in order to allow passing of the larger vehicles by smaller vehicles in the capacity and congested regimes, which is referred as the seepage behavior as explained in Sec. 6.3.2. The general approach for seepage functionality is shown in Alg. 7.1 and discussed next. In the free flow regime, faster vehicles can overtake slower vehicles and therefore, passing is also allowed on the link.

[3] See Sec. 7.3 for the set up and approach to generate FDs. Various other FDs are discussed in subsequent sections.

[4] A clear difference between the FDs for the queue model with holes presented here and FDs presented in the Agarwal et al. (2016) can be observed which is a reaction of the correction due to link geometry (see Sec. 7.2.2.3 and Appen. B.1).

Algorithm 7.1: Seepage algorithm for the queue model.

```
Data: define one or more seep vehicle class(es)
Input: A finite set of links L = {l_1, l_2, ..., l_n}
for at every time step until simulation ends do
    for all links (i.e., l_i ∀ i ∈ (1, n)) do
        if vehicle queued (i.e., t_{l_i,now} > t_{l_i,earliest}) then
            for all queued vehicles do
                if queued vehicle == seep vehicle then
                    if m ≤ C then
                        m++;
                        send queued vehicle to front of the queue;
                        move vehicle to next link;
                    else
                        m = 0;
                        move vehicle to next link;
                else
                    go to next queued vehicle;
        else
            go to next link;
```

1. Define one or more vehicular seep mode(s).

2. On every link, if the (in)flow exceeds its flow capacity, a queue appears. Thus, in the simulation framework, an agent is queued if the current time step ($t_{l,now}$) exceeds the precomputed earliest link exit time ($t_{l,earliest}$) of the agent.

3. In the next step, the vehicles whose earliest link exit time has passed (basically queued vehicle), are identified.

4. For each identified vehicle, it is checked if it belongs to a seep mode. If yes, then it is pushed to the front of queue and, afterwards, the front vehicle (seep mode) leaves the link depending on the flow capacity of the current link and storage capacity of the next link (see last two conditions in Sec. 7.2).

5. After every C seep mode steps, the first vehicle (e.g., car or bicycle) in the queue is allowed to leave. Thus, in traffic streams with significant share of seep mode vehicles, a cyclic process is initiated. E.g., four seep mode vehicles, a front vehicle, four seep mode vehicles, etc. Even in the practical situations, all smaller vehicles do not perform seepage altogether and therefore, the assumption is reasonable. The constant C in this chapter, is assumed to 4 (equivalent to space corresponding to 1 *PCU*), however, the true value need to be calibrated from the scenario specific survey data.

6. If a seep mode vehicle is not found in the queue, the flow dynamic remains unaltered i.e., first vehicle in the queue leaves the link as long as the flow and storage capacities of the involved links are not violated (see conditions in Sec. 7.2).

7. A vehicle class in the simulation framework is differentiated by its size (*PCU*) and

maximum speed of the vehicle class, therefore, in the MATSim simulation framework, seepage is not possible among vehicles of the same vehicle class.

7.3 Experimental design

To understand the traffic flow models and primary relationship between the fundamental variables of the traffic flow (flow q, density ρ and speed v), the FDs play an important role (see Sec. 7.4). In this section, the experimental set up to generate FDs for various link and traffic dynamics of the queue model is presented briefly.

7.3.1 Set up

An equilateral triangular race track network is selected as shown in Fig. 7.3. A triangular track is the simplest form of the network in which agents can continue rotating until they are stopped and different states of the FDs can be achieved. Each link of the network is 1000 m long and the allowed speed on the link is 60 km/h. The flow capacity (outflow) and storage capacities of each link are 1600 PCU/h and 133.33 PCU/km respectively.

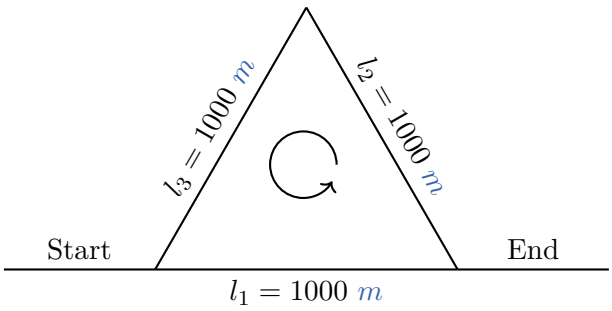

Figure 7.3: Network for race track experiment.

The PCUs and maximum speeds for car, motorbike and bicycle are assumed as 1, 0.25, 0.25 and 60, 60, 15 km/h respectively (Agarwal et al., 2013) unless otherwise stated. Further, in order to check the behavior of the heavy vehicles, truck mode is also used. The maximum speed and PCU of the truck vehicle class are assumed as 30 km/h and 3 respectively.

7.3.2 Steady state

A simulation is run for each discrete density point in the FD. The flow and speed are measured at the end of the track (i.e., at the end of the link l_3). In each simulation run, the modal split and density determine the number of agents for each vehicle class. Thus, these agents are allowed to run on the track until the fluctuations in the flow and speed of each vehicle class are damped. Fig. 7.4 shows the box plots of FDs for the car only simulation. The inset figure shows a few points of the same FD but at a higher resolution. Clearly, the variations in the flow and speed at every density point are low. This situation is referred to as steady state. The average values of the flow and speed at each density point are recorded at steady state condition. For the cases, a steady state is not achieved at the end of the simulation run, the data is not recorded.

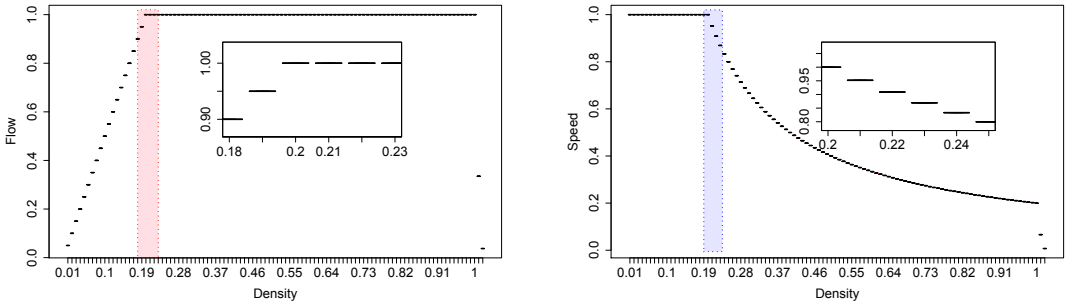

Figure 7.4: Truncated box plots (inset) showing variations in the flow and speed at different densities. Traffic dynamics = without holes; link dynamics =FIFO.

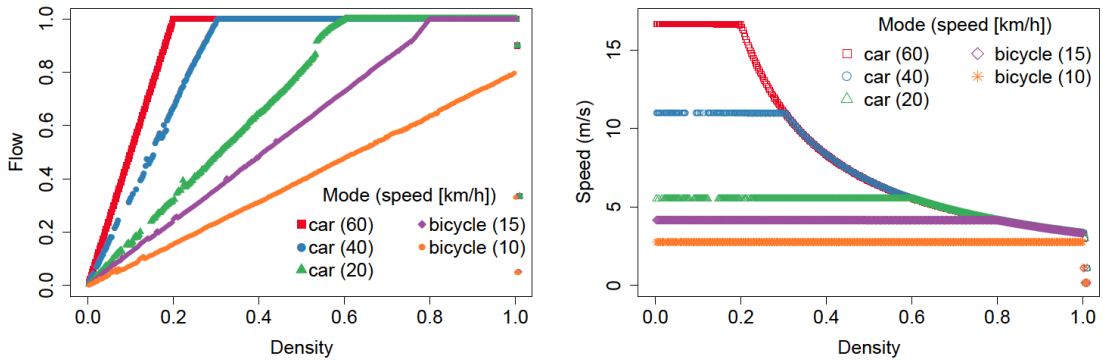

Figure 7.5: FDs from simulations of car only and bicycle only simulations. The car and bicycle vehicle classes with different maximum speeds are considered. Traffic dynamics = without holes; link dynamics = FIFO.

7.4 Fundamental Diagrams (FDs)

For various link and traffic dynamics of the queue model, FDs are plotted to show the relationship between the three fundamental quantities of the traffic flow, i.e., flow (q), density (ρ) and speed (v) and to compare the various traffic and link dynamics with each other.

7.4.1 Traffic dynamics : without holes

First, FDs for the FIFO link dynamics (default in MATSim), passing link dynamics (Agarwal et al., 2015) and seepage link dynamics, in combination with the default traffic dynamics (i.e., without holes; see Sec. 7.2.1) are demonstrated.

7.4.1.1 Link Dynamics : FIFO

Homogeneous traffic Fig. 7.5 shows the flow density curves for different types (classes) of cars and bicycles.[5] Three different car types and 2 different bicycle types are used and

[5]The car with maximum speed of 60 km/h is a different vehicle class than the car with maximum speed of 40 and 20 km/h. The same is true for bicycle vehicle classes.

differentiated based on their speeds only. For each vehicle class, a different simulation run is set up as explained in Sec. 7.3. The slopes of the left branches of the FDs are approximately equal to the maximum speeds of the corresponding vehicle classes. Thus, this branch of the FD is called free flow regime and the flow density relationship is linear in this regime. The primary relationship between the three fundamental variables of the traffic flow ($q = \rho \cdot v$) holds. Afterwards, this branch meets with a horizontal section, where the flow remains constant (maximum flow) over a certain density range. This horizontal section is called as capacity regime. Further, the horizontal section meets with nearly vertical branch of the FD, which is known as jammed regime (Simon and Nagel, 1999). This transition from the capacity regime to the jammed regime is very steep and unrealistic, which is a shortcoming of the standard queue model (Simon et al., 1999).

Comparing the different vehicle classes, one can observe that as the maximum speed of the vehicle class decreases, the slope of the left branch of FD also decreases and consequently, the horizontal section of the capacity regime shrinks. For the slowest vehicle class (i.e., bicycle with maximum speed as 10 km/h), the slope of the left branch of the FD is so low such that the horizontal section of the FD does not exist, and in consequence, maximum flow is smaller than the link outflow (Agarwal et al., 2015).

Heterogeneous traffic Different vehicle types can be simulated together with the FIFO link dynamics. In mixed traffic, if two vehicle classes have almost the same maximum speed, the FDs for the two vehicle classes are about the same. This can also be observed from the FDs of car and motorbike in Fig. 7.10. On the contrary, if the maximum speeds of the two vehicle classes differ significantly and FIFO link dynamics is used, the FDs is mainly governed by the FD of the slowest vehicle class (see Agarwal et al., 2013, 2015, for some examples). Such combinations are avoided here due to the unrealistic nature.

7.4.1.2 Link Dynamics : passing

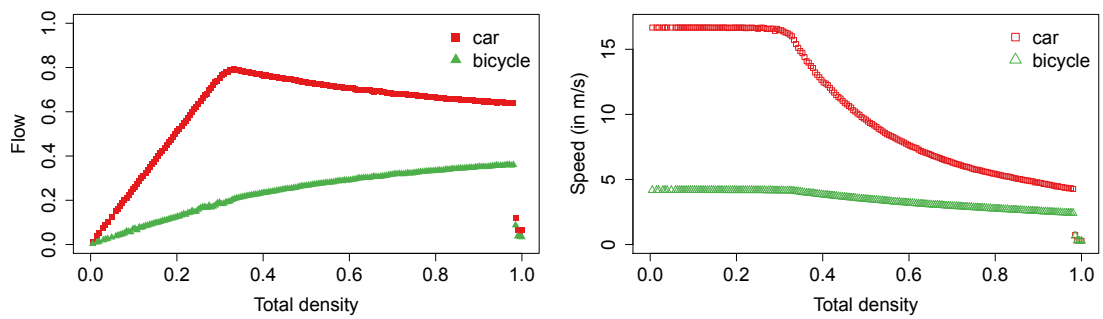

Figure 7.6: FDs from simulation of car and bicycle vehicle classes. Traffic dynamics = without holes; link dynamics = passing. Adapted after Agarwal et al. (2015).

As explained in Sec. 7.2.1, different vehicle types are added to the queue model to observe the passing behavior (Agarwal et al., 2015). The resulting FDs are presented here for reference purpose and to compare with other FDs. Fig. 7.6 shows the FDs from simulation of car and bicycle in equal modal split (in PCU). Clearly, the slope of the

FDs in the free flow regimes are given by the minimum of two speeds (vehicle and link). The capacity regime of the FD for car has approximately linear section with a marginally decreasing slope whereas due to the slower speed of the bicycle vehicle class, flow increases with a smaller rate in the capacity regime. The jammed regimes of FDs for both the vehicle classes have almost vertical sections.

7.4.1.3 Link Dynamics : Seepage

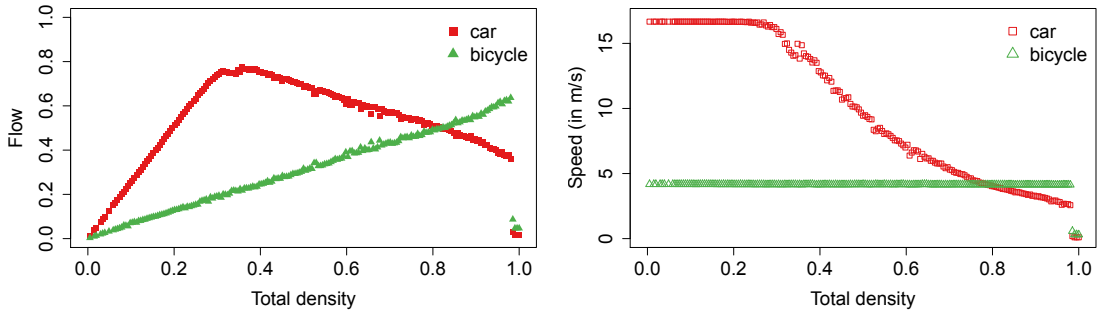

Figure 7.7: FDs from simulation of car and bicycle vehicle classes, and bicycle is considered as seep mode. Traffic dynamics = without holes; link dynamics = seepage.

Fig. 7.7 shows the FDs from the simulation of car and bicycle vehicle classes while bicycle performs seepage. Comparing it with the FDs for passing link dynamics (see Fig. 7.6), it is clear that,

a) the FDs in the free flow regime are about the same for passing and seepage link dynamics,

b) as a reaction to the seepage, in the capacity regime, the flow of car decreases rapidly and the flow of bicycle increases with almost same slope as that of the free flow regime,

c) similar to the jammed regime in the FDs for passing link dynamics (see Fig. 7.6), the transition from capacity to the jammed regime is sudden. Consequently, flow and speed drops to zero with almost vertical slope and

d) the speed of the bicycle remains unchanged until jammed regime is reached.

With these observations, the seepage behavior of the bicycle can be confirmed (also see Fig. 7.12), however, the intra-link interaction is still absent in it and consequently, the jammed regime has steep slope. The backward traveling holes introduces the intra-link interaction (see Sec. 7.2.2) and corresponding FDs are presented in the next section.

7.4.2 Traffic dynamics : with holes

This section illustrates the FDs for different link dynamics in combination with the with holes traffic dynamics. The effect of the introduction of the intra-link interaction is discussed while comparing the FDs of the queue model with and without holes traffic dynamics.

7.4.2.1 Link Dynamics : FIFO

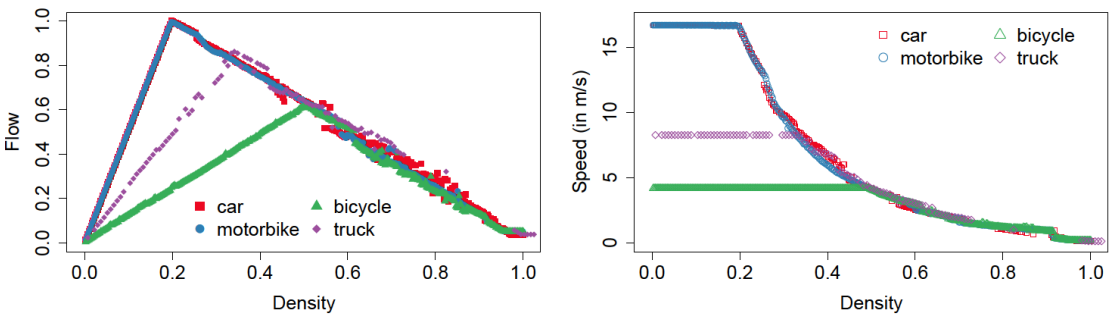

Figure 7.8: FDs from simulations of single vehicle classes (car, truck, motorbike and bicycle). Traffic dynamics = with holes; link dynamics = FIFO.

Initially, the FDs for the homogeneous traffic (single vehicle classes) simulations, namely car, truck, motorbike, and bicycle are generated. For each vehicle class, a different simulation is set up. The resulting FDs are shown in Fig. 7.8. All vehicle classes show triangular FDs due to introduction of the intra-link interaction such that the slopes of the left (free flow regime) and right (capacity and jammed regimes) branches are determined by the lower of the two speeds (link speed $v_{l,max}$ and vehicle speed $v_{v,max}$) and speed of the backward traveling holes respectively. The car and motorbike vehicle types have different *PCU*s but same speeds (see Sec. 7.3.1). This result in the similar FDs for car and motorbike (points are overlapped on the top of each other). Similar overlapping FDs are also obtained for queue model without holes (see FDs in Agarwal et al., 2015). For truck and bicycle,

a) the maximum flow is achieved at a density which is higher than the density at which the flows of car and motorbike vehicle classes are maximum

b) the maximum flow is lower than the maximum flow of car and motorbike.

In other words, lower the maximum speed of the vehicle type is, higher is the density at which flow/speed starts decreasing and lower is the maximum flow achieved. This is a combined effect of their slower speeds and the implicit inflow capacity constraint. This can also be confirmed from Fig. 7.5 in which, a decrease in the speed results in the lower maximum flow.

7.4.2.2 Link dynamics : Passing

To simulate the heterogeneous traffic conditions, the queue model with holes is also extended for multiple vehicle types as explained in Sec. 7.2.2. For an illustration, the car and bicycle vehicle classes are simulated in the equal modal split (in *PCU* units) and the resulting FDs are shown in Fig. 7.9.

The maximum flow of car is higher than bicycle in a combined simulation because i) car is faster than bicycle and ii) car can overtake the bicycle. Further, as expected, due to

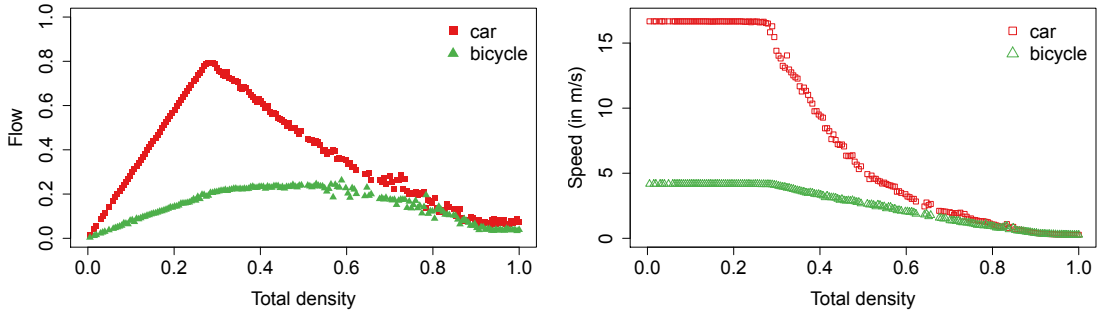

Figure 7.9: FDs from simulation of equal modal split (in *PCU*) of car and bicycle. Traffic dynamics = with holes; link dynamics = passing.

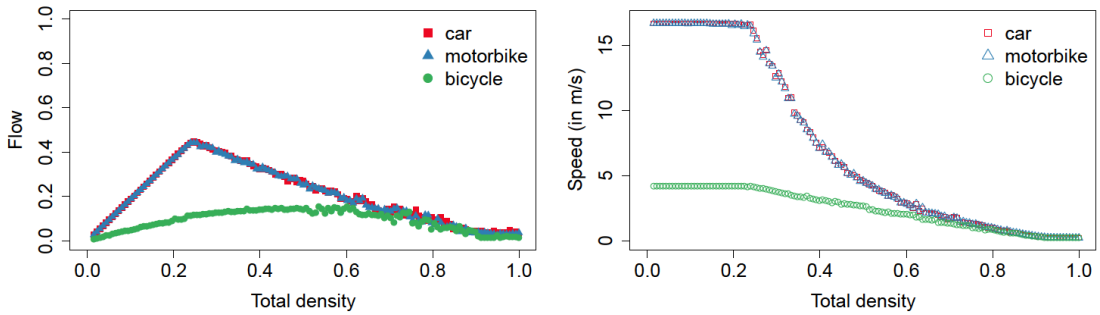

Figure 7.10: FDs from simulation of equal modal split (in *PCU*) of car, motorbike and bicycle. Traffic dynamics = with holes; link dynamics = passing.

the slower speed of the bicycle vehicle class, the maximum flow of bicycle is achieved at a density higher than that of for the car vehicle class. In contrast to the FDs for passing without holes (see Fig. 7.6), the flow of car starts decreasing rapidly after attaining maximum flow and eventually reaches to zero at the jammed density. The rate of decrease in the flow is given by the speed of the backward traveling holes.

In order to observe the behavior of the vehicle types with different *PCU*s and same speeds, another experiment is performed. Fig. 7.10 presents the FDs for car, motorbike and bicycle simulation in equal modal split (in *PCU*) using the passing link dynamics. The FDs for car and motorbike resemble closely with each other because

a) car and motorbike vehicle types have identical maximum speeds and

b) equal modal split (in *PCU*) of car and motorbike is simulated.

The shape of the FD for bicycle is similar to the FD of bicycle in Fig. 7.9 however the maximum flow of the bicycle is lower in the former. Thus, the passing of the slower vehicle (bicycle) by the faster vehicles (car, motorbike) can be observed. This approach can be applied to any number of vehicle types in the queue model.

7.4.2.3 Link Dynamics : Seepage

Single seep mode

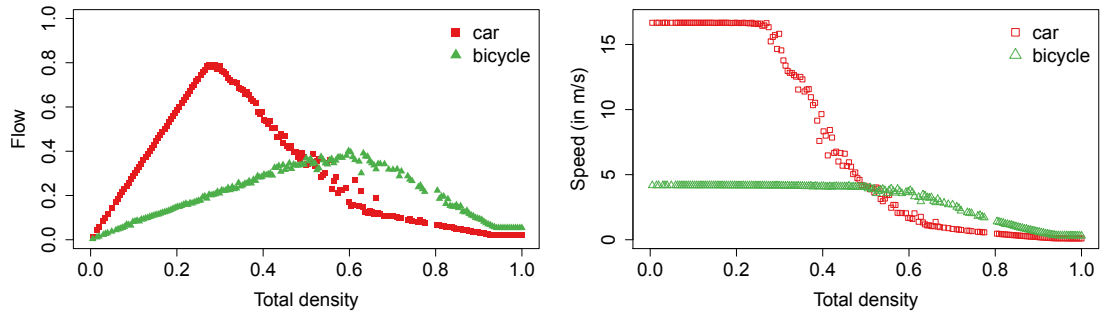

Figure 7.11: FDs from simulation of equal modal split of car and bicycle, and bicycle is considered as seep mode. Traffic dynamics = with holes; link dynamics = seepage.

Car and bicycle vehicle classes (equal modal split in *PCU*) are simulated simultaneously and seepage of bicycle is allowed. The resulting FDs are shown in Fig. 7.11. Comparing Figs. 7.9 and 7.11, following can be observed:

a) the FDs in the free flow regime are identical i.e., passing occurs in the free flow regime,

b) bicycle flow is higher than the car flow at higher densities due to the seepage of bicycle in the capacity and congested regimes (also see Fig. 7.6),

c) the bicycle flow and speed start decreasing at a density higher than in the passing queue model and

d) the flow characteristics of bicycle is marginally affected by the presence of cars but on the contrary, the flow characteristics of the car is significantly affected by the presence of bicycles.

The seepage behavior can be observed both in queue model without holes and with holes (Figs. 7.7 and 7.11 respectively). However, in the former, the flow and speed of bicycle start decreasing almost at the jam density because the space freed by leaving vehicle is available immediately at the upstream end of the link; whereas, in the latter, the transition from free flow/capacity regime to the jammed regime is smooth due to the intra-link interaction.

Multiple seep modes

Due to its small size, motorbike also has high maneuverability and therefore can show the seepage behavior as shown in Fig. 6.1. Therefore, in another experiment, the FDs are also plotted for the mixed traffic situations in which bicycle and motorbike both perform seepage behavior.

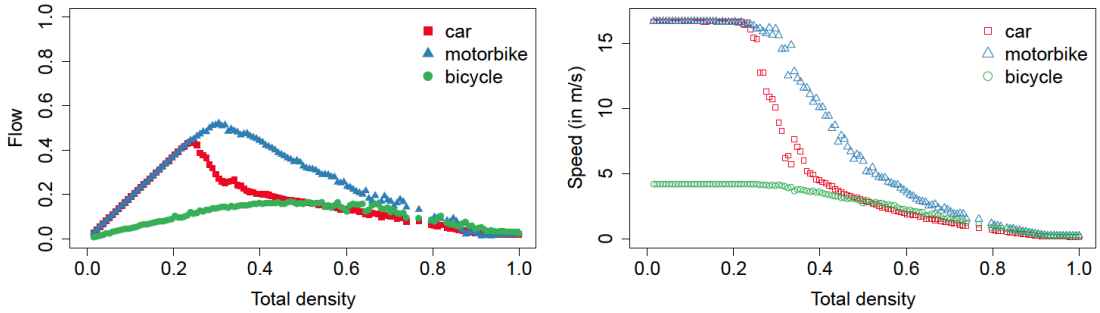

Figure 7.12: FDs from simulation of equal modal split of car, motorbike and bicycle. Bicycle and motorbike are considered as seep modes. Traffic dynamics = with holes; link dynamics = seepage.

Fig. 7.12 shows the FDs from the simulation of car, motorbike and bicycle modes in equal modal split (in *PCU*) using seepage link dynamics. Motorbike and bicycle modes are assumed as seep modes. Again, similar to the Fig. 7.10, the left branch of the FDs for car and motorbike are same due to their same maximum speeds (overlapping data points in Figs. 7.10 and 7.12). Due to the slower maximum speed of the bicycle, the left branch of the FD for bicycle has a flatter slope than the left branch of the FDs for car and motorbike vehicle types. In contrast to Fig. 7.10, after the free flow regime, the FDs for car and motorbike differ significantly. In capacity and jammed regimes, the average flow and speed of the car vehicle class is lower than the average flow and speed of motorbike respectively. Clearly, this is the result of the seepage of motorbike. Therefore, the FD for motorbike looks similar to FD for motorbike in Fig. 7.10.

Though, the bicycle is also chosen as seep mode, the FDs for bicycle vehicle type in Figs. 7.10 and 7.12 differ marginally. This marginal effect is consequence of the lower maximum speed of the bicycle vehicle class. Hence, an important observation is that, if in a traffic stream, the modal share of faster seep mode is significant, the slower seep mode perform seepage marginally. Thus, seepage is producing a behavior similar to what is observed in the developing nations where mixed traffic has smaller vehicles in abundance.

7.5 Sensitivity

In this section, the robustness of the proposed extensions of the queue model is tested. Sec. 7.5.1 shows the various FDs from the simulation of homogeneous and heterogeneous traffic conditions using the queue model with holes by increasing the storage capacity without changing the link (out)flow capacity. The impact of the bicycle share on seepage is illustrated in Sec. 7.5.2. The FDs for the heterogeneous traffic conditions presented in Sec. 7.4 are generated from the equal modal share in *PCU*. The sensitivity of different modal share is demonstrated in Secs. 7.5.2.1 and 7.5.2.2 in terms of the flow-density contours and the average bicycle passing rate contours respectively. These contour plots are also generated using the same experimental set up as described in Sec. 7.3. The car and bicycle vehicle classes are used for the different modal split combinations. For each modal split combination, a separate simulation set up is created. With these, the idea is

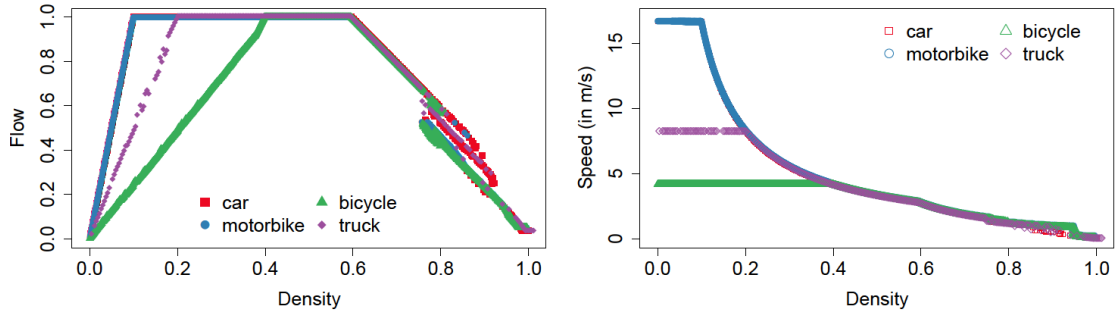

(a) Homogeneous vehicle classes (bicycle, car, motobicycle and truck). Link dynamics = FIFO

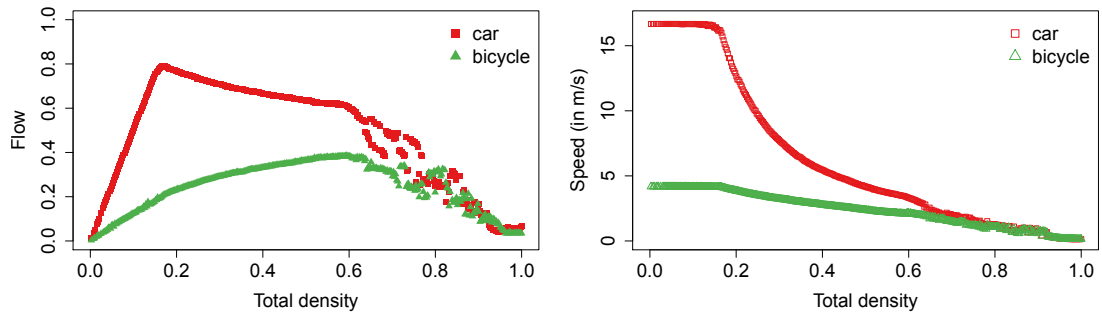

(b) Equal modal split (in *PCU*) of car and bicycle. Link dynamics = Passing

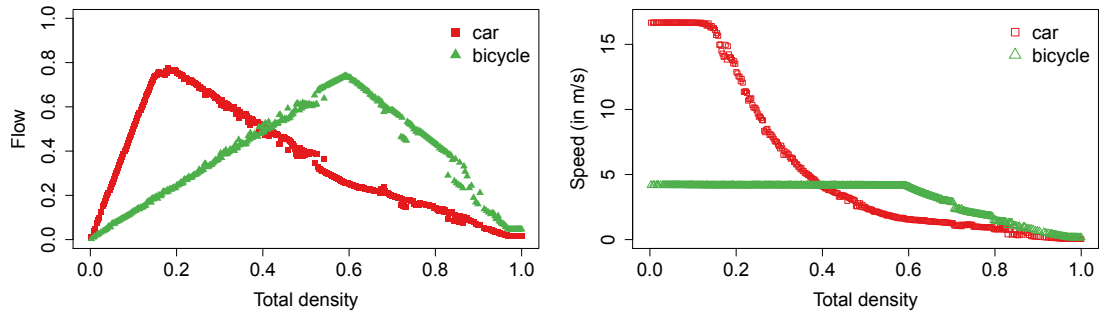

(c) Equal modal split (in *PCU*) of car and bicycle. Link dynamics = Seepage

Figure 7.13: FDs with storage capacity equivalent to 2 lanes. Traffic dynamics = with holes.

to test if the proposed model for the queue model with holes and seepage link dynamics is applicable to different scenarios and also if it produces reasonable FDs in such scenarios.

7.5.1 Storage capacity

In the real-world, roads such as arterials may have the same flow capacity as in the above examples, but increased storage capacity. This could, e.g., happen from having more lanes, but a signal at the downstream and of the link. Therefore, the effect of more lanes (= a higher storage capacity while maintaining the same outflow) on the queue model with holes is shown in Fig. 7.13. In the current simulation framework, lane changing behavior

is not modeled, however, passing (Agarwal et al., 2015) and seepage link dynamics are included in it.

7.5.1.1 Homogeneous traffic

Fig. 7.13a shows the FDs from the simulation of car, motorbike, bicycle and truck separately. It can be observed that, the maximum flow for each vehicle class is capped by the link flow capacity. That is, once the flow reaches the maximum possible flow (1600 PCU/h), it remains constant, until it reaches the jammed branch of the FD, at this point, the flow follows that branch to zero. The slopes of the left and right branches are given by the minimum of two speeds (link and vehicle speed) and speed of the backward traveling holes respectively. The horizontal section appears due to the increased storage capacity. The maximum flows for truck and bicycle also approach to the link flow capacity, however, the horizontal sections in the FDs for truck and bicycle are shorter than the horizontal sections in the FDs for car and motorbike due to their lower maximum speeds.[6]

7.5.1.2 Heterogeneous traffic

Passing only

Fig. 7.13b shows the FDs from the simulation of car and bicycle in equal modal split (in PCU) with storage capacity equivalent to the two lanes. The queue model with holes and passing link dynamics is used. The maximum flow of car is about the same as in the flow of car in Fig. 7.9. However, due to an increase in the storage capacity, the flow of car decreases marginally in the capacity regime and then in the jammed regime, it decreases with the slope equivalent to the speed of the backward traveling holes. In the capacity regime, the rate of decrease in the car flow and the rate of increase in the bicycle flow are about the same i.e., the overall flow (car flow and bicycle flow) is capped by the link capacity i.e., 1600 PCU/h (similar to the car and motorbike FDs in Fig. 7.13a).

Passing with seepage

Fig. 7.13c shows the FDs from the simulation of car and bicycle in equal modal split (in PCU) with storage capacity equivalent to two lanes. The queue model with holes and seepage link dynamics is used i.e., in the free flow regime, car can overtake bicycle whereas in the capacity and jammed regime bicycle can pass car. From Figs. 7.13b and 7.13c, it can be observed that the FDs of car and bicycle are identical in the free flow regimes. Afterwards, similar to Fig. 7.11, the bicycle flow continues to rise with the same rate (= maximum speed of bicycle) as that of the free flow regime until it reaches to its maximum value and meets the right branch of the FD which has the slope equal to the backward traveling wave. From Fig. 7.13c, it can also be observed that as a reaction to the seepage, the maximum flow of bicycle is approximately the same as the maximum flow of car, though at a higher density.

[6] One important consequence of higher storage capacities is that at higher densities, queue model with holes displays higher fluctuations.

7.5.2 Bicycle mixing ratio

For simplicity, the FDs illustrated above are for equal modal share (in *PCU*) of car and bicycle. However, it it important to study the behavior of the queue model with holes and seepage link dynamics for different bicycle share. For this, different combinations of car and bicycle modes are simulated on the race track network using different link and traffic dynamics. For the seepage simulations, only bicycle is considered as seep mode. The results are discussed in the following sections.

7.5.2.1 Flow density contours

Fig. 7.14 shows the flow density contours for the queue models with and without holes using the passing link dynamics.[7] In Fig. 7.14a, the flow density contours for the queue

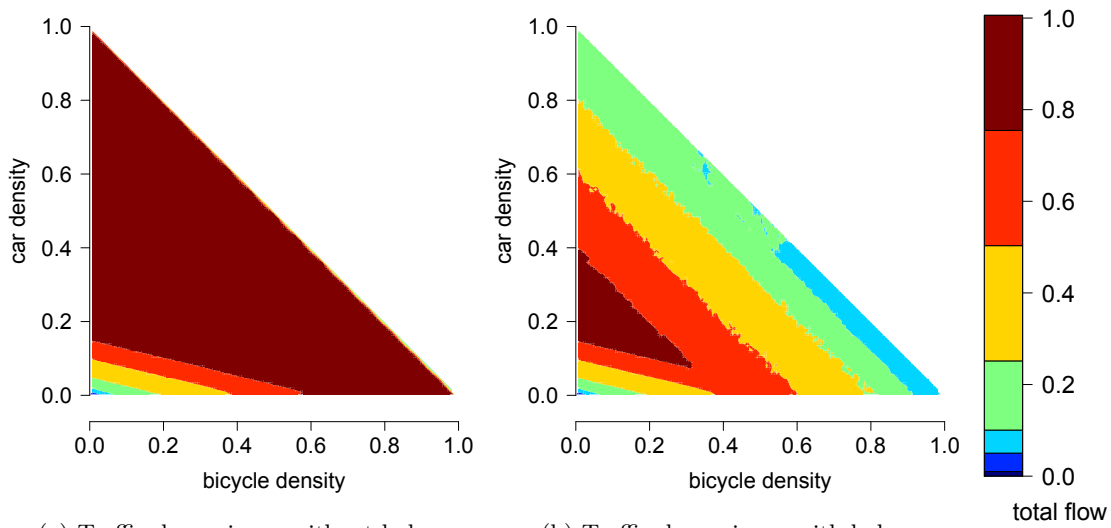

(a) Traffic dynamics = without holes.

(b) Traffic dynamics = with holes.

Figure 7.14: Flow density contours from the simulations of car and bicycle vehicle classes. Traffic dynamics = with and without holes; link dynamics = passing.

model without holes are shown. Clearly, due to nearly vertical slope at higher densities, the contours pointing towards zero flow are hardly visible. One can observe that at diagonal values in the jammed regime, the flow pattern is not realistic due to a sudden drop of flow from maximum ($\approx$ link outflow capacity $\approx$ 1.0) to minimum ($\approx$ 0.0) (see also Figs. 7.2 and 7.5). The effect of the introduction of holes in the queue model is clearly visible from flow density contours in Fig. 7.14b. It can be observed that at lower densities, i.e., in the free flow regime, similar to the FDs in Fig. 7.2, both contour plots look equivalent (i.e., for car density $<= 0.1$ and bicycle density $<= 0.4$). In the jammed regime, a clear demarcation of continuous change in the overall flow can be noted. In other words, the

[7] As discussed previously in Sec. 7.2.3, the queue model with holes introduces the implicit inflow capacity and alters the overall flow (see Fig. 7.2). The flow density contours on a normalized scale for seepage link dynamics are similar to the Fig. 7.14, therefore, the flow density contours only for passing link dynamics are presented here.

transition from the capacity to jammed regime is smoother and realistic than the transition in the queue model without holes. The contour plot in Fig. 7.14b has a close resemblance to the contour plot generated by extending the LWR model analytically (Zhang and Jin, 2002).

7.5.2.2 Average bicycle passing rate contours

As presented previously in Sec. 7.2.4, a major difference between the passing and seepage link dynamics is that in the former, the faster vehicles (e.g., car, motorbike) overtake the slower vehicles (e.g., bicycle) in the free flow regime and in the latter, the smaller vehicles (e.g., bicycle, motorbike) overtake the larger vehicles (e.g., car) in the capacity and/or jammed regimes. Therefore, in this section, the contours for average bicycle passing rate are demonstrated.[8]

The average bicycle passing rate is defined as the average number of bicycles passed by one car on a one km road segment. The detailed methodology is described in Appen. B.2 and resulting contour plots are shown in Figs. 7.15 and 7.16.

Comparison between traffic dynamics Comparing Figs. 7.15a and 7.16a for the passing link dynamics and Figs. 7.15b and 7.16b for the seepage link dynamics, it can be observed that the average bicycle passing rate is significantly lower in the queue model with holes than in the queue model without holes. For the queue model without holes, the average bicycle passing rate increases with an increase in the bicycle density until the jammed regime is reached (see Figs. 7.15a and 7.15b) whereas it increases with an increase in the bicycle density and decreases afterwards for the queue model with holes (see Figs. 7.16a and 7.16b). In contrast to the queue model with holes which introduces an implicit inflow capacity, at higher density, the average bicycle passing rate is unrealistically high due to nearly vertical slope in the jammed regime.

Comparison between link dynamics Figs. 7.15 and 7.16 show the contours from the simulation of car and bicycle vehicle classes using the queue model without holes and with holes respectively. As discussed in the previous paragraph, the average bicycle passing rate in the former is significantly higher than the average bicycle passing rate in the latter. However, as a consequence of the seepage, at higher car density (≈ 0.6 or higher), the average bicycle passing rate is approximately zero (see Figs. 7.15b and 7.16b).[9] Further, as the bicycle density increases (or car density decreases) the average bicycle passing rate increases. As expected, the rate of increase of the average bicycle passing is slower with the seepage link dynamics.

[8] The average bicycle passing rate can express the chances of accidents since the probability of the accidents depends on the vehicular interactions (Newbery, 1988, p. 169). However, in contrast to the average bicycle passing rate in Figs. 7.15b and 7.16b, the number of interactions for the seepage link dynamics will be significantly higher. Thus, in such scenarios, the average bicycle passing rates should be replaced by the *average passing rate* to include all the interactions (passing, seepage). For the simplicity and to highlight the differences between the passing and seepage, the scope of this thesis is limited to estimate only average bicycle passing rate.

[9] It should be noted that for simplicity, the average bicycle passing rate only includes the passing of bicycle vehicle class by car and not passing of car by bicycle. The latter is only possible with the seepage link dynamics. Thus, the plots for the seepage link dynamics do not incorporate all possible passing events.

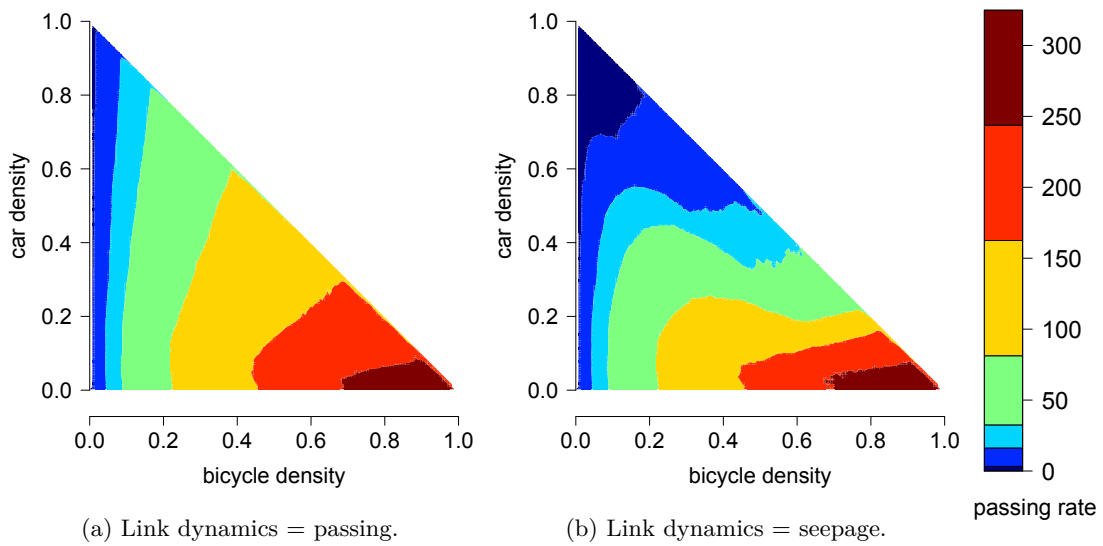

(a) Link dynamics = passing.

(b) Link dynamics = seepage.

Figure 7.15: Average bicycle passing rate contours from the simulations of car and bicycle vehicle classes. Traffic dynamics = without holes; link dynamics = passing and seepage.

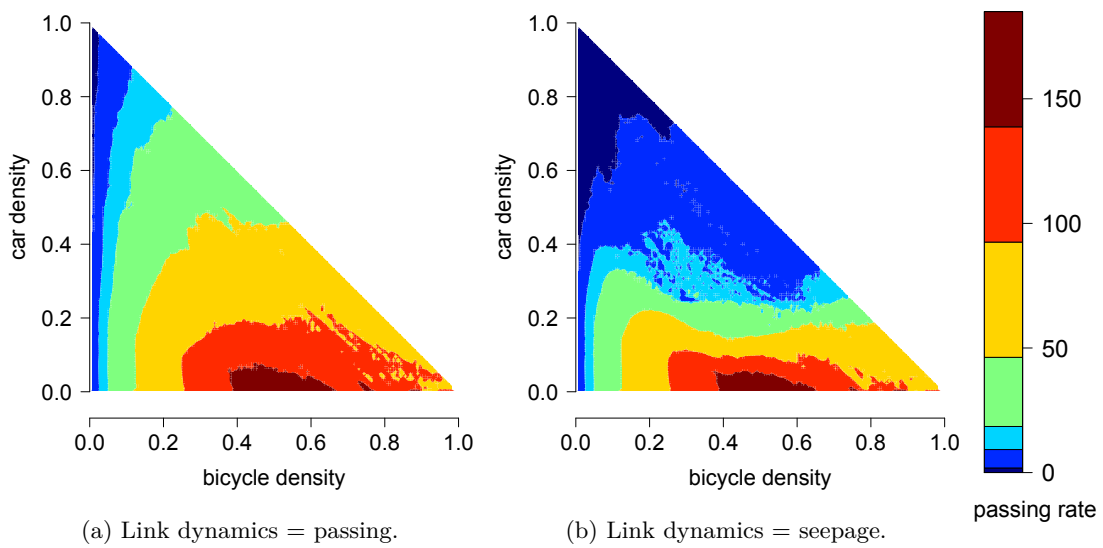

(a) Link dynamics = passing.

(b) Link dynamics = seepage.

Figure 7.16: Average bicycle passing rate contours from the simulations of car and bicycle vehicle classes. Traffic dynamics = with holes; link dynamics = passing and seepage.

7.5.2.3 Speed density profile

The FDs shown in Figs. 7.7, 7.11 and 7.13c are plotted only for the equal modal split and therefore, it is important to test the applicability and to observe the traffic flow characteristics of the seepage queue model under different modal share. Hence, a sensitivity test is conducted using the triangular race track to test the seepage behavior under different bicycle shares and then compare the results with the passing link dynamics. The speed density plots for the passing and seepage link dynamics are shown in Fig. 7.17. Total density, bicycle speed and bicycle share are plotted together such that the sum of bicycle and car share is always unity.

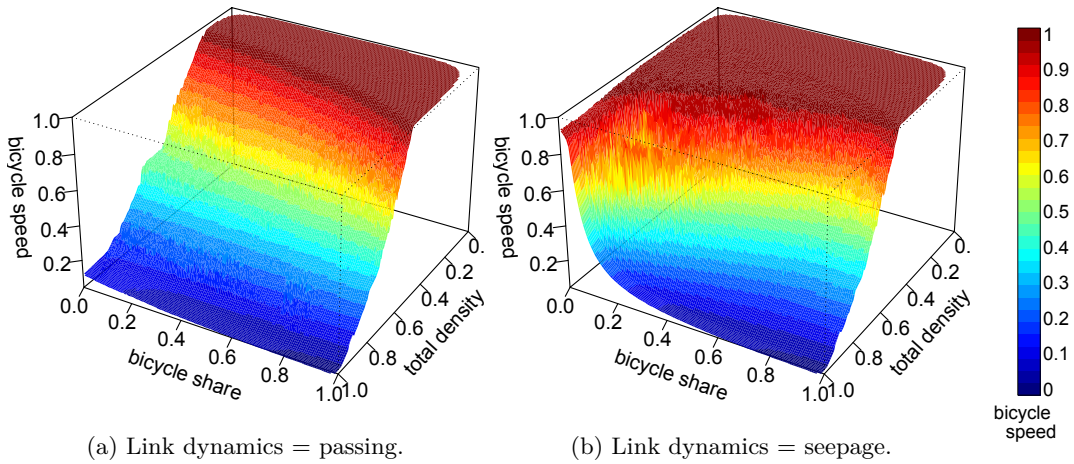

(a) Link dynamics = passing.

(b) Link dynamics = seepage.

Figure 7.17: Speed density profiles from the simulations of car and bicycle vehicle classes. Traffic dynamics = with holes; link dynamics = passing and seepage.

Comparing the speed density profiles for the passing and seepage link dynamics (see Figs. 7.17a and 7.17b respectively), followings can be observed:

1) The speed density profiles for the passing and seepage link dynamics are similar at
   a) density lower than 0.2 i.e., in free flow regime for all bicycle share and
   b) all densities and at higher bicycle share (≥ 0.9) i.e., traffic stream contains mainly bicycle vehicle class.

2) The total density at which the speed of bicycle starts decreasing, increases with an increase in the bicycle share for the passing link dynamics and decreases with an increase in the bicycle share for the seepage link dynamics. Clearly, this is a consequence of seepage; for instance, at bicycle share ≈ 0.2 and in the capacity or jammed regime (i.e., total density ≥ 0.2), the seepage of bicycle allows the agents with bicycle mode to maintain their free flow speed. This, in turn, is not possible with the passing link dynamics.

With the discussion above, it can be noted that the with holes traffic dynamics and seepage link dynamics introduce more realistic traffic flow patters and applicable for all kind of scenarios and traffic mixes.

7.6 Spatio-temporal plots

In order to understand and differentiate the queue model with and without holes, space time trajectories are presented in this section. As described before in Sec. 7.2, the queue model controls the agents only during the link entry/exit to make it computationally faster. Therefore, these trajectories are plotted by interpolating the intermediate points on the link.

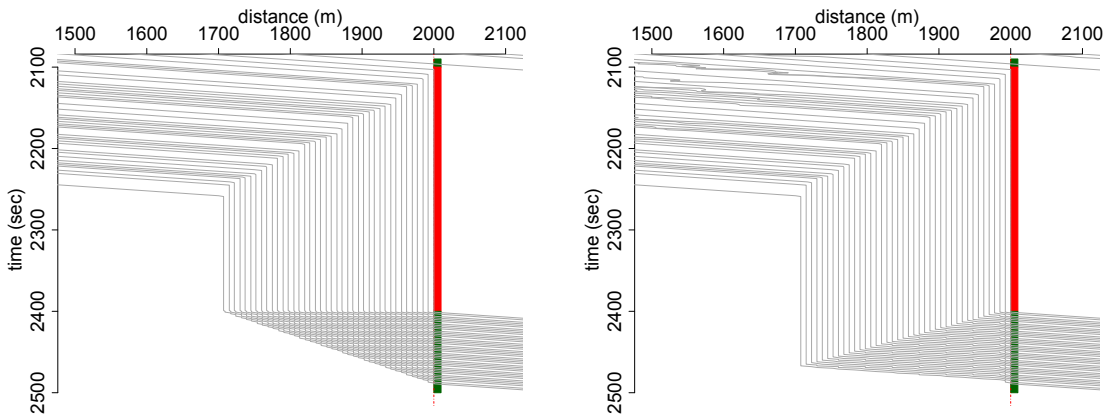

(a) Traffic dynamics = without holes.

(b) Traffic dynamics = with holes.

Figure 7.18: Space time trajectories at density 13.33 PCU/km.

For simplicity, only the car vehicle class is simulated on the triangular race track (see Sec. 7.3) with minor modification i.e., a hypothetical bottleneck is created to stop the outflow on the middle link (l_2) for 5 min (between $t = 2100$ and $t = 2400$). This is done in order to observe the queuing pattern. The steps to interpolate the intermediate points on the link at every time step ($= 1$ sec) are shown in Appen. B.3.

Figs. 7.18a and 7.18b show the spatio-temporal plots for the queue model without holes and with holes respectively.[10] As soon as the outflow of the middle link (l_2) comes to a halt, queuing starts. However, as expected, the queuing patterns in both models are different. In the queue model without holes, the position of the leading vehicle is occupied immediately by the following vehicle, consequently, a sudden shock (all vehicle move one step ahead simultaneously) is observed at $t = 2400$ (see Fig. 7.18a). This (horizontal) shock travels backward until the last vehicle moves forward in the same time step. On the contrary, in the queue model with holes, the space is occupied by the following vehicle after some time depending on the speed of backward traveling holes. In other words, the shock is not sudden and all the vehicles do not move instantly at $t = 2400$ (see Fig. 7.18b). Clearly, this results in a higher queue dissipation time and a shock is observed which moves

[10] These trajectories are derived in the post-processing, therefore, minor rounding errors can be observed in the trajectories.

backward with the time. Hence, the proposed approach produces the realistic traffic flow patterns.

7.7 Discussion

This chapter presents the various extensions of the queue model to make the realistic traffic patters. These extensions are equally applicable to a wide variety of simulation frameworks. As discussed in Sec. 7.2, the queue model is a simple model which tracks vehicles at the entry/exit of the link and easy to implement. Clearly, it has several limitations while comparing with the most of the detailed modeling approaches (see Sec. 6.3), however, the simplicity of the queue model makes it computationally faster and the ability to include all types of vehicles in the simulation for a large urban agglomeration. This section discusses a few issues and their possible influences on the overall traffic patterns. However, every additional approach to improve the queue model will increase the computational complexities.

7.7.1 Validation with real-traffic data

Though, there are several arguments, FDs, space-time plots are presented in the support of the proposed queue model extensions, it is equally important to validate the model with the real-world traffic data. In future, it would be very interesting to plan and conduct a traffic survey to validate the model and to calibrate the scenario-specific parameters. Clearly, the fruitful results could be achieved only if the traffic surveys are conducted in the urban area of one of the industrializing nations. Alternatively, similar to Mallikarjuna and Rao (2011), a video image processing application could be used to validate the presented queue model extensions.

7.7.2 Passing link dynamics

The passing link dynamics is introduced by Agarwal et al. (2015) and this thesis continues from there. In this, it is assumed that a faster vehicle can overtake the slower vehicles irrespective of the number of lanes on the link.[11] This is valid for most of the urban arterial/sub-arterials, however, not always true. Including this in the future research will most likely help to identify the probable single lane bottlenecks with high demand.

Similarly, the overtaking in the queue model is simply introduced by sorting the data structure based on the earliest link exit time. However, in the practical situations, overtaking opportunities depends on several factors, e.g., divided vs undivided roads, speed of the front vehicle, etc. These factors are completely ignored in the queue model, however, adding such feature will make the queue model less attractive for the large-scale scenarios. In future research, a possible way would be to introduce some penalty for every passing event while calibrating the results against a detailed model.

[11] The seepage is likely to occur even on the single lane links.

7.7.3 Seepage link dynamics

The seepage link dynamics in the queue model is introduced according to the Alg. 7.1. Thus, in the capacity and congested regimes, the smaller vehicles with high maneuverability can move across the gaps between the stationary or almost stationary vehicles and can appear in front of the queue. The approach is applicable not only for the smaller vehicles but for any type of the vehicle type across the world. Sometimes, the car seeps between the truck on a multi-lane highway. The seepage also plays an important role in the situation where ambulance vehicles or other fire engines need to seep through the large pedestrian crowds. This situation happens for example during some large music festivals or other public events. In those situations, the seep mode is not assigned to the smaller vehicle, instead the smaller "vehicles" (i.e., pedestrians) give space to the large vehicles (i.e., ambulances). Albeit those situations seem to be quite different from the seepage observed on the road networks, it seems to be reasonable to apply a similar approach as the one that has been proposed in this contribution.

For future prospect, two weakness of the seepage algorithm are discussed below.

i) **Stochasticity in the seepage** Though, the seepage is a common practice in most of the industrializing nations, not all smaller vehicles perform seepage. Therefore, to increase the stochasticity in the simulation, it would be interesting to introduce the randomization in the seepage of the queued seep modes. Presumably, this will introduce the complexities and thus, become slightly more resource-intensive

ii) **Limit on the seepage events** There is a constant parameter (C) in Alg. 7.1, it determines the number of seep modes which are brought in front of the queue. In this thesis, it is assumed as the space equivalent to 1 PCU, however, this is a scenario-specific parameter which depends on the share of the seep modes in the traffic stream, type of the seep mode, etc. Hence, before applying it to any scenario, it needs to be calibrated using the traffic survey at various urban intersections. This parameter could not be kept same for all the different sample sizes, therefore, similar to the flow and storage capacity (see Appen. B.5), it must also be scaled down.

7.7.4 Speed of backward traveling holes

The speed of backward traveling holes (v^h) is assumed as 15 km/h. This corresponds to a reaction time (l_v/v_h) of 1.8 sec, where l_v is the length of the 1 PCU ($= 7.5m$).[12] The effect of vehicle length is incorporated implicitly in the simulation, e.g., if a vehicle is a quarter of the length of a car, for the same reaction time, the hole speed will be 3.75 km/h ($= (7.5\ m/4)/1.8\ sec$). Hence, a constant reaction time would return different implicit hole speeds depending on the length of the vehicle. In future studies, it would be interesting to model the vehicle classes with different backward traveling hole speeds with some stochasticity in it because the actual speed of the hole also depends on the underlying traffic mix on the link.

[12] Please note that the links are modeled as one dimensional unit and length of the vehicle includes the longitudinal clearance between the two vehicles.

7.8 Summary

The implementation of the network loading algorithm in MATSim is a queue model. This chapter starts by illustrating the queue model. The queue model is then extended to replicate the realistic traffic patterns using the backward traveling holes. The queue model is further extended for the seepage of smaller vehicles in the mixed traffic conditions.

The extensions of the queue model are followed by the generation of the FDs for various traffic and link dynamics combinations. These FDs demonstrates the interrelationship between the fundamental variables of the traffic flow. Moreover, the robustness of the queue model are tested using the different contour plots and speed density profiles. In the end, the chapter discusses a few limitations of the queue model.

Chapter 8

Real-World Simulation Experiments

8.1 Overview

Ch. 7 extends the computationally efficient queue model to include (a) realistic traffic pattern using backward traveling holes and (b) seepage of the smaller vehicles. In this direction, in order to

1) explore the possibility of application of the presented queue model extensions to a large-scale real-world scenario and

2) compare the computational efficiency in terms of the average simulation time for various traffic and link dynamics of the queue model

a few simulation experiments are performed. In the first experiment, an evacuation scenario for Patna, India is presented to show an application of the seepage link dynamics. Next experiment compares the simulation times of various link and traffic dynamics of the queue model extensions using the Patna scenario. This part of the chapter is an edited version of Agarwal and Lämmel (2016).

8.2 Real-world evacuation

As described previously, in the Sec. 6.3.2, a small experiment is conducted within the project *Last–Mile–Evacuation* (Taubenböck et al., 2013). That experiment studies the evacuation of the pedestrians using seepage action while moving through a group of stationary cars (Klüpfel and Hebben, 2010). That is a static example however; this thesis proposes the evacuation of a scenario with the mixed traffic conditions and seepage behavior. This section presents an application of the seepage to a real-world evacuation scenario. The objectives of presenting this real-world scenario is to show and to quantify the influence of seepage for disaster management. This approach is useful to simulate large-scale evacuations (e.g., in case of tsunamis or forest fires) in densely populated areas where small vehicles/pedestrians are expected to seep from the free space between the stationary vehicles.

8.2.1 Simulation inputs

The initial scenario is taken from a previous study by Agarwal et al. (2013) and therefore, described here briefly. The initial network is created using the shape files and it consists of 3505 nodes and 7542 links. A disaster prone area is identified as an evacuation area. The aim is to evacuate all the persons inside this area (see Fig. 8.1). In the simulation, the network is connected with some of the exit (safe or evacuation) links (see blue links in Fig. 8.1) which lead to a safer location (see Lämmel, 2011, for detailed methodology to prepare the evacuation network)

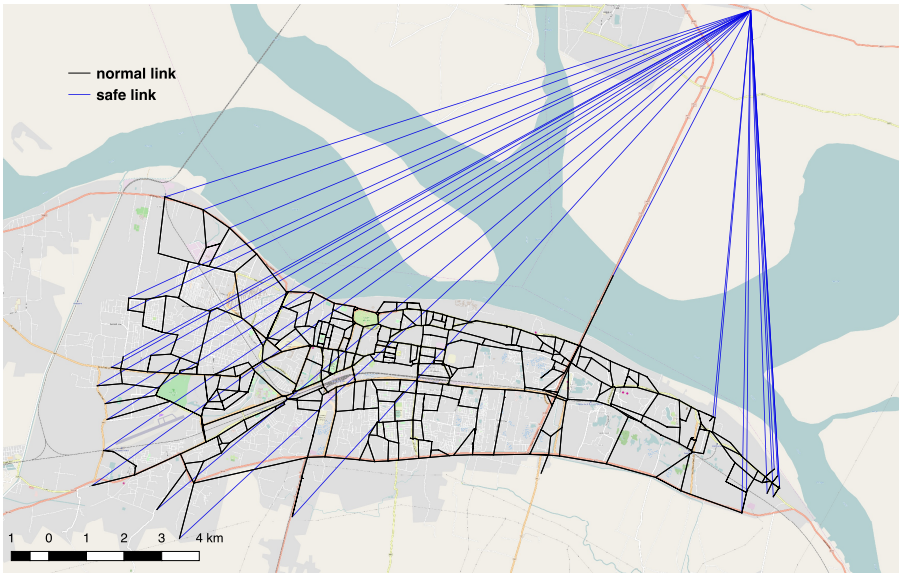

Figure 8.1: Evacuation Patna network for the experiment.

The initial activity locations and travel modes of the persons are taken from the Patna comprehensive mobility plan (Patna CMP; TRIPP et al., 2009). For simplicity, it is assumed that all persons start evacuating simultaneously as soon as the warning is announced (at 09:00:00 in this experiment) and all persons start evacuating from their home locations. Thus in the simulation run, all persons inside the evacuation area are considered for evacuation. Assuming everyone starts at once is a conservative assumption, since it would lead to a high initial load onto the network and thus to high densities resulting in a lower throughput (cf. FDs in Figs. 7.9 and 7.11) compared to widely distributed departure times. A study that investigates the influence of the departure time distribution on the overall evacuation performance is presented by Lämmel and Klüpfel (2012). In absence of the travel schedule for PT, it is excluded from the simulation.[1] The walk mode cannot be simulated using the regular vehicular traffic model and therefore skipped in the simulation. Thus, car, motorbike and bicycle (bike) modes are considered as main congested modes (see Sec. 9.3.3) in the simulation [2]. Overall about 1% sample size is taken. Next section

[1] In the regular simulation experiments, PT is included in the simulation, however, it may not be simulated on the network as congested mode rather logically simulated between origin and destination as uncongested mode (see Sec. 9.3.3 for further details).

[2] Please refer to Agarwal et al. (2013), for the details about the calibration of the scenario. In this

illustrates the simulation set up for this experiment.

8.2.2 Simulation set up

Apart from the passing link dynamics scenario, two more situations based on the chosen seep mode(s) are considered. In the first situation, only bicycle is chosen as seep mode and in the second situation, both, bicycle and motorbike are chosen as seep modes. Overall, the following three simulation scenarios are considered as follows.

i) Scenario 1: passing only

ii) Scenario 2: seepage; bicycle as seep mode

iii) Scenario 3: seepage; bicycle and motorbike as seep modes

Each simulation scenario is run for 100 iterations. For the re-planning, until the 75 iterations, 10% of the agents are allowed to change their route and remaining agents until 75 iterations and all the agents after 75 iterations, select a plan from their generated choice sets. The plan selection is according to a probability distribution which converges to the MNL model (see Nagel and Flötteröd, 2012, and also Sec. 2.2.2.3). In the initial iteration, basically the shortest path is assigned to each agent between its origin and destination. Afterwards, agents learn and adapt to the system as described in the Sec. 2.2.2. Finally, the outcome of the last iteration shows the routes corresponding to a Nash equilibrium like equilibrium. Therefore, based on the agents' behavior, the results are also analyzed for two cases (see Fig. 8.2 and Tab. 8.1), namely

(1) shortest path (SP) (= initial iteration in the MATSim sense) and

(2) Nash equilibrium (NE).

The simulation results in terms of the average travel time and evacuation progress for each scenario are elaborated in the next section.

8.2.3 Simulation results

8.2.3.1 Average travel time

Tab. 8.1 shows the comparison of the average trip time from for the three scenarios and for both the cases (SP and NE). Clearly, as expected, the average SP trip time is significantly higher than the average trip time for NE for all scenarios. Interestingly, the effect of the seepage behavior can be observed in the first iteration (SP) itself. For the SP case, the average trip time for bicycle in scenario 1 is about 13% and 3% higher than the average trip time for bicycle in scenario 2 and 3 respectively. In the latter, both, motorbike and bicycle are allowed to seep, however, due to the presence of the faster seep mode (in this case, motorbike), the slower seep mode (i.e., bicycle) can seep marginally (also see Fig. 7.12). This results in the

a) lower average motorbike trip time in scenario 3 than in scenario 1 and 2 and

b) higher average bicycle trip time in scenario 3 than in scenario 2.

Table 8.1: Average trip time (in *min*) for various scenarios.

Scenario		travel modes		
		bicycle	car	motorbike
Scenario 1	SP	382.73	301.94	329.57
	NE	184.12	127.07	153.96
Scenario 2	SP	331.88	369.66	449.90
	NE	145.48	178.94	216.51
Scenario 3	SP	370.21	410.28	312.54
	NE	166.15	207.40	139.45

In the NE case, the average trip time for each mode is significantly shorter than the average trip time in SP case for both the simulation runs. Furthermore, in the scenario 2, only bicycle seep from the space between car and motorbike. Consequently, the average bicycle trip time is about 21% lesser than average trip time for the passing (= no-seep) scenario. As a consequence of the seepage of bicycle mode, the average trip time of car and motorbike is approximately 40% higher than the average trip time for the passing scenario. In the scenario 3, while motorbike and bicycle both modes perform seepage and motorbike is faster, the average trip times of bicycle and motorbike are about 9% lower and average trip time of car is about 63% higher than the average trip time in passing scenario.

Clearly, with the comparison made above, it can be observed that the seepage has decreased the average trip time for seep mode(s) and increased the average trip time for other modes significantly. However, for the evacuation scenario, it is important to analyze the evacuation progress and the total clearing time, therefore, the next section compares the evacuation progress of different scenarios.

8.2.3.2 Evacuation progress

Fig. 8.2 shows the evacuation progress for all three simulation runs categorized based on the modes. Firstly, as expected, NE (blue lines) leads to the shorter evacuation times as compared to SP (red lines) for all the scenarios and, for all modes separately or together. This is in line with the literature (Lämmel et al., 2010). In terms of policy making, this would mean the shortest path solution does not take congestion into consideration and thus it is not a good solution. Further, comparing the scenarios 1 and 2 (solid and dotted lines respectively), seepage of the bicycle mode in scenario 2 has led to a higher evacuation rate for the bicycle mode and slower evacuation rate for the car and motorbike. Eventually, with time, for car and motorbike, the evacuation rate in scenario 2 catches up and becomes almost the same as that of the scenario 1. Moreover, comparing scenario 2 an 3 (dotted and dashed line respectively), for bicycle, the evacuation rate in the scenario 3 is lower than in the scenario 2 because, seepage of the motorbike is possible which decreases the rate

simulation experiment, the calibrated scenario is used.

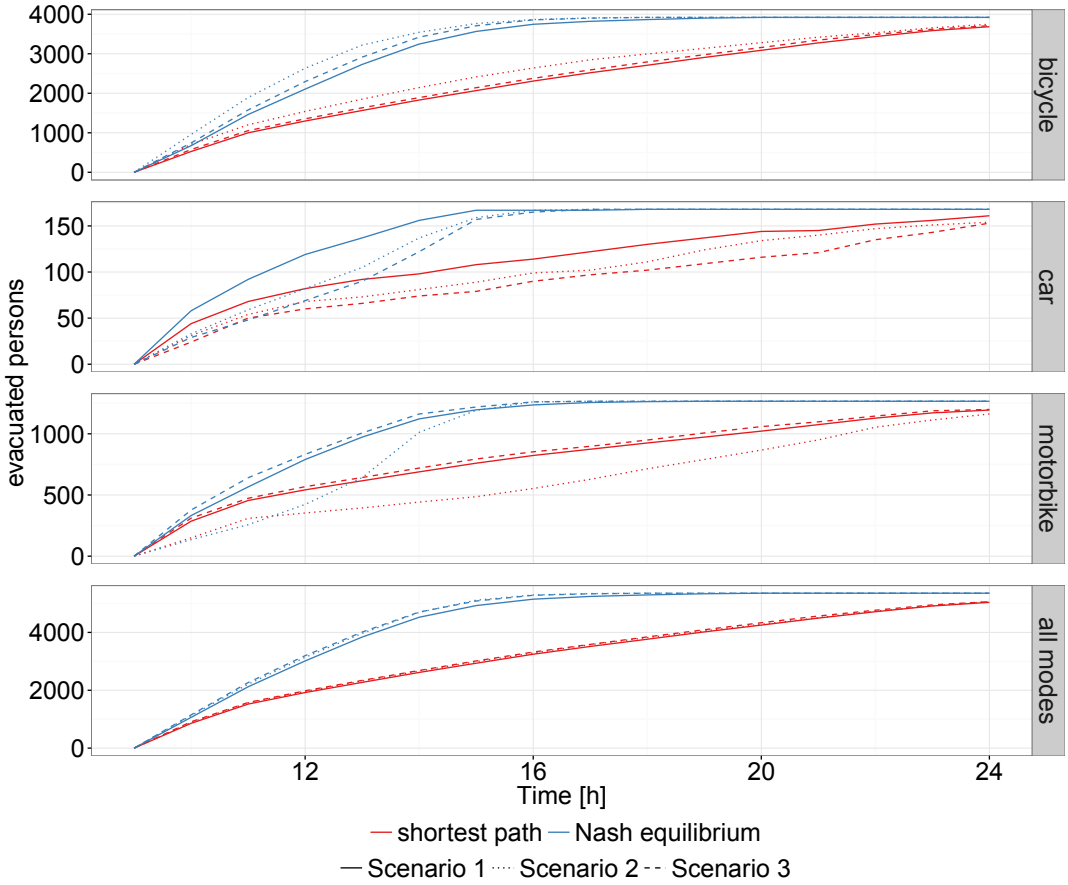

Figure 8.2: Comparison of the evacuation progress.

of seepage for bicycle mode (also see Fig. 7.12). The evacuation rate for the motorbike in scenario 3 is highest among the three scenarios. For car, the evacuation rate is the slowest as the car is hindered by the seep modes. Comparing all the modes altogether, the rate of evacuation is more or less same in scenario 2 and 3, and (slightly) higher than that in the scenario 1. Thus, looking on the time bound evacuation scenario, more people can be evacuated using the seepage behavior. Overall, with this experiment, it can be summarized that the seepage has no negative impact in terms of the evacuation rate and in order to model the various real-world situations practically, the seepage behavior can be included in the model (see Sec. 8.4 for more discussion).

8.3 Computation performance

In order to compare the simulation time for the queue model with different link and traffic dynamics, a real-world example of Patna, India is used. A comparison between the runtime of MATSim and three other simulators (TRANSIMS, VISSIM and SUMO[3]) is given by Maciejewski (2010). The author finds that MATSim is about 10 times faster than its nearest neighbor TRANSIMS. Although, the comparison is performed using a small

[3]Based on SUMO distribution (Krajzewicz et al., 2012), there exists a package – MESO – which computes the vehicle movements with queues and appears to be faster (http://sumo.dlr.de/wiki/MESO). A comparison of the results and simulation time using MESO, is beyond the scope of this thesis.

network example, a similar outcome is expected because the queue model in MATSim only tracks agent's entry/exit to the link. A thorough comparison between different simulators is beyond the scope of this thesis; however, this provides an opportunity for the future research and can be tackled by the author or other researchers.

8.3.1 Simulation time in MATSim

Simulation time The total simulation time in MATSim comprises several parts e.g., mobility simulation (mobsim), re-planning, scoring, dumping data, etc. The mobsim time is the time required to execute all the agents on the network and therefore only mobsim time is used for the comparison purpose. In this chapter, here onwards, the simulation time refers to only mobsim time and QSim is used as the mobility simulation for all the simulation experiments (see Sec. 2.2.2.1).

In the QSim, mainly two data structures are used for each link to process the agents. In every time step, the flow and storage capacities of the link are accumulated. Additionally, in every time step, status of the agent is also checked and updated if the agent(s) can move over the node based on the conditions described in Sec. 7.2. This is the most time consuming step of the QSim (Dobler, 2013, pp. 35-56).

Parallel computing It is a common practice to distribute the computational load using multi-threaded architecture. MATSim also supports the use of multiple threads for various steps e.g., mobility simulation, re-planning, event handling, etc., (Nagel, 2016b). Dobler (2013, pp. 35-56) introduces the parallel QSim in MATSim. It is found that the simulation time decreases with the number of threads linearly for the large scenarios. To reduce the computational load of the mobility simulation, Fourie et al. (2013) use somewhat different approach. The authors introduce a simplified meta-model or PSim (also called as Pseudo-simulation) and integrated it with QSim. The basic idea is that the congestion pattern does not vary too much a) by adding a few synthetic agents and b) from one iteration to the next iteration. Thus, it is not necessary to run QSim for every iteration and can save considerable simulation time. The selection of the approach from above depends on the scale of the scenario and available hardware infrastructure. However, in this thesis, the default QSim is used. Presumably, use of the multi-threading and PSim would further reduce the simulation time.

Factors affecting the simulation time There are several factors which affect the simulation time, e.g., number of agents, number of nodes and links, etc. There is another optional approach to further cut down the runtime by simplifying the network. A network is simplified by reducing the number of nodes and links by merging them based on the nodes classification given by Balmer et al. (2005b) or by removing the unconnected nodes/link. This in turn reduces the computational effort during the network loading process.

In the QSim, if the three conditions described in Sec. 7.2.1 are satisfied, the front most (head) agent in the data structure is removed from the link and added to the tail of the data structure of the downstream link. Minimally, this process is same for all link dynamics, however, different functionalities of link dynamics are provided by the different sorting criteria of the data structure before removing an agent. For passing, the data

structure is sorted based on the earliest link exit time of the agents whereas for seepage the Alg. 7.1 is used to find the seep mode. Based on the sorting criteria, the computational effort increases.

It is important to mention that there are some other factors that affect the simulation time and are not considered explicitly; e.g., the traffic pattern for the FIFO link dynamics will behave like a wide moving jams and agents will stay on the network for a longer period of time than in the simulation with passing link dynamics or seepage link dynamics. Similarly, the traffic patterns will be different in the simulation with the passing and seepage link dynamics. The traffic patterns from the simulation of mixed traffic conditions using different link dynamics cannot be identical, however, in this chapter, the simulation time is compared without explicitly considering the above effects.

8.3.2 Simulation set up

For illustration purpose, scenario of Patna is considered (also see Ch. 9). For simplicity, only the urban trip diaries are considered as demand for this experiment (see Sec. 9.3.2.1). The scenario is briefly described below.[4]

The simplified network has 702 nodes and 1934 links. The 1% sample population has 13278 persons and each person make two trips per day. The scenario has about 2% car, 33% bicycle, 14% motorbike, 22% public transport and 29% walk trips. Car, motorbike and bicycle are physically simulated on the network and therefore considered as the main congested modes for the scenario (see Sec. 9.3.3 for a comparison of the congested and uncongested modes in the simulation framework). Each simulation is run for 200 iterations. In order to compare the performance between different sample sizes, same experiment is repeated again with 10% and 100% samples. The synthetic demand is generated by cloning 1% population sample by randomizing the activity locations and the departure times.[5]

From the three link dynamics (FIFO, passing and seepage) and two queue models (with and without holes), 6 cases are considered (see x-axis of Fig. 8.3). Each case is run for 5 different random seeds to check the robustness of the simulation time.

8.3.3 Computational hardware

The runs for this experiment were conducted on the computing cluster of the mathematics faculty of Technische Universität Berlin. These simulation runs are processed on a machine which has Supermicro X9DRT type main board, two Intel Xeon E5-2630v3 @ 2.4 *GHz* CPU each with Octa core. The machine has 64 *GB* of DDR memory clocked at 1866 *MHz*. However, for each run, only 4 cores are used. The Java virtual machine, JVM: 1.8.0_92; Oracle Corporation; mixed mode; 64-bit is used which can use maximum

[4] The scenario in the simulation time experiment is different than the scenario in the evacuation scenario (see Sec. 8.2.1). The demand for the former is synthesized directly from the trip diaries. The ASCs for this demand are calibrated using the given modal share and output of the calibrated demand is used for the evacuation scenario (see Agarwal et al., 2013, for complete methodology of the calibration). The simulation time experiment is performed for the different sample sizes by cloning the initial plans. Cloning the calibrated plan would produce biased plans and therefore could influence the overall results and therefore, different travel demands are used in the evacuation and the simulation time for the different sample size experiments.

[5] An illustration of the traffic patterns from the simulation of the different sample sizes is shown in Appen. B.5.

of 30 *GB* by setting −Xmx30G in the run script. The experimental runs are performed between September and November 2016.

8.3.4 Outcome

The box plot comparisons of the average simulation times for 1%, 10% and 100% samples are shown in Fig. 8.3. The average simulation time per iteration for with holes traffic dynamics is shown in Tab. 8.2. From the Fig. 8.3 following can be summarized.

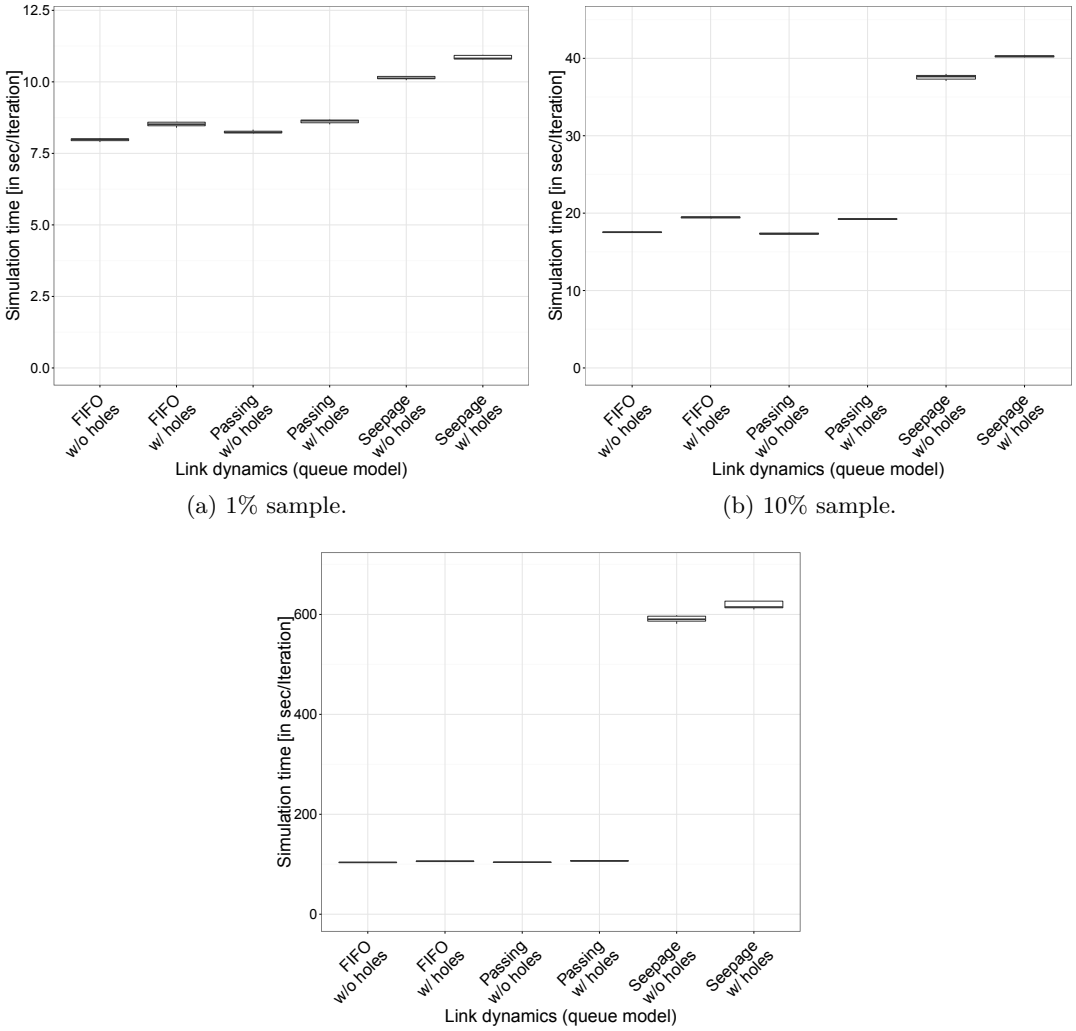

(a) 1% sample.

(b) 10% sample.

(c) 100% sample.

Figure 8.3: Average simulation time for 200 runs of Patna scenario.

- The default variant of the queue model i.e., the queue model with FIFO link and without holes traffic dynamics, has least simulation time for 1% sample size despite of the fact that car/motorbike cannot overtake bicycle and thus stays longer in the simulation. For 1%, 10% and 100% samples, the average simulation times per iteration are 7.98 *sec*, 17.54 *sec* and 103.56 *sec* respectively.
- For passing link dynamics, the simulation time is about the same as that of in FIFO link dynamics. This is the combined effect of at least two factors which balances each

other (also see Tab. 8.2): a) for passing link dynamics, sorting of the data structure increases the simulation time marginally and b) for FIFO link dynamics, the faster vehicles are trapped behind the slower vehicles and thus are forced to stay longer in the simulation; consequently, the longer simulation time is required to process them.

- For 1% sample size, the increase in the average simulation times – if using backward traveling holes – for FIFO, passing and seepage link dynamics are 0.5 *sec*, 0.4 *sec* and 0.7 *sec* respectively. It means that the introduction of backward traveling holes increases the simulation time marginally. This happens due to the requirements of an additional data structure per link to process the holes. A likewise increment in the simulation time is observed for other sample sizes too.
- Looking on the simulation time for the seepage link dynamics, it can be observed that the look up for the seep mode on every link (see Alg. 7.1) is more costly than other link dynamics in terms of the computational load. The average simulation time for the seepage link dynamics is significantly higher than the average simulation time for the FIFO and passing link dynamics (see Tab. 8.2).

8.3.5 Average simulation time

From the experiments in the Sec. 8.3, it can be observed that the QSim is able to handle the large-scale scenario and it is not very resource hungry. Furthermore, in this direction, the average simulation times per iteration for different sample sizes and link dynamics are shown in Tab. 8.2. From the table, it can be noted that the average time to simulate 10%

Table 8.2: Average simulation time per iteration (in *sec*).

		sample sizes		
traffic dynamics	**link dynamics**	**1%**	**10%**	**100%**
without holes	FIFO	7.98	17.54	103.56
	passing	8.23	17.36	103.67
	seepage	10.14	37.56	590.65
with holes	FIFO	8.51	19.46	105.74
	passing	8.61	19.23	106.85
	seepage	10.86	40.28	618.31

and 100% sample size scenarios, for FIFO and passing link dynamics are approximately 2 and 12 times higher than the average time to simulate 1% sample size scenario. In other words, the average simulation times do not increase in the same ratio as the sample sizes. This highlights the advantage of using the queue model to simulate a sample of agents (1%, 10% etc.) rather than simulating the millions of agents from a huge agglomeration area. The average simulation times for seepage scenario with 10% and 100% sample sizes are significantly higher than the average simulation time for the seepage scenario with 1% sample size (about 4 and 57 times respectively for 10% and 100% sample sizes) because with higher sample sizes, the look up of the seep mode (see Alg. 7.1) is more often which increases the computational effort.

8.4 Discussion

In this chapter, two important simulation experiments are presented, with the aim of showing an application of seepage and comparing the average simulation times of different link and traffic dynamics of the queue model. Some of the restrictions with the queue model are discussed in Sec. 7.7, a few other points are discussed in this section which show an opportunity for the future research.

8.4.1 Application of seepage

The seepage queue model is able to replicate the real-world traffic conditions. This chapter makes an attempt to apply it to an evacuation scenario. In this experiment, the average time for the seep mode is reduced significantly and it is found that seepage does not produce any negative impacts on the overall evacuation time.

In the seepage experiment (see Sec. 8.2) , it is assumed that the seep mode consumes the storage capacity of the link. However, as shown in the Fig. 1.1, during seepage in the practical situations, the seep mode do not occupy the additional space, instead use the space between the two cars in the same lane which in turn can relief the additional storage space. This additional space can enhance the saturation flow and overall result in lesser clearing time for the evacuation scenarios.

8.4.2 Comparison with other models

This chapter compares the time to simulate the 1%, 10% and 100% sample sizes for the different link and traffic dynamics. A comparison between the runtime of MATSim and three other simulators (TRANSIMS, VISSIM and SUMO) is given in Maciejewski (2010). The author finds that MATSim is about 10 times faster than its nearest neighbor TRANSIMS. Putting all these studies together, it can be implied that the proposed queue model extensions are fast and useful to simulate the large-scale scenario. However, from future perspective, a detailed comparison of the simulation time and simulation outcome from different simulation framework would support the findings in this thesis.

8.5 Summary

This chapter illustrates a few real-world experiments based on the queue models. With the Patna evacuation scenario, it has been showed that the seepage link dynamics can be used with various real-world traffic conditions and overall, for Patna, there is no negative impact of the seepage on the evacuation rate. A comparison of different combinations of traffic and link dynamics of queue model is also presented. The default FIFO link dynamics appears to be the fastest whereas the simulation time for passing link dynamics is also about the same. A significant increase in the run time is observed for the seepage link dynamics. The introduction of the backward traveling holes increases simulation time marginally. These experiments are performed on a real-world scenario for the different sample sizes. For a huge urban agglomeration, the simulation time is further reduced by using the small sample size.

Part III

Integrated Scenario

Chapter 9

Patna Scenario

9.1 Overview

In order to apply the queue model extension to a large-scale scenario with mixed traffic condition and to test the policy measures, a medium sized city in eastern India, Patna, is chosen. It is one of the highly populated eastern cities in India. Development of Patna is east to west (along river Ganga). The streets are heavily encroached and in poor condition. The total available road network in Patna is only around 5% of the total development area (Singh and Misra, 2004).

In this part, the traffic queue model is applied to this scenario. The external demand is synthesized from traffic counts data by extending Cadyts to mixed traffic conditions. The urban and external demand is calibrated simultaneously. Further, based on the given modal share and traffic characteristics, a bicycle superhighway[1] is proposed. The optimum number of bicycle superhighway connectors are identified using an iterative process and thereby, the impacts of the policy measures are discussed.

9.2 Scenario background

The population of the Patna agglomeration area was 5.77 M in 2011 (Census, 2011). The study area includes 72 zones of the Patna Municipal Corporation (PMC) with a population of 1.57 M for the year 2008.

Different motorized and non-motorized modes are used; however, low income households are captive to bicycle (cycle) and PT. On almost all road sections, all modes share the same road space and the lane discipline is absent. Tab. 9.1 shows the modal income statistics for households of Patna city. This data is calculated from individual monthly income form trip diaries.[2] Car is predominantly used by high income persons whereas motorbike is used by mid to high income persons. Bicycle and walk trips are limited to

[1] A bicycle or cycle superhighway is a physically segregated link for bicycles which allow safer and faster trips (see http://denmark.dk/en/green-living/bicycle-culture/cycle-super-highway,http://lcc.org.uk/pages/cycle-superhighways for some practical examples.)

[2] For some persons, the monthly income data is not available, therefore, the data is randomly imputed based on the income distribution from TRIPP et al. (2009).

Table 9.1: Average income (Indian Rupee (*INR*)) statistics for Patna city; data is generated from trip diaries (TRIPP et al., 2009).

travel mode	number of persons	mean income	median income
bicycle	3878	5903.24	4000.0
car	526	13482.41	20000.0
motorbike	2668	10341.26	6250.0
PT	3527	8343.99	4000.0
walk	2679	6383.35	4000.0
all modes	13278	7840.43	4000.0

low income households.

9.3 Inputs

9.3.1 Network

The road network of Patna is divided into 3 major road categories namely major arterial, arterial and collector street. The three major arterials are Ashok Rajpath, Old bypass and New bypass, which are spread along the length of the city (see Fig. 9.1). 36% of total road length have a width less than 5 *m*, with an accordingly low capacity. Any location inside Patna is at most one *km* away from a major arterial or an arterial. The network is shown in Fig. 9.1.

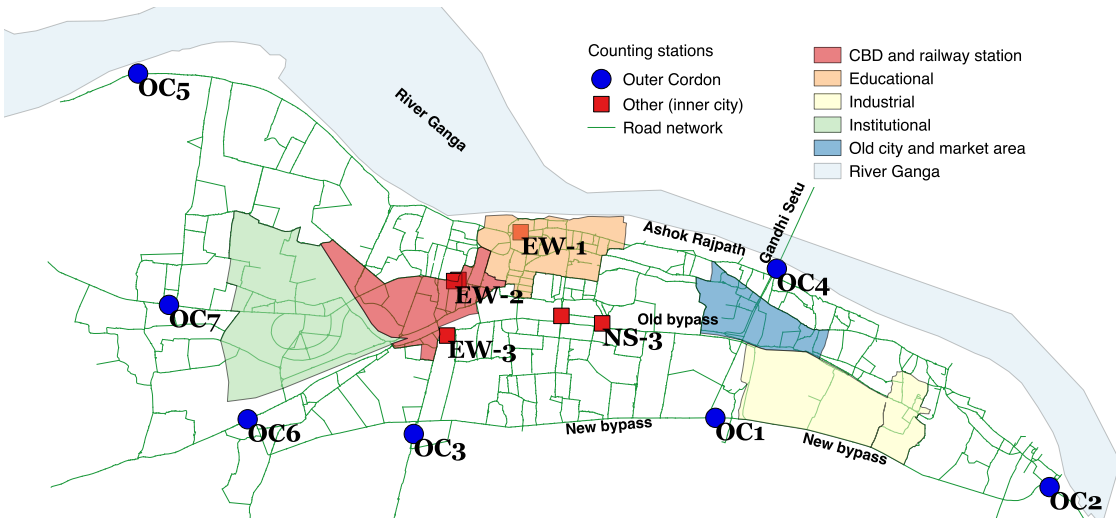

Figure 9.1: Patna road network, survey and activity location zones.

To create a digital MATSim network for the Patna scenario, TransCad (TransCAD, 2012) files are used as input files. These files are a part of the data provided by TRIPP et

al. (2009).[3] The hourly flow capacity is then computed according to Chandra and Kumar (2003) as follows (see Agarwal, 2012, for more details):

$$Capacity = -2184 - 22.6 \cdot w^2 + 857.4 \cdot w \tag{9.1}$$

where w is the width of the road in m. A minimum flow capacity of 300 PCU/h per direction is used.

9.3.2 Demand

The data available is based on a comprehensive transportation planning study conducted for Patna, (from hereonwards named as Patna Comprehensive Mobility Plan (CMP) TRIPP et al., 2009). The demand is mainly categorized in two sub-populations, namely urban and external traffic. The latter is further classified into commuters and through traffic (see Sec. 9.3.2.2).

9.3.2.1 Urban demand

Urban travel demand for Patna is generated directly from a trip diary survey provided by TRIPP et al. (2009). Parts of the data in the household survey were unavailable; for such cases the required data was imputed randomly based on other available data in the Patna CMP. This results in 13,278 records. Every such record is translated into one MATSim person with one MATSim plan. The trip production rate is 79% and absolute population of all zones are between 18,000 and 21,000. This results in approximately 1.24 million trips corresponding to the 2008 population of Patna (TRIPP et al., 2009) and represents approximately 1% sample of all trips. In absence of other data, two trips in each urban plan are synthetically generated. In order to get significant number of plans for commuters and through traffic in various categories (see Sec. 9.3.2.2), 10 % sample is used. Therefore, urban plans are also cloned by randomizing origin, destination and departure time to get 10% sample.[4] According to the reference study (Patna CMP; TRIPP et al., 2009), shares of bicycle, car, motorbike, PT and walk share are 33%, 2%, 14%, 23% and 29% respectively (see Tab. 9.6).

Table 9.2: Values of time and vehicle operating costs (IRC:SP:30, 2009).

travel mode	vehicle operating costs ($USDct/km$)	value of time ($USDct/h$)
car	3.75	93.84
motorbike	1.55	48.05
PT	–	59.31

[3] A few disconnected links are joined together which are out of scope and some other minor adjustments are made. This concerns some major arterials, and is verified from open street maps (www.openstreetmap.org). The reasons for the errors are unknown.

[4] As long as schedule-based transit assignment is not used, decent results with MATSim can already be obtained from 1% population samples (Nagel, 2008, 2011). Appen. B.5 shows an approach to update the flow and storage capacities for different sample sizes and a comparison of the traffic patters for different sample sizes of the Patna scenario in shown in Appen. B.5.2.

As presented in Sec. 2.2.2.2, to evaluate a plan, MATSim uses a scoring function and needs explicit values for utility parameters. In order to determine the utility parameters, the value of time and vehicle operating costs is taken from IRC:SP:30 (2009) and converted to US Dollar (*USD*)[5] for a common interpretation (see Tab. 9.2). These values are then translated into MATSim utility parameters as demonstrated in Sec. 9.4. The average trip cost for PT is taken from Kumar et al. (2004) and shown in Eq. 9.2. The value are on the lower side, however, seems appropriate due to significant share of low cost "tuk-tuks" in Patna.

$$\text{PT trip cost } (USD) = \begin{cases} 0.045, & \text{if } d \leq 4\ km \\ 0.045 + (d-4) \cdot 0.0047, & \text{if } d > 4\ km \end{cases} \tag{9.2}$$

9.3.2.2 External traffic

The Patna CMP also provides classified hourly counts for 7 outer cordon stations (see Fig. 9.1) in both directions.[6] The external traffic is categorized in two categories, namely through traffic and commuters. The former is the traffic which just pass through Patna and makes at most a trip per day whereas, in the latter case, agents commute between Patna and nearby area of Patna.[7] Further, the hourly classified counts can be thus divided into through and commuters traffic using directional split factors (see Tab. C.2).

Through traffic MATSim is an activity-based simulation framework, therefore require a full plan rather than only origin-destination (OD) flows. An OD matrix (see Tab. C.3) is provided for through traffic. This, together with hourly modal counts determines the origin, destination, departure time and travel mode for each plan. The shares given in OD matrix are used for all modes (bicycle, car, motorbike and truck) in 1 h time bin. Consequently, a 10% sample is created from the counts such that each plan has one trip only. Since, the actual origins and destinations of through traffic are unknown, the trip is assumed to originate and terminate before and after the counting stations respectively.

Commuters traffic For commuters, the exact locations of the trip destinations are unknown. However, a few potential locations are identified based on the land-use pattern from Patna CMP as shown in Fig. 9.1. Thus, a random point inside any of these probable activity location zones is taken as the trip destination. It means, for every agent (i.e., for every count) 5 different destinations are plausible . Subsequently, 5 plans are generated and added to the choice set of the agent. The location choice is performed in order to determine the unknown destination using the traffic counts (see Sec. 9.4.1).

[5] 1 *USD* ≈ 66.6 *INR*. Exchange rate on 8 June 2016.

[6] Demand originating and terminating from the counting station "OC1" (see Fig. 9.1) is included in the simulation. However, this counting station is excluded from the comparison of traffic counts (see Fig. 9.2) because of the uncertain location (link) of the counting station.

[7] Steps to estimate the external trip counts are shown in Appen. C.1. It also shows the directional split for through and commuters traffic and origin destination matrix for through traffic. This data is taken from Patna CMP (TRIPP et al., 2009).

9.3.3 Travel modes

Congested modes Modes which are physically simulated on the network using the queue model are called as *congested* modes or *main* modes. As described before in Sec. 7.2, these modes consume flow and storage capacities. Consequently, these modes affect the network capacities and thus, also affect the route choice decision making process of the individual travelers.

Uncongested modes This means that every time the traffic flow simulation encounters a leg with a mode that is not registered as "congested" mode, it will note a departure, compute the expected arrival time according to the beeline distance[8] of the leg divided by the mode-specific teleportation speed, and set a timer. When the arrival is due, the traffic flow simulation will note an arrival and the person will start its next activity. It means that trips with modes that are not physically executed in the traffic flow simulation are still logically executed, with the difference that there is no information about the chosen route through the network,[9] and these trips are not influenced by other events in the system and events in turn are not influenced by them. A big advantage of this is that, in this way, a simulation can be started with an arbitrary set of modes, and most types of analysis (e.g., modal trip distance/time distribution) are still possible. Clearly, they are approximated, but also a congested network loading model is an approximation, albeit a better one.

Travel mode characteristics for Patna demand As described above in Secs. 9.3.2.1 and 9.3.2.2, demand is categorized as urban and external.

a) Urban travelers use bicycle, car, motorbike, PT or simply walk. All modes are included in the simulation, but only bicycle, car and motorbike modes are physically simulated on the network. PT and walk trips are teleported.

b) Travel modes for external demand are bicycle, car, motorbike, PT, truck and walk. However, PT and walk trips are excluded from external demand because these modes are teleported and rest of the travelers from external demand cannot switch to these modes.

Tab. 9.3 provides the assumed speeds for all modes and *PCU*s for congested modes. In a traffic mix, the *PCU*s of bicycle and motorbike are on lower side if share of bicycle and motorbike is high (Chandra and Sikdar, 2000); therefore, the *PCU*s of bicycle and motorbike is assumed as 0.15. Tab. 9.3 also shows beeline distance factors for uncongested modes. The beeline distance, in principle, is a concept in MATSim that designates how much detour an actual trip takes compared to the direct teleported distance.

[8] The beeline distance is defined as the direct distance between the two activity locations.

[9] In a different implementation by Dobler and Lämmel (2011), uncongested modes are not teleported, but moved along a network. There is, however, no congestion on the links, but vehicles leave links at their free flow link exit times. Compared to teleportation, this has the advantage that a sequence of links will be noted by the simulation, which may be beneficial for some analyses, and is the minimal requirement for meaningful en-route re-planning in these modes. That approach was not used for this case study, since it is unrealistic to assume that pedestrians would only use the planning network that was available.

Table 9.3: Modal attributes for Patna scenario.

	congested mode					uncongested mode
	bicycle	car	motorbike	truck	PT	walk
Speed (km/h)	15	60	60	30	20	5
PCU	0.15	1	0.15	3	–	–
Beeline distance factor	–	–	–	–	1.5	1.5

9.4 Calibration

Before testing a policy measure, the calibration of the Patna scenario is necessary for the followings.

a) Destinations (activity locations) of the commuters are unknown.

b) Some of the trip diaries do not have mode and income information which is randomly assigned based on the modal distribution from Patna CMP (TRIPP et al., 2009).

c) The mode-specific utility parameters are taken from other sources. The ASCs for all modes are unknown.

Following section illustrates the procedure for calibration. In the whole simulation experiment, for simplicity, passing link dynamics and without holes traffic dynamics is used.

9.4.1 Calibrator : Cadyts

MATSim lacks in generating the plans using traffic counts data itself. Though, a probable choice set is generated using the possible activity locations (see Sec. 9.3.2.2), the destination for the commuters is not fixed. Hence, it cannot be used in the simulation directly. Cadyts (Flötteröd, 2010) bridges this gap by a Bayesian calibration process Flötteröd et al. (2011a). The procedure to integrate it with MATSim is described next.

Cadyts can be used as a tool to calibrate the initial demand based on the real-world traffic counts data. In this chapter, it is used to solve the problem of location choice similar to a previous work by Ziemke et al. (2015). Mainly it is used for homogeneous traffic (see Flötteröd et al., 2011b; Ziemke et al., 2015, for calibration of car traffic and; Moyo Oliveros and Nagel, 2012, for calibration of PT traffic). Though, in absence of mode choice as a re-planning strategy (see Sec. 2.2.2.3), Cadyts can be used for calibration of mixed traffic condition. However, this is not the case for the urban demand, thus, the set up is extended to use Cadyts for heterogeneous traffic conditions.

Cadyts applies a plan-specific utility correction to the score of the selected plan in the choice set of an agent. This correction for the homogeneous traffic is calculated as

$$\Delta V_l(k) = \frac{y_l(k) - q_l(k)}{\sigma_l^2(k)}$$

where $y_l(k)$ is the real-world traffic count on the link l, $q_l(k)$ is the count in the simulation for the same link l, and $\sigma_l^2(k)$ is the variance of the traffic count at link l and time bin k. Sum of all such corrections corresponding to different counting station is added to

the MATSim utility function with a weight w. In contrast to this, for heterogeneous conditions, the correction for every vehicle type *mode* on link l is calculated as shown in Eq. 9.3.

$$\Delta V_{mode,l}(k) = \frac{y_{mode,l}(k) - q_{mode,l}(k)}{\sigma^2_{mode,l}(k)} \tag{9.3}$$

From this, one can observe that for a given variance, if the simulated count is too low than the real-world traffic count, the correction will be positive and vice versa. This will eventually bring simulated counts close to the real-world traffic counts.

9.4.2 Utility function

The explicit values of utility parameters for Patna is unknown therefore, value of time and costs for car, motorbike and PT are taken from IRC:SP:30 (2009) and Kumar et al. (2004). In general, the value of time is the opportunity cost of time an individual traveler spends on the trip; this is highly dependent on the income level of individual. The income levels of the individuals in Patna is highly differentiated, many users are captive to only non-motorized or PT modes (see Tab. 9.1). Therefore, the default MATSim utility function is modified as follows.

1. **Income-dependent value of time:**

   a) To get started, let us assume a (partial) utility function for trip q by mode $mode(q)$ as

   $$V_q = -\widetilde{\beta}_{trav,mode(q)} \cdot t_{trav,q} + \bar{\beta}_{m,q} \cdot m$$

   where $\widetilde{\beta}_{trav,mode(q)}$ is the marginal utility of travel time, $t_{trav,q}$ is the travel time for trip q, $\bar{\beta}_{m,q}$ is the marginal utility of money and m is the monetary payments. The sign convention is such that $\widetilde{\beta}_{trav,mode(q)}$ typically is positive, $t_{trav,q}$ always positive, $\bar{\beta}_m$ typically positive, and m typically negative. In consequence, the VTTS is

   $$VTTS = \frac{-\widetilde{\beta}_{trav,mode(q)}}{\bar{\beta}_m} \tag{9.4}$$

   b) In order to incorporate the high income differentiation across different modes (see Tab. 9.1), the perception of income is added to behavioral decision making process of individual. Therefore, it is assumed that the marginal utility of money ($\bar{\beta}_m$) is no longer uniform, rather it depends on the income y_j of individual j. Hence the VTTS, as in Eq. 9.4, also depends on the income. As is common (e.g., see Franklin, 2006) , we will assume that the income-dependent marginal utility of money is indirectly proportional to the income:

   $$\beta_{m,j} = \frac{\bar{y}}{y_j} \ ,$$

   where $\bar{y}$ is the median income for all individuals, and y_j is the income of indi-

vidual j.

c) It is assumed that the (dis)utility of traveling by car, $\widetilde{\beta}_{trav,car}$, is the same for every individual however car is predominantly used by high income persons. Therefore,

$$VTTS_{car} \stackrel{!}{=} \frac{-\widetilde{\beta}_{trav,car}}{\beta_{m,highIncome}} \qquad \beta_{m,highIncome} = \frac{\bar{y}}{y_{highIncome}}$$

where $y_{highIncome}$ is the median income for car users (see Tab. 9.1). Thus, the marginal utility of traveling by car will become:

$$\widetilde{\beta}_{trav,car} = VTTS_{car} \cdot \frac{\bar{y}}{y_{highIncome}} = 0.94 \cdot \frac{4000}{20000} = 0.19 \ \frac{util}{h},$$

where the VTTS comes from Tab. 9.2.

d) Similarly, for motorbike, the marginal utility of traveling will be:

$$\widetilde{\beta}_{trav,mb} = VTTS_{mb} \cdot \frac{\bar{y}}{y_{midIncome}} = 0.48 \cdot \frac{4000}{6250} = 0.31 \ \frac{util}{h}$$

e) For PT, the marginal utility of traveling:

$$\widetilde{\beta}_{trav,PT} = VTTS_{PT} \cdot \frac{\bar{y}}{y_{lowIncome}} = 0.59 \cdot \frac{4000}{4000} = 0.59 \ \frac{util}{h}$$

f) In absence of the values of time for bicycle and walk modes, (dis)utility (or disagreeability) of being (stuck) in traffic for bicycle and walk mode is assumed same as motorbike; i.e.,

$$\widetilde{\beta}_{trav,bicycle} = \widetilde{\beta}_{trav,walk} = \widetilde{\beta}_{trav,mb} = 0.31 \ \frac{util}{h}$$

These values express that car is the most agreeable of all available modes, and PT the least agreeable. The fact that the VTTS of car in Tab. 9.2 comes out as the one with the *highest* willingness-to-pay to shorten its duration is thus now explained by the higher income of car users, and not as a general inconvenience of car. This seems to be more plausible.

2. **Utility of performing:** Considering the marginal utility of time as resource, a unit reduction in travel time (Δt) would not only save the direct (dis)utility of travel $\beta_{trav} \cdot \Delta t$ but also increase the score by the utility of time as a resource, which approximately is $\beta_{dur} \cdot \Delta t$ (Kickhöfer and Nagel, 2016a, pp. 391–392). The latter is the opportunity cost of time gained by performing the activities for the saved time (Δt). This results in

$$\widetilde{\beta}_{trav,mode} = \beta_{dur} - \beta_{trav,mode}$$

where the sign convention is such that the MATSim parameter β_{dur} is typically positive and the MATSim parameter $\beta_{trav,mode}$ is typically negative. The MATSim

scoring function (see Eq. 2.2) requires an explicit value of β_{dur}. Thus, similar to Kickhöfer and Nagel (2016a, pp. 391–392), the marginal utility of performing (or marginal utility of activity duration) an activity (β_{dur}) is taken as the lowest of marginal utility of traveling for different modes ($\beta_{dur} = \widetilde{\beta}_{trav,car} = 0.19\ util/h$), and the corresponding direct marginal utility, $\beta_{trav,car}$ is set to zero. All other direct marginal utilities of traveling are set relative to this value, i.e.,

$$\beta_{trav,mode} = 0.19\ util/h - \widetilde{\beta}_{trav,mode}$$

The resulting mode-specific marginal utilities of traveling for MATSim scoring function are shown in Tab. 9.4 and Eq. 9.5.

3. **Scoring function:** Following, Eq. 2.4 and Tab. 9.4, the income dependent, simplified utility of traveling can be re-written as:

$$\begin{aligned}
S_{trav,bicycle(q)} &= C_{bicycle(q)} - 0.12 \cdot t_{trav,q} + \beta_{d,bicycle(q)} \cdot d_{trav,q} \\
S_{trav,car(q)} &= C_{car(q)} - 0.0 \cdot t_{trav,q} + \frac{\bar{y}}{y_j} \cdot (\gamma_{d,car(q)} \cdot d_{trav,q}) \\
S_{trav,mb(q)} &= C_{mb(q)} - 0.12 \cdot t_{trav,q} + \frac{\bar{y}}{y_j} \cdot (\gamma_{d,mb(q)} \cdot d_{trav,q}) \\
S_{trav,PT(q)} &= C_{PT(q)} - 0.40 \cdot t_{trav,q} + \frac{\bar{y}}{y_j} \cdot (\gamma_{d,PT(q)} \cdot d_{trav,q}) \\
S_{trav,walk(q)} &= C_{walk(q)} - 0.12 \cdot t_{trav,q} + \beta_{d,walk(q)} \cdot d_{trav,q}
\end{aligned} \tag{9.5}$$

$\bar{y}/y_j$ is now the income-dependent marginal utility of money, depending on the income y_j of individual j. $\gamma_{d,car(q)}$ and $\gamma_{d,mb(q)}$ are monetary distance rates, taken from Tab. 9.4. $\gamma_{d,PT(q)}$ is the distance based fare for PT, taken from Eq. 9.2. Further, the ASCs for different modes are calibrated to capture the influence of variables not explicitly included in the scoring function. Along with this, to include the physical effort in bicycle and walk mode, the marginal utilities of distance for bicycle and walk, $\beta_{d,bicycle}$ and $\beta_{d,walk}$, are also calibrated.

In absence of the data, utility parameters for bicycle, car and motorbike from urban and external traffic are assumed same. For trucks, a different behavioral model is required, which is out of the scope of this thesis. However, for the scenario completion and to include the congestion effects from commercial vehicles, trucks are also included in the simulation with MATSim default utility parameters.

9.4.3 Simulation set up

For the simulation, the combined demand (urban and external traffic) is used. For MATSim scoring function, the utility parameters except ASCs are listed in Tab. 9.4. The modal split of the urban travelers from reference study and initial plans is shown in Tab. 9.6. In order to replicate this modal split, mode choice is allowed for urban travelers and the ASCs are calibrated.

The calibration is performed for 200 iterations together with the Cadyts in order to generate the synthetic plans for the external demand (see Sec. 9.4.1). The Cadyts adds

Table 9.4: Utility parameters converted to MATSim format.

travel mode	monetary distance rate (γ_d) [USD/m]	marginal utility of traveling (β_{trav}) [$util/h$]
car	$-3.7 \cdot 10^{-5}$	-0.0
motorbike	$-1.6 \cdot 10^{-5}$	-0.12
PT	see Eq. 9.2	-0.40
bicycle	–	-0.12
walk	–	-0.12
marginal utility of activity duration (β_{dur}) [$util/h$]		0.19

a corrector factor to the utility function so that the simulation counts match the real traffic counts. Recall that in the initial plans, each external commuter has five plans corresponding to five different destinations. For the calibration process, the maximum limit of plans in the choice set of an agent is increased to 10 for the initial 200 iterations. After calibrating with Cadyts, only the best plans for each agent and in consequence only the destinations best matching the traffic counts are kept. The simulation is then continued for another 1000 iterations to stabilize the urban and external demand in absence of the Cadyts correction factor from the utility function.

Re-planning Different innovative modules are used for different sub-populations.

a) **Urban:** 15% of the urban travelers are allowed to change their route, 10% are allowed to change mode and 5% are allowed to mutate the departure time of the activity. The mutation of the departure time of the activity is performed randomly between -2 to $+2$ h (see Sec. 2.2.2.3). The time mutation is turned off after Cadyts calibration, the departure times of the urban travelers are then fixed.

b) **External:** 15% of the agents from external traffic area allowed to change route until innovation is turned on i.e., initially until 160 iterations ($= 0.8 \cdot 200$) and then until 1000 iterations ($= 200 + 0.8 \cdot (1200 - 200)$). However, after 200 iterations, the origin-destination of the external demand is fixed, as explained above.

The innovation is used until 80% of iteration (i.e., initially for 1-160 iterations and then 201-1000 iterations). The remaining agents until 80% of the iterations and all agents afterwards chose a plan from their generated choice set.

9.4.4 Calibration results

In this section, the results of the calibration are presented and the modal splits from reference study, initial plans and calibrated demand are compared. Afterwards, the real-world traffic counts are compared with the simulation counts. In order to understand the impact of the income-dependent scoring function, a comparison of income-dependent distance distribution from first and last iterations are presented.

9.4.4.1 Calibrated utility parameters

The calibrated ASCs for all modes and marginal utility of distance for bicycle and walk modes are shown in Tab. 9.5. The ASCs for bicycle and walk modes are estimated to zero which can be interpreted as no initial impedance. Car/motorbike and PT often have some initial overhead either in terms of getting the car out of the garage or in terms of walking to PT stop. In this scenario, walking to PT stop is marginally less burdensome as getting the car/motorbike out of the garage/parking location.

As a consequence of mode choice, the share of walk mode increases which can be controlled either by a negative ASC or by having marginal utility of distance for walk mode ($\beta_{d,walk}$). The former has less significance for walk mode and therefore the latter is chosen. Eventually, in contrast to bicycle, walk mode is teleported and thus the utility for a person with walk mode is not affected by congestion. The marginal utility of distance for walk mode ($\beta_{d,walk} = -1.2 \cdot 10^{-4}\ util/m$) is estimated to marginally higher than the marginal utility of distance for bicycle mode ($\beta_{d,walk} = -1.1 \cdot 10^{-4}\ util/m$). This means, for walking 1 km, an agent will loose 0.12 $Util(util)$. At a speed of 5 km/h, it will take 12 min which could be used for performing an activity. Thus, the agent will also loose 0.024 $util$ ($= \beta_{trav,walk(q)} \cdot 0.2h$) for traveling and 0.038 $util$ ($= \beta_{dur} \cdot 0.2h$) opportunity cost of time which could be used for performing an activity.

Table 9.5: Calibrated utility parameters.

	travel mode				
Parameter	**bicycle**	**car**	**motorbike**	**PT**	**walk**
after Cadyts calibration (it.1200)					
ASC ($util$)	0.0	−0.6	−0.58	−0.545	0.0
$\beta_{d,mode(q)}$ ($util/m$)	−0.00011	–	–	–	−0.00012

9.4.4.2 Modal split

A comparison of the modal splits at different stages is shown in Tab. 9.6. Importantly, it can be observed that modal share for walk mode is significantly different in reference study and in the initial plans. The aim of the calibration is set to replicate the modal shares from the reference study. Clearly, the modal split after calibration (column "it.1200" in Tab. 9.6) has close resemblance with the reference study.

9.4.4.3 Traffic counts

Fig. 9.2 shows the comparison of average weekday real counts and average weekday simulation counts after 1200 iterations. The counts are scaled up for 100% population. In the first step, Cadyts pushes agents on the routes by adding a correction factor to the scoring function such that the simulation counts match to the real counts. Afterwards, in absence of the Cadyts correction factor, the simulation counts become higher than the real counts (see Fig. 9.2), however, the calibration results after 1200 iterations provide a good fit for

Table 9.6: Modal splits for urban demand.

mode	reference study TRIPP et al. (2009)	initial urban plans from travel diaries; it.0	after calibration it.1200
bicycle	33%	29.0%	32.3%
car	2%	4.0%	2.7%
motorbike	14%	20.3%	14.7%
PT	22%	26.6%	21.7%
walk	29%	20.1%	28.6%

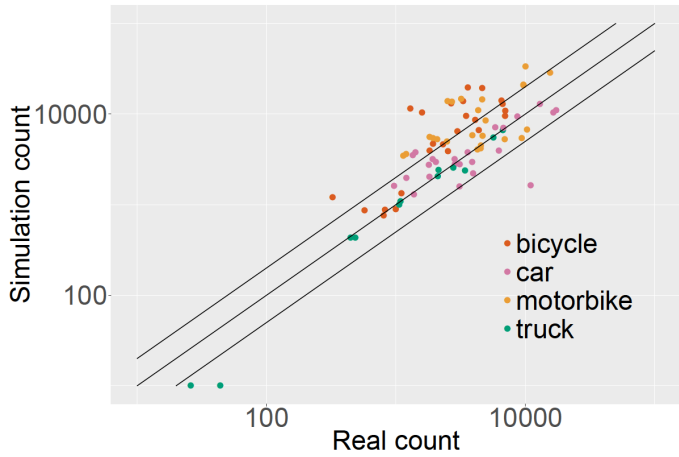

Figure 9.2: Comparison of 24 h simulation and real traffic counts.

modal split and synthetic plans for external traffic. Therefore, the output of the iteration 1200 is used for further policy testing and referred as the "base case".

9.4.4.4 Income distance distribution

In order to understand the impact of the income-dependent scoring function for different modes, income distance distribution is plotted in Fig. 9.3. The income attributes are taken from the initial trip diaries and trip distances are the beeline distances between origin and destination activities. Thus, following important observations are made:

a) Car is restricted to mainly high income group in initial plans as well as in the base case, however, in contrast to the initial plans, in the base case, car is used for the longer distances.

b) PT is used mainly for longer distances ($> 4km$) whereas bicycle and walk modes are used for relatively shorter distances ($< 6km$). A few longer bicycle trips can be observed for very low income households.

c) To replicate the modal share from the reference study, the scenario is calibrated such that share of walk trips is about 8% higher in the base case (see Tab. 9.6). A higher share of walk trips (relatively shorter distance i.e., $< 4km$) can be noticed in the Fig. 9.3b. Additionally, the scoring function forces the impractical longer ($> 8km$)

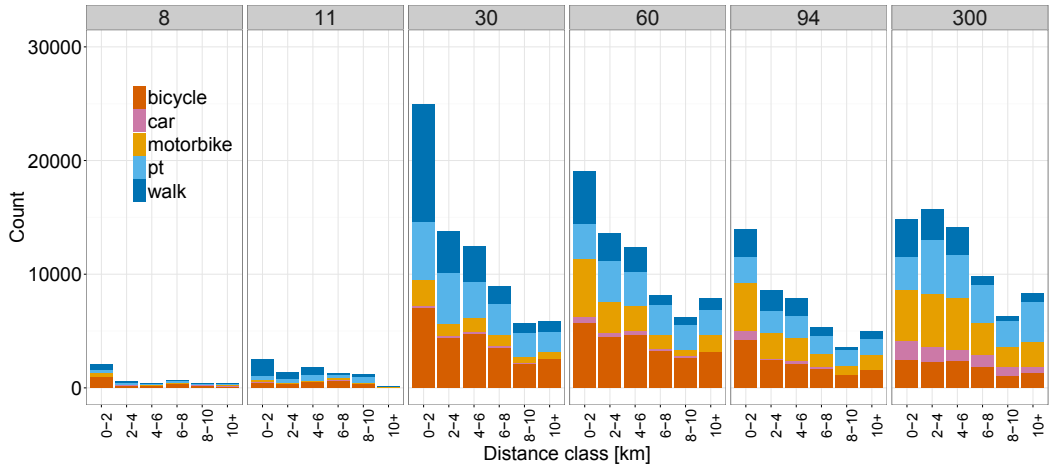

(a) it.0 (initial plans)

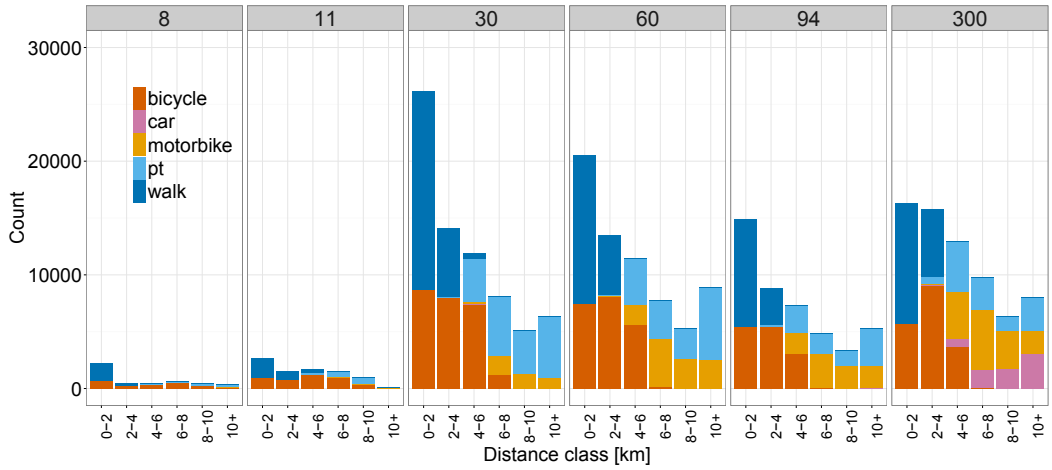

(b) it.1200 (calibrated plans)

Figure 9.3: Income-dependent distance distributions for initial plans and calibrated base case. The x- and y-axes depict the distance classes (in *km*) and number of trips respectively. The average income (in *USD*) is shown at the top of each frame.

walk trips to other plausible modes. A similar effect is also observed for the longer bicycle trips from higher income groups.

It can be observed that the modal income-dependent distance distribution for the initial plans is irregular (see distributions for bicycle and walk modes in Fig. 9.3a). The calibration against such non-linear distribution is beyond the scope of this thesis, however, plausibly, in future, this can be achieved with the help of Optimization of dynamic traffic simulations (Opdyts) (Flötteröd, 2016a).

9.5 Policy measures

Transport planners decide a policy minimally based on the traffic patters, pressure on the supply, income levels of the households, modal share, objectives of the policy (e.g., generate revenues, abate transport externalities, etc.). An effective policy for a particular

situation might not be effective in other situations. Therefore, in the context of Patna, a few policy measures are discussed in terms of the applicability and then suitable policy measures are proposed.[10]

1. **Tolls for transport externalities:** Several pricing schemes are available in the literature (see Sec. 3.2), in which, mostly, private vehicles and commercial traffic are tolled. Two such similar pricing schemes presented in Chs. 4 and 5. Application of these schemes to Patna would be less effective because

   i) the potential toll payers are car users and share of the car trips is very low (about 2%)

   ii) share of non-motorized trips is about 50% (see Tab. 9.6) and thus, the city is not severely struggling with the problem of emission externality and

2. **Tolled lane:** The differences in the income levels of the individuals in Patna are large (see Tab. 9.1); travelers from low income households are captive to non-motorized or PT modes. In such cases, policies are very sensitive to the household income levels, e.g., for the travelers with low income money would be more important than time or comfort, whereas travelers with high income would prefer to travel with faster and comfortable mode. In such scenarios, a possible measure would be to reserve a lane if the link has 2 or more lanes, and apply a toll on the reserved lane (Powell, 2001, pp. 271–290; Bar-Gera, 2012; Anderson and Geroliminis, 2015). This can restrict the further possible switches from non-car to car trips and make a balance between the different user preferences (travel time/cost). The toll values in such cases, mainly, depends on the demand and supply. About 36% of the total road length in Patna have a width less than 5 m (TRIPP et al., 2009) which narrows the chances of success of such policy.

3. **Physical segregation of bicycle:** For Patna, the bicycle share is about 33% which is highest among all modes (see Tab. 9.6). This favors the need of a segregated infrastructure for bicycle modes. A desired bicycle superhighway would be on ground however, it could be overhead if space on the ground is limited or not available. As discussed above, the pricing schemes for Patna might not be a successful policy measure; even though, if a pricing scheme is applied, the generated revenue should be used for positive efforts towards sustainable transport. The bicycle superhighway is one such positive effort. There are at least two major hurdles for laying a bicycle superhighway in the urban area:

   a) **Land acquisition:** This is a common problem before laying any kind of road and it becomes sever if required land is in built-up area. The widening of existing road infrastructure for bicycle lane is not possible for the similar reasons.

   b) **Restriction on motorbike:** Generally, bicycle lane in India is about 2.5 m wide so that cycle rickshaw can also use them (Tiwari, 2001). A major drawback of this is that due to wide bicycle lane, it is also used by motorbike and it is hard to restrict the motorbikes on the bicycle superhighway.

[10] In this thesis, PT is not physically simulated on the network therefore policy measures related to improvements for the PT infrastructure is out of scope of the thesis.

Derived from the foregoing discussion, a bicycle superhighway is proposed while considering the two major hurdles (land acquisition and restriction of motorbike on bicycle superhighway). It is proposed to lay the bicycle superhighway along the railway line because

a) it is more likely that there is enough space available on both side of the railway line,

b) the railway line is spread from east to west and

c) is parallel to the one of the major arterial (see Fig. 9.4).

Since, it is a physically segregated bicycle superhighway (rather than a bicycle lane parallel to arterials), motorbike can be restricted by law enforcements. However, a what-if case is considered in which bicycle superhighway is used by bicycle and motorbike simultaneously.

9.5.1 Policy scenarios

Following scenarios are considered for Patna.

1. **BAU:** Business as usual
2. **BSH-b:** Bicycle superhighway used by bicycle mode only
3. **BSH-mb:** Bicycle superhighway used by motorbike and bicycle modes.

The output results of the calibrated base case is used for the three scenarios.

9.5.2 Policy set up

For comparison, the calibrated base case (see Sec. 9.4.4) scenario is further run for 200 iterations and named as business as usual (BAU) i.e. no policy measure is applied.

A bicycle superhighway is added to the existing network as shown in Fig. 9.4. The entry/exit to the bicycle superhighway is decided based on an optimization approach (see Sec. 9.5.3). For each link of the bicycle superhighway, it is assumed that bicycles are about two times faster than on the regular network and the effort to ride a bicycle is reduced to half.[11] For the first policy measure (BSH-b) only bicycle mode is allowed on the superhighway whereas for the second policy measure (BSH-mb), both bicycle and motorbike modes are allowed on the superhighway.

All three scenario (see Sec. 9.5.1) are run for 200 iterations. Output plans of the base case (it.1200) is used for all three scenarios. Further, for re-planning, plans innovation is used until 80% of the iterations (see Fig. 2.2). Similar to the base case, in each iteration 10% urban travelers are allowed to change mode , 15% are allowed to change route. For all external trips, only reroute is allowed for 15% of the agents. Rest of the agents until innovation and all the agents after it, select a plan from their generated choice sets. The base case scoring function (see Eq. 9.5) and calibrated parameters (see Tab. 9.5) are used for all three scenarios.

[11] Technically, this is achieved by giving each link of the bicycle superhighway only half of its true length.

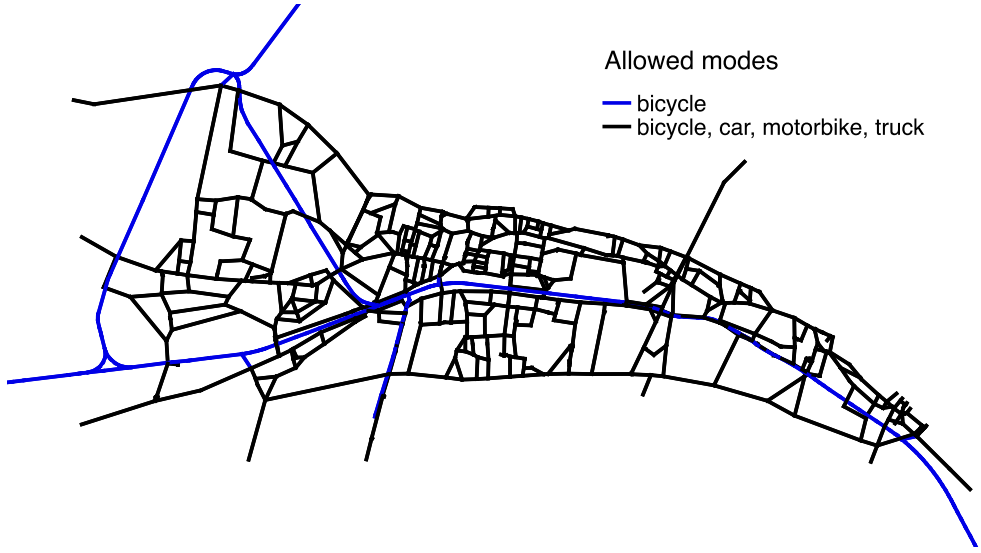

Figure 9.4: Patna network with bicycle superhighway.

9.5.3 Bicycle superhighway connectors

For successful laying of a vehicle-specific superhighway depends on the benefits and usage of the superhighway. This, in turn, depends on the links which connects the regular network to the superhighway. The number of connectors may be constrain by the budget of the project or on other factors, however, in this chapter, the optimum number of connectors are identified based on the usage of the connector links.

Algorithm 9.1: Identification of the bicycle superhighway connectors.

Input: Nodes of existing network $N_{e,n}$
Input: Node of proposed bicycle superhighway network $N_{b,m}$
for *every node* $N_{b,i}$ *in set* $N_{b,m}$ **do**
  $N_{e,i} \leftarrow$ get nearest node from $N_{e,n}$;
  $N_i \leftarrow$ connect $N_{b,i}$ to $N_{e,i}$ to get connector;
Output: Number of connectors (N_c) between bicycle superhighway and existing networks

Data: $N_c \leftarrow$ total number of connectors
Input: $K_c \leftarrow$ total number of required connectors
Input: $I_r \leftarrow$ iterations to let the agents react under all connectors
Input: $I_u \leftarrow$ iterations after which a connector is removed
for *each iteration* I **do**
  for *for each connector until,* $N_c - K_c == 0$ **do**
    if $I <= I_r$ **then**
      let the agent react ;
    else if $(I - I_r)\%I_u == 0$ **then**
      get the least used connector and remove it;

The Alg. 9.1 shows the steps to identify the optimum number of bicycle superhighway connectors. In the first step, the bicycle superhighway is connected with the Patna network with all possible connectors. For initial I_r iterations, agents are allowed to react (change mode, route) under all possible connectors. Thereupon, after every I_u iterations, the least

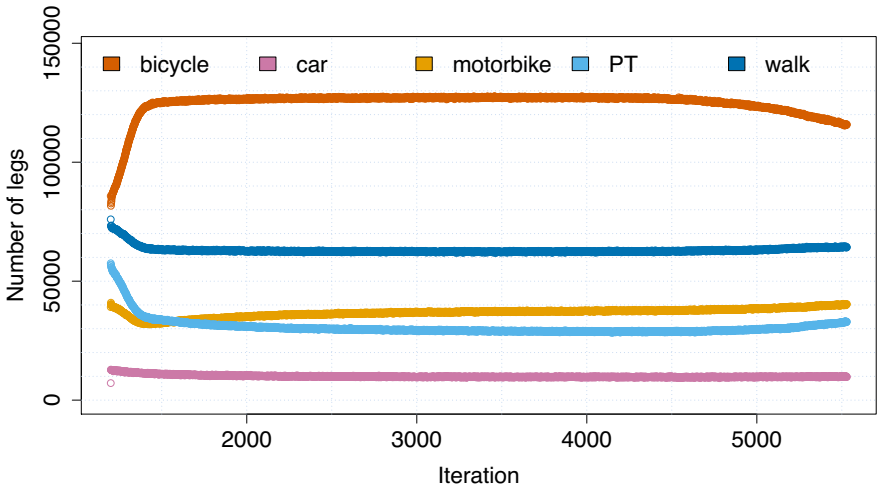

Figure 9.5: Modal share of urban travelers during identification of bicycle superhighway connectors.

used[12] connector is identified and removed from the network. For the Patna scenario, initially, the agents are allowed to react in the presence of the all connectors for 100 iterations ($= I_r$) and least used link is removed after every 10 iterations ($= I_u$). The resulting modal share is shown in Fig. 9.5. From this, it can be observed that, initially, the bicycle share (orange color) increases steeply in the presence of all possible bicycle superhighway connectors, become constant until 4500 iterations and then start decreasing after 4500 iterations. Therefore, the connectors at iteration 4500 are taken as the optimum locations of the connectors and the output network from iteration 4500 is chosen for the two policy measures (BSH-b and BSH-mb).

9.6 Results

This section mainly exhibits and compares the results of the three scenarios. Firstly, in order to show the broad picture of the impact of the bicycle superhighway, the congestion patterns from the three scenarios are presented in Sec. 9.6.1. This is followed by a comparison of the modal split for all three scenarios in Sec. 9.6.2 and an detailed analyses of the mode switcher and retainer in Sec. 9.6.3. The results of the two policy scenarios (BSH-b and BSH-mb) are compared with the BAU scenario. Since, the external demand is added to the scenario for completeness of the scenario and having congestion effects from the external demand, the results are mainly analyzed for urban travelers only.

9.6.1 Congestion patterns

Fig. 9.6 shows a comparison of the congestion patterns[13] from three scenarios for car, motorbike and bicycle traffic at 08:00:00. The left column (Figs. 9.6a, 9.6d and 9.6g)

[12]The selection criteria to remove a link could be determined by any criteria e.g., budget constrain, economic benefits etc. However, for simplicity, in this case, least used link is selected for removal.

[13]These congestion patters are generated using the visualization tool VIA (see http://www.via.senozon.com).

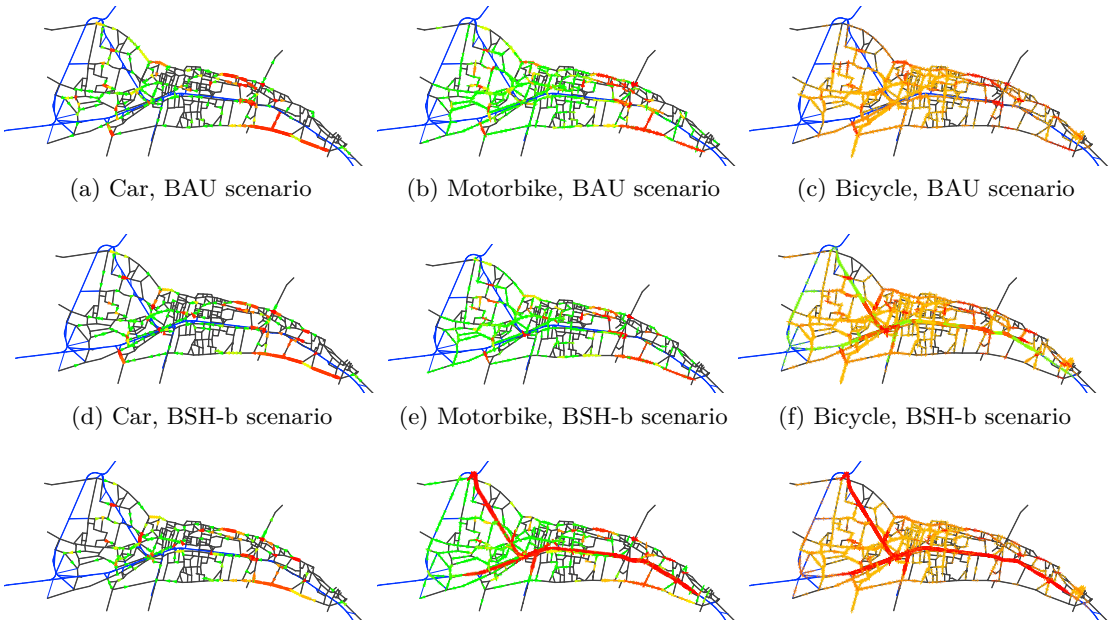

(a) Car, BAU scenario (b) Motorbike, BAU scenario (c) Bicycle, BAU scenario

(d) Car, BSH-b scenario (e) Motorbike, BSH-b scenario (f) Bicycle, BSH-b scenario

(g) Car, BSH-mb scenario (h) Motorbike, BSH-mb scenario (i) Bicycle, BSH-mb scenario

Figure 9.6: Comparison of the congestion patterns at 08:00:00 for three scenarios.

shows the congestion patterns for car. Though, a capacity relief on the new bypass can be observed in the BSH-mb scenario, the traffic patterns for the car traffic remain mostly same in the three scenarios because the share of the car does not change much (approximately 2%; Tab. 9.7). The middle column (Figs. 9.6b, 9.6e and 9.6h) shows the congestion patterns for motorbike. The former two depicts approximately similar patterns whereas the long queues appear in the latter (BSH-mb scenario) which is an effect of allowing motorbikes on the bicycle superhighway. The right column (Figs. 9.6c, 9.6f and 9.6i) shows the congestion patterns for bicycle traffic. A few small bicycle queues appear on the few links of the bicycle superhighway in BSH-b scenario. The queues become longer in the BSH-mb scenario in which both motorbike and bicycle travel on the bicycle superhighway. Overall, a capacity relief effect on the new bypass road (see Fig. 9.1) and other streets can be observed.

9.6.2 Modal split

Tab. 9.7 shows the modal splits for various scenario. In business as usual scenario (BAU), the modal split is about the same as the base case scenario and reference study. The effect of the bicycle superhighway is clearly visible in BSH-b and BSH-mb scenarios. In BSH-b scenario, approximately half of the urban trips are made by bicycle mode. The increase in the bicycle share comes mainly from PT trips and, partly from motorbike and walk trips (also see Tab. 9.8b). On the other hand, in BSH-mb scenario, motorbike can also travel on the bicycle superhighway; this increases the share of motorbike to more than 18%. Consequently, the share of the bicycle is about 44% which is significantly higher than the modal share in BAU scenario but lesser than the modal share in BSH-b scenario. Further, the detailed analysis for mode switcher and retainer is presented in the next section.

Table 9.7: Modal splits for urban travelers (in %) for various policy scenarios.

mode	reference study	it.1200	it.1400		
		base case	BAU	BSH-b	BSH-mb
bicycle	33.0	32.3	32.5	48.7	44.0
car	2.0	2.7	2.5	2.1	1.9
motorbike	14.0	14.7	15.3	11.2	18.5
PT	22.0	21.7	21.2	12.9	10.3
walk	29.0	28.6	28.6	25.1	25.3

9.6.3 Mode switcher analysis

9.6.3.1 Change in number of trips

Tab. 9.8a shows the number of trips for mode switchers (e.g., car to bicycle, motorbike to car, etc.) and mode retainers (the diagonal values in the matrix; e.g., car to car, bicycle to bicycle, etc.) for BAU scenario. Clearly, for the BAU scenario, most of the agents retain their modes.

Tab. 9.8b and Tab. 9.8c show the change in the number of trips of mode switcher/retainer with respect to BAU scenario for BSH-b and BSH-mb policy measures respectively. In the BSH-b scenario, with respect to BAU, the increase in the bicycle share is mainly contributed from motorbike, PT and walk to bicycle mode switchers (11712, 20330 and 9058 trips respectively). The contributions from motorbike, PT and walk to bicycle mode switchers have significantly decreased in BSH-mb scenario (7166, 13560 and 8594 trips respectively). This is an effect of allowing motorbikes on the bicycle superhighway. In addition to this, for BSH-mb scenario, (a) significant number of PT trips are shifted to motorbike mode (12892 trips) and (b) the number of motorbike retainers is approximately 5000 higher than the number of motorbike retainers in the BSH-b scenario. The driving forces behind this are discussed in the next section.

9.6.3.2 Change in the average speed

Tab. 9.9 shows the changes in average route speed and in average beeline speed for mode switcher/retainer. The changes are computed with respect to the first iteration (it.1200) of each policy measure. The route speed is the ratio of the route distance (along traveled links)[14] to the travel time in the simulation whereas the beeline speed is the ratio of the direct distance between the activity locations (beeline distance) to the travel time.[15]

Tab. 9.9a and Tab. 9.9b show the changes in the average route speed and average beeline speed for BSH-b scenario and Tab. 9.9c and Tab. 9.9d show the changes in the average route and beeline speeds for BSH-mb scenario. In BSH-b scenario, for bicycle

[14] As mentioned before in Sec. 9.5.2, to make the bicycle twice as faster as on the normal network, the length of the links of bicycle superhighway is halved. For the analysis of the average route speed, the actual link length of the bicycle superhighway is taken while making the speed of the bicycle double on these links.

[15] In general, if the activity locations does not change, the positive change in average beeline speed denotes the lesser travel time for the same beeline distance and vice versa.

Table 9.8: Analysis for number of trips of mode switcher/retainer.

(a) Absolute number of trips for BAU Scenario

		last iteration (it.1400)					
		bicycle	car	motorbike	PT	walk	total
	bicycle	82408	56	430	774	2140	85808
first	car	48	4772	1712	622	2	7156
iteration	motorbike	526	1056	36186	1308	16	39092
(it.1200)	PT	1084	702	2296	53408	28	57518
	walk	2176	4	18	22	73766	75986

(b) The change in the number of trips for BSH-b scenario with respect to BAU

		last iteration (it.1400)				
		bicycle	car	motorbike	PT	walk
	bicycle	+1092	−28	−228	−484	−352
first	car	+990	−804	+10	−194	−2
iteration	motorbike	+11712	−348	−10674	−682	−8
(it.1200)	PT	+20330	+210	+74	−20618	+4
	walk	+9058	−2	−10	0	−9046

(c) The change in the number of trips for BSH-mb scenario with respect to BAU

		last iteration (it.1400)				
		bicycle	car	motorbike	PT	walk
	bicycle	+942	−26	−204	−522	−190
first	car	+542	−1734	+1538	−344	−2
iteration	motorbike	+7166	−432	−5806	−920	−8
(it.1200)	PT	+13560	+554	+12892	−27014	+8
	walk	+8594	−4	+64	−2	−8652

retainers, the average route speed *in*creases by +1.09 km/h and the average beeline speed increases by +0.37 km/h. This indicates that the bicycles are faster and also travel longer distances. Since significant number of bicycle trips are using the bicycle superhighway, a capacity relief on the network also increases the average route speeds of car and motorbike retainers (+3.20 and +4.28 km/h). This also translates in higher beeline speeds (+2.49 and +3.03 km/h), i.e., reduced origin-to-destination travel times.

The average route speeds for car and motorbike to bicycle mode switchers *de*crease by −7.28 and −12.73 km/h respectively whereas the average beeline speeds *de*crease by −4.88 and −9.31 km/h respectively. This indicates that switching from car/motorbike to bicycle makes the travel speed considerably slower, while the direct origin-to-destination speed and thus the travel time does not suffer as much.

In the BSH-mb scenario, due to congestion on the bicycle super highway, the average

Table 9.9: The changes in average speeds (in km/h) for mode switcher/retainer with respect to first iteration (it.1200).

(a) The changes in average route speed for BSH-b scenario

		last iteration (it.1400)				
		bicycle	car	motorbike	PT	walk
	bicycle	+1.09	+13.92	+17.07	+9.66	−5.42
first	car	−7.28	+3.20	+6.92	+6.37	–
iteration	motorbike	−12.73	+2.90	+4.28	+3.56	−26.59
(it.1200)	PT	−9.22	−1.91	+3.01	0.00	−15.01
	walk	+6.82	+30.04	+19.75	+15.02	0.0

(b) The changes in average beeline speed for BSH-b scenario

		last iteration (it.1400)				
		bicycle	car	motorbike	PT	walk
	bicycle	+0.37	+9.47	+11.47	+5.50	−3.22
first	car	−4.88	+2.49	+4.82	+2.94	–
iteration	motorbike	−9.31	+2.33	+3.03	+1.24	−15.20
(it.1200)	PT	−5.39	+0.29	+2.49	0.00	−10.16
	walk	+2.90	+16.09	+10.74	+9.78	0.0

(c) The changes in average route speed for BSH-mb scenario

		last iteration (it.1400)				
		bicycle	car	motorbike	PT	walk
	bicycle	−2.34	+7.26	+14.07	9.74	−5.83
first	car	−16.12	+4.82	−3.18	+6.66	–
iteration	motorbike	−21.87	+2.70	−3.95	+1.51	−25.21
(it.1200)	PT	−13.24	−1.67	−8.40	0.00	−15.01
	walk	+2.90	–	+14.56	+15.01	0.0

(d) The changes in average beeline speed for BSH-mb scenario

		last iteration (it.1400)				
		bicycle	car	motorbike	PT	walk
	bicycle	−1.76	+4.35	+8.72	+5.49	−3.42
first	car	−10.35	+3.82	−2.54	+2.86	–
iteration	motorbike	−15.21	+2.22	−3.76	−0.50	−14.73
(it.1200)	PT	−8.48	+0.79	−5.16	0.00	−9.43
	walk	+0.90	–	+6.12	+10.51	0.0

route and beeline speed for bicycle retainers *de*creases by -2.34 km/h and -1.76 km/h respectively i.e., the bicycle retainers move more slowly, but somewhat compensate by more direct routes. Similar to the BSH-b scenario, the average route speed *de*creases for car/motorbike to bicycle mode switchers. In contrast to the BSH-b scenario, the average route speeds for car to motorbike switchers and motorbike retainers *de*crease significantly and yet they are better off by traveling shorter distances.

Overall from the mode switcher/retainer analysis, it can be summarized that share of bicycle increases significantly even if the motorbikes are allowed on the bicycle superhighway. Further, in the next section, the emissions externalities for all scenarios are estimated, which will emphasize the importance of the bicycle superhighway towards sustainable transport.

9.6.4 Emissions calculation

Estimation approach In order to assess the impact of the policy scenarios, the emissions are estimated as a post-processing step. To estimate the emissions from motorbike, the EMT (see Sec. 4.2.2 for detailed methodology; Kickhöfer et al., 2013) is extended to mixed traffic conditions. Thereafter, the emissions[16] are calculated for all three scenarios.

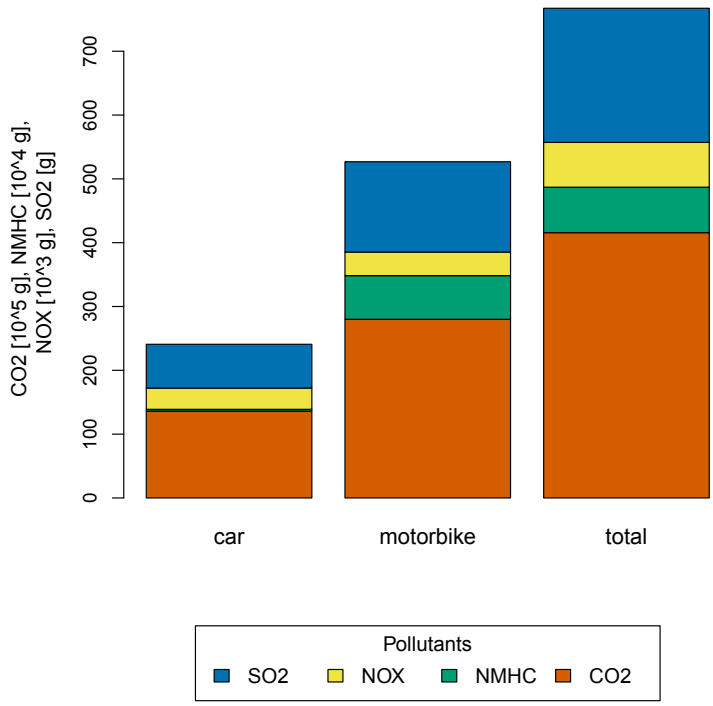

Figure 9.7: Absolute emissions for Patna BAU scenario.

[16]For Patna scenario, HBEFA version 3.2 is used. For motorbike, it does not provide i) the cold start emissions and ii) *PM* emissions. Thus, *PM* emissions are not shown in the analysis.

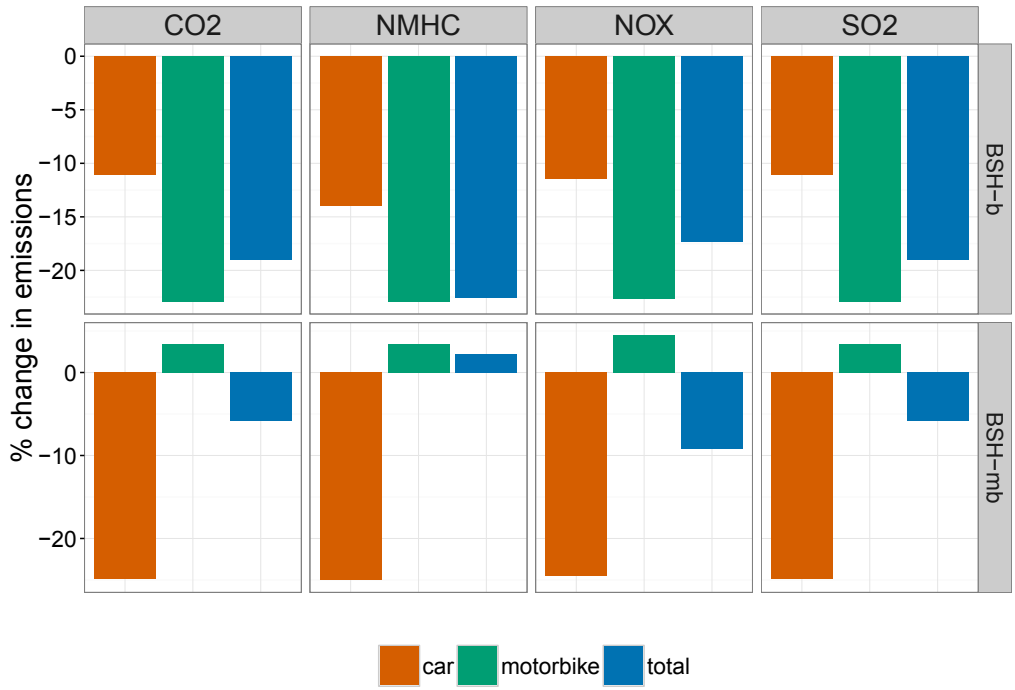

Figure 9.8: Change in emissions (in %) for the BSH-b and BSH-mb scenarios with respect to BAU scenario.

Absolute emissions for BAU Fig. 9.7 shows the emissions from car and motorbike for BAU scenario. Though, the emissions per km is higher for car than motorbike (e.g., 200, 83 gCO_2/km for car and motorbike respectively), the emissions from motorbike is significantly higher than the emissions from car due to higher modal share of the motorbike. An important observation is that the $NMHC$ from motorbike is approximately 95% of the total $NMHC$ because in contrast to other pollutants, motorbike emits significantly higher $NMHC$ emissions than car.[17] The estimated per kilometer emissions from car and motorbike (e.g., 0.49, 0.11 gNO_x/km) are in line with the literature (Goel and Guttikunda, 2015).

Changes in emissions for policy measures The % change in emissions for the two policy measures (BSH-b and BSH-mb) are shown in Fig. 9.8. The values are relative to the business as usual (BAU) scenario. For the BSH-b scenario, all emissions are *de*creased significantly. This is a positive effect of higher bicycle share and lower motorized traffic (see Tab. 9.7). Further, in BSH-mb scenario, a significant reduction in emissions for car mode is observed, however, the increase in the share of motorbike results to an *in*crease in the emissions for motorbike. Interestingly, overall, total emissions is still lesser than the BAU scenario except $NMHC$. The share of $NMHC$ emissions from motorbike is approximately 95% in the BAU scenario and an increase in the share of motorbike for BSH-mb scenario increases the total $NMHC$ emissions.

To summarize this, the BSH-b policy measure reduced the emissions most by increasing

[17] The $NMHC$ emissions from 2-stroke motorcycles are significantly higher than 4-stroke motorcycles (Tsai et al., 2000). Therefore, it is likely that in Indian context, the motorbike emissions estimated in this chapter are underestimated.

the share of bicycle and reducing the share of motorized vehicles. In the BSH-mb scenario, the increase in the share of motorbike increases the emissions from motorbike and the overall emissions decreases with an exception for *NMHC* emissions.

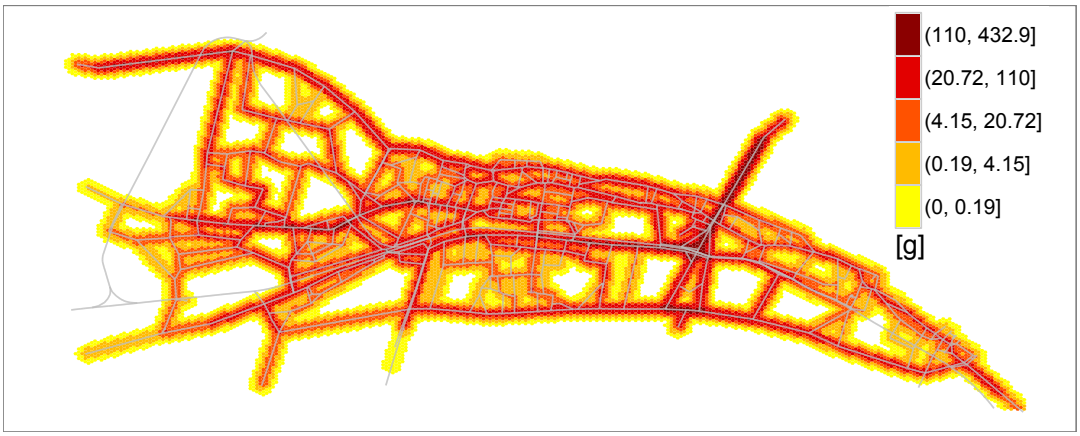

(a) Absolute emissions for BAU scenario.

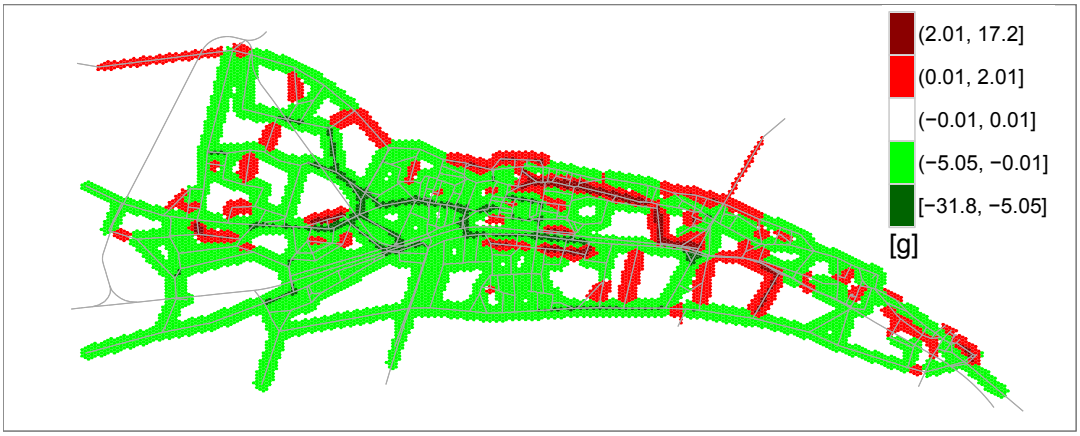

(b) Change in emissions for BSH-b scenario.

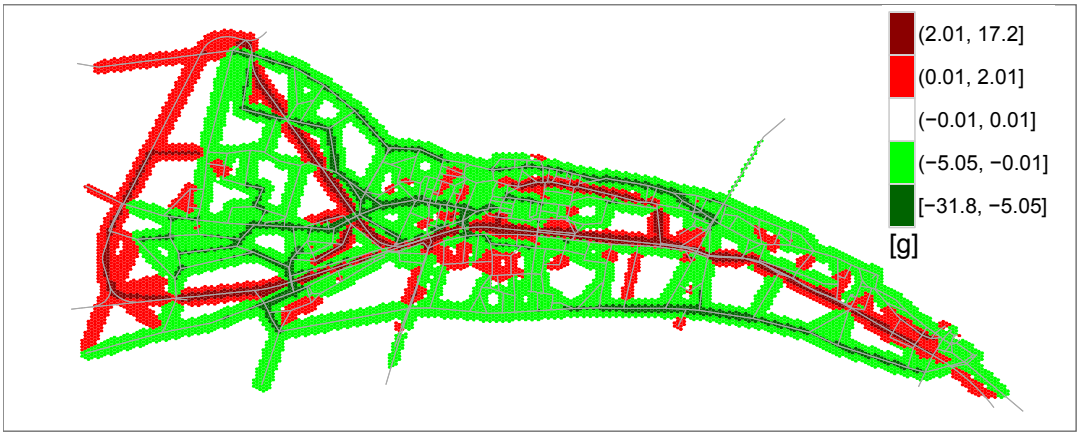

(c) Change in emissions for BSH-mb scenario.

Figure 9.9: Absolute NO_2 emissions (in g) for BAU scenario and change in emissions (in g) for BSH-b and BSH-mb policy measures. The values are scaled to full population.

Spatial distribution Fig. 9.9 shows the spatial distribution of NO_2 emissions.[18] Fig. 9.9a shows the absolute emissions (in g) for BAU scenario. The emissions on all major arterials (see Fig. 9.1), arterials, "Gandhi Setu" are high. Figs. 9.9b and 9.9c show the change in NO_2 emissions with respect to BAU scenario for BSH-b and BSH-mb policy measures respectively. An increase in emissions is indicated by red hexagons, a decrease in emissions is indicated by green hexagons and white hexagons denotes very minor change in NO_2 emissions. From the spatial distribution plots, it can be observed that emissions on most of the portion of major arterial and arterials decreases. This is an effect of decrease in the share of motorized vehicles. The decrease in NO_2 emissions on major arterials is more significant in the BSH-mb scenario due to capacity relief effect (dark green hexagons). In BSH-mb scenario, a significant increase in the emissions on the bicycle superhighway can be observed. This is the result of allowing motorbikes on the bicycle superhighway. Thus, BSH-b policy measure reduces emissions significantly (approximately 18%; see Fig. 9.8) mainly from the inner city. In contrast to this, BSH-mb policy reduces total emissions by only about 5% (see Fig. 9.8), and mainly increases the emissions in the inner city.

9.7 Discussion

The objective of this chapter is to simulate a large-scale scenario under mixed traffic conditions and to propose and test policy measures. For this, a scenario of Patna, India is chosen. The chapter presents the calibration process of the scenario and based on the traffic characteristics, proposes a policy measure. In the following, the influence of several assumptions to the overall results and an interpretation of the findings are discussed.

9.7.1 Plans from traffic counts

The urban demand for the Patna scenario is calibrated using the trip diaries which are recorded using the extensive surveys. The collection of the hourly traffic counts data is relatively easier than the trip diary surveys. This chapter shows that the hourly traffic counts are enough to generate the activity-based demand by extending the Cadyts to mixed traffic conditions. Thus, the approach is very helpful and can be applied to any scenario if the origin-destination matrix data or the trip diaries are not available and performing extensive trip diary surveys is not an option.

9.7.2 Calibration of utility parameters

Firstly, in absence of the data, the travel related utility parameters for this case study are taken from the IRC:SP:30 (2009). However, in future, a better estimates of the parameters should be evaluated using the stated or revealed preference surveys for the individual travelers of Patna or other similar urban area.

This chapter calibrates the ASC and marginal utility of distance for various modes manually. The calibration process is performed against the mode-specific, distance-based

[18] For illustration purposes, the emission plot only shows NO_2. For the visual presentation, a Gaussian distance weighting function is used to smooth emissions. Uniform hexagonal cells of size 100 m are used for this purpose. The smoothing radius is assumed to be 100 m. In contrast to Kickhöfer (2014) which assumes the emissions at the center of the link, the emissions are linearly distributed on the link. For more information on the exact visualization procedure, please refer to Appen. A.

income distribution. For this, an income-dependent utility function is used which eventually produces practical choices. However, the process of manual calibration is complex, error-prone and time-consuming, therefore, in future, it would be helpful to replace the manual calibration with an automatic calibrator – Opdyts – which also takes care of the non-linearity of the given distributions. The Opdyts optimizes a given objective functions (e.g., variation in the mode-specific income-dependent distribution), using a set of decision variables (e.g., utility parameters) in a transport simulation framework (e.g., MATSim) (Flötteröd, 2016a).

9.7.3 Inclusion of public transit

This chapter simulates car, motorbike and bicycle on the network physically whereas the PT and walk modes are teleported. In future studies, it would be interesting to see the impact of the policy measure while simulating the PT physically on the network. In absence of the transit schedules, the para-transit simulation could be useful (see, Neumann, 2014, for detailed description and methodology).

This chapter ignores the emissions from the public transit vehicles such as "tuk-tuks" which presumably emits significantly higher emissions than rest of the vehicles i.e., the total emission estimates are underestimated. The proposed policy measures show a significant shift from PT to bicycle, therefore, inclusion of the emissions from the public transit will further cut down the total emissions for the policy measures.

9.7.4 Policy implications

Based on the traffic characteristics and composition for Patna, this chapter proposes a bicycle superhighway. Firstly, it is recommended to lay it on the ground rather than overhead which will benefit the cycle-rickshaws (both for passengers and for goods). Since a railway line passes approximately in the middle of the Patna and parallel to the old bypass road, the problem of land acquisition can be circumvented by laying it along the railway line. This would still need the strong political intervention. Secondly, in absence of strict enforcements, possibly the motorbike riders will use the bicycle superhighway. To investigate this, this chapter considers a second policy scenario, in which both, bicycle and motorbike, are allowed to travel on it.

This thesis assumes that the bicycles are twice as fast on the bicycle superhighway as on the retular links, and require only half of the efforts. This is an optimistic assumption which shows that the share of bicycle increases significantly, even if the motorbikes are allowed on the bicycle superhighway. However, before a possible implementation, simulation studies with more realistic values should be done. Further, this chapter uses an iterative process to identify the optimum locations of connectors between the network and the proposed bicycle superhighway. A budget constraint could be added to the iterative process to limit the maximum number of connectors.

It is possible to calculate the emissions for highly differentiated vehicle types. However, in absence of the vehicle specific data, this chapter uses the average values from HBEFA. This results in the average NO_x emissions for car and motorbike as 0.49, 0.11 g/km which are approximately in the same order as in the literature (Goel and Guttikunda, 2015). The total emissions decrease significantly if only bicycles are allowed on the bicycle

superhighway. Though, except *NMHC* emissions, total emissions for BSH-mb scenario decrease, a significant increase in the emissions along the bicycle superhighway is observed which is inside the city and thus undesirable. This provides a strong reason to implement strict law-enforcements to stop the motorbikes on the bicycle superhighway.

For the policy makers and transport planners, this chapter shows the potential to reduce the emissions by laying a bicycle superhighway rather than a pricing measure. The latter has lesser public acceptance (Schade and Schlag, 2000). Thus, the insights from findings of this chapter can be transferred to other urban areas in order to increase the share of non-motorized vehicles for sustainable transport.

9.7.5 Benefit-cost analysis

Though, the benefits from the proposed policy measures are cited by showing the reductions in the emissions, an economic policy appraisal (e.g., benefit cost analysis) would help as decision support tool in transport planning (OECD, 2006). This would include the possible benefits from the reductions in emissions, congestion, etc., and the cost of laying the bicycle superhighway. Further, it would also be interesting to compare system welfare from the pricing based on the marginal social costs and from the benefits of laying bicycle superhighway.

9.8 Summary

In this chapter, a real world scenario of Patna, India is presented to show the simulation capabilities under mixed traffic conditions and then to test the policy measures. The urban demand is synthesized using the trip diary surveys. To include the congestion effects from the external traffic, the external plans are generated using the traffic counts data by extending Cadyts to mixed traffic conditions. The income diversity is included in the utility function and then the scenario is calibrated.

Further, this chapter proposes a bicycle superhighway while allowing only bicycle and, bicycle and motorbike both. The optimum locations of connectors between the bicycle superhighway and existing network are identified using an iterative process. It is shown that in both policy scenarios, the share of bicycle increases significantly. Further, the EMT is extended to mixed traffic conditions and the emissions are estimated for both scenarios. In the first policy scenario in which only bicycle travel on the bicycle superhighway, the emissions from car and motorbike both decreases significantly. In the second policy scenario in which motorbike is also allowed on the bicycle superhighway, the share of motorbike increases. Here, the emissions from car decrease whereas the emissions from motorbike increase. Though, except *NMHC* emissions, total emissions decrease, a significant increase in the emissions along bicycle superhighway is observed.

Chapter 10 Conclusions and Further Challenges

The thesis focuses on the evaluation of policy measures to abate the negative transport externalities while considering inter-relationships between different externalities and politically motivated goals. Since the model was to be applied to a city in India, additionally a computationally efficient model to simulate mixed traffic conditions was developed, which can replicate mixed traffic patterns realistically.

The background of the research problem was stated in Ch. 1. The travel simulator used in this thesis was briefly described in Ch. 2. Further, the thesis was divided into three parts; the first two parts mainly focused on the policies to internalize the transport negative externalities and modeling of heterogeneous traffic conditions respectively.

In Part I, first the review of the existing literature towards the estimation and internalization of the externalities was made in Ch. 3, a joint internalization approach for the congestion and emissions externalities was proposed to optimize the system using the damage costs in Ch. 4 and then a backcasting approach was proposed in Ch. 5 to derive the toll levels, as multiples of the original damage cost estimates, in order to achieve the politically motivated emission reduction targets.

Part II first reviewed the literature for traffic flow modeling in Ch. 6, introduced the *with holes* traffic dynamics and *seepage* link dynamics to the queue model in Ch. 7 and demonstrated two simulation experiments in Ch. 8.

Part III presented the demand generation, calibration for a case study of Patna, India and a bicycle superhighway is proposed to ease the traffic and increase the bicycle share in Ch. 9. Finally, the thesis contributions and further challenges are summarized in the present chapter.

10.1 Conclusions

Transport externalities

Starting at the level of individual externality, this thesis first investigated the separate marginal social cost pricing strategies for congestion and emission externalities to examine the impact of congestion pricing on emissions and vice versa. For this, a real-world case study of the Munich Metropolitan Area (MMA) was used. As expected and found in the

literature, the results indicated that the two externalities are positively correlated. The two pricing strategies are then combined to obtain a simulation-based approach to calculate and internalize the correct dynamic price levels for both externalities simultaneously. Since the underlying multi-agent simulation framework is computationally efficient, the presented approach is—in contrast to analytical models—suitable for the calculation of highly differentiated tolls in large-scale simulations with dynamic traffic flows and activity-based demand. With this, it was demonstrated that the joint internalization yields the lowest level of emission and congestion externalities for the whole population as well as for individual user groups. It also returned the highest level of system welfare. The main driving forces behind this overall effect was found to be modal shift from car towards public transit. Interestingly, this effect is present on the aggregated level but it was also found that external cost pricing can increase the car share of urban travelers who profit from a capacity relief which results from the reduction in the car share of other travelers. It was demonstrated that the potential efficiency gains can only be obtained when the implicit price elasticities of the car travel demand are captured in an accurate way, i.e., by carefully modeling substitutes to the car mode. Without substitutes, pricing can not unfold its full power and contribute to a meaningful reduction in transport-related externalities.

Furthermore, it was found that simply combining the average toll levels obtained from the isolated pricing schemes or from uncorrected exogenous cost estimates will result in overpricing. The amplitude of this effect was shown to be more important in peak hours for emissions and in off-peak hours for congestion. Therefore, the hypothesis that "combining the toll levels obtained from the separate pricing schemes would not yield toll levels above those of the economic optimum" is rejected. Policy makers should, hence, account for the correlations between the different externalities and correct the cost estimates. As one of the main contributions of this thesis, it was shown that the joint internalization approach makes it possible to identify the amplitude of this correlation between the externalities under consideration. The methodology is then used to derive corrected average toll levels per vehicle kilometer. An aggregation according to any other desired simplification rule seems feasible, which offers opportunities for policy design. With the help of the spatial distribution of changes in the externalities, it was shown that pricing emissions steers agents on shorter distance routes and pricing congestion pushes agents on shorter travel times routes with potentially longer distance routes. Thus, for congested areas, route choice behavior of agents is by tendency affected into opposite direction by the two pricing schemes. This needs to be accounted for when designing real-world policies: an emission (or distance)-based toll might increase congestion whereas a congestion-based toll might increase emissions. Therefore, the presented model seems necessary to simultaneously account for both externalities.

Further, in the context of the politically motivated emission reduction targets, a parametric backcasting approach was proposed in order to estimate the costs – in additional to the damage costs – required to reduce the EU's GHG emissions by 20% from the 1990 levels. In this direction, the approach was again applied to to Munich Metropolitan Area (MMA) with the simplified objective of reducing the CO_2 emissions by 20%. In the first step, the toll values were identified by internalizing the damage cost estimates from the literature. In order to achieve the 20% reductions in CO_2 emissions, the damage cost estimates are increased parametrically which are called as avoidance charge.

It has been showed that a factor of 10 is required to reduce the total emission costs by 20% and a factor of 5 is enough to obtain a 20% reduction in the CO_2 emissions in city area, metropolitan area or in the whole area together. The reduction in the CO_2 emissions was mainly due to modal shift from car to public transit. The highest contribution came from commuters and reverse commuters. As an effect of capacity relief, at lower values of the avoidance charge (a factor of 5 or lower), the car share of urban travelers increases; consequently, an increase in the CO_2 emissions for urban travelers were observed. Further investigation of emission pollutants indicated that the number of short urban car trips increased which in turn increased the *NMHC* levels except at very high levels of avoidance charge. Similarly, minor increase in the *NMHC* levels for freight user group was also observed due to shift in the routes from motorway to local and distributor roads. A 6 times increase in the system welfare was observed while applying the toll equivalent to 5 times of the damage costs.

To achieve the 20% reduction in the CO_2 emissions, the cost estimates from the literature must be increased 5 times thus the avoidance charge will become 350 EUR/ton. This value is significantly higher than the projected avoidance costs in literature (Maibach et al., 2008, pp. 262-264). However, the case study points out that a steep avoidance charge is required to achieve the 20% reductions in CO_2 emissions with respect to 1990 levels from road transport sector.

Mixed traffic

To investigate a policy measure for the urban area in industrializing countries, it is important to replicate the heterogeneous traffic conditions in the simulation framework. In this regard, the Part II extended an existing queue model to heterogeneous traffic conditions. The queue models play an important role for the simulation of large-scale scenarios because it controls agents at entry/exit of the link and never in between. The simple to implement and understandable logic of the queue model makes it computationally efficient. This thesis extended the queue model for a more realistic behavior by introducing the backward traveling holes for mixed traffic conditions. In this approach, the space freed by the leaving vehicles was not immediately occupied by the following vehicles. Thus, the proposed queue model is realistic and show characteristics similar to the simplified Kinematic Wave Model (KWM) and double-ended queue model. The Fundamental Diagrams (FDs) for homogeneous (only one vehicle class) and heterogeneous (multiple vehicle classes) traffic conditions were presented. The resulting FDs were mainly triangular in shape, in which, the slopes of the left and right branches is approximately equal to the lower of the vehicle and link speeds, and speed of backward traveling holes respectively.

Further, the queue model was further extended to include the "seepage" behavior which is a common behavior in most of the urban areas of industrializing nations. Due to the smaller size and easier maneuverability, smaller vehicles (bicycle, motorbike) creep across the gaps between the stationary or almost stationary vehicles and come in front of the queue. With this, the faster vehicle can overtake slower vehicle in the free flow regime and smaller vehicle can overtake larger vehicle in capacity or congested regimes. The FDs for the seepage link dynamics were also presented and it has been showed that due to inclusion of seepage of bicycle, the flow characteristics of bicycle is marginally affected by the presence of cars, while on the contrary, the flow characteristics of the

car are significantly affected by the presence of bicycles. The FDs for car, motorbike, bicycle modes were plotted while allowing motorbike and bicycle to seep. The resulting FDs showed that the seepage is more effective for faster seep mode (e.g., motorbike) rather than slower seep mode (e.g., bicycle). By visualizing the speed density profiles for seepage, it was demonstrated that a higher share of bicycle led to a higher frequency of the seepage events and thus, the seep mode retained its maximum speed even at very high densities.

Furthermore, the proposed queue model extension for seepage was applied to a real-world scenario of Patna, India for the evacuation modeling in mixed traffic conditions. The passing and seepage queue model extensions were compared based on this scenario. It was showed that due to seepage, a significant decrease in the average trip time for bicycle mode and an increase in the average trip time for car and motorbike mode were observed. Though, the total evacuation time for the two evacuation scenarios were more or less same, the initial evacuation rate was higher for the seepage link dynamics i.e., if looking on the time bound evacuation scenario, more people can be evacuated using the seepage behavior.

The computational efficiency of the queue model for various link and traffic dynamics was compared. It was found that due to an additional data structure, simulation time for queue model with holes was increased marginally. Interestingly, the simulation times for simulating 10% and 100% samples were only about 2 and 13 times higher than simulation time for simulating 1% of sample size. The seep mode look up on every link appeared to be costly with respect to the other link dynamics of the queue model. The simulation time with the seepage link dynamics increases rapidly with the sample size while comparing to the other link dynamics.

Integrated scenario

Finally, the last part integrated the two previous parts by presenting a real-world scenario from one of the industrializing nations. To simulate the mixed traffic conditions, a case study of Patna was chosen which is a highly populated city in the eastern part of India. The urban demand was synthesized from trip diaries. To include the congestion effects from the commuters, reverse commuters and through traffic, external demand was also included in it. However, for external traffic, only hourly classified counts data was available rather than the daily plans. Therefore, the external plans are generated by extending Cadyts to the mixed traffic conditions. The income effect of the individuals was included in the utility function. The scenario was then calibrated to estimate the Alternative (mode) specific constants (ASCs) and marginal utilities of distance for bicycle and walk modes.

Further, the calibrated scenario was used for the policy testing. The highest share of the bicycle emphasized the need of a segregate bicycle infrastructure, therefore, a bicycle superhighway was proposed for the Patna scenario along the railway line such that only bicycles are allowed on it (BSH-b). An iterative optimization approach was used to determine the locations of the connectors between the bicycle superhighway and the existing network. In mixed traffic conditions, in absence of the enforcements, it is possible that motorbike riders use the bicycle superhighway; therefore, another scenario (BSH-mb) was also considered in which the bicycle superhighway is also used by the motorbike riders. The results showed that bicycle superhighway leads to a significant increase in the bicycle share for both scenarios, and increase in the motorbike share for the BSH-mb scenario. A

capacity relief was observed on the existing network while looking on the average speeds of the mode switchers and mode retainers.

Further, to estimate the contributions to the emissions, the Emission Modeling Tool (EMT) was extended to mixed traffic conditions. The emissions are calculated for all scenarios. In BSH-b scenario, significant reduction in emissions from car and motorbike was observed whereas in BSH-mb scenario, significant increase in the emissions along the bicycle superhighway was observed. This emphasize the need of strict enforcements to stop motorbikes on the bicycle superhighway.

10.2 Summary and future challenges

The goals for the thesis were to investigate the policy measures in a simulation framework to mitigate the transport related negative externalities and to extract the valuable information for the policy makers in the industrialized and industrializing countries. Thus, this thesis addressed two important issues in the context of the urbanization processes: the transport negative externalities, and modeling the heterogeneous traffic from a large urban agglomeration.

For the first issue, two policy measures were investigated with the help of a metropolitan area from industrialized nation.

- **Joint internalization** The first policy measure was to internalize the multiple externalities simultaneously due to their inter-relationship since introducing a correction term in the form of a toll for one externality also reduced the other externality. The individual tolls were obtained using the idea of the marginal social cost pricing in an agent-based context. In this agent-based simulation framework, it was possible to calculate the highly differentiated, time-dependent toll values corresponding to the different transport externalities and consequently, the behavioral reactions to the time-dependent vehicle-specific congestion and/or emission tolls are modeled for every agent of the system.

  Though, it is unclear if users would actually understand the ever-changing price signals correctly and if such dynamic tolls levels from marginal social cost pricing are feasible to implement. From this, the important takeaway towards policy implications is to transfer the insights from the marginal social cost pricing scheme into recommendations for the policy makers in terms of the corrected average toll levels per kilometer for different transport externalities.

  Though, the reactions of the different user groups (urban, commuters and reverse commuters) were observed while allowing them to change their route or mode, the behavior modeling of the commercial vehicles and externalities from public transit were lacking which lays an opportunity for future research.

  For the emissions costs, the damage costs estimates from the literature were used and for the congestion costs, the approximate average VTTS was used. However, for the latter, in future, it would be helpful to estimate the disaggregated VTTS for the agents (Kaddoura and Nagel, 2016) and then observe the user reaction.

  Though, in this thesis, only congestion and emission externalities were internalized, the approach can be applied to any other combinations of the externalities and any

number of externalities (e.g., congestion, emissions, noise, accidents etc.) to generate the correction terms for policy implications. E.g., simultaneous internalization of exposure of air pollution (Kickhöfer and Kern, 2015), exposure of noise (Kaddoura et al., 2016) and congestion.

- **Parametrized backcasting** The thesis proposed a parametric backcasting approach to derive the toll levels, as a multiple of the damage costs estimates from the literature to achieve the political goals. This approach is different than the joint internalization of multiple externalities based on marginal social cost pricing in which the system was optimized using the damage cost estimates. The damage costs are difficult to estimate due to the complexities and uncertainties in the long-term cause and effect (Tol, 2005; Downing et al., 2005), therefore, in order to achieve a future state of the environment, avoidance costs approach is more acceptable. In this thesis, for the road transport sector, a avoidance charge were estimated with the objective to cut the CO_2 emissions by 20% for MMA, transferred from the EU's goal of 20% reduction in GHG emissions by 2020 with respect to 1990 levels. This thesis discussed several issues structurally which can forfeit a part of the positive effects achieved from the government initiatives. Using the case study of MMA, it was shown that a toll value equivalent to 5 times of the damage cost estimates are required to cut the CO_2 emissions by 20%. The result for the case study is an approximate value for the MMA scenario due to the simplified assumptions, however, the approach is applicable for any scenario to derive the avoidance costs based on the given damage cost estimates.

  The estimation of the avoidance costs depends on the time horizon (short/mid/long term), the target levels of the emissions, system to which the target is applied (e.g., transport sector vs. all sectors, regional vs. national level etc.), penetration rate of efficient fuel/vehicle technology, assessment of the possible rebound effects etc. Thus, it remains a future task to consider these factors to derive the avoidance costs for a greater region. A very high avoidance costs would also require very strong political intervention. From the perspective of an efficient climate change policy, the avoidance costs for the transport sector could be higher than the average avoidance costs for all sectors (Maibach et al., 2008). This is also visible from the Fig. 5.1 in which, total GHG emissions from all sectors have already achieved the target of 20% reduction with respect to 1990 levels, whereas the GHG emissions from transport (or road) sector are about 15% higher with respect to 1990 levels.

For the second issue, this thesis considered to extend the existing computationally efficient queue model rather than looking into the detailed modeling of the mixed traffic conditions. This allowed to simulate all possible vehicle types in an agent-based simulation framework. In this thesis, the queue model was extended in the following two steps.

- **Traffic dynamics : with holes** The queue propagation of the queue model was unrealistic i.e., if a vehicle leaves the downstream end of the link, the freed space is available immediately at the upstream end of the link. This thesis overcame this by introducing the backward traveling holes into the queue model for mixed

traffic i.e., the space freed by leaving vehicle will travel towards upstream with the pre-configured hole speed. The hole speed of 15 km/h is derived by assuming the reaction time of 1.8 sec i.e., the implicit hole speed would depend on the length of the vehicle class. For instance, if a vehicle is a quarter of the length of a car, the hole speed would be 4 times that of the car. From the future perspectives, it would also be interesting to add stochasticity in the hole speed so that the reaction time of every vehicle will be different.

- **Link dynamics : seepage** Fig. 6.2 showed different combinations of the traffic and link dynamics of the queue model. Though, seepage is a common behavior in the industrializing nations, a few studies (e.g., Aupetit et al., 2014) report presence of this behavior in the industrialized nations too. For instance, motorbike/car seep between the other vehicles on the motorway. For the industrializing nations, it is more important on the urban streets than on the motorways. This thesis assumed that all seep vehicles perform seepage which is not true in all cases, therefore, it would be helpful to introduce the randomization in the seepage of the queue model. The seep mode look-up on each link is resource-intensive with respect to other link dynamics. The computational burden increases with the sample size due to increase in the occurrences of the seepage for higher sample size.

The with holes traffic dynamics and seepage link dynamics were justified using several FDs, contour plots, simulation of the real-world experiments, however, it is a future task to validate these models with the help of real-world traffic survey data. These queue model extensions made the queuing pattern realistic without significant decrease in the computational efficiency. Thus, millions of agents from a large urban agglomeration can be simulated on a normal machine within the reasonable time.

The two issues in the context of the urbanization were dealt in the first two parts of this thesis. In the third part, an attempt is made to combine the two issues by presenting a real-world scenario of Panta, India. The travel demand for Patna was synthesized using the urban and external demand. In absence of the daily plans for the external demand, Cadyts was extended to calibrated the daily plans for the external demand. The joint demand is then manually calibrated to estimate the ASCs against the modal split. In future, the manual calibration could be replaced by an automatic calibrator – Opdyts – (Flötteröd, 2016a), which requires an objective function, a set of decision variables and a transport simulation framework (in this case MATSim).

For Patna, the possible target for a toll is car users, however, the share of car is only 2%. Thus, a pricing scheme is less likely to be effective in such conditions. Therefore, a bicycle superhighway is proposed which is becoming a popular measure in the EU to increase the share of the bicycle. For the case study, in order to show the possible gains of the bicycle superhighway, it is assumed that the bicycle are two times faster on the bicycle superhighway than the existing network and requires only half of the efforts. Though, this is not completely unrealistic if looking on the future use of electric bicycles, a practical value could be used in practice. The need of the electric bicycle would increase if the bicycle superhighway is overhead. The proposed policy measure shows reduction in the emissions and increase in the bicycle share which shows the potentials to use it for other urban areas to increase the bicycle share and/or to reduce the emissions. In addition to

this, as an additional policy, the motorbikes were also allowed on the bicycle superhighway. The visualization of spatial distribution of emissions showed that allowing motorbikes on the bicycle superhighway increases the emissions along the bicycle superhighway i.e., in the inner city which is undesirable. This indicates that a strict law enforcement should be included in order to restrict the bicycle superhighway to bicycle users only.

Appendix A

Spatial Averaging

A.1 Parametric equation

A brief information about parametric equation and line integration is presented here which is further used in Appen. A.2.

Parametric equation for a line is defined as :

$$\begin{aligned} r(\vec{t}) &= (1-t)\ \langle x_1, y_1\rangle + t\ \langle x_2, y_2\rangle \quad \forall \quad 0 \le t \le 1 \\ &= \langle x_1 + (x_2 - x_1)\ t, y_1 + (y_2 - y_1)\ t\rangle \end{aligned} \tag{A.1}$$

where, (x_1, y_1) and (x_2, y_2) are the two end points of the line.

The line integral of a function $(f(x, y))$ alone the line (L) with respect to small arc length $\mathrm{d}s$ is given by

$$\int_L f(x, y)\mathrm{d}s$$

where $\mathrm{d}s = \sqrt{(\frac{\mathrm{d}x}{\mathrm{d}t})^2 + (\frac{\mathrm{d}y}{\mathrm{d}t})^2}\mathrm{d}t$ and

$$x = x_1 + (x_2 - x_1)\ t, \quad y = y_1 + (y_2 - y_1)\ t$$

$$\forall\ (x_1, y_1) \le (x, y) \le (x_2, y_2)\ \Rightarrow\ 0 \le t \le 1$$

$$\Rightarrow \frac{\mathrm{d}x}{\mathrm{d}t} = (x_2 - x_1), \quad \frac{\mathrm{d}y}{\mathrm{d}t} = (y_2 - y_1)$$

$$\mathrm{d}s = \sqrt{(x_2 - x_1)^2 + (y_2 - y_1)^2}\ \mathrm{d}t \tag{A.2}$$

A.2 Spatial smoothing

To determine the smoothened influence of the emissions in the nearby area, the *Gaussian distance weighting* function is used. Area under consideration is divided into n equal square cells and influence of the emission emitted on every link is distributed over these

cells. In contrast to the spatial smoothing in the work by (Kickhöfer, 2014), in which it is assumed that the emissions are concentrated at the center of the link, in this thesis, it is assumed that, emissions on the link are uniformly distributed. Thus, the effect of emission emitted at location i on the cell j can be written as –

$$w_{i,j} = \frac{E}{\ell_e} \cdot e^{-\frac{r_{i,j}^2}{R^2}} \tag{A.3}$$

where, E is total emissions emitted on the link, ℓ_e is euclidean distance of the link, $r_{i,j}$ is distance between location i (x, y) and cell centroid (x_0, y_0) and R is the smoothing radius of of a three dimensional Gaussian distribution.

Thus, the total weighted emission for the cell j due to emissions emitted on the link is given by –

$$x_j = \int_L w_{i,j} \cdot \mathrm{d}s \tag{A.4}$$

Now, using the parametric equation (see Appen. A.1) for the link. If from node (x_1, y_1) and to node (x_2, y_2) are two ends of the link, small arc length from Eq. A.2 can be re-written as –

$$\begin{aligned} \mathrm{d}s &= \sqrt{(x_2 - x_1)^2 + (y_2 - y_1)^2}\ \mathrm{d}t \\ &= \ell_e \cdot \mathrm{d}t \end{aligned}$$

Further, $r_{i,j}$ can also be converted into parametric equation as follows –

$$\begin{aligned} r_{i,j}^2 &= (x - x_0)^2 + (y - y_0)^2 \\ &= (x_1 + (x_2 - x_1)\ t - x_0)^2 + (y_1 + (y_2 - y_1)\ t - y_0)^2 \\ &= ((x_1 - x_0) + (x_2 - x_1)\ t)^2 + ((y_1 - y_0) + (y_2 - y_1)\ t)^2 \\ &= A + {\ell_e}^2 \cdot t^2 + 2 \cdot B \cdot t \\ &= (\ell_e \cdot t + \frac{B}{\ell_e})^2 + (A - \frac{B^2}{{\ell_e}^2}) \end{aligned} \tag{A.5}$$

where $A = (x_1 - x_0)^2 + (y_1 - y_0)^2$ and $B = (x_2 - x_1)\ (x_1 - x_0) + (y_2 - y_1)\ (y_1 - y_0)$ Using these parametric equations in Eq. A.4 will give –

$$\begin{aligned} x_j &= \int_L w_{i,j}\ \mathrm{d}s \\ &= \int_{(x_1,y_1)}^{(x_2,y_2)} \frac{E}{\ell_e}\ exp\left(-\frac{r_{i,j}^2}{R^2}\right)\ \mathrm{d}s \\ &= \int_0^1 \frac{E}{\ell_e} exp\left(-\frac{(\ell_e \cdot t + \frac{B}{\ell_e})^2 + (A - \frac{B^2}{\ell_e^2})}{R^2}\right) \cdot \ell_e \cdot \mathrm{d}t \\ &= E \cdot \int_0^1 exp\left(-\frac{(A - \frac{B^2}{\ell_e^2})}{R^2}\right) \cdot exp\left(-\frac{(\ell_e \cdot t + \frac{B}{\ell_e})^2}{R^2}\right) \mathrm{d}t \end{aligned} \tag{A.6}$$

Now, substituting $(\ell_e \cdot t + \frac{B}{\ell_e}) = z \Rightarrow \mathrm{d}t = \frac{1}{\ell_e}\mathrm{d}z$, the weighted emission for the cell j reduces to –

$$\begin{aligned} x_j &= E \cdot exp\left(-\frac{(A - \frac{B^2}{l^2})}{R^2}\right) \cdot \frac{1}{\ell_e} \int\limits_{\frac{B}{\ell_e}}^{l+\frac{B}{\ell_e}} e^{-(\frac{z}{R})^2}\ \mathrm{d}z \\ &= C \cdot \left(erf\left(\frac{\ell_e}{R} + \frac{B}{\ell_e \cdot R}\right) - erf\left(\frac{B}{\ell_e \cdot R}\right)\right) \end{aligned} \tag{A.7}$$

where $C = E \cdot exp\left(-\frac{\left(A - \frac{B^2}{\ell_e^2}\right)}{R^2}\right) \cdot \frac{R}{\ell_e} \cdot \frac{\sqrt{\pi}}{2}$ and $erf(z) = \frac{2}{\sqrt{\pi}} \cdot \int\limits_0^z e^{-y^2}\mathrm{d}y$. At this point, all the values are deterministic.

Thus, the weighted emissions for each cell due to every link are calculated and summed up. Further, the values are normalized by taking the ratio of cell area and area under Gaussian distance weighting function, which is defined as $\int_0^{2\pi}\int_0^{\infty} e^{-\frac{r^2}{R^2}}\ (r\mathrm{d}r\ \mathrm{d}\varphi) = \pi R^2$ (see Appendix A.2 in Kickhöfer, 2014, for detailed derivation).

Appendix B

Queue Model

B.1 Consequences for the link geometry

In order to function properly, a link modeled with holes needs to have certain geometrical properties. This can be seen as follows:

1. At critical density ρ_c, the flow from free flow branch and congested branch will be equal, i.e.,

$$\begin{aligned} \rho_c \cdot v_{l,max} &= v_h \cdot (\rho_{jam} - \rho_c) \\ \rho_c &= \frac{v_h \cdot \rho_{jam}}{(v_h + v_{l,max})} \end{aligned} \tag{B.1}$$

2. The maximum flow, which is the flow at the critical density, is

$$\begin{aligned} q_{max} &= \rho_c \cdot v_{l,max} \\ &= v_{l,max} \cdot \frac{v_h \cdot \rho_{jam}}{(v_h + v_{l,max})} \end{aligned} \tag{B.2}$$

3. Now ρ_{jam} needs to be large enough that q_{max} in Item 2 is at least as large as the link's flow capacity q_l, given by the assignment network:

$$q_l \leq q_{max} = v_{l,max} \cdot \frac{v_h \cdot \rho_{jam}}{(v_h + v_{l,max})} \ .$$

Out of these variables, ρ_{jam} is the only one that is somewhat flexible, since it can be increased by assuming a larger number of lanes, and the number of lanes is rarely a reliable quantity in assignment networks. In consequence,

$$\begin{aligned} \rho_{jam} &\geq \frac{q_{max} \cdot (v_h + v_{l,max})}{v_{l,max} \cdot v_h} \\ N_{PCU} &\geq \frac{q_{max} \cdot \ell_l \cdot (v_h + v_{l,max})}{v_{l,max} \cdot v_h} \end{aligned}$$

$$N_{PCU} = q_{max} \cdot \ell_l \cdot \left(\frac{1}{v_{l,max}} + \frac{1}{v_h} \right) \tag{B.3}$$

where N_{PCU} is the number of PCU units that can be placed on the link. In consequence, in the simulation the condition Eq. B.3 is checked for each link, and if the condition is not fulfilled, this link's storage capacity is increased accordingly. As stated early, the assumption is that a link that is assumed to have a certain flow capacity in the assignment network needs to be physically able to process this flow; if this is not the case, the input data must be erroneous and thus be corrected in a plausible way. Maintaining the flow and increasing the storage seems the best way to do this in an assignment context.

B.2 Average bicycle passing rate

As demonstrated in Sec. 7.5.2.2, the average bicycle passing rate is defined as number of bicycles passed by every car on a one km link. The steps to calculate it on the race track network (see Fig. 7.3) are given below.

- Following assumptions are made.
  a) Only car and bicycle modes are used for this experiment.
  b) The passing among same vehicle type is restricted.
  c) The counting of the number of bicycles on the race track is started as soon as first bicycle leaves the track.
- Every time a car leaves the track, number of bicycles ($n_{bicycle}$) passed by the leaving car is counted. This is simply the number of bicycles entered before the car.
- The number of bicycles passed by the car on one km link will be

  $$= \frac{n_{bicycle} \cdot 1000}{3 \cdot \ell_l}$$

  where ℓ_l is length of the link in m.
- Thus, the passing rate ($N_{bicycle}$) is given by –

  $$N_{avg}^{bicycle} = \frac{1}{k} \cdot \sum_{i=1}^{k} \left(\frac{n_{bicycle} \cdot 1000}{3 \cdot \ell_l} \right) \tag{B.4}$$

  where k is the total number of times, cars leave the track until the stability is reached.

B.3 Spatio temporal trajectories

Following steps are used to generate the distance-time trajectories in Fig. 7.17.

1. It is assumed that the position of backward traveling holes is not affected by the position of the vehicles. It means, once a hole is generated, it will keep traveling with constant speed until it reaches upstream end of the link.

2. In a capacity/congested regimes, a link is filled with the vehicles and holes.

3. Thus, the position of the vehicles can be determine as follows.

   a) First, the position of the hole (x_t^h) from upstream end of the link is computed using the queue logic.

   $$x_t^h = \left(\frac{t_{l,remaining}^h}{t_{l,free}^h} \right) \cdot \ell_l$$

   where $t_{l,remaining}^h$ is the time remaining for hole to reach upstream end of the link and $t_{l,free}^h$ is the minimum time required for the hole to reach upstream end of the link (see Eq. 7.2).

   b) The position of the vehicle (x_t^v) from upstream end of the link is also determined using queue logic.

   $$x_t^v = \left(1 - \frac{t_{l,remaining}^v}{t_{l,free}^v} \right) \cdot \ell_l$$

   where, $t_{l,remaining}^v$ is the time remaining to reach the downstream end of the link and $t_{l,free}^v$ is the minimum time for the vehicle to reach the downstream end of the link (see Eq. 7.1).

   c) Now, for each vehicle, identify the holes such that

   $$x_t^h \geq x_t^v$$

   and then for each such holes, vehicle position is recalculated as

   $$x_t^v = x_t^v - PCU_h \cdot Size_{PCU}$$

   where PCU_h and $Size_{PCU}$ are PCU equivalent of the respective hole and size of the 1 PCU ($= 7.5m$) on the link respectively. Thus, all the vehicles are positioned on the link.

B.4 Capacity update in queue model

B.4.1 QSim structure

In short, the steps of the QSim structural can be descried as (Dobler, 2013, pp. 43-45):

(1) The requisite inputs (see Sec. 2.2.1), simulation agents are created and simulation begins.

(2) In an iterative loop, the state of the simulation is observed for each time step (typically 1 sec) until all time steps are simulated. The method to observe state of the simulation is called as `doSimStep`

(3) `doSimStep` is composed of two more methods, `moveNodes` and `moveLinks`.

(4) The former is responsible for moving of agents over the node i.e., from upstream link to the downstream link if possible (see three conditions in Sec. 7.2). If agents from more than one in-going links are ready to move to downstream link, one of the agent is selected randomly based on the capacities of the in-going links.

(5) The later simulates departures, the movement of vehicles along the network's link, arrivals.

B.4.2 Fast capacity update

The flow and storage capacities of a link (see Sec. 7.2) are updated under `moveLinks` call. This means, the flow and storage capacities of every link is updated in every time step, even if link is not used at all; thus clearly, this would be a time consuming for a large urban-network (e.g., see network of MMA in Fig. 4.2).

An agent is moved over the node during `moveNodes`, if the flow capacity of the in-going link and the storage capacity of the downstream link are observed (see Sec. 7.2). That is, update of flow and storage capacities of a link is necessary only if agent is moved over the node. Based on this, a new capacity updated approach is proposed, in which the flow and storage capacities are updated during `moveNodes` rather than in `moveLinks`. In other words, the flow capacity of a link is updated only if agent is arrived at the end of a link and storage capacity of a link is updated if agent can be moved over the node. This reduces the computational effort for un-necessary updating of the capacities for every link at every time step. Though, there is a minor change in the implementation of QSim, however, as expected, the differences between the results of the the approaches are negligible (see Fig. B.1). The Fig. B.1 shows the FDs from the simulation of car and bicycle in equal

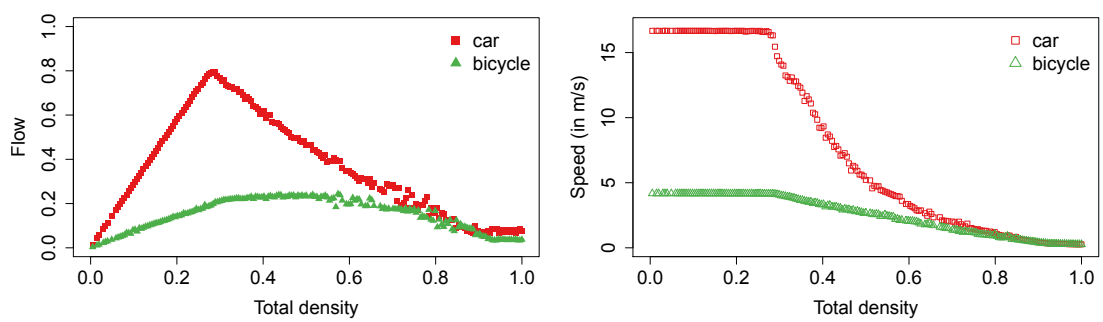

Figure B.1: FDs from simulation of equal modal split (in *PCU*) of car and bicycle using fast capacity update approach. Traffic dynamics = with holes, link dynamics = passing.

modal split (in *PCU*) while using fast capacity update approach. Clearly, there are no significant differences between the Fig. B.1 and Fig. 7.9. The latter is the FDs generated using the slow (default) capacity update approach of QSim.

B.4.3 Performance analysis

In order to compare the performance of fast capacity update, the scenario is set up same as in Sec. 8.3.2 and same computational resources are used (see Sec. 8.3.3). The comparison is made for 1% and 10% sample sizes with passing link dynamics and both (with and without holes) traffic dynamics.

Table B.1: Average simulation time per iteration (in *sec*) for fast and slow capacity update approaches.

sample size	1%		10%	
capacity update	slow	fast	slow	fast
without holes	8.23	6.78	17.36	16.35
holes	8.61	7.86	19.23	18.15

Tab. B.1 compares the average simulation time from fast and slow capacity updates. Use of the fast capacity update for 1% sample size reduces the average simulation time per iteration by 17.6% and 8.7% for without holes and with holes traffic dynamics respectively. The same numbers for 10% sample size are 5.8% and 5.6%. Clearly, a significant improvement in the simulation time can be observed; however, the lesser improvement in average simulation time for 10% sample size is an effect of the more frequent update of the capacities of the link. Presumably, this improvement would be even higher for huge urban networks depending on the network usage.

The average modal travel time and distance from the simulation of 1% and 10% sample size scenarios using fast and slow capacity update approaches are also compared. It has been found that the differences between the average modal travel times from two capacity update approaches is below 2% and the average modal travel distances from the two capacity update approaches is below 0.5%. This difference is marginally lower for 10% sample size scenario than 1% sample size scenario which explains the possible impact of lower artefacts in 10% sample size scenario.

B.5 Scaling of a scenario

The simulation time and complexities of a scenario can be reduced considerably by observing only a sub-sample of the population. This means, e.g., in a 10% sample scenario, every agent will represent 10 agents therefore, the other parts (flow and storage capacities, etc.) of the simulation infrastructure needs to be scaled down accordingly. The sampling of a scenario can be random at individual level or at household level, however, it may also result in some artefacts.[1]

B.5.1 Sample sizes in MATSim

The flow capacity of a link in the network is set from the actual flow capacities in the real-world and corresponding to full population. The QSim controls the consumption of

[1] See (Dobler, 2013, pp. 33-34) for some more discussion and examples about possible artefacts due to sampling of a scenario.

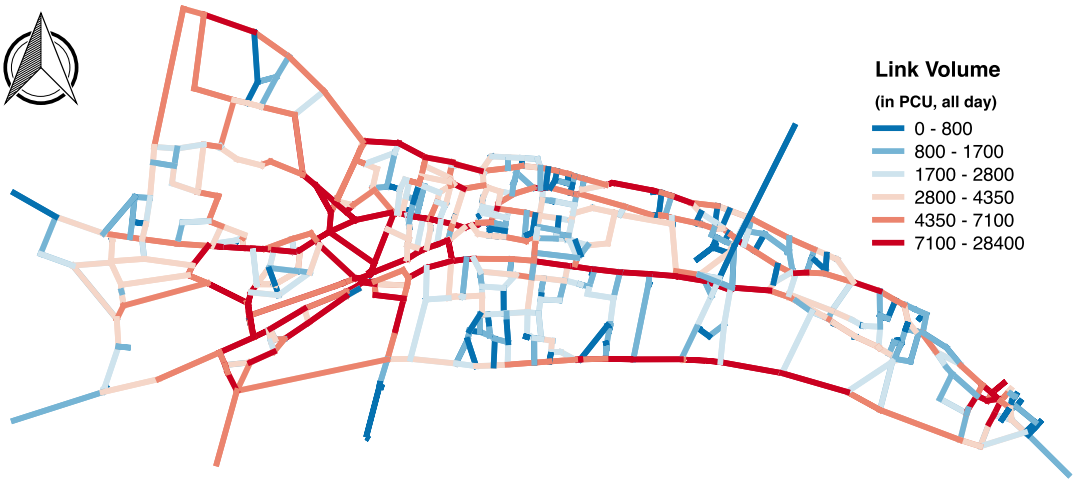

(a) 1%

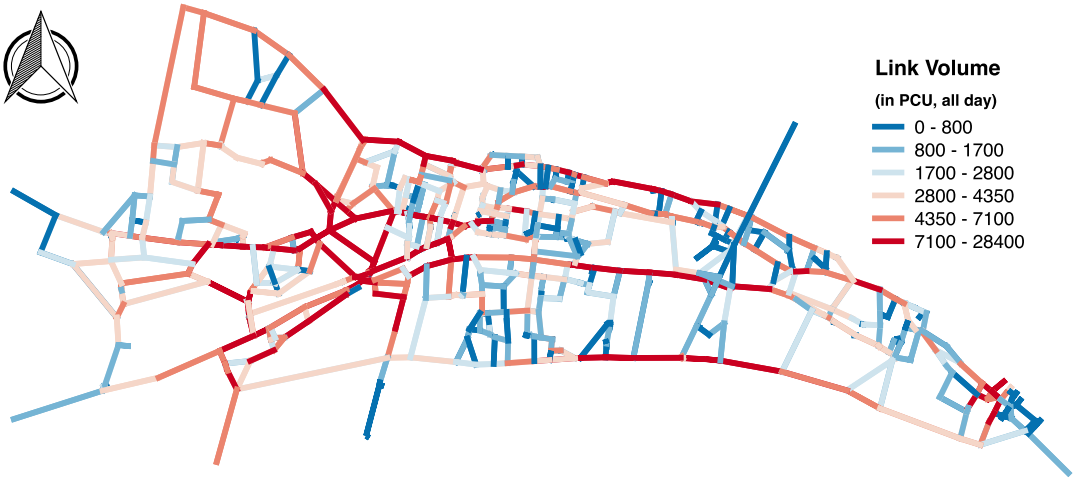

(b) 10%

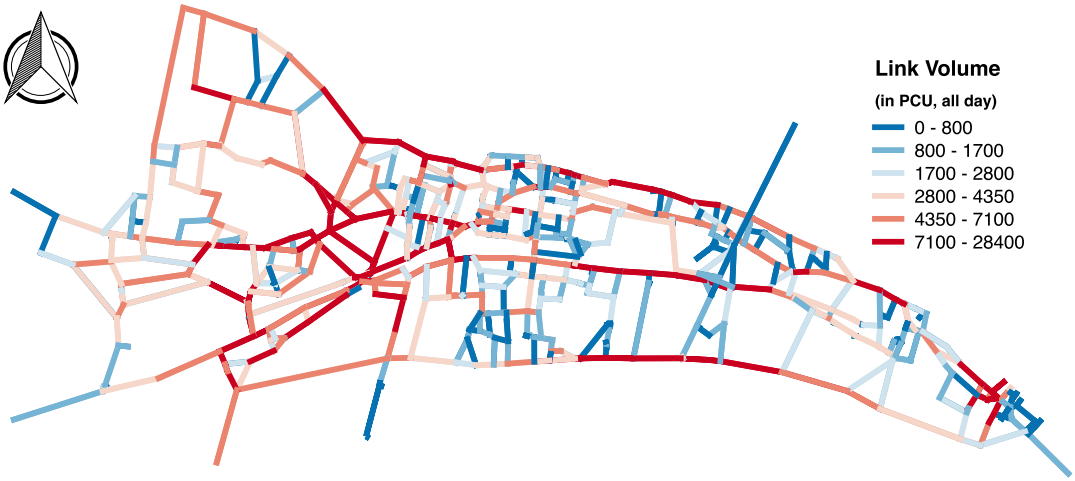

(c) 100%

Figure B.2: An illustration of traffic patterns. Traffic dynamics = with holes; link dynamics = passing. Values are scaled up to whole population.

flow and storage capacities on the link i.e., the flow and storage capacities can be scaled down to the corresponding sample sizes. It means, for example, for a 1% sample scenario,

the flow capacity of a link with a capacity of 1 PCU/sec will allow only 1 PCU for every 100 sec, because, every agent represents 100 agents. Thus, the smaller links or links with smaller flow capacities could produce large fluctuations. In order to dampen some of these fluctuations, the link storage capacities, which produce spillback, is set to about 3 times the flow capacity factor (i.e., $3 \cdot 1\% = 3\%$). This approach is sufficient to obtain realistic congestion patterns (Nagel, 2008, 2011).

B.5.2 Traffic patterns

Further, in this section, the traffic patterns from different sample sizes are compared. For illustration purpose, the output of one of the run for the passing link dynamics and with holes traffic dynamics is chosen.

Fig. B.2 shows the link volume (in PCU) for all three sample sizes. From these figures, it can be observed that the traffic pattern for all three sample sizes have close similarities. A few minor differences can be noticed which are the effect of mainly artefacts. With this, it can be summarized that to decrease the computational effort significantly, a smaller sample size can be used without getting significant differences in traffic patterns.

In this experiment, only traffic patterns from the simulations of different sample sizes are compared. In general, the average travel time and distance would differ marginally for simulations of different sample sizes due to the artefacts. This shows an opportunity for the future research with detailed comparison of the travel characteristics using different sets of the storage capacity factors for different sample sizes.

Appendix C

Patna Scenario

C.1 Patna external demand

The external demand for Patna scenario is generated as follows.

Table C.1: An example of hourly classified traffic counts data.

time bin	car	motorbike	truck	bicycle	total
1	34	5	142	1	182
...	...	...	...	...	...
6	43	38	210	68	359
7	48	93	139	101	381
8	76	123	141	137	477
9	56	33	42	36	167
...	...	...	...	...	...
22	115	55	165	10	345
23	95	40	225	3	363
24	49	16	186	1	252

1) TRIPP et al. (2009) provides hourly classified traffic counts data for all counting stations in both (inbound and outbound) directions (see Tab. C.1 for an example). For each mode, the sum of hourly inbound and outbound counts must be equal, if this is not the case, the counts are adjusted. For instance, total inbound car count is 990 and outbound count is 1000, thus, the outbound counts are reduced by a factor calculated as $(1000 - 990)/990$.

2) Further, the directional split for each counting station is available (see Tab. C.2). In absence of the classified hourly factors, the directional split is used together with the adjusted hourly classified counts (from step 1) to get the hourly modal counts for commuters and through traffic. E.g., at OC1, for time bin 2, the car count is 100; 70% of this will be commuters and the remaining 30 will be through traffic.

Table C.2: Share of through and commuters traffic.

	Share of ...	
Outer cordon location	**commuters traffic**	**through traffic**
OC1	0.70	0.30
OC2	0.58	0.42
OC3	0.94	0.06
OC4	0.66	0.34
OC5	0.76	0.24
OC6	0.86	0.14
OC7	0.95	0.05

3) Further, Patna CMP also provides an origin-destination (OD) matrix for through traffic which helps to determine the origin and destination of the through trip. Again, in absence of the hourly classified OD matrix, the through traffic counts obtained in step 2 are used along with the OD matrix (see Tab. C.3) to get the through trips. From the example in step 2, of the 30 through car trips that originate at OC1 in time bin 2, 49% trips (≈ 15) terminate at OC4, 15% trips (≈ 5) terminate at OC5, etc.

Table C.3: Origin-destination (O-D) matrix for through traffic.

O-D	**OC1**	**OC2**	**OC3**	**OC4**	**OC5**	**OC6**	**OC7**
OC1	0%	0%	2%	49%	15%	3%	31%
OC2	1%	0%	0%	84%	5%	0%	10%
OC3	19%	4%	0%	4%	17%	23%	33%
OC4	76%	16%	0%	0%	3%	0%	5%
OC5	35%	7%	4%	38%	0%	8%	8%
OC6	30%	7%	23%	0%	13%	0%	27%
OC7	34%	7%	0%	9%	50%	0%	0%

List of Symbols and Acronyms

M Million, 1×10^6

CO_2 Carbon Dioxide

CO Carbon Monoxide

$EURct$ Euro cent, 1/100 EUR

EUR Euro

INR Indian Rupee

$NMHC$ Non-Methane Hydrocarbons

NO_2 Nitrogen Dioxide

NO_x Nitrogen Oxides

PCU Passenger car unit

PM Particular Matter

SO_2 Sulfur Dioxide

$USDct$ US Dollar cent, 1/100 USD

USD US Dollar

g Gram, 1/1000 kg

h Hour, 60 min

km Kilometer, 1000 m

min Minute, 60 sec

m Meter, the SI base unit of length

sec Second, the SI base unit for time

ton Ton, 1000 kg

$util$ Util, a unit of utility

ASC Alternative (mode) specific constant xvii, xxi, 16, 37–39, 109, 120, 123–125, 139, 146, 149

CA Cellular Automata 72, 74

Cadyts Calibration of dynamic traffic assignment xvii, xxi, 11, 115, 120, 123–126, 139, 141, 146, 149

CMP Comprehensive Mobility Plan 117, 118, 120, 164

CTM Cell Transmission Model 73–75, 77

ECMF Emission Cost Multiplication Factor 57, 59–65

EMT Emission Modeling Tool xvii, xxii, 11, 32, 33, 136, 141, 147

EU European Union 5, 7, 24, 53–57, 66, 67, 144, 148, 149

FD Fundamental Diagram xvi, xx, xxi, 11, 79, 81, 83, 84, 86–97, 101, 102, 104, 145, 146, 149, 158

FIFO First-in-first-out 10, 15, 73, 75, 76, 79, 81, 82, 84, 87, 88, 90, 94, 109–112

GDP Gross Domestic Product 5, 21

GHG Green House Gases xvi, xx, 3, 7, 8, 10, 24, 53–57, 65, 66, 144, 148

HBEFA Handbook on Emission Factors for Road Transport, see www.hbefa.net 32, 33, 35, 50, 136, 140

Java JAVA programming language, see www.java.com 13, 15, 109

KWM Kinematic Wave Model 72, 73, 78, 83, 145

LTM Link Transmission Model 73–75

LWR Lighthill–Whitham–Richards 74, 75, 78, 96

MATSim Multi-Agent Transport Simulation, see www.matsim.org 9, 10, 13–15, 17, 18, 28, 31–34, 36, 37, 40, 43, 71, 78, 79, 81, 82, 86, 87, 102, 107, 108, 112, 116–124, 140, 149, 159

MCM A MATSim re-planning module 16, 17, 38

MEC Marginal External Cost 5, 33, 34

MMA Munich Metropolitan Area 11, 25, 28, 29, 31, 33, 36, 37, 41, 51, 53, 56–59, 65, 67, 143, 144, 148, 158

MNL Multinomial Logit 18, 38, 105

MPC Marginal Private Cost 5, 33

MSC Marginal Social Cost 5, 33, 57

Opdyts Optimization of dynamic traffic simulations 127, 140, 149

PMC Patna Municipal Corporation 115

PQM Point Queue Model 72–74, 79

PT Public Transport 8, 14, 22, 34, 37–39, 42, 44, 45, 50, 59, 62, 65, 104, 115–126, 128, 132–135, 140

RCM A MATSim re-planning module 16, 17, 38

SQM Spatial Queue Model xvi, xx, xxi, 72–74, 78, 79

SUMO Simulation of Urban Mobility, see www.sumo.dlr.de 75, 107, 112

TAMM A MATSim re-planning module 16

VISUM Verkehr In Städten – UMlegung, see www.ptv.de 36

VTTS Value of Travel Time Savings 4, 32, 35, 38, 39, 50, 121, 122, 147

XML Extensible Markup Language, see www.w3.org/XML 13

Bibliography

2008/101/EC (2008). *Directive 2008/101/EC of the European Parliament and of the Council*. Official Journal of the European Union (cit. on pp. 7, 51).

Agarwal, A. (2012). "Agent based simulation of the travel demand for Patna City, India". MA thesis. India: Indian Institute of Technology, Delhi (cit. on pp. 6, 10, 117).

— (2016). "Patna". In: *The Multi-Agent Transport Simulation MATSim*. Ed. by A. Horni, K. Nagel, and K. W. Axhausen. Ubiquity, London. Chap. 77. DOI: 10.5334/baw. URL: http://matsim.org/the-book (cit. on p. 80).

Agarwal, A. and B. Kickhöfer (2015). "Agent-based simultaneous optimization of congestion and air pollution: A real-world case study". In: *Procedia Computer Science* 52.C, pp. 914–919. ISSN: 1877-0509. DOI: 10.1016/j.procs.2015.05.165 (cit. on pp. 21, 29, 40, 48).

— (2016). "The correlation of externalities in marginal cost pricing: lessons learned from a real-world case study". In: *Transportation*. DOI: 10.1007/s11116-016-9753-z (cit. on pp. 21, 29).

Agarwal, A. and G. Lämmel (2015). "Seepage of smaller vehicles under heterogeneous traffic conditions". In: *Procedia Computer Science* 52.C, pp. 890–895. ISSN: 1877-0509. DOI: 10.1016/j.procs.2015.05.147 (cit. on pp. 69, 79).

— (2016). "Modeling seepage behavior of smaller vehicles in mixed traffic conditions using an agent based simulation". In: *Transp. in Dev. Econ.* 2.2, pp. 1–12. DOI: 10.1007/s40890-016-0014-9 (cit. on pp. 69, 79, 103).

Agarwal, A., M. Zilske, K. Rao, and K. Nagel (2013). "Person-based dynamic traffic assignment for mixed traffic conditions". In: *Conference on Agent-Based Modeling in Transportation Planning and Operations*. Also VSP WP 12-11, see http://www.vsp.tu-berlin.de/publications. Blacksburg, Virginia, USA (cit. on pp. 73, 76, 84, 86, 104, 109).

— (2015). "An elegant and computationally efficient approach for heterogeneous traffic modelling using agent based simulation". In: *Procedia Computer Science* 52.C, pp. 962–967. ISSN: 1877-0509. DOI: 10.1016/j.procs.2015.05.173 (cit. on pp. 10, 73, 76, 77, 79, 80, 85, 86, 88, 93, 99).

Agarwal, A., G. Lämmel, and K. Nagel (2016). "Modelling of Backward Travelling Holes in Mixed Traffic Conditions". In: *Traffic and Granular Flow '15*. Ed. by V. L. Knoop and W. Daamen. 1st ed. Delft, NL: Springer International Publishing. Chap. 53, pp. 419–426. ISBN: 978-3-319-33482-0. DOI: 10.1007/978-3-319-33482-0_53 (cit. on pp. 69, 79, 82).

Anderson, P. and N. Geroliminis (2015). "Dynamic lane restrictions on congested arterials". In: *94th Transportation Research Board Annual Meeting*. 15-1838 (cit. on p. 128).

Arnott, R., A. de Palma, and R. Lindsey (1993a). "A structural model of peak-period congestion: A traffic bottleneck with elastic demand". In: *The American Economic Review* 83.1, pp. 161–179. ISSN: 00028282. URL: http://www.jstor.org/stable/2117502 (cit. on p. 25).

— (1993b). "Properties of dynamic traffic equilibrium involving bottlenecks, including a paradox and metering". In: *Transportation Science* 27.2, pp. 148–160. DOI: 10.1287/trsc.27.2.148 (cit. on p. 27).

Arsan, V. T. and R. Z. Koshy (2005). "Methodology for modeling highly heterogeneous traffic flow". In: *Journal of Transportation Engineering* 131.7, pp. 544–551. DOI: 10.1061/(ASCE)0733-947X(2005)131:7(544) (cit. on p. 73).

Asaithambi, G., R. V. Y. Kumar, and R. Sivanandan (2013). "Evaluation of exclusive stopping space for motorcycles at signalized intersections under mixed traffic conditions using simulation model". In: *92nd Transportation Research Board Annual Meeting* (cit. on pp. 10, 75).

Attard, M. and S. Ison (2015). "The effects of road user charges in the context of weak parking policies: The case of Malta". In: *Case Studies on Transport Policy* 3.1. Urban Transport Policy, pp. 37–43. ISSN: 2213-624X. DOI: http://dx.doi.org/10.1016/j.cstp.2014.07.001 (cit. on p. 49).

Aupetit, S., S. Espié S., and S. Bouaziz (2014). "Naturalistic study of riders' behaviour in lane–splitting situations". English. In: *Cognition, Technology & Work*, pp. 1–13. ISSN: 1435-5558. DOI: 10.1007/s10111-014-0293-z (cit. on pp. 74, 149).

Aziz, H. M. A. and S. V. Ukkusuri (2012). "Integration of environmental objectives in a system optimal dynamic traffic assignment model". In: *Computer-Aided Civil and Infrastructure Engineering* 27.7, pp. 494–511. DOI: 10.1111/j.1467-8667.2012.00756.x (cit. on pp. 22, 26).

Babisch, W., G. Pershagen, J. Selander, D. Houthuijs, O. Breugelmans, E. Cadum, F. Vigna-Taglianti, K. Katsouyanni, A. S. Haralabidis, K. Dimakopoulou, P. Sourtzi, S. Floud, and A. L. Hansell (2013). "Noise annoyance – A modifier of the association between noise level and cardiovascular health?" In: *Science of The Total Environment* 452–453, pp. 50–57. DOI: 10.1016/j.scitotenv.2013.02.034 (cit. on p. 3).

Balijepalli, N. C., D. Ngoduy, and D. P. Watling (2014). "The two-regime transmission model for network loading in dynamic traffic assignment problems". In: *Transportmetrica A: Transport Science* 10.7, pp. 563–584. DOI: 10.1080/18128602.2012.751680 (cit. on p. 71).

Balmer, M. (2007). "Travel demand modeling for multi-agent transport simulations: Algorithms and systems". PhD thesis. Switzerland: Swiss Federal Institute of Technology (ETH) Zürich (cit. on p. 16).

Balmer, M., B. Raney, and K. Nagel (2005a). "Adjustment of activity timing and duration in an agent-based traffic flow simulation". In: *Progress in activity-based analysis*. Ed. by H. Timmermans. Oxford, UK: Elsevier, pp. 91–114 (cit. on pp. 13, 17).

Balmer, M., M. Bernard, and K. W. Axhausen (2005b). "Matching Geo-Coded Graphs". In: *Swiss Transport Research Conference (STRC)*. See http://www.strc.ch. Monte Verita, Switzerland. URL: http://www.strc.ch (cit. on p. 108).

Balmer, M., M. Rieser, K. Meister, D. Charypar, N. Lefebvre, K. Nagel, and K. Axhausen (2009). "MATSim-T: Architecture and Simulation Times". In: *Multi-Agent Systems for Traffic and Transportation*. Ed. by A. Bazzan and F. Klügl. IGI Global, pp. 57–78 (cit. on pp. 13, 14).

Banister, D. and R. Hickman (2009). "Techno-optimism: progress towards CO2 reduction targets in transport: a UK and London perspective". In: *International Journal of Sustainable Development* 12.1, pp. 24–47. DOI: 10.1504/IJSD.2009.027527 (cit. on p. 27).

Bar-Gera, H. (2012). "The fast lane to Tel-Aviv: high occupancy toll project with a pareto package". In: *91st Transportation Research Board Annual Meeting*. 12-0712 (cit. on p. 128).

Barla, P., B. Lamonde, L. F. Miranda-Moreno, and N. Boucher (2009). "Traveled distance, stock and fuel efficiency of private vehicles in Canada: price elasticities and rebound effect". In: *Transportation* 36.4, pp. 389–402. DOI: 10.1007/s11116-009-9211-2 (cit. on p. 53).

Barth, M. and K. Boriboonsomsin (2009). "Traffic congestion and greenhouse gases". In: *ACCESS Magazine, University of California Transportation Center* 35 (cit. on p. 25).

Basso, L. J., C. A. Guevara, A. Gschwender, and M. Fuster (2011). "Congestion Pricing, Transit Subsidies and Dedicated Bus Lanes: Efficient and Practical Solutions to Congestion". In: *Transport Policy* 18, pp. 676–684 (cit. on pp. 22, 23).

Beamon, B. M. and P. M. Griffin (1999). "A simulation-Based methodology for analyzing congestion and emissions on a transportation network". In: *Simulation* 72.2, pp. 105–114. DOI: 10.1177/003754979907200204 (cit. on p. 25).

Beevers, S. D. and D. C. Carslaw (2005). "The impact of congestion charging on vehicle emissions in London". In: *Atmospheric Environment* 39, pp. 1–5. DOI: 10.1016/j.atmosenv.2004.10.001 (cit. on pp. 22, 25, 40).

Behrisch, M., L. Bieker, J. Erdmann, and D. Krajzewicz (2011). "SUMO - Simulation of Urban MObility: An Overview". In: *SIMUL 2011, The Third International Conference on Advances in System Simulation*. Barcelona, Spain, pp. 63–68 (cit. on p. 73).

Beria, P. (2015). "Effectiveness and monetary impact of Milan's road charge, one year after implementation". In: *International Journal of Sustainable Transportation*. DOI: 10.1080/15568318.2015.1083638 (cit. on p. 25).

Bickel, P., R. Friedrich, A. Burgess, P. Fagiani, A. Hunt, G. de Jong, J. Laird, C. Lieb, G. Lindberg, P. Mackie, S. Navrud, T. Odgaard, A. Ricci, J. Shires, and L. Tavasszy (2006). *Proposal for Harmonised Guidelines, Deliverable 5 of HEATCO [Harmonised European Approaches for Transport Costing and Project Assessment] commissioned by the European Union*. URL: http://heatco.ier.uni-stuttgart.de/ (cit. on pp. 4, 5).

Bliemer, M. C. J. (2007). "Dynamic Queuing and Spillback in Analytical Multiclass Dynamic Network Loading Model". In: *Transportation Research Record: Journal of the Transportation Research Board* 2029, pp. 14–21 (cit. on p. 73).

Böhme, S. and L. Eigenmüller (2006). *Pendlerbericht Bayern*. Tech. rep. IAB (cit. on p. 35).

Börjesson, M. and J. Eliasson (2014). "Experiences from the Swedish Value of Time study". In: *Transportation Research Part A: Policy and Practice* 59, pp. 144–158. ISSN: 0965-8564. DOI: 10.1016/j.tra.2013.10.022 (cit. on p. 24).

Börjesson, M. and I. Kristoffersson (2015). "The Gothenburg congestion charge. Effects, design and politics". In: *Transportation Research Part A: Policy and Practice* 75, pp. 134–146. DOI: 10.1016/j.tra.2015.03.011 (cit. on p. 25).

Buchanan, J. M. and W. C. Stubblebine (1962). "Externality". In: *Economica* 29.116, pp. 371–384. ISSN: 00130427, 14680335. DOI: 10.2307/2551386. URL: http://www.jstor.org/stable/2551386 (cit. on p. 2).

Buehler, R. and J. Pucher (2011). "Sustainable transport in Freiburg: lessons from Germany's environmental capital". In: *International Journal of Sustainable Transportation* 5.1, pp. 43–70. DOI: 10.1080/15568311003650531 (cit. on pp. 22, 49).

Cai, H. and S. Xie (2011). "Traffic-related air pollution modeling during the 2008 Beijing Olympic games: the effects of an odd-even day traffic restriction scheme". In: *Science of The Total Environment* 409.10, pp. 1935–1948. DOI: 10.1016/j.scitotenv.2011.01.025 (cit. on p. 22).

Calthrop, E., S. Proost, and K. van Dender (2000). "Parking policies and road pricing". In: *Urban Studies* 37.1, pp. 63–76. DOI: 10.1080/0042098002294 (cit. on p. 22).

Calthrop, E. and S. Proost (1998). "Road Transport Externalities". In: *Environmental and Resource Economics* 11.3–4, pp. 335–348. DOI: 10.1023/A:1008267917001. URL: http://dx.doi.org/10.1023/A%3A1008267917001 (cit. on p. 22).

Census (2011). *Census of India 2011*. http://www.censusindia.gov.in/ (cit. on p. 115).

Centre for Road Safety (accessed 2014). *Transport for New South Wales*. URL: http://roadsafety.transport.nsw.gov.au/stayingsafe/motorcyclists/lanefiltering/ (cit. on p. 74).

Cetin, N., A. Burri, and K. Nagel (2003). "A Large-Scale Agent-Based Traffic Microsimulation Based On Queue Model". In: *Swiss Transport Research Conference (STRC)*. See http://www.strc.ch. Monte Verita, Switzerland. URL: http://www.strc.ch (cit. on pp. 9, 15, 69, 76).

Chandra, S. and P. K. Sikdar (2000). "Factors affecting PCU in mixed traffic situations on urban roads". In: *Road and transport research* 9.3, pp. 40–50 (cit. on p. 119).

Chandra, S. and U. Kumar (2003). "Effect of lane width on capacity under mixed traffic conditions in India". English. In: *Journal of Transportation Engineering* 129.2, pp. 155–160. DOI: 10.1061/(ASCE)0733-947X(2003)129:2(155) (cit. on p. 117).

Charypar, D. and K. Nagel (2005). "Generating complete all-day activity plans with genetic algorithms". In: *Transportation* 32.4, pp. 369–397. ISSN: 0049-4488. DOI: 10.1007/s11116-004-8287-y (cit. on p. 15).

Charypar, D., K. Axhausen, and K. Nagel (2007a). "An event-driven parallel queue-based microsimulation for large scale traffic scenarios". In: *World Conference on Transport Research (WCTR'07)*. Also VSP WP 07-03, see http://www.vsp.tu-berlin.de/publications. Berkeley, CA (cit. on p. 15).

— (2007b). "Event-Driven Queue-Based Traffic Flow Microsimulation". In: *Transportation Research Record* 2003, pp. 35–40. DOI: 10.3141/2003-05 (cit. on pp. 10, 15, 76, 81).

Chen, L. and H. Yang (2012). "Managing congestion and emissions in road networks with tolls and rebates". In: *Transportation Research Part B: Methodological* 46, pp. 933–948. DOI: 10.1016/j.trb.2012.03.001 (cit. on p. 26).

Clarke, D. D., P. Ward, C. Bartle, and W. Truman (2004). *In–depth study of motorcycle accidents*. Tech. rep. 54. School of Psychology, University of Nottingham (cit. on p. 74).

Clarkson, R. and K. Deyes (2002). *Estimating the social cost of carbon emissions*. Government Economic Service Working Paper 140. Department for Environment, Food and Rural affairs (cit. on pp. 4, 31).

Creutzig, F. and D. He (2009). "Climate change mitigation and co-benefits of feasible transport demand policies in Beijing". In: *Transportation Research Part D: Transport and Environment* 14.2, pp. 120–131. ISSN: 13619209. DOI: 10.1016/j.trd.2008.11.007 (cit. on p. 5).

Daganzo, C. (1994). "The cell transmission model: A dynamic representation of highway traffic consistent with the hydrodynamic theory". In: *Transportation Research B* 28B.4, pp. 269–287 (cit. on p. 71).

Daganzo, C. (1995). "The cell transmission model, part II: Network traffic". In: *Transportation Research B* 29B.2, pp. 79–93 (cit. on p. 71).

Daniel, J. I. and K. Bekka (2000). "The environmental impact of highway congestion pricing". In: *Journal of Urban Economics* 47, pp. 180–215. DOI: 10.1006/juec.1999.2135 (cit. on pp. 22, 25, 42).

Dijkstra, E. (1959). "A note on two problems in connexion with graphs". In: *Numerische Mathematik* 1, pp. 269–271 (cit. on p. 16).

Divjak, M. S. (2009). "Strategic land use planning for low carbon cities in Ljubljana urban region". In: *45th ISOCARP Congress 2009* (cit. on p. 53).

Dobler, C. (2013). "Travel behaviour modelling for scenarios with exceptional events - methods and implementations". PhD thesis. ETH Zürich (cit. on pp. 108, 157, 159).

Dobler, C. and G. Lämmel (2011). "Integration of a microscopic force-based 2D pedestrian simulation into a framework for large-scale transport systems simulation". In: URL: https://svn.vsp.tu-berlin.de/repos/public-svn/publications/vspwp/2011/11-24 (cit. on p. 119).

Downing, T. E., D. Anthoff, R. Butterfield, M. Ceronsky, M. Grubb, J. Guo, C. Hepburn, C. Hope, A. Hunt, A. Li, A. Markandya, S. Moss, A. Nyong, R. Tol, and P. Watkiss (2005). *Social cost of carbon: a closer look at uncertainty*. Final project report. Department for Environmental, Food and Rural Affairs (cit. on pp. 4, 5, 31, 148).

EEA (2008). *Climate for a transport change*. Tech. rep. 1/2008. European Environment Agency. DOI: 10.2800/3320 (cit. on p. 54).

— (2014). *Focusing on environmental pressures from long–distance transport – Term 2014 : transport indicators tracking progress towards environmental targets in Europe*. EEA Report 7/2014. European Environment Agency (cit. on p. 53).

— (2015). *New cars' CO2 emissions well below Europe's 2015 target*. Tech. rep. European Environment Agency (cit. on pp. 24, 52).

Eissfeldt, N., D. Krajzewicz, K Nagel, and P. Wagner (2006). *Simulating traffic flow with queues*. VSP Working Paper. See http://www.vsp.tu-berlin.de/publications (cit. on pp. 10, 76, 81).

Eliasson, J., L. Hultkrantz, L. Nerhagen, and L. S. Rosqvist (2009). "The Stockholm congestion – charging trial 2006: Overview of effects". In: *Transportation Research Part A: Policy and Practice* 43, pp. 240–250. DOI: 10.1016/j.tra.2008.09.007 (cit. on p. 25).

Ellis, T. (2006). "Inquiry into managing transport congestion Victoria". In: *Motorcycle Riders' Associations (MRA)* (cit. on p. 75).

Elmberg, C. M. (1972). "The Gothenburg traffic restraint scheme". In: *Transportation* 1.1, pp. 1–27. ISSN: 0049–4488. DOI: 10.1007/BF00167506 (cit. on pp. 22, 51).

Emberger, G. (2015). "Low carbon transport strategy in Europe - a critical review". In: *International Journal of Sustainable Transportation*. DOI: 10.1080/15568318.2015.1106246 (cit. on p. 54).

Erlang, A. K. (1909). "The theory of probabilities and telephone conversations". In: *Nyt Tidsskrift for Matematik B* 20.16, pp. 33–39 (cit. on p. 69).

Essen, H. van, A. Schroten, M. Otten, D. Sutter, R. Schreyer C. Zandonella, M. Maibach, and C. Doll (2011). *External Costs of Transport in Europe*. Tech. rep. CE Delft (cit. on p. 5).

European Commission (2009). *A sustainable future for transport : towards an integrated, technology-led and user-friendly system*. Tech. rep. Directorate - General for Energy and Transport. DOI: 10.2768/13118 (cit. on p. 51).

— (2011). *Roadmap to a Single European Transport Area - Towards a competitive and resource efficient transport system*. White Paper. DOI: 10.2832/30955. URL: http://ec.europa.eu/transport/themes/strategies/doc/2011_white_paper/white-paper-illustrated-brochure_en.pdf (cit. on pp. 7, 51).

European Environment Agency (2016). *Eurostat: your key to Eurpoean statistics*. European Commission. URL: http://ec.europa.eu/eurostat/data/database (cit. on p. 52).

Fan, S. and D. Work (2015a). "A cell transmission model for heterogeneous multiclass traffic flow with creeping". In: *94th Transportation Research Board Annual Meeting* (cit. on p. 75).

— (2015b). "A heterogeneous multiclass traffic flow model with creeping". In: *SIAM Journal on Applied Mathematics* 75.2, pp. 813–835. DOI: 10.1137/140977977 (cit. on p. 75).

FCCC/CP/2015/L.9/Rev.1 (2016). *Adoption of the Paris agreement*. Framework Convention on Climate Change, United Nations (cit. on pp. 7, 51).

FEMA (2009). *A European agenda for motorcycle safety: The motorcyclists' point of view*. Tech. rep. Federation of European Motorcyclists Associations (cit. on pp. 74, 75).

Ferguson, E., J. Duthie, and S. Waller (2011). "Comparing delay minimization and emissions minimization in the network design problem". In: *Computer-Aided Civil and Infrastructure Engineering* 27.4, pp. 288–302. DOI: 10.1111/j.1467-8667.2011.00746.x (cit. on pp. 22, 26).

Fernandes, P., J. M. Bandeira, T. Fontes, S. R. Pereira, B. J. Schroeder, N. M. Rouphail, and M. C. Coelho (2014). "Traffic restriction policies in an urban avenue: a methodological overview for a trade-off analysis of traffic and emission impacts using microsimulation". In: *International Journal of Sustainable Transportation*. DOI: 10.1080/15568318.2014.885622 (cit. on p. 22).

Flötteröd, G. (2010). *Cadyts – Calibration of dynamic traffic simulations – Version 1.1.0 manual*. Transport and Mobility Laboratory, École Polytechnique Fédérale de Lausanne. URL: http://home.abe.kth.se/~gunnarfl/files/cadyts/Cadyts_manual_1-1-0.pdf (cit. on p. 120).

— (2016a). *Fast approximate optimization subject to transport simulation constraints* (cit. on pp. 127, 140, 149).

— (2016b). "Queueing Representation of Kinematic Waves". In: *The Multi-Agent Transport Simulation MATSim*. Ed. by A. Horni, K. Nagel, and K. W. Axhausen. Ubiquity, London. Chap. 50. DOI: 10.5334/baw. URL: http://matsim.org/the-book (cit. on p. 76).

Flötteröd, G., M. Bierlaire, and K. Nagel (2011a). "Bayesian demand calibration for dynamic traffic simulations". In: *Transportation Science* 45.4, pp. 541–561. DOI: 10.1287/trsc.1100.0367 (cit. on p. 120).

Flötteröd, G., Y. Chen, and K. Nagel (2011b). "Behavioral Calibration and Analysis of a Large-Scale Travel Microsimulation". In: *Networks and Spatial Economics* 12.4, pp. 481–502. ISSN: 1566-113X. DOI: 10.1007/s11067-011-9164-9 (cit. on p. 120).

Follmer, R., U. Kunert, J. Kloas, and H Kuhfeld (2004). *Mobilität in Deutschland – Ergebnisbericht*. Tech. rep. Bonn: infas/DIW. URL: www.kontiv2002.de (cit. on pp. 35, 37, 54, 55, 63).

Fourie, P., J. Illenberger, and K. Nagel (2013). "Increased Convergence Rates in Multi-agent Transport Simulations with Pseudo-simulation". In: *Transportation Research Record* 2343, pp. 68–76. DOI: 10.3141/2343-09 (cit. on p. 108).

Franklin, J. (2006). "The distributional effects of transportation policies: The case of a bridge toll for Seattle". PhD thesis. Seattle: University of Washington (cit. on p. 121).

Frederix, R., F. Viti, and C. Tampère (2010). "A density-based dynamic OD estimation method that reproduces within-day congestion dynamics". In: *Intelligent Transportation Systems (ITSC), 2010 13th International IEEE Conference on*, pp. 694–699. DOI: 10.1109/ITSC.2010.5625220 (cit. on p. 71).

Frondel, M., N. Ritter, and C. Vance (2012). "Heterogeneity in the rebound effect: further evidence for Germany". In: *Energy Economics* 34.2, pp. 461–467. DOI: 10.1016/j.eneco.2011.10.016 (cit. on p. 53).

Gajjar, H. and J. D. Mondol (2015). "Techno-economic comparison of alternative vehicle technologies for South Africa road transport system". In: *International Journal of Sustainable Transportation*. DOI: 10.1080/15568318.2015.1026007 (cit. on pp. 22, 24).

Gawron, C. (1998). "An Iterative Algorithm to Determine the Dynamic User Equilibrium in a Traffic Simulation Model". In: *International Journal of Modern Physics C* 9.3, pp. 393–407 (cit. on pp. 7, 9, 13, 15, 69, 76).

Geurs, K. and B. van Wee (2000). "Backcasting as a tool to develop a sustainable transport scenario assuming emission reductions of 80-90%". In: *Innovation: The European Journal of Social Science Research* 13.1, pp. 47–62. DOI: 10.1080/135116100111658 (cit. on pp. 22, 27).

— (2004). "Backcasting as a tool for sustainable transport policy making: the environmentally sustainable transport study in the Netherlands". In: *European Journal of Transport Infrastructure Research* 4.1, pp. 47–69 (cit. on pp. 22, 27).

Ghafghazi, G. and M. Hatzopoulou (2014). "Simulating the environmental effects of isolated and area-wide traffic calming schemes using traffic simulation and microscopic emission modeling". In: *Transportation* 41, 633–649 (cit. on pp. 22, 23, 49).

Goel, R. and S. Guttikunda (2015). "Evolution of on-road vehicle exhaust emissions in Delhi". In: *Atmospheric Enivronment* 105, pp. 78–90. DOI: 10.1016/j.atmosenv.2015.01.045 (cit. on pp. 137, 140).

Grether, D., Y. Chen, M. Rieser, and K. Nagel (2009). "Effects of a Simple Mode Choice Model in a Large-scale Agent-Based Transport Simulation". In: *Complexity and Spatial Networks. In Search of Simplicity*. Ed. by A. Reggiani and P. Nijkamp. Advances in Spatial Science. Springer. Chap. 13, pp. 167–186. DOI: 10.1007/978-3-642-01554-0 (cit. on p. 17).

Gundaliya, P. J., T. V Mathew, and S. L. Dhingra (2008). "Heterogeneous traffic flow modelling for an arterial using grid based approach". In: *Journal of Advanced Transportation* 42.4, pp. 467–491. DOI: 10.1002/atr.5670420404 (cit. on p. 72).

Hall, R. (1994). "Non-recurrent congestion: How big is the problem? Are traveler information systems the solution?" In: *Transportation Research C* 36, p. 67 (cit. on p. 30).

Haszpra, L. and I. Szilágyi (1994). "Non-Methane Hydrocarbon composition of car exhaust in Hungary". In: *Atmospheric Environment* 28.16, pp. 1609–2614. DOI: 10.1016/1352-2310(94)90434-0 (cit. on p. 60).

Henderson, J. V. (1974). "Road congestion: A reconsideration of pricing theory". In: *Journal of Urban Economics* 1, pp. 354–365. DOI: 10.1016/0094-1190(74)90012-6 (cit. on p. 25).

Hickman, R., O. Ashiru, and D. Banister (2009). "Achieving carbon-efficient transportation : backcasting from London". In: *Transportation Research Record: Journal of the Transportation Research Board* 2139, pp. 172–182. DOI: 10.3141/2139-20 (cit. on pp. 22, 27).

Hoekman, S. K. (1992). "Speciated measurements and calculated reactivities of vehicle exhaust emissions from conventional and reformulated gasolines". In: *Environmental Science and Technology* 26.6, pp. 1206–1216. DOI: 10.1021/es50002a610 (cit. on p. 60).

Horni, A. and K. Nagel (2016). "More About Configuring MATSim". In: *The Multi-Agent Transport Simulation MATSim*. Ed. by A. Horni, K. Nagel, and K. W. Axhausen. Ubiquity, London. Chap. 4. DOI: 10.5334/baw. URL: http://matsim.org/the-book (cit. on p. 14).

Horni, A., K. Nagel, and K. W. Axhausen (2016a). "Introducing MATSim". In: *The Multi-Agent Transport Simulation MATSim*. Ed. by A. Horni, K. Nagel, and K. W. Axhausen. Ubiquity, London. Chap. 1. DOI: 10.5334/baw. URL: http://matsim.org/the-book (cit. on p. 15).

— (2016b). *The Multi-Agent Transport Simulation MATSim*. Ed. by A. Horni, K. Nagel, and K. W. Axhausen. Ubiquity, London. DOI: 10.5334/baw. URL: http://matsim.org/the-book (cit. on p. 13).

Hülsmann, F., R. Gerike, B. Kickhöfer, K. Nagel, and R. Luz (2011). "Towards a multi-agent based modeling approach for air pollutants in urban regions". In: *Conference on "Luftqualität an Straßen"*. Also VSP WP 10-15, see http://www.vsp.tu-berlin.de/publications. Bundesanstalt für Straßenwesen. FGSV Verlag GmbH, pp. 144–166. ISBN: 978-3-941790-77-3 (cit. on p. 30).

Hurdle, V. F. and B. Son (2001). *Shock wave and cumulative arrival and departure models: Partners without conflict*. Annual Meeting Preprint 01-2189. Washington, D.C.: Transportation Research Board (cit. on pp. 70, 71).

Hurt, H. H., J. V. Ouellet, and D. R. Thom (1981). *Motorcycle accident cause factors and identification of countermeasures volume I*. Tech. rep. Traffic Safecty Center, University of Southern California, Los Angeles, California (cit. on pp. 74, 75).

IPCC (2014). *Climate change 2014: mitigation of climate change. Contribution of working group III to the fifth assessment report of the intergovernmental panel on climate change*. Ed. by O. Edenhofer, R. Pichs-Madruga, Y. Sokona, E. Farahani, S. Kadner, K. Seyboth, A. Adler, I. Baum, S. Brunner, P. Eickemeier, B. Kriemann, J. Savolainen, S. Schlömer, C. von Stechow, T. Zwickel, and J. Minx. Cambridge University Press, Cambridge, United Kingdom and New York,

NY, USA. URL: https://www.ipcc.ch/pdf/assessment-report/ar5/wg3/ipcc_wg3_ar5_full.pdf (cit. on p. 53).

IRC:SP:30 (2009). *Manual on economic evaluation of highway projects in India*. Indian Roads Congress. New Delhi, India (cit. on pp. 117, 118, 121, 139).

ITP and BVU (2007). *Prognose der deutschlandweiten Verkehrsverflechtungen 2025*. Tech. rep. Intraplan Consult GmbH, Beratergruppe Verkehr+Umwelt GmbH. URL: http://daten.clearingstelle-verkehr.de/220/ (cit. on p. 35).

IWW, IFEU, KuP, PÖU, and PTV (1998). *Entwicklung eines Verfahrens zur Aufstellung umweltorientierter Fernverkehrskonzepte als Beitrag zur Bundesverkehrswegeplanung*. Schlussbericht für Forschungsprojekt FE Nr. 10506001(alt) / 295 54 001 (neu). Im Auftrag des Umweltbundesamtes. Institut für Wirtschaftspolitik und Wirtschaftsforschung, Universität Karlsruhe; Institut für Energie- und Umweltforschung GmbH; Kessel und Partner; Planungsgruppe Ökologie + Umwelt; PTVConsult GmbH (cit. on p. 27).

Jacob, R. R., M. V. Marathe, and K. Nagel (1999). "A computational study of routing algorithms for realistic transportation networks". In: *ACM Journal of Experimental Algorithms* 4.1999es, Article No. 6. DOI: 10.1145/347792.347814 (cit. on p. 16).

Jakob, A., J. L. Craig, and G. Fisher (2006). "Transport cost analysis: a case study of the total costs of private and public transport in Auckland". In: *Environmental Science & Policy* 9.1, pp. 55 –66. DOI: 10.1016/j.envsci.2005.09.001 (cit. on p. 5).

Jansson, J. O. (1994). "Accident externality charges". In: *Journal of Transport Economics and Policy* 28.1, pp. 31–43 (cit. on p. 2).

Jara-Díaz, S. (2007). *Transport Economic Theory*. Bingley: Emerald Group Publishing Limited, p. 140. ISBN: 9780080450285 (cit. on p. 24).

Kaddoura, I. and B. Kickhöfer (2014). *Optimal Road Pricing: Towards an Agent-based Marginal Social Cost Approach*. VSP Working Paper 14-01. See http://www.vsp.tu-berlin.de/publications. TU Berlin, Transport Systems Planning and Transport Telematics (cit. on pp. 9, 28, 30).

Kaddoura, I. and K. Nagel (2016). "Agent-based congestion pricing and transport routing with heterogeneous values of travel time savings". In: *Procedia Computer Science* 83, pp. 908–913. DOI: 10.1016/j.procs.2016.04.184 (cit. on p. 147).

Kaddoura, I., B. Kickhöfer, A. Neumann, and A. Tirachini (2015a). "Agent-based optimisation of public transport supply and pricing: Impacts of activity scheduling decisions and simulation randomness". In: *Transportation* 42.6, pp. 1039–1061. ISSN: 0049-4488. DOI: 10.1007/s11116-014-9533-6 (cit. on p. 41).

— (2015b). "Optimal public transport pricing: Towards an agent-based marginal social cost approach". In: *Journal of Transport Economics and Policy* 49.2. Also VSP WP 13-09, see http://www.vsp.tu-berlin.de/publications. Awarded as the Best PhD Student Paper at hEART 2013., pp. 200–218 (cit. on p. 48).

Kaddoura, I., L. Kröger, and K. Nagel (2016). "User-specific and dynamic internalization of road traffic noise exposures". In: *Networks and Spatial Economics*. DOI: 10.1007/s11067-016-9321-2 (cit. on p. 148).

Kickhöfer, B. (2014). "Economic Policy Appraisal and Heterogeneous Users". PhD thesis. Berlin: TU Berlin. DOI: 10.14279/depositonce-4089 (cit. on pp. 8, 30, 36, 45, 139, 152, 153).

Kickhöfer, B. and A. Agarwal (2015). "Is marginal emission cost pricing enough to comply with the EU CO2 reduction targets?" In: *hEART 2015 – 4th Symposium of the European Association for Research in Transportation*. Also see VSP WP 15-16 http://www.vsp.tu-berlin.de/publications (cit. on p. 51).

Kickhöfer, B. and J. Kern (2015). "Pricing local emission exposure of road traffic: An agent-based approach". In: *Transportation Research Part D: Transport and Environment* 37.1, pp. 14–28. ISSN: 1361-9209. DOI: 10.1016/j.trd.2015.04.019 (cit. on pp. 22, 25, 39, 44, 48, 148).

Kickhöfer, B. and K. Nagel (2016a). "Microeconomic Interpretation of MATSim for Benefit-Cost Analysis". In: *The Multi-Agent Transport Simulation MATSim*. Ed. by A. Horni, K. Nagel, and K. W. Axhausen. Ubiquity, London. Chap. 51. DOI: 10.5334/baw. URL: http://matsim.org/the-book (cit. on pp. 38, 122, 123).

— (2016b). "Towards High-Resolution First-Best Air Pollution Tolls". In: *Networks and Spatial Economics* 16.1, pp. 175–198. DOI: 10.1007/s11067-013-9204-8 (cit. on pp. 9, 22, 25, 28, 31, 34–36).

Kickhöfer, B., F. Hülsmann, R. Gerike, and K. Nagel (2013). "Rising car user costs: comparing aggregated and geo-spatial impacts on travel demand and air pollutant emissions". In: *Smart Transport Networks: Decision Making, Sustainability and Market structure*. Ed. by T. Vanoutrive and A. Verhetsel. NECTAR Series on Transportation and Communications Networks Research. Edward Elgar Publishing Ltd, pp. 180–207. ISBN: 978-1-78254-832-4. DOI: 10.4337/9781782548331.00014 (cit. on pp. 30, 136).

Kim, H., Y. Lim, and K. Lim (2003). "Two traffic flow models for dynamic network loading". In: *Journal of Eastern Aisa Society for transportation Studies* 5 (cit. on p. 70).

Klüpfel, H. and S. Hebben (2010). *Numerical tsunami early warning system "Last-mile - Evacuation" WP 4100 : Evacuation analysis and traffic optimization, evacuation plans for buildings and geometrically complex areas*. Tech. rep. TraffGo HT GmbH (cit. on pp. 75, 103).

Knight, F. H. (1924). "Some fallacies in the interpretation of social cost". In: *The Quarterly Journal of Economics* 38.4, pp. 582–606 (cit. on p. 21).

Krajzewicz, D., J. Erdmann, M. Behrisch, and L. Bieker (2012). "Recent Development and Applications of SUMO - Simulation of Urban MObility". In: *International Journal On Advances in Systems and Measurements* 5.3&4, pp. 128–138 (cit. on p. 107).

Krewitt, W. and B. Schlomann (2006). *Externe Kosten der Stromerzeugung aus erneuerbaren Energien im Vergleich zur Stromerzeugung aus fossilen Energieträgern*. Tech. rep. Zentrums für Sonnenenergie- und Wasserstoff-Forschung Baden-Württemberg (ZSW) (cit. on p. 64).

Kumar, C. V. P., D. Baus, and B. Maitra (2004). "Modeling generalized cost of travel for rural bus users: a case study". In: *Journal of Public Transportation* 7.2, pp. 59–72. DOI: 10.5038/2375-0901.7.2.4 (cit. on pp. 118, 121).

Lämmel, G. (2011). "Escaping the Tsunami: Evacuation Strategies for Large Urban Areas. Concepts and Implementation of a Multi-Agent Based Approach". PhD thesis. Berlin: TU Berlin. URL: http://opus.kobv.de/tuberlin/volltexte/2011/3270/ (cit. on p. 104).

Lämmel, G. and H. Klüpfel (2012). "Slower is faster: the influence of departure time distribution on the overall evacuation performance". In: *International Conference on Evacuation Modeling and Management*. see also vspwp = 11-29. Northwestern University, Evanston, Illinois, USA. DOI: 10.13140/RG.2.1.3787.9201 (cit. on p. 104).

Lämmel, G., D. Grether, and K. Nagel (2010). "The representation and implementation of time-dependent inundation in large-scale microscopic evacuation simulations". In: *Transportation Research Part C: Emerging Technologies* 18.1, pp. 84–98. ISSN: 0968-090X. DOI: 10.1016/j.trc.2009.04.020 (cit. on p. 106).

Lee, T.-C. and K. Wong (2016). "An agent-based model for queue formation of powered two-wheelers in heterogeneous traffic". In: *Physica A: Statistical Mechanics and its Applications* 461, pp. 199–216. ISSN: 0378-4371. DOI: 10.1016/j.physa.2016.05.005 (cit. on p. 75).

Leong, S. T., S Muttamara, and P. Laortanakul (2002). "Applicability of gasoline containing ethanol as Thailand's alternative fuel to curb toxic {VOC} pollutants from automobile emission". In: *Atmospheric Environment* 36.21, pp. 3495–3503. DOI: 10.1016/S1352-2310(02)00288-1 (cit. on pp. 22, 24).

Li, X., G. Li, S.-S. Pang, X. Yang, and J. Tian (2004). "Signal timing of intersections using integrated optimization of traffic quality, emissions and fuel consumption: a note". In: *Transportation Research Part D: Transport and Environment* 9.5, pp. 401–407. DOI: 10.1016/j.trd.2004.05.001 (cit. on pp. 22, 23, 49).

Li, Z.-C., W. H. K. Lam, S. C. Wong, and A. Sumalee (2012). "Environmentally sustainable toll design for congested road networks with uncertain demand". In: *International Journal of Sustainable Transportation* 6.3, pp. 127–155. DOI: 10.1080/15568318.2011.570101 (cit. on pp. 22, 26).

Lighthill, M. J. and J. B. Whitham (1955). "On kinematic waves. II: A Theory of traffic flow on long crowded roads". In: *Proceedings of the Royal Society A* 229, pp. 281–345. DOI: 10.1098/rspa.1955.0089 (cit. on p. 70).

Lindley, J. A. (1987). "Urban freeway congestion: quantification of the problem and effectiveness of potential solutions". In: *ITE Journal* 57.1, pp. 27–32 (cit. on p. 30).

Lindsey, R. and E. T. Verhoef (2001). "Traffic Congestion and Congestion Pricing". In: *Handbook of Transport Systems and Traffic Control*. Ed. by D. Hensher and K. Button. Vol. 3. Handbooks in Transport, pp. 77–105. ISBN: 9780080435954 (cit. on p. 27).

Link, H., C. Nash, A. Ricci, and J. Shires (2014). "A generalised approach for measuring the marginal social costs of road transport in Europe". In: *International Journal of Sustainable Transportation*. DOI: 10.1080/15568318.2013.861044 (cit. on pp. 27, 62).

Litman, T. (2012). *Climate change emission valuation for transportation economic analysis*. Tech. rep. Victoria Transport Policy Institute (cit. on p. 3).

Liu, J. and G. Santos (2015). "Decarbonizing the road transport sector: break-even point and consequent potential consumers' behavior for the U.S. case". In: *International Journal of Sustainable Transportation* 9.3, pp. 159–175. DOI: 10.1080/15568318.2012.749962 (cit. on p. 27).

Maciejewski, M. (2010). "Parametric calibration of queue-based traffic flow model in MATSim". In: *VII Konferencja Naukowo-Techniczna "Systemy Transportowe – Teoria i Praktyka"* (cit. on pp. 107, 112).

Madireddy, M., B. D. Coensel, A. Can, B. Degraeuwe, B. Beusen, I. D. Vlieger, and D. Botteldooren (2011). "Assessment of the impact of speed limit reduction and traffic signal coordination on vehicle emissions using an integrated approach". In: *Transportation Research Part D: Transport and Environment* 16.7, pp. 504 –508. ISSN: 1361-9209. DOI: 10.1016/j.trd.2011.06.001 (cit. on pp. 22, 23).

Maerivoet, S. and B. D. Moor (2005). "Transportation Planning and traffic flow models". In: *ArXiv Physics e-prints*. eprint: physics/0507127 (cit. on p. 70).

Maibach, M., D. Schreyer, D. Sutter, H. van Essen, B. Boon, R. Smokers, A. Schroten, C. Doll, B. Pawlowska, and M. Bak (2008). *Handbook on estimation of external costs in the transport sector*. Tech. rep. Internalisation Measures and Policies for All external Cost of Transport (IMPACT). CE Delft. URL: http://ec.europa.eu/transport/sites/transport/files/themes/sustainable/doc/2008_costs_handbook.pdf (cit. on pp. 4, 5, 27, 28, 31, 39, 64, 145, 148).

MAIDS (2003). *In–depth investigation of motorcycle accidents*. Association des Constructeurs Européens de Motocyles (cit. on p. 74).

Mallikarjuna, C. and K. R. Rao (2007). "Identification of a suitable cellular automata model for mixed traffic". In: *Proceedings of the Eastern Asia Society for Transportation Studies*. Vol. 6. DOI: 10.11175/eastpro.2007.0.321.0 (cit. on p. 72).

Mallikarjuna, C. and K. R. Rao (2011). "Heterogeneous traffic flow modelling: A complete methodology". In: *Transportmetrica* 7.5, pp. 321–345. DOI: 10.1080/18128601003706078 (cit. on pp. 72, 99).

Manjunatha, P., P. Vortisch, and T. V. Mathew (2013). "Methodology for the calibration of VISSIM in mixed traffic". In: *92nd Transportation Research Board Annual Meeting*. 13-3677 (cit. on p. 8).

Mathew, T., C. Munigety, and A. Bajpai (2013). "Strip-based approach fo the simulation of mixed traffic conditions". In: *Journal of Computing in Civil Engineering* 29.5, p. 04014069. DOI: 10.1061/(ASCE)CP.1943-5487.0000378 (cit. on pp. 8, 73).

May, A. D. (2013). "Urban transport and sustainability: the key challenges". In: *International Journal of Sustainable Transportation* 7.3, pp. 170–185. DOI: 10.1080/15568318.2013.710136 (cit. on pp. 24, 54).

Mayeres, I., S. Ochelen, and S. Proost (1996). "The marginal external costs of urban transport". In: *Transportation Research Part D: Transport and Environment* 1.2, pp. 111–130. DOI: 10.1016/S1361-9209(96)00006-5 (cit. on p. 4).

Mock, P., U. Tietge, V. Franco, J. German, A. Bandivadekar, N. Ligterink, U. Lambrecht, J. Kühlwein, and I. Riemersma (2014). *From laboratory to road : A 2014 update of official and "Real–World" Fuel consumption and CO_2 values for passenger cars in Europe*. White Paper. International Council on Clean Transportation (cit. on p. 53).

Moyo Oliveros, M. and K. Nagel (2012). *Automatic Calibration of Microscopic, Activity-Based Demand for a Public Transit Line*. Annual Meeting Preprint 12-3279. Also VSP WP 11-13, see http://www.vsp.tu-berlin.de/publications. Washington, D.C.: Transportation Research Board (cit. on p. 120).

MVV (2007). *Regionaler Nahverkehrsplan für das Gebiet des Münchner Verkehrs- und Tarifverbundes*. Tech. rep. Munich Local Transport Provider (cit. on p. 37).

Nagel, K. (2008). *Towards simulation-based sketch planning: Some results concerning the Alaskan Way viaduct in Seattle WA*. VSP Working Paper 08-22. See http://www.vsp.tu-berlin.de/publications. TU Berlin, Transport Systems Planning and Transport Telematics. URL: https:

//svn.vsp.tu-berlin.de/repos/public-svn/publications/vspwp/2008/08-22 (cit. on pp. 117, 161).
— (2011). *Towards simulation-based sketch planning, part II: Some results concerning a freeway extension in Berlin*. VSP Working Paper 11-18. See http://www.vsp.tu-berlin.de/publications. TU Berlin, Transport Systems Planning and Transport Telematics. URL: https://svn.vsp.tu-berlin.de/repos/public-svn/publications/vspwp/2011/11-18 (cit. on pp. 117, 161).
— (2016a). "Matrix-Based pt router". In: *The Multi-Agent Transport Simulation MATSim*. Ed. by A. Horni, K. Nagel, and K. W. Axhausen. Ubiquity, London. Chap. 20. DOI: 10.5334/baw. URL: http://matsim.org/the-book (cit. on p. 14).
— (2016b). "Other Experiences with Computational Performance Improvements". In: *The Multi-Agent Transport Simulation MATSim*. Ed. by A. Horni, K. Nagel, and K. W. Axhausen. Ubiquity, London. Chap. 40. DOI: 10.5334/baw. URL: http://matsim.org/the-book (cit. on p. 108).
Nagel, K. and G. Flötteröd (2012). "Agent-based traffic assignment: Going from trips to behavioural travelers". In: *Travel Behaviour Research in an Evolving World – Selected papers from the 12th international conference on travel behaviour research*. Ed. by R. Pendyala and C. Bhat. International Association for Travel Behaviour Research, pp. 261–294. ISBN: 978-1-105-47378-4 (cit. on pp. 18, 32, 105).
Nagel, K. and M. Schreckenberg (1992). "A cellular automaton model for freeway traffic". In: *Journal de Physique I France* 2, pp. 2221–2229. DOI: 10.1051/jp1:1992277 (cit. on pp. 70, 72).
Nagel, K., B. Kickhöfer, A. Horni, and D. Charypar (2016a). "A Closer Look at Scoring". In: *The Multi-Agent Transport Simulation MATSim*. Ed. by A. Horni, K. Nagel, and K. W. Axhausen. Ubiquity, London. Chap. 3. DOI: 10.5334/baw. URL: http://matsim.org/the-book (cit. on pp. 15, 16).
Nagel, K., K. W. Axhausen, B. Kickhöfer, and A. Horni (2016b). "Research Avenues". In: *The Multi-Agent Transport Simulation MATSim*. Ed. by A. Horni, K. Nagel, and K. W. Axhausen. Ubiquity, London. Chap. 97. DOI: 10.5334/baw. URL: http://matsim.org/the-book (cit. on p. 16).
Nagurney, A. (2000). "Congested urban transportation networks and emission paradoxes". In: *Transportation Research Part D: Transport and Environment* 5.2, pp. 145–151. DOI: 10.1016/S1361-9209(99)00031-0 (cit. on p. 25).
Nair, R., H. S. Mahmassani, and E. Miller-Hooks (2011). "A porous flow approach to modeling heterogeneous traffic in disordered systems". In: *Transportation Research Part B: Methodological* 45.9, pp. 1331–1345. DOI: 10.1016/j.trb.2011.05.009 (cit. on pp. 10, 75).
Neumann, A. (2014). "A paratransit-inspired evolutionary process for public transit network design". PhD thesis. Berlin: TU Berlin. urn: urn:nbn:de:kobv:83-opus4-53866 (cit. on p. 140).
Newbery, D. M. (1988). "Road user charges in Britain". In: *The Economic Journal* 98.390, pp. 161–176. ISSN: 00130133, 14680297. DOI: 10.2307/2233312. URL: http://www.jstor.org/stable/2233312 (cit. on pp. 2, 95).
Newell, G. (1993). "A simplified theory of kinematic waves in highway traffic. I: General theory. II: Queueing at freeway bottlenecks. III: Multi-destination flows". In: *Transportation Research B* 27B, pp. 281–313 (cit. on p. 71).
Nie, X. and H. M. Zhang (2005). "A comparative study of some macroscopic link models used in dynamic traffic assignment". In: *Networks and Spatial Economics* 5.1, pp. 89–115. DOI: 10.1007/s11067-005-6663-6 (cit. on pp. 71, 72).
OECD (2006). *Cost-benefit Analysis and the Environment: Recent Developments*. Organisation for Economic Cooperation and Development. ISBN: 92-64-01004-1 (cit. on p. 141).
Oketch, T. (2000). "New modeling approach for mixed-traffic streams with nonmotorized vehicles". In: *Transportation Research Record: Journal of the Transportation Research Board* 1705.00–0285, pp. 61–69. DOI: 10.3141/1705-10 (cit. on pp. 10, 74, 75).
— (2003). *Modeled performance characteristics of heterogeneous traffic streams containing nonmotorized vehicles*. Annual Meeting Preprint 03–0721. Washington, D.C.: Transportation Research Board (cit. on pp. 74, 75).
Osorio, C. and K. Nanduri (2015a). "Energy-efficient urban traffic management: A microscopic simulation-based approach". In: *Transportation Science* 49.3, pp. 637–651. DOI: 10.1287/trsc.2014.0554 (cit. on pp. 22, 23).

— (2015b). “Urban trasportation emission mitigation: coupling high-resolution vehicular emissions and traffic models for traffic signal optimization”. In: *Transportation Research Part B: Methodological* 81.2, pp. 520–538. ISSN: 0191-2615. DOI: 10.1016/j.trb.2014.12.007 (cit. on pp. 22, 23, 49).

Panis, L. I., S. Broekx, and R. Liu (2006). “Modeling instantaneous traffic emission and the influence of traffic speed limits”. In: *Science of The Total Environment* 371.1-3, pp. 270–285. DOI: 10.1016/j.scitotenv.2006.08.017 (cit. on p. 23).

Parry, I. W. H., M. Walls, and W. Harrington (2007). “Automobile externalities and policies”. In: *Journal of Economic Literature* 45.2, pp. 373–399 (cit. on p. 22).

Parry, I. W., D. Evans, and W. E. Oates (2014). “Are energy efficiency standards justified?” In: *Journal of Environmental Economics and Management* 67.2, pp. 104–125. DOI: 10.1016/j.jeem.2013.11.003 (cit. on p. 54).

Parry, I. and K. Small (2005). “Does Britain or the United States Have the Right Gasoline Tax?” In: *The American Economic Review* 95.4, pp. 1276–1289. DOI: 10.1257/0002828054825510 (cit. on pp. 39, 43, 53, 62).

Percoco, M. (2014). “The effect of road pricing on traffic composition: Evidence from a natural experiment in Milan, Italy”. In: *Transport Policy* 31.0, pp. 55–60. ISSN: 0967-070X. DOI: 10.1016/j.tranpol.2013.12.001 (cit. on p. 25).

— (2015). “Heterogeneity in the reaction of traffic flows to road pricing: a synthetic control approach applied to Milan”. In: *Transportation* 42.6, pp. 1063–1079. ISSN: 0049–4488. DOI: 10.1007/s11116-014-9544-3 (cit. on p. 25).

Pigou, A. (1920). *The Economics of Welfare*. MacMillan, New York (cit. on pp. 7, 21, 24).

Powell, T. (2001). *The Transport System - Markets, Modes and Policies*. PTRC (cit. on p. 128).

Proost, S. and K. van Dender (2001). “The welfare impacts of alternative policies to address atmospheric pollution in urban road transport”. In: *Regional Science and Urban Economics* 31.4, pp. 383–411. ISSN: 0166-0462. DOI: 10.1016/S0166-0462(00)00079-X (cit. on pp. 22, 26).

Qu, T., L. Rilett, and J. Zietsman (2003). “Estimating the impact of freeway speed limits on automobile emissions”. In: *82nd TRB Annual Meeting*. 001972 (cit. on pp. 22, 23).

Raney, B. and K. Nagel (2004). “Iterative Route Planning for Large-Scale Modular Transportation Simulations”. In: *Future Generation Computer Systems* 20.7, pp. 1101–1118. ISSN: 0167-739X. DOI: 10.1016/j.future.2003.11.001 (cit. on p. 13).

— (2006). “An improved framework for large-scale multi-agent simulations of travel behaviour”. In: *Towards better performing European Transportation Systems*. Ed. by P. Rietveld, B. Jourquin, and K. Westin. London: Routledge, pp. 305–347 (cit. on p. 13).

Ricci, A., R. Enei, N. Piccioni, G. L. Adele Vendetti Peter Bickel and, C. Nash, S. Grant-Muller, B. Matthews, H. Link, J. C. martin, C. Ruijgrok, and T. Pauwels (2008). *Generalization of marginal social cost estimates*. Deliverable 7 of GRACE (Generalisation of Research on Accounts and Cost Estimation), Funded by Sixth Framework Programme. ITS, University of Leeds, Leeds (cit. on p. 62).

Richards, P. (1956). “Shock waves on the highway”. In: *Operations Research* 4.1, pp. 42–51 (cit. on p. 70).

Rieser, M., D. Grether, and K. Nagel (2009). “Adding mode choice to a multi-agent transport simulation”. In: *Transportation Research Record* 2132, pp. 50–58. DOI: 10.3141/2132-06 (cit. on p. 17).

Rieser, M., A. Horni, and K. Nagel (2016). “Let’s Get Started”. In: *The Multi-Agent Transport Simulation MATSim*. Ed. by A. Horni, K. Nagel, and K. W. Axhausen. Ubiquity, London. Chap. 2. DOI: 10.5334/baw. URL: http://matsim.org/the-book (cit. on p. 18).

Romm, J. (2006). “The car and fuel of the future”. In: *Energy Policy* 34.17, pp. 2609–2614. DOI: 10.1016/j.enpol.2005.06.025 (cit. on pp. 22, 24, 52).

Rotaris, L., R. Danielis, E. Marcucci, and J. Massiani (2010). “The urban road pricing scheme to curb pollution in Milan, Italy: Description, impacts and preliminary cost–benefit analysis assessment”. In: *Transportation Research Part A: Policy and Practice* 44.5, pp. 359–375. DOI: 10.1016/j.tra.2010.03.008 (cit. on pp. 22, 25).

RSB (2005). *Municipality of Munich: Referat für Stadtplanung und Bauordnung* (cit. on p. 34).

Schade, J. and B. Schlag (2000). *Acceptability of urban transport pricing*. Research Report 72. ISBN 951-561-354-X. Helsinki: VATT. URL: www.vatt.fi/en/publications (cit. on p. 141).

Schmitz, T., D. Hassel, and F.-J. Weber (2000). "Determination of VOC-components in the exhaust of gasoline and diesel passenger cars". In: *Atmospheric Environment* 34.27, pp. 4639–4647. ISSN: 1352-2310. DOI: 10.1016/S1352-2310(00)00303-4 (cit. on p. 60).

Schoemaker, J., A. Scholtz, and R. Enei (2012). *Towards low carbon transport in Europe*. Tech. rep. Transport Research and Innovation Portal (TRIP) (cit. on pp. 51, 52).

Schrank, D., B. Eisele, T. Lomax, and J. Bak (2015). *2015 urban mobility scorecard*. Tech. rep. Texax A&M Transportation Institute and INRIX (cit. on p. 3).

Schröder, S., M. Zilske, G. Liedtke, and K. Nagel (2012). *A computational framework for a multi-agent simulation of freight transport activities*. Annual Meeting Preprint 12-4152. Also VSP WP 11-19, see http://www.vsp.tu-berlin.de/publications. Washington D.C.: Transportation Research Board (cit. on p. 47).

Sharma, S. and T. Mathew (2011). "Multiobjective network design for emission and travel-time trade-off for a sustainable large urban transportation network". In: *Environment and Planning B: Planning and Design* 38.3, pp. 520–538. DOI: 10.1068/b37018 (cit. on pp. 22, 26).

Shepherd, S. P. (2008). "The effect of complex models of externalities on estimated optimal tolls". In: *Transportation* 35.4, pp. 559–577. ISSN: 0049–4488. DOI: 10.1007/s11116-007-9157-1 (cit. on p. 26).

Simon, P. and K. Nagel (1999). *Simple queueing model applied to the city of Portland*. Annual Meeting Preprint 99-0861. Washington, D.C.: Transportation Research Board (cit. on p. 86).

Simon, P., J. Esser, and K. Nagel (1999). "Simple queueing model applied to the city of Portland". In: *International Journal of Modern Physics* 10.5, pp. 941–960. DOI: 10.1142/S0129183199000747 (cit. on pp. 69, 70, 76, 86).

Singh, S. K. and A. Misra (2004). "Road Accident Analysis: A case study of Patna City". In: *Urban Transport Journal* 2.2, pp. 60–75 (cit. on p. 115).

Smits, E.-S., M. Bliemer, and B. van Arem (2011). "Dynamic network loading of multiple user-classes with the link transmission model". In: *2nd International Conference on Models and Technologies for Intelligent Transportation Systems*. 057. Leuven, Belgium (cit. on p. 73).

Sperley, M. and A. J. Pietz (2010). *Motorcycle lane–sharing: Literature review*. Tech. rep. OR–RD–10–20. Oregon Department of Transportation Research Section (cit. on pp. 74, 75).

Stassen, K. R., P. Collier, and R. Torfs (2008). "Environmental burden of disease due to transportation noise in Flanders (Belgium)". In: *Transportation Research Part D: Transport and Environment* 13, pp. 355–358. DOI: 10.1016/j.trd.2008.04.003 (cit. on p. 3).

Sumalee, A., R. Zhong, T. Pan, and W. Szeto (2011). "Stochastic cell transmission model (SCTM): a stochastic dynamic traffic model for traffic state surveillance and assignment". In: *Transportation Research Part B: Methodological* 45.3, pp. 507 –533. ISSN: 0191-2615. DOI: 10.1016/j.trb.2010.09.006 (cit. on pp. 71, 73).

Szeto, W., Y. Jiang, and A. Sumalee (2011). "A cell-based model for multi-class doubly stochastic dynamic traffic assignment". In: *Computer-Aided Civil and Infrastructure Engineering* 26.8, pp. 595–611. DOI: 10.1111/j.1467-8667.2011.00717.x (cit. on p. 73).

Taubenböck, H., N. Goseberg, G. Lämmel, N. Setiadi, T. Schlurmann, K. Nagel, F. Siegert, J. Birkmann, K.-P. Traub, S. Dech, V. Keuck, F. Lehmann, G. Strunz, and H. Klüpfel (2013). "Risk reduction at the "Last-Mile": an attempt to turn science into action by the Example of Padang, Indonesia". In: *Natural Hazards* 65.1, pp. 915–1945. DOI: 10.1007/s11069-012-0377-0 (cit. on pp. 75, 103).

Thomas, B. A. and I. L. Azevedo (2013). "Estimating direct and indirect rebound effects for U.S. households with input–output analysis Part 1: theoretical framework". In: *Ecological Economics* 86, pp. 199–210. DOI: 10.1016/j.ecolecon.2012.12.003 (cit. on p. 53).

Timilsina, G. R. and H. B. Dulal (2011). "Urban road transportation externalities: costs and choice of policy instruments". In: *World Bank Research Observer* 26.1, pp. 162–191. DOI: 10.1093/wbro/lkq005 (cit. on p. 8).

Tiwari, G. (2001). *Traffic segregation: a case for bus priority lanes with segregated cycle tracks - case study Delhi*. Workshop on Transportation, Landuse, and The Environment, Pune (cit. on p. 128).

Tol, R. S. J. (2005). "The marginal damage costs of carbon dioxide emissions: an assessment of the uncertainties". In: *Energy Policy* 33.16, pp. 2064–3074. DOI: 10.1016/j.enpol.2004.04.002 (cit. on pp. 4, 5, 31, 64, 148).

Tordeux, A. (2010). “Étude de Processus en Temps Continu Modélisant l’écoulement de Flux de Trafic Routier”. PhD thesis. Univerité Paris-Ext, Marne-laVallée, France (cit. on p. 71).

Tordeux, A., M. Roussignol, J.-P. Lebacque, and S. Lassarre (2014). “A stochastic jump process applied to traffic flow modelling”. In: *Transportmetrica A: Transport Science* 10.4, pp. 350–375. DOI: 10.1080/23249935.2013.769648 (cit. on p. 71).

TransCAD (2012). *TransCAD, Transporation Planning software*. http://www.caliper.com/tcovu.htm (cit. on p. 116).

Treiber, M. and A. Kesting (2013). *Traffic flow dynamics*. Springer-Verlag Berlin Heidelberg. DOI: 10.1007/978-3-642-32460-4 (cit. on p. 71).

TRIPP, iTrans, and VKS (2009). *Comprehensive mobility plan for Patna urban agglomeration area*. Tech. rep. Department of Urban Development. Government of Bihar (cit. on pp. 104, 115–118, 120, 126, 128, 163).

Tsai, J.-H., Y.-C. Hsu, H.-C. Weng, W.-Y. Lin, and F.-T. Jeng (2000). “Air pollutant emission factors from new and in-use motorcycles”. In: *Atmospheric Environment* 34.28, pp. 4747–4754 (cit. on p. 137).

Tuerprasert, K. and C. Aswakul (2010). “Multiclass cell transmission model for heterogeneous mobility in general topology of road network”. In: *Journal of Intelligent Transportation Systems* 14.2, pp. 68–82. DOI: 10.1080/15472451003719715. eprint: http://www.tandfonline.com/doi/pdf/10.1080/15472451003719715 (cit. on p. 73).

Turvey, R. (1963). “On divergences between social and private cost”. In: *Economica* 30.119, pp. 309–313. DOI: 10.2307/2601550 (cit. on pp. 5, 27, 32).

United Nations (2014). *World Urbanization prospects : The 2014 revision, highlights*. Tech. rep. ST/ESA/SER.A/352. Department of Economic and Social Affairs, Population Division (cit. on pp. 1, 2, 5).

Vickrey, W. (1969). “Congestion Theory and Transport Investment”. In: *The American Economic Review* 59.2, pp. 251–260 (cit. on pp. 25, 27).

Wall, G. (2011). “Environmental parking charging policies: a case study of Winchester”. In: *Local Economy* 26.4, pp. 246–259. ISSN: 0269-0942. DOI: 10.1177/0269094211404624 (cit. on pp. 22, 49).

Walters, A. A. (1961). “The theory and measurement of private and social costs of highway congestion”. In: *Econometrica* 29.4, pp. 676–699. DOI: 10.2307/1911814 (cit. on pp. 5, 32).

Wang, H., P. Zhou, and D. Zhou (2012). “An empirical study of direct rebound effect for passenger transport in urban China”. In: *Energy Economics* 34.2, pp. 452–460. DOI: 10.1016/j.eneco.2011.09.010 (cit. on p. 53).

Wang, J., L. Chi, X. Hu, and H. Zhou (2014). “Urban traffic congestion pricing model with the consideration of carbon emissions cost”. In: *Sustainability* 6(2), pp. 676–691. DOI: 10.3390/su6020676 (cit. on pp. 22, 26).

Wang, J., J. Yang, Q. Li, and Z. Wang (2004). “The effect of nonstandard vehicle’s special behavior on mixed-traffic modeling”. In: *Applications of Advanced Technologies in Transportation Engineering*, pp. 589–594. DOI: 10.1061/40730(144)109 (cit. on p. 74).

Waraich, R., D. Charypar, M. Balmer, and K. Axhausen (2009). *Performance Improvements for Large Scale Traffic Simulation in MATSim*. Tech. rep. ETH Zürich, IVT (cit. on p. 14).

Watkiss, P., D. Anthoff, T. Downing, C. Hepburn, C. Hope, A. Hunt, and R. Tol (2005). *The social cost of carbon (SCC) review: methodological approaches for using SCC estimates in policy assessment*. Final Report. Department for Environment, Food and Rural Affairs (Defra), London (cit. on pp. 4, 27, 31).

WBCSD (2004). *Mobility 2030: meeting the challenges to sustainability*. Tech. rep. World Business Council for Sustainable Development (cit. on p. 1).

WEC (2011). *Global transport scenarios 2050*. Tech. rep. World Energy Council (cit. on p. 1).

Weinreich, S., K. Rennings, B. Schlomann, C. Geßner, and T. Engel (1998). “External costs of road, rail and air transport – A bottom-up approach”. In: *ZEW Discussion Papers* 98-06 (cit. on p. 4).

Weinreich, S., G. Bühler, S. Schmid, P. Bickel, R. Friedrich, A. Ricci, R. Enei, O. Baccelli, C. Vaghi, R. Zucchetti, T. Cini, and M. Henriques (2000). *Real cost reduction of door-to-door intermodal transport (RECORDIT) Deliverable 1 : accounting framework*. Tech. rep. Commission of the European Commutnities - DG TREN (cit. on p. 5).

Whitehead, J, J. P. Franklin, and S. Washington (2014). "The impact of a congestion pricing exemption on the demand for new energy efficient vehicles in Stockholm". In: *Transportation Research Part A: Policy and Practice* 70, pp. 24–40. DOI: 10.1016/j.tra.2014.09.013 (cit. on p. 25).

Wong, G. and S. Wong (2002). "A multi-class traffic flow model — an extension of LWR model with heterogeneous drivers". In: *Transportation Research Part A* 36.9, pp. 827–841. DOI: 10.1016/S0965-8564(01)00042-8 (cit. on p. 72).

Wright, L. and L. Fulton (2005). "Climate change mitigation and transport in developing nations". In: *Transport Reviews* 25.6, pp. 691–717. DOI: 10.1080/01441640500360951 (cit. on p. 7).

Yin, Y. and S. Lawphongpanich (2006). "Internalizing emission externality on road networks". In: *Transportation Research Part D: Transport and Environment* 11, pp. 292–301. DOI: 10.1016/j.sbspro.2014.07.198 (cit. on p. 41).

Yperman, I. (2007). "The link transmission model for dynamic network loading". PhD thesis. Katholieke Universiteit Leuven (cit. on p. 71).

Zhang, A., A. E. Boardman, D. Gillen, and W. Waters II (2004). *Towards estimating the social and environmental costs of transportation in Canada*. Tech. rep. Center for Transportation Studies, The University of British Columbia (cit. on pp. 4, 5).

Zhang, H. M. and W. L. Jin (2002). "Kinematic wave traffic flow model for mixed traffic". In: *Transportation Research Record: Journal of the Transportation Research Board* 1802, pp. 197–204. DOI: 10.3141/1802-22 (cit. on pp. 72, 73, 95).

Zhang, H. M. and Y. Nie (2005). *Modeling network flow with and without link interaction: properties and implication*. Presented at the 84th annual meeting of the Transportation Research Board (cit. on pp. 70, 71).

Zhang, H. M., Y. M. Nie, and Z. S. Qian (2013). "Modelling network flow with and without link interactions: the cases of point queue, spatial queue and cell transmission model". In: *Transportmetrica B: Transport Dynamics* 1.1, pp. 33–51. DOI: 10.1080/21680566.2013.785921 (cit. on p. 71).

Zhou, X. and J. Taylor (2014). "DTALite: A queue-based mesoscopic traffic simulator for fast model evaluation and calibration". In: *Cogent Engineering* 1.1, p. 961345. ISSN: 2331-1916. DOI: 10.1080/23311916.2014.961345 (cit. on p. 70).

Zhou, Y., Y. Wu, L. Yang, L. Fu, K. He, S. Wang, J. Hao, J. Chen, and C. Li (2010). "The impact of transportation control measures on emission reductions during the 2008 Olympic games in Beijing, China". In: *Atmospheric Environment* 44.3, pp. 285–293. DOI: 10.1016/j.atmosenv.2009.10.040 (cit. on p. 22).

Ziemke, D., K. Nagel, and C. Bhat (2015). "Integrating CEMDAP and MATSim to increase the transferability of transport demand models". In: *Transportation Research Record* 2493, pp. 117–125. DOI: 10.3141/2493-13 (cit. on p. 120).

Zilske, M., S. Schröder, K. Nagel, and G. Liedtke (2012). *Adding freight traffic to MATSim*. VSP Working Paper 12-02. See http://www.vsp.tu-berlin.de/publications. TU Berlin, Transport Systems Planning and Transport Telematics (cit. on p. 47).